Turbo-Discharging the Internal Combustion Engine

Alan Baker – BEng (Hons) DIS

A Doctoral thesis submitted in partial fulfilment of the requirements for the award of Doctor of Philosophy of Loughborough University

Abstract

This thesis reports original research on a novel internal combustion (IC) engine charge air system concept called Turbo-Discharging. Turbo-Discharging depressurises the IC engine exhaust system so that the engine gas exchange pumping work is reduced, thereby reducing fuel consumption and CO_2 emissions.

There is growing concern regarding the human impact on the climate, part of which is attributable to motor vehicles and transport. Recent legislation has led manufacturers to improve the fuel economy and thus reduce the quantity of CO_2 generated by their vehicles. As this legislation becomes more stringent manufacturers are looking to new and developing technologies to help further improve the fuel conversion efficiency of their vehicles. Turbo-Discharging is such a technology which benefits from the fact it uses commonly available engine components in a novel system arrangement.

Thermodynamic and one-dimensional gas dynamics models and experimental testing on a 1.4 litre four cylinder four-stroke spark ignition gasoline passenger car engine have shown Turbo-Discharging to be an engine fuel conversion efficiency and performance enhancing technology. This is due to the reduction in pumping work through decreased exhaust system pressure, and the improved gas exchange process resulting in reduced residual gas fraction. Due to these benefits, engine fuel conversion efficiency improvements of up to 4% have been measured and increased fuel conversion efficiency can be realised over the majority of the engine operating speed and load map. This investigation also identified a measured improvement in engine torque over the whole engine speed range with a peak increase of 12%.

Modelling studies identified that both fuel conversion efficiency and torque can be improved further by optimisation of the Turbo-Discharging system hardware beyond the limitations of the experimental engine test. The model predicted brake specific fuel consumption improvements of up to 16% at peak engine load compared to the engine in naturally aspirated form, and this increased to up to 24% when constraints imposed on the experimental engine test were removed.

Contents

Acknowledgements

Throughout this work I have been supported by many people. I would like to thank Loughborough University for their funding and support of the project.

I would like to thank Doctor Andy Williams and Professor Colin Garner for the opportunity to work on the project, and for their tireless support throughout. With their support I have achieved a great deal, both academically and professionally. It has been challenging almost every step of the way, and I wish you both all the best in taking the project and all your other research at Loughborough forward.

Crucial to the success of this project was the support offered by the university staff, especially the technical staff. There was a significant amount to achieve in a comparatively short space of time, and without your help I would not have come close. Thank you.

I would like to thank my family and friends for their continual support throughout this period of my life, especially my dearest Abby. Our experience going through this together means we can achieve anything we wish. In hindsight I am glad we went through it together, no matter how difficult it was at times!

List of Figures

List of Tables

Nomenclature

c_P	specific heat at constant pressure
D	Cylinder bore
E	Efficacy
h_W	Heat transfer coefficient
k	ratio of specific heats
m	mass
P	Pressure
Q_{CH}	Gross heat release rate
Q_{HV}	Heating value
T	Temperature
U	Blade speed
V	Volume
v	specific volume
v_c	Characteristic velocity
Vc	Cylinder clearance volume
v_m	Mean piston speed
v_w	Tangential velocity
W	Work
W_n	Non-dimensional cumulative burn rate
γ	Specific weight
η	Efficiency
θ	Engine crank angle
λ	Air fuel ratio or excess air
ρ	Density

Abbreviations

1-D	One dimensional
abs	Absolute
BDC	Bottom dead centre
BMEP	Brake mean effective pressure
bsfc	Brake specific fuel consumption
CA	Crank angle
CO	Carbon monoxide
CO2	Carbon dioxide
CoV	Coefficient of variance
DAQ	Data acquisition
DEP	Divided exhaust period
DI	Direct injection
DPF	Diesel particulate filter
ECU	Engine control unit
EGR	Exhaust gas recirculation

EIVC	Early inlet valve closing
ETC	Electric turbo compound
EVC	Exhaust valve closing
EVO	Exhaust valve opening
F/A	Fuel to air ratio
FTP	Federal test procedure
HC	Hydrocarbons
HP	High pressure
IC	Internal combustion
IMEP	Indicated mean effective pressure
IVC	Intake valve closing
IVO	Intake valve opening
LIVO	Late inlet valve closing
LP	Low pressure
MBT	Minimum advance best torque
MTC	Mechanical turbo compound
NA	Naturally aspirated
NDIR	Non-dispersive infra red
NEDC	New european drive cycle
Nox	Nitrogen oxides
NVH	Noise, vibration and harshness
PFI	Port fuel injection
PMEP	Pumping mean effective pressure
RGF	Residual gas fraction
SCR	Selective catalytic reduction
SI	Spark ignition
TDC	Top dead centre
TEG	Thermoelectric generator
TTL	Transistor-transistor logic
U/C	Blade to speed ratio
VEMB	Valve event modulated exhaust period
VGT	Variable geometry turbine
VI	Virtual instrument
VNT	Variable nozzle geometry
VTG	Variable turbine geometry
VVT	Variable valve geometry
WOT	Wide open throttle

1. Introduction

This chapter introduces the reasons why internal combustion engines are an important future technology and the relevance of this thesis to the field. It then describes the objectives of this thesis and gives an overview of its composition before summarising the major contributions to knowledge and the publications that have arisen as a result of this work that has investigated the novel concept called “Turbo-Discharging”.

1.1 IC Engines

Internal combustion (IC) engines have been the most popular means of vehicle propulsion for over 100 years. The first recorded application of an IC engine in an automobile is attributed to Karl Benz (1844 – 1929) for his Benz Patent Motorwagen built in 1885. The Motorwagen was powered by a single cylinder 954 cc two-stroke gasoline engine giving the vehicle a purported top speed of 9 mph (National Motor Museum Trust Limited 2010).

The use of IC engines for propulsion grew and still dominates the road transport market. There are many reasons for this including:

I. high fuel energy density giving extended range;
II. high engine specific powers and fuel economy;
III. relative low cost of manufacture and ownership;
IV. reliability and robustness;
V. fuel distribution infrastructure;
VI. ease of fuel storage and handling.

Each of the reasons given above will now be discussed in more detail as Turbo-Discharging can be beneficial to specific power and fuel consumption, but its implementation must not be detrimental to, for example, engine reliability and robustness.

I. High Fuel Energy Density

Fuels such as gasoline, diesel and natural gas have high energy per unit mass compared to other methods of storing energy. Table 1-1 gives a summary of fuels and other forms of energy storage.

Fuel Type	Energy density by mass
	MJ/kg
Pure Uranium-235	$82x10^{6}$
Hydrogen	120
Natural Gas	45
Gasoline	44
Diesel	42.5
Coal	32.5
Lithium ion (Li-ion) battery	$72\ x10^{-3}$
Nickel Metal Hydride (NiMH) battery	$4\ x10^{-3}$
Lead Acid battery	$1.4\ x10^{-3}$

Table 1-1 – Energy densities by mass of different energy storage methods (Boyle *et al* 2003, Heywood 1988)

High energy density fuels are desirable since, for a fixed energy conversion efficiency, they allow a vehicle to travel further when carrying a given mass of fuel.

It can be seen that the difference in energy density between fossil fuels and electric batteries is significant. For example, 20 kg of Gasoline contain over 60 times more energy than a Lithium-Ion (Li-ion) battery of the same mass. Internal combustion engines are less efficient

converting fuel energy into crankshaft rotational energy than electric motors converting electricity to rotational energy operating at their rated speed; the useful work produced by IC engines is only about 30-40% of the total available energy (Martyr and Plint 2007), whereas permanent magnet electric motors are significantly more efficient at 96% (Sergaki 2012), (de Almeida *et al* 2011). However, even when taking into account this difference in efficiency of energy usage, the gasoline engine could still produce over 20 times as much shaft work as a Li-ion battery powered electric motor with the same mass of energy store.

Another major advantage of fossil fuels is that re-fuelling the vehicle takes only a matter of minutes as opposed to charging an electric vehicle which, depending on the facilities available, can take from several hours to over-night for a full recharge. For example, the Nissan Leaf with a battery of approximately 24 kWh takes 7 hours to fully charge from a domestic source in Europe or the US (Ikezoe *et al* 2012). This is could be an inconvenience when trying to complete a journey greater than the range of the vehicle on a single charge.

Batteries do offer some advantages such as the ability to capture energy that would otherwise be lost. An example of this is regenerative braking, where during the process of braking the kinetic energy of the vehicle is recovered by a generator which charges the batteries, allowing the energy to be re-used to propel the vehicle. This system amongst others has led to the interest in hybrid and full electric vehicles, with the former becoming increasingly popular through vehicles such as the Toyota Prius and the Honda Insight which use regenerative braking systems to help increase the overall efficiency of the vehicle (Uehara *et al* 2012).

II. High Specific Powers and Fuel Economy

Figure 1-1 shows a graph of specific energy vs specific power for leading electric vehicle technology and internal combustion engines. The electrical system includes the mass of the energy store and a nominal electric motor mass of 80 kg. The internal combustion engine systems include only the engine and mass of fuel. For all systems the drivetrain is excluded. As explained previously, it can be seen that the specific energy is an order of magnitude higher to most battery technology; this is based on the mass of the vehicle power and drivetrain and the mass of fuel the vehicle carries.

The specific power of IC engines is significantly better than most of the electric vehicle technologies. It should be noted that the best Li-ion battery shown has not been used in a

vehicle (Alamgir and Sastry 2008), and ultracapacitors are only used in conjunction with other energy sources due to their very low specific energy (Miller *et al* 2007).

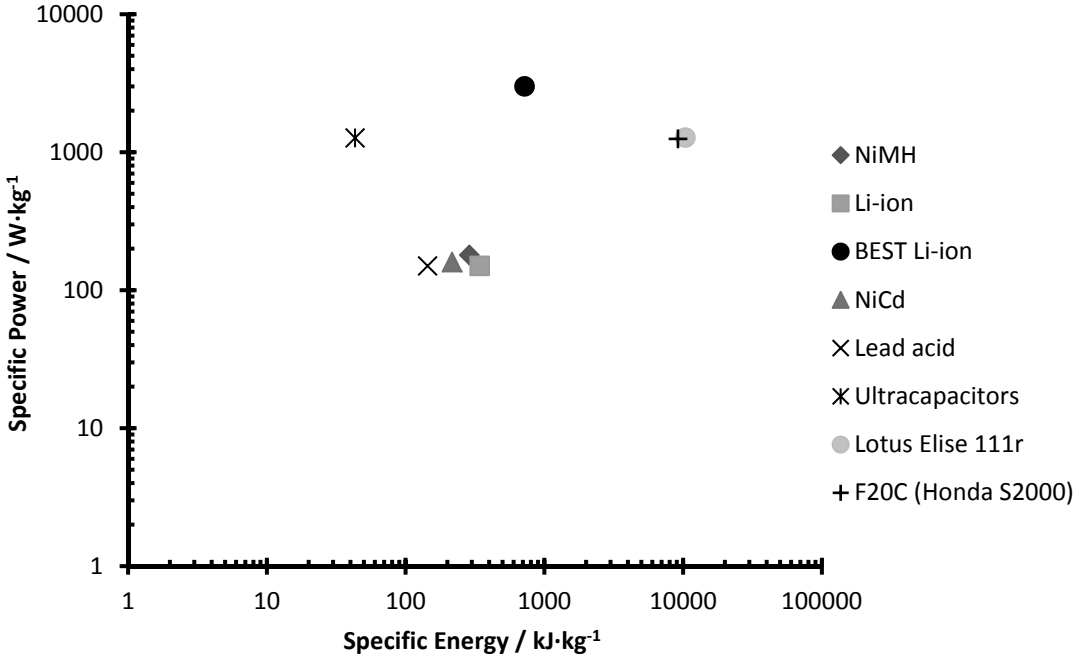

Figure 1-1 - Comparison of Specific Power vs Specific Energy for a number of propulsion systems

The IC engine therefore still exceeds the specific powers offered by realistic electric vehicle alternatives. This specific power helps lead to increased fuel economy; a lower mass of powertrain reduces overall vehicle mass, reducing rolling resistance and therefore requiring less power to maintain the same velocity. Furthermore, vehicle inertia is reduced, which in turn reduces the energy required to accelerate the vehicle. This is especially important with current drive-cycle based emissions legislation.

III. Use of Low Cost Materials

Only one out of the four strokes of the Otto cycle is at high temperature. For the other three quarters of the engine cycle the cylinder contents are at a comparatively low temperature, giving the heat transferred to the cylinder walls time to dissipate. This time for heat dissipation means that expensive, rare earth materials can be avoided and more common lower cost materials and their associated manufacturing processes can be used.

In comparison, electric and fuel cell vehicles require the use of more expensive, scarcer materials. For example, most electric vehicles now use lithium-ion batteries such as the Nissan Leaf (Ikezoe *et al* 2012)and GM Volt; the cost of lithium batteries is four times that of a lead

acid battery (Buchmann 2001). Furthermore, the 2010 cost of the battery and motor are shown as $22/kW + $700/kWh + $680, and $21.7/kW + $425 respectively, compared to that of an IC engine at $14.5/kw + $531 (Brooker *et al* 2010). Thus, for 60 kW of motive power, an IC engine costs ~$2700 less than an electric vehicle powertrain (assuming a battery discharge rate of 0.5 kWh).

IV. Reliability and Robustness

IC engines have been developed for over 120 years and in that time have become a well-established technology. Components have been developed and optimised to a point that they are robust, reliable and are becoming increasingly inexpensive; the latter mainly due to advanced mass production techniques.

Batteries as a competing technology to IC engines are able to operate over a comparatively small temperature range, and even within these limits their operating characteristics can deteriorate significantly. For example, if a Nickel Metal Hydride (NiMH) battery is discharged at 30°C the usable life reduces to 80% of that at 20°C; at 40°C this further reduces to 60%. At low temperature the battery chemistry ceases to function correctly. The absolute limit for NiMH batteries is -20°C, below this the battery will not discharge (Buchmann 2001). A battery's ability to accept charge is similarly affected at extreme temperatures.

IC engines are more forgiving to ambient conditions. A gasoline engine rejects ~30% of the fuel energy to the engine coolant as heat (Martyr and Plint 2007); this allows the engine to operate in cold conditions as it is self heating, assuming that it is possible to start the engine in the first place. This lower temperature limit is governed primarily by the viscosity of the oil and the freezing point of engine coolant and fuel.

High temperature operation of an IC engine is limited by the heat produced by combustion and the ability of the cylinder head, valve, piston and block materials to withstand this, and the ability of the engine cooling system to reject this heat. Owing to the fact IC engines have to operate over a wide range of load conditions, the cooling system is designed to cope with a maximum load at vehicle rated speed for a maximum ambient temperature. Thus, as the ambient temperature increases the maximum load permitted decreases as the cooling system becomes insufficient.

V. Practicality of Fuel Distribution Network

Fuel distribution is a significant concern for any fuel other than those which are already used and widely distributed. For example, there would be substantial cost in implementing a hydrogen storage and distribution network for use with polymer electrolyte membrane (PEM) fuel cells or other hydrogen powered vehicles.

It could be argued that the distribution network for electricity already exists as almost every home in the developed world has an electrical power supply. However, if every commuter was to purchase an electric vehicle to travel to and from their workplace, a large proportion would return home and plug their vehicles in at the same time. This would soon overload the current electrical distribution network. It could also be argued that the current electricity distribution network could not support charging vehicles in the manner which is required by the consumer (Berkheimer *et al* 2014).

For example, the Tesla Roadster claims to be able to charge to full capacity in 4 hours. However, this is charging at 70 Amps from a 90 Amp supply. Not all homes in the United Kingdom have a main fuse to the house which would allow charging at this current, not taking into account the ability to use any other piece of electrical equipment at the same time as charging. For these reasons, IC engines will remain the prime mover for the foreseeable future.

VI. The Ease of Fuel Storage and Handling

Most liquid fuels are comparatively easy to store compared with some of the other options presented above. By way of an example, storing gaseous fuels requires either high pressure or low temperature storage conditions, which are expensive to engineer and provide, whereas diesel fuel is commonly kept on farms throughout the United Kingdom in relatively inexpensive plastic containers. Until the electricity distribution grid is capable of storing and supplying energy in a similar manner to the supply of liquid fuels it is unlikely to become prevalent as a propulsion method.

1.2 Emissions and Climate Change

Although the core technology of IC engines is well developed there are still significant opportunities to improve their performance and reduce their negative impact on our local and global environment. Products of combustion can be harmful to the environment and to humans, including those from gasoline and diesel fuels. During the infancy of the IC engine there were no laws governing the levels of pollutants generated. California and the US were the first to introduce emissions legislation in the late 1960s with the Californian Air Resources Board (CARB), largely due to the photochemical smog over Los Angeles that was generated by nitrogen oxides (NO_x) produced largely by IC engines. Since that time legislation regarding exhaust gas emissions from IC engines has become increasingly stringent.

The vast majority of modern passenger car gasoline and diesel engines now use catalytic converters to control the emission of carbon monoxide (CO), NO_x and hydrocarbons (HC). The use of particulate filters in the exhausts of diesel engines is becoming increasingly common, and the use of cooled EGR for controlling NO_x is common for diesel engines, and is becoming increasingly common in gasoline engines. Recently, Selective Catalytic Reduction (SCR) systems are being employed on diesel engines to further reduce NO_x emissions. Applications of technologies such as Turbo-Discharging must not prevent application of established emissions after-treatment technologies.

In the past decade there has been growing interest in climate change, and it is believed that the carbon dioxide (CO_2) produced by passenger vehicles is having a significant negative impact on the environment. In the United Kingdom since March 2005 the Vehicle Excise Duty (VED), or road tax, paid by the consumer is charged according to the levels of CO_2 emitted from the vehicle when operating over the New European Drive Cycle (NEDC). From 2015 all manufacturers will also be charged if the average CO_2 produced by their fleet is greater than their target. This will be done on a sliding scale such that if they are more than 3 $g \cdot km^{-1}$ over the limit they will pay €95 per excess gram (g) per km per car, and lesser transgressions charged between €5-25 (ACEA 2010).

Data from government and other agencies has shown that the amount of CO_2 emitted from the UK passenger car fleet is continuously decreasing, down to 68.7 million tons of CO_2 in 2007 from 72.2 million tons of CO_2 in 1997 (SMMT 2010). This is largely due to the efforts of

manufacturers making vehicles more fuel efficient, and thus producing less CO_2 through less fuel being burned.

Many technologies have been employed to increase fuel efficiency. These technologies are wide and varied, ranging from improvements in materials allowing the use of less viscous oil reducing frictional losses to the introduction of fully variable valve train for more efficient engine load control.

One technology being applied to both compression and spark ignition engines is that of pressure charging – most commonly achieved with a turbocharger. The combination of turbocharging and engine downsizing, whilst retaining their peak load capability, is becoming common in the majority of internal combustion engines. This will now be explored in more detail.

1.3 Pressure charging the Internal Combustion Engine

One particular technique that has helped to improve the fuel economy and therefore reduce CO_2 emissions of the internal combustion engine is that of increased charge density. This is generally termed pressure charging and there are two common methods of pressure charging the IC engine.

The first method is to use a mechanically-driven supercharger, used to increase the mass of the contents, or charge, of the cylinder per cycle in an internal combustion engine (Baines 2005).

A supercharger extracts work from the crankshaft, which is then used to compress the intake air. Increasing the density of the intake air allows more fuel to be injected and burned for a fixed air-fuel ratio, allowing the engine to generate more useful work. However, the supercharger uses some of the useful work produced by the engine and therefore tend not to be used when an increase in engine efficiency is required.

A further issue affecting some superchargers is the disparity between the speed at which they need to rotate to compress the air and the speed of rotation of the engine. One example is the centrifugal compressor; the size of compressor for the mass of air required by the engine is relatively small, but the speed of rotation required is over an order of magnitude higher. To

achieve this high speed of rotation requires a gear set, introducing an extra inefficiency in the system. Positive displacement superchargers such as the roots type spin slower than a centrifugal compressor, but still faster than an IC engine.

The second widely used method of pressure charging is turbocharging which utilises energy that would otherwise be wasted in the exhaust to provide power to a turbine which drives a compressor via a shaft to achieve the same pressure charging effect as a supercharger. It too was initially used for increasing the rated power of engines, however, more recently it has been seen as an opportunity or an enabling technology to increase the efficiency of the IC engine.

To achieve comparable power densities to engines powered by other fuels, diesel fuelled engines require turbocharging, reflected by the fact that in 1999 more than 80% of diesel fuelled passenger car engines were turbocharged. This has now increased to nearly 100%. The diesel engine has an inherent lean air-fuel ratio operation at rated torque due to emissions limits; a denser charge air allows for more fuel to be burned or for a more complete burn of the fuel. Compression ignition engines do not suffer from knock as can occur in spark ignition (SI) engines, so boost pressures can be higher than those in gasoline engines and these higher boost pressures are sometimes required when using high levels of exhaust gas recirculation (EGR) to drive the same mass of air into the cylinder.

The use of turbocharging in gasoline engines is more limited due to knock (the uncontrolled auto ignition of the charge mixture) and the wider engine speed range. However, with advances in engine materials and control technologies to minimise the propensity to knock and growing pressure to increase fuel economy, turbocharging gasoline engines is gaining significant popularity. Most manufacturers are now developing and marketing turbocharged downsized gasoline engines.

The aforementioned limits in turbocharging gasoline engines have given rise to an opportunity for a new turbocharging technology which will be the subject of this work, called Turbo-Discharging. This concept uses exhaust gas energy transferred from a turbine to a compressor situated downstream in the exhaust system. Through the application of a divided exhaust event the cylinder is exposed to a depressurisation generated by the compressor. This technology can increase the fuel conversion efficiency of both non-pressure charged and turbocharged IC engines, whilst offering significant secondary benefits which may lead to even

further increases in efficiency. This makes it an important research opportunity given increasing fuel costs and tightening emissions legislation.

1.4 Thesis Aim and Objectives

The overall aim of this research is to study the impact and potential of Turbo-Discharging, a novel exhaust system technology offering potential benefits in fuel economy and therefore emissions of IC engines. As an entirely new concept, anything contained within this thesis pertaining to the Turbo-Discharging system is considered to be novel.

More specifically, the major objectives of the research reported in this thesis were to:

1. Study, optimise and evaluate Turbo-Discharging as a technology for fuel economy improvements with respect to valve events, manifold design and turbocharger specification;

2. Study the thermodynamic cycle characteristics of Turbo-Discharging to quantify maximum possible benefits and understand key energy flows within the system;

3. Quantify the effect of Turbo-Discharging on the combustion process with specific regard to cylinder residual gas fraction. Identify how Turbo-Discharging may result in an increase in knock resistance;

4. Investigate the impact of valving strategies, particularly at high engine speed and load (i.e. high flow condition). Recommend and evaluate strategies to maximise system effectiveness in this condition.

1.5 Thesis Overview

Chapter 1 of this thesis has discussed the context as to where a new technology such as Turbo-Discharging could add value. It has also identified the aim and objectives of this research, and will continue to detail which publications have arisen as a result of this work and then identify the contribution to knowledge arising.

Chapter 2 discusses in detail how air systems technology can improve fuel efficiency, identifying the most significant recent developments and highlighting their benefits and drawbacks. A conceptual description of Turbo-Discharging is then given.

Chapter 3 details the creation of a thermodynamic Turbo-Discharging model before using the model to define performance limits of a Turbo-Discharging system and identify performance critical parameters. This provides a basis of comparison for the further modelling and experimental work.

Chapter 4 provides details on the baseline engine test and measurement methods used throughout this research.

Chapter 5 describes the construction and calibration of the One-Dimensional (1-D) gas dynamics model of the naturally aspirated baseline engine. It then describes how the model was modified to include a Turbo-Discharging system.

Chapter 6 gives details on the design and fabrication of the experimental Turbo-Discharging system, and associated hardware to support its operation.

Chapter 7 describes how the 1-D Turbo-Discharging model was calibrated and validated to data gathered from the experimental engine test. It then investigates the modelled energy flows, and identifies variables the primary benefit of Turbo-Discharging is sensitive to.

Chapter 8 investigates two main secondary benefits of Turbo-Discharging both through experimental investigation and modelling. The impact of reduced residual gas fraction and increased charge momentum are shown to arise from Turbo-Discharging, and the benefits to engine fuel efficiency and performance are quantified.

Chapter 9 explores how the 1-D model could be modified by removing constraints imposed for the experimental rig and gives direction on the achievable benefits of Turbo-Discharging on a base naturally aspirated gasoline passenger car engine.

Chapter 10 presents the major conclusions of the research work presented here, and provides recommendations for further work.

1.6 Publications Arising

The following papers have been published as a result of this research:

Williams, A., Baker, A., and Garner, C., "Turbo-Discharging: Predicted Improvements in Engine Fuel Economy and Performance", 2011, SAE Technical Paper 2011-01-0371

Williams, A., Baker, A., Vijayakumar, R., and Garner, C., "Turbo-Discharging for Improved Torque and Fuel Economy", 2012, *Institution of Mechanical Engineers – 10th International Conference on Turbochargers and Turbocharging,* p 15-23, 2012

Williams, A., Baker, A., Vijayakumar, R., and Garner, C., "Turbo-Discharging Turbocharged Internal Combustion Engines", *Proceedings of the Institution of Mechanical Engineers Part D, Journal of Automobile Engineering,* v227, n 1, p 52-65, January 2013

1.7 Contribution to Knowledge

The work presented in this thesis is the first work to have thoroughly examined the Turbo-Discharging concept. This has generated the following novel contributions to the body of knowledge:

1. For the first time the behaviour of a Turbo-Discharging system on an internal combustion engine has been shown experimentally.
2. The maximum potential thermodynamic benefit of a Turbo-Discharging system has been quantified for some common engine arrangements.
3. A method of measuring the performance of a Turbo-Discharging system compared to a thermodynamic ideal has been defined.
4. The effect of depressurisation from an exhaust driven compressor on an IC engine has been quantified and factors influencing the depressurisation achieved have been identified.
5. The effect of exhaust pressure, including depressurisation, on knock margin has been explored.
6. An optimisation study of a Turbo-Discharging system has been completed, identifying areas of focus for future studies.

1.8 Closing Comments

The case for the continued use of the IC engine has been made, and justification for further improvement has been shown. A path of potential development has been highlighted in the form of pressure charging, which will now be investigated along with other fuel efficient engine technologies relevant to this research to understand the technologies that Turbo-Discharging will work with or compete against.

2. Air Systems and Fuel Saving

This chapter describes how air system technologies are being used to improve the fuel conversion efficiency of internal combustion engines. It discusses the most recent developments in this area and describes how the proposed Turbo-Discharging concept offers an alternative or additional approach to these. Finally the Turbo-Discharging concept will be introduced in detail.

The purpose of this chapter is to make clear the value of this research and explain how the concept presented is novel, technologically plausible and worthwhile investigating.

2.1 Improving Engine Fuel Efficiency

To improve engine thermal efficiency it is first important to define energy flows in an internal combustion engine. Vehicle thermal efficiency describes fuel energy that is transferred to the crankshaft, the desired output from the engine system. Typical values for production vehicle thermal efficiency generally lie between 30-37%, and of the remaining fuel energy 30% is rejected to the engine coolant, 7% radiated and convected to ambient and a further 30% rejected in the exhaust (Martyr and Plint 2007). However, these are optimum steady state values which do not accurately reflect how engines are actually used in vehicles where they operate over a range of operating conditions, varying in both speed and load.

Some more recent studies have analysed engine thermal efficiency over drive cycles which show a much lower percentage of useful work is extracted from the fuel energy. Conklin and Szybist (2010) show that for a modern turbocharged engine performing a Federal Test Protocol (FTP)-75 engine cycle only 10.4% of the fuel energy is converted to useful work. 61.9%, the majority of fuel energy is lost to friction, coolant and other losses, whilst 27.7% of fuel energy is transferred into thermal energy in the exhaust gas. This is shown in Figure 2-1.

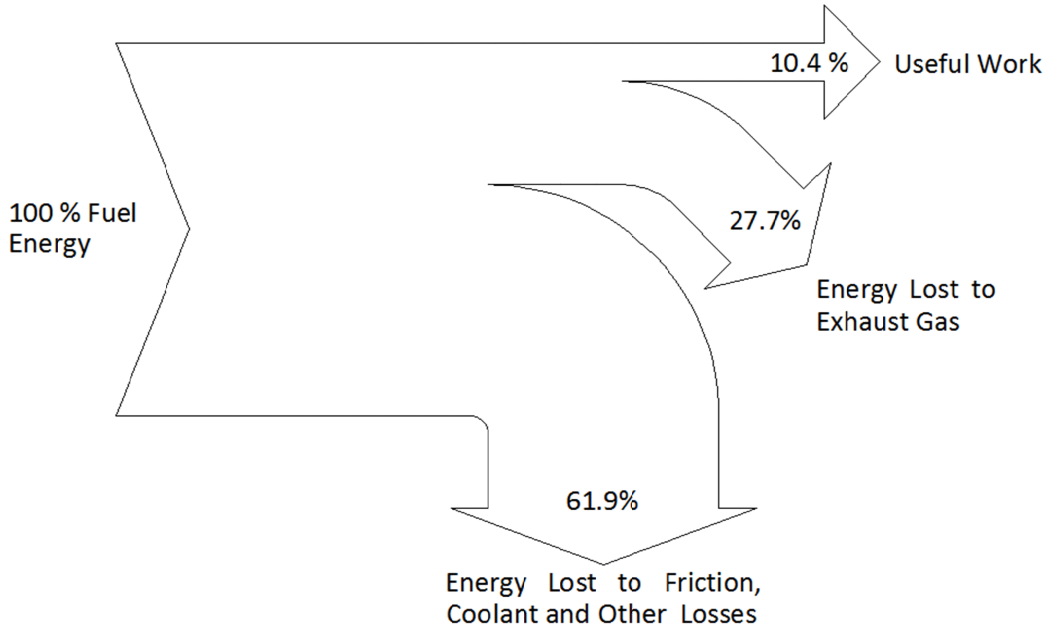

Figure 2-1 - Sankey diagram illustrating typical fuel energy usage in a gasoline engine from (Conklin and Szybist 2010)

Conklin goes on to show from a second law analysis that 81.9% of the fuel exergy, the energy possible to extract from the fuel with ideal processes with respect to a reference condition, is lost through irreversibilities, friction, coolant and other losses, whilst 9.7% goes to brake work and 8.4% is lost through the exhaust.

It is therefore important to eliminate, or minimise any irreversibilities through friction, energy transfer to coolant and any other losses. There is substantial ongoing work into reducing these losses, but this work will focus on the energy available in the exhaust gas.

Nearly the same quantity of fuel exergy used for brake work is available as thermal energy in the exhaust gas over the FTP-75 drive cycle. Recovering a fraction of this energy could therefore significantly improve fuel economy. As such there has been an increasing amount of research into utilising this energy in the past decade.

The amount of energy contained in the exhaust gas is dependent on many factors. It is often impossible for the cylinder to fully expand the combustion gases due to the fixed geometry nature of engines. Commonly the engine expansion ratio is equal (and fixed) to that of the compression ratio. With a fixed expansion ratio it is not possible to fully expand the exhaust gas if the pressure at the start of the expansion stroke is higher than that at the end of the compression stroke.

Efforts have been made to further expand the burned gases in engines through variable valve timing and engine cycles incorporating Early Intake Valve Closing (EIVC) or Late Intake Valve Opening (LIVO), such as the miller cycle. Both of these strategies reduce the compression ratio by limiting the amount of air induced into the cylinder. Reducing the compression ratio reduces the pressure in the cylinder before the exhaust stroke which allows for a more complete expansion of the combustion gases. This results in a reduced amount of energy in the exhaust gas and increased engine thermal efficiency. However, these systems still cannot fully expand the burned gases and therefore energy can still be extracted.

One of the most significant factors that makes extracting energy from the exhaust gases attractive is their high temperature. The large temperature differential between the exhaust gas and the ambient leads to a large amount of energy availability, similar in quantity to that of the fuel energy that does positive work on the crankshaft as mentioned previously. High mass flow rates can also aid the energy extraction process.

However, almost any device placed in the exhaust to recover energy will cause a restriction and thus raise the pressure the engine is working against during the exhaust stroke (commonly referred to as back pressure). This increases the work required from the crankshaft to forcibly remove the gases from the cylinder, decreasing the fuel efficiency of the engine. The device in the exhaust must therefore recover and transfer as much energy as this to the crankshaft for the system to have no effect on the engine, or more energy to improve fuel efficiency.

In conclusion, there is significant value in and potential for recovering energy from exhaust gases. The following section will discuss different approaches to recover this energy.

2.2 Recovering Exhaust Gas Energy

There are various methods which have been developed to extract energy from the exhaust gas of IC engines. These will now be discussed.

2.2.1 Turbines

One of the most established means of recovering energy from the exhaust gas of an IC engine is to use a turbine. The reciprocating internal combustion engine was first combined with a rotating turbomachine by Alfred Büchi in 1905 in the form of a turbocharger (Baines 2005).

A turbine expands the exhaust gas passing through it, converting a portion of the enthalpy in the exhaust gas into rotor work. The exhaust gas is guided into the turbine such that it exerts a tangential force on the rotor. This manifests as a reduction in the angular momentum of the exhaust gas. This can be calculated using Euler's turbine equation;

$$\frac{\dot{W}}{\dot{m}} = U_1 \cdot v_{W1} - U_2 \cdot v_{W2} \qquad \textbf{2-1}$$

where $\dot{W}$ is the work output of the turbine, $\dot{m}$ is the mass flow rate of exhaust through the turbine, U_1 and U_2 are the inlet and outlet blade speeds respectively, and v_{W1} and v_{W2} are the tangential (to the axis of rotation) exhaust gas velocities. It can be seen that the power output of the turbine is a function of the mass flow, tangential gas velocities and blade speeds (hence rotational speed) only. There are other equations for estimating turbine work using thermodynamic parameters to describe the change in energy of the gas across the turbine. These are commonly used as it is difficult to measure the velocity components of the flow entering and exiting a turbine.

The exhaust flow from an internal combustion engine is highly pulsating. This is a significantly different environment to turbomachinery such as gas turbines where there is constant combustion which provides a comparatively steady flow of gas.

Each exhaust event from one cylinder of an IC engine commonly contains two distinct periods:

1. *Blowdown pulse.* This occurs immediately after exhaust valve opening and is caused by the burned gas at high pressure expanding from the cylinder into the exhaust. The magnitude of the blowdown event varies with engine speed and load.

2. *Displacement pulse.* After the burned gases have expanded to exhaust manifold pressure the remaining gas in the cylinder needs to be displaced by the piston which does so by travelling from BDC (Bottom Dead Centre) to TDC (Top Dead Centre). This part of the exhaust stroke requires work from the crankshaft, and is a major source of exhaust pumping work as the gas is forced through the exhaust valves.

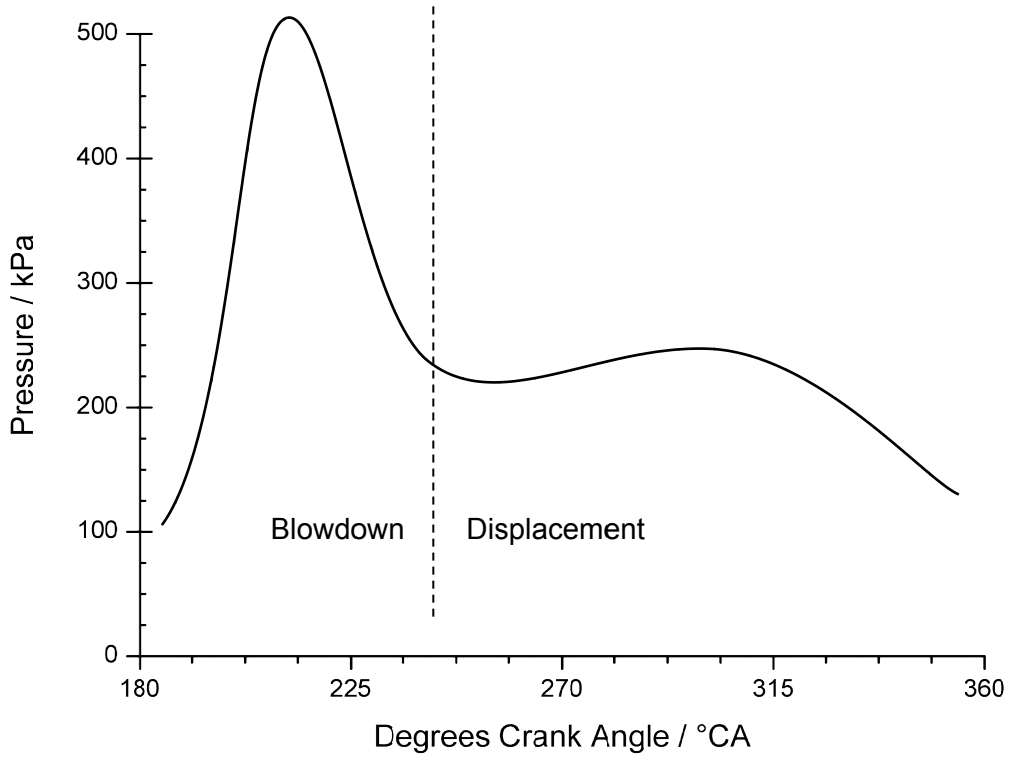

Figure 2-2 - Example exhaust pressure pulsation highlighting the blowdown and displacement pulses

The pulsating mass flow of exhaust through the turbine means that even for a steady state engine condition the turbine operates over a range of its pressure ratio and mass flow map. This, coupled with the fact that the turbocharger has to operate over a range of exhaust mass flowrates and pressure ratios from varying engine speed and load, means that matching a turbocharger to an engine is always a compromise between performance at a single point and performance across the entire engine operating range. This will be discussed more in section 2.2.2.

Placing a turbine in the exhaust flow can have a negative effect on engine breathing. The turbine acts as a restriction, across which there is a pressure drop, thus the pressure upstream of the turbine is higher than that of the exhaust system. This means that during the

displacement pulse the piston has to do extra work by driving the exhaust gases from the cylinder and through the turbine, rather than just through the exhaust to atmospheric pressure. The effect of this is increased pumping work during the displacement part of the exhaust stroke.

Commonly radial inflow turbines are used in passenger car applications. Recent developments in turbocharger turbines include the use of mixed flow and axial turbines to reduce exhaust pumping work.

Mixed flow turbines are becoming more prevalent in their application due to the increasing requirement on turbine efficiency under pulsating conditions. Radial inflow turbines are commonly quoted as having peak efficiency at a blade speed ratio (U/C) of 0.7; however, the U/C for high pressure ratio, low speed operation will be lower than this (Lüddecke *et al* 2012). For gasoline engines, it is desirable to sacrifice efficient energy extraction at high U/Cs to improve energy extraction at low U/Cs as there is generally a surplus of energy at high U/Cs, whereas turbine energy is the limitation for low U/C operation.

Honeywell turbo technologies have introduced their dual boost turbocharger which incorporates an axial turbine, as well as parallel back-to-back compressor wheels (Lei *et al* 2012). The point of peak efficiency for the axial turbine is achieved at a lower U/C than that of a radial turbine. Similarly to mixed flow turbines, this enables the axial turbine to operate more effectively during transients and pulsed flows, where low U/C's are frequently encountered. Furthermore, reductions in shaft inertia are possible as the hub of the turbine wheel is closer to the axis of rotation compared to a radial or mixed flow turbine.

2.2.2 Pulse and Constant Pressure Turbine Operation

Pulse and constant pressure turbocharging are two philosophies on the best method to manage extraction of exhaust gas energy using a turbine.

Constant pressure turbocharging necessitates the use of a large volume manifold. The exhaust gas from the engine expands into this large volume, ideally completely removing the gas flow pulsations. This constant pressure gas then flows through the turbine, allowing for better matching for a given steady state condition allowing the turbine to operate at a higher efficiency. For a steady state engine condition the turbine will operate at a single mass flow and pressure ratio, allowing optimisation of turbine sizing for that operating condition.

Pulse turbocharging requires the use of a small manifold to maintain as much kinetic energy in the exhaust gas as possible. This means there is more energy available to the turbine, but the pulsating flow means the efficiency oscillates around its optimum which can give a lower overall efficiency. The difference in efficiency is shown in Figure 2-3.

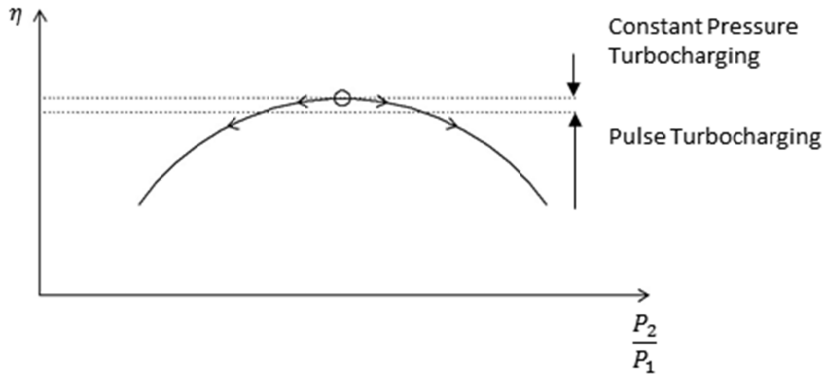

Figure 2-3 - Efficiencies of Constant Pressure and Pulse Turbocharging

It is commonly believed that pulse turbocharging is the better method of the two as more of the exhaust gas energy is maintained, rather than being wasted in the expansion of gas in the large volume manifold required for constant pressure turbocharging. Even though the turbine is operating at a lower efficiency, the fact there is more energy in the gas to extract means the net work to the turbine is higher. Another benefit of this system is that it is more compact, which allows for a smaller powertrain package giving the vehicle designers more versatility with regard to performance, safety and cooling design.

2.2.3 Wastegates and Variable Geometry Turbines

It is sometimes desirable to control the power extracted by a turbine, whether it is to provide control over the device it is connected to or in some cases to reduce back pressure on an engine to improve fuel economy.

It has already been identified that for a steady state engine condition the turbine is operating over a range of mass flows and pressure ratios. Passenger car engines very rarely operate in a steady state condition; in fact they operate over a wide speed and load range for which the exhaust gas conditions vary substantially. Therefore turbines are generally sized to extract energy efficiently over as much of the speed and load map as possible.

One method of maximising the engine speed and load range a turbine functions over is to use a smaller turbine rather than a turbine sized to produce maximum boost at high engine rpm. This smaller turbine will extract more power than is required at a lower engine speed, as shown as curve 2 in Figure 2-4, as opposed to the large turbine of curve 1.

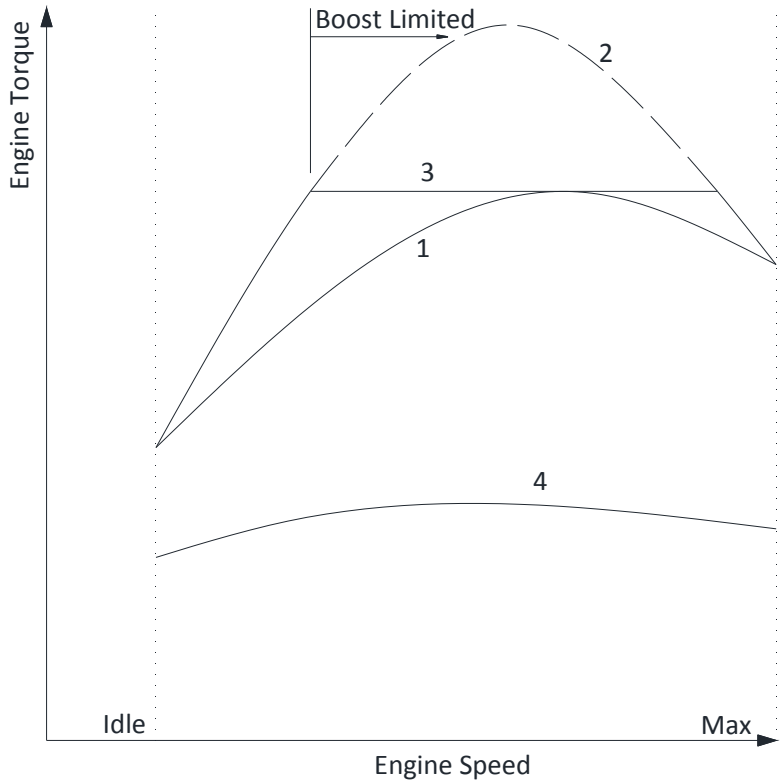

Figure 2-4 - Torque-Speed characteristics for a turbocharged engine application modified from (Baines 2005)

Using a smaller turbine will allow the turbocharger to achieve too high a pressure ratio across the compressor across some of the engine speed range. It is therefore necessary to employ a

device such as a wastegate to limit the energy recovered by the turbine by bypassing some of the exhaust gas around the turbine.

One alternative technology to wastegates that is being implemented on almost all passenger car compression ignition engines and on some spark ignition engines is that of Variable Geometry Turbines (VGTs). There are several variations on these, but none of them actually vary the turbine wheel or blade geometry; they simply affect how the exhaust gas enters the turbine.

The most common type is a Variable Nozzle Turbine (VNT), where pivoting inlet guide vanes rotate to adjust the angle of incidence of the gas onto the turbine. This system has the ability to increase the energy extracted by the turbine at lower exhaust mass flow rates to aid transient response and to minimise the low speed torque deficit commonly observed in turbocharged engines. As the vanes rotate to a more closed position the gas enters the turbine at a higher angle of incidence, but is also accelerated through the narrowed flow area of the guide vanes. This can be shown using Euler's turbine equation 2-1. For constant mass flow and blade speeds, increasing the tangential velocity of the exhaust gas entering the turbine will increase the power extracted by the turbine.

However, the energy to accelerate the gas through the vanes is partially generated by the piston, and manifests as an increase in engine pumping work. It is still beneficial to do this as it aids transient response, allowing the turbocharger to increase in speed and to reach a more efficient operating condition faster.

The variable guide vanes can also be used for limiting the power extracted by the turbine and transferred to a compressor or other device. This is achieved by the guide vanes opening, rotating the gas through an angle such that it enters the turbine at a lower angle of incidence, reducing the tangential gas velocity and thus the energy extracted. This has a significant benefit over that of a wastegated turbine in that by doing this the pressure drop over the turbine reduces. In a wastegated turbine the wastegate opens and exhaust gas mass flow is bypassed, but to extract the same power from the turbine the pressure ratio must remain constant. Thus the engine is still exposed to the same back pressure and thus the same pumping work.

Currently the use of VGTs has largely been limited to passenger or small commercial vehicle compression ignition engines. This is due to material cost and high temperature capability; the

lower exhaust temperatures experienced in a compression ignition engine allow the use of low cost materials to be used for the VGT mechanism. However, for SI gasoline engines with higher exhaust temperatures more expensive materials such as Inconel 917 must be used, significantly increasing the cost of the unit such that the increase in performance cannot be justified.

2.2.4 Alternate Forms of Exhaust Gas Energy Extraction

There are two significant alternate technologies currently considered in research for extracting energy from the exhaust gas. These are thermoelectric devices and Rankine cycle energy recovery systems.

Thermo-Electric Generators (TEGs) utilise the Seebeck effect to generate electrical energy, where two dissimilar metals are joined and energy is generated when there is a temperature differential between the two metals. These junctions are then joined together in an array to form a thermopile. The resulting energy can be used to offset the power required by the alternator, reducing parasitic losses and increasing the amount of useful work output of the engine.

If the electrical energy is proportional to the transfer of heat through the device, then it is important to maximise both the high temperature on the exhaust side and the low temperature on the ambient side. However, common material thermal limits for the hot side of TEGs are in the region of 230°C (Martins *et al* 2011), limiting the potential conversion efficiency by reducing the potential heat transfer through the device.

To maximise the high temperature on the device, it is important to transfer as much thermal energy from the exhaust gas into the device as possible. Common methods of achieving this involve increasing the surface area available for heat transfer from the gas and to increase turbulence of the gas across the surface. The drawback of both of these methods is that they will cause a restriction in the exhaust, increasing engine back pressure and thus pumping work. This will directly detract from the benefit offered by the device, such that to achieve a fuel efficiency benefit the device must extract and transfer more energy back to the engine than the pumping work required to overcome the restriction in the exhaust.

Another drawback of the TEG is their very low energy conversion efficiency, commonly as low as 1% system efficiency, peaking at less than 10%. This leads to low total energy conversion quantities, commonly less than 1 kW (Ibrahim *et al* 2010). Mori *et al* (2009) modelled their TEG device on four US drive cycles where the output from the device was based on exhaust temperature and mass flow. The result of this was a maximum improvement in fuel economy of 0.36% with a corresponding reduction in CO_2 of 0.42%.

Rankine cycle systems for exhaust gas energy recovery use the heat energy from the exhaust to evaporate a working fluid in a Rankine cycle. This working fluid is contained within a separate circuit comprised of a pump, evaporator, turbine, condenser and adjoining pipework.

The pump provides the energy required to pressurise the liquid coolant. This requires work, which generally originates as fuel energy, detracting from the engine thermal efficiency.

From the pump, the fluid passes through the evaporator. This is a heat exchanger, transferring heat from the exhaust gas into the working fluid. The same drawbacks apply here as for TEGs; to increase the effectiveness of heat transfer the heat exchanger must cause a restriction in the exhaust, increasing back pressure and increasing pumping work.

Once the fluid has passed through the evaporator and the thermal energy has been transferred (turning the working fluid into vapour), it passes through the turbine. This expands the fluid, extracting a portion of the energy transferred to it from the exhaust gas. This work recovered is the primary benefit of the system.

Finally the fluid passes through a further heat exchanger or condenser, returning the fluid to a liquid state so it can be pumped round the system efficiently and so it can effectively absorb more thermal energy.

Teng *et al* claim a 20% improvement in rated power based on a second law analysis of a heavy duty diesel engine (Teng *et al* 2007). Ringler *et al* (2009) claim a more modest 10% improvement when travelling in top gear at a steady speed from a 1-D model and simulation on a 4 cylinder SI engine.

Weerasinghe *et al* (2010) claim for a 22% improvement in fuel economy from their modelling results of a rankine steam hybrid system even though there was only a 7.8% benefit in engine power. They argue that the reason for this is the steam hybrid system acts as a buffer; the steam allows for storage of energy which is then released slowly, enabling power to be

produced by the expander even when there is no hot exhaust from higher load conditions from the engine.

There are a number of common drawbacks with Rankine systems for recovering exhaust gas energy from passenger gar IC engine exhausts. A considerable amount of mass would be added to the vehicle due to the working fluid and the components required, unless it is integrated with a secondary cooling loop such as that for charge cooling (Teng *et al* 2007). This will also take up a significant amount of volume on the vehicle, add substantial cost and the condensing heat exchanger will increase vehicle drag. It is anticipated that vehicle manufacturers will find this increase in complexity and cost unattractive (Hussain *et al* 2009). Weerasinghe *et al* (2010) also state that typically secondary fluid power systems are unattractive to manufacturers, but argue that the level of complexity is similar to that of an air conditioning circuit, and that a rankine cycle system would add only 20 kg more mass than a turbo-compounding system.

Currently the author is not aware of any rankine cycle systems that have been used on a production passenger vehicle. It is likely that the increase in complexity, package volume, mass and cost are currently restricting their use, even though the claimed benefits are comparatively higher than those of competing systems. As such, turbines for extracting energy from the exhaust gas are considered the most effective and appropriate technology for passenger car IC engines.

2.3 Turbocharging

Turbocharging is a common method of using work extracted by a turbine in the exhaust flow to improve the performance of an internal combustion engine. The turbine is connected to a radial compressor to compress the intake charge air. The primary purpose of this is to increase the charge air density such that more air is trapped in the cylinder so more fuel can be burned, increasing the power output for a given displacement.

There are also a number of secondary benefits which Table 2-1 summarises along with challenges associated with using a turbocharger.

Benefits	Challenges
1. More engine power through increased air density meaning more fuel can be burned.	1. Exhaust pumping work can be increased due to the exhaust restriction of the turbine.
2. A more complete burn can be achieved in compression ignition engines from the increased mass of air in the cylinder.	2. Turbocharged spark ignited engines can have a higher propensity to knock due to the increased charge pressure.
3. Positive pumping work is possible during the intake stroke in compression ignition engines and at WOT.	3. Complexity is increased from turbocharger cooling, packaging and thermal management.
4. Higher charge pressure can allow for higher levels of cooled EGR to be used.	4. Increased time to catalyst light off due to increased thermal mass of exhaust system.
5. Scavenging can be improved through an improved pressure ratio between intake and exhaust manifolds.	5. Extracting energy from the exhaust gas may leave less energy for energy recovery systems such as thermoelectric or rankine cycle and after-treatment systems.

Table 2-1 – Benefits and challenges of turbocharging

These benefits and challenges will now be discussed in more detail.

2.3.1 Benefits

1. More engine power through increased air density meaning more fuel can be burned

The power produced by an IC engine can be shown to be

$$\dot{W} = \eta_f \cdot \dot{m}_f \cdot Q_{HV} \quad \textbf{2-2}$$

where $\dot{W}$ is the power produced by the engine, η_f is the fuel conversion efficiency of the engine, $\dot{m}_f$ is the mass of fuel inducted per unit time and Q_{HV} is the heating value of the fuel. This equation can be expanded using the following two equations:

$$\dot{m}_f = \dot{m}_a \cdot [F/A] \quad \textbf{2-3}$$

where $\dot{m}_a$ is the mass of air inducted into the cylinder and $[F/A]$ is the mass based ratio of fuel to air,

$$\dot{m}_a = \rho_i \cdot \eta_{vol} \cdot V_{swept} \cdot {}^{N}/_{2} \quad \textbf{2-4}$$

where ρ_i is the density of the charge, η_{vol} is the volumetric efficiency of the engine, V_{swept} is the swept volume of the cylinder and ${}^{N}/_{2}$ is the engine crankshaft rotation speed corrected for a four stroke engine as there is only one induction stroke per two revolutions.

These equations give an equation for the power produced by an IC engine of the following form;

$$\dot{W} = \rho_i \cdot V_{swept} \cdot \eta_{vol} \cdot {}^{N}/_{2} \cdot [F/A] \cdot Q_{HV} \cdot \eta_f \quad \textbf{2-5}$$

Thus an increase in intake charge density for a fixed air to fuel ratio will give an increase in output power.

2. A more complete burn can be achieved with a more dense charge in compression ignition engines

Compression ignition engines inject fuel directly into the cylinder once the intake valve has closed. Combustion begins very shortly after injection; there is only minimal time for the fuel and air to mix, so it is common for there to be areas of high fuel/air ratio across the cylinder. Turbocharging increases the mass of air in the cylinder, giving more chance for the fuel to

react with oxygen during combustion. This helps to minimise hydrocarbon emissions and decreases the cyclic variance as mixing is less dependent on in-cylinder motion.

3. Positive pumping work is possible during the intake stroke

For a compression ignition engine, or a spark ignited engine in a wide open throttle condition, it is possible for the turbocharger to do work on the piston during the intake stroke. Naturally aspirated engines create a low pressure in the cylinder by the downward motion of the piston which draws air into the cylinder. If the intake manifold pressure is higher than that of the cylinder at Intake Valve Opening (IVO) then air will flow into the cylinder without the need for the piston to draw a low pressure. Furthermore, if the pressure above the piston is higher than that of the crankcase as it is travelling towards BDC, positive work is done on the piston.

However, this must be balanced with the extra pumping work required during the exhaust stroke when exhausting the burned gases. Turbines can cause a restriction in the exhaust and as such present the engine with increased back pressure compared to an NA engine. Depending on the efficiency of the turbocharger, the operating condition of the engine and a number of other parameters the engine thermal efficiency may increase or decrease.

4. Higher charge pressure can allow for higher levels of cooled EGR to be used

One method of controlling NO_x emissions is to use cooled EGR to reduce peak cylinder temperatures. With increasingly stringent emissions targets, manufacturers are being forced to use higher levels of EGR to further decrease NO_x.

If the mass of EGR in the cylinder increases then the mass of air in the cylinder will decrease unless the density of the air increases, increasing the demand on the boosting system. Thus, higher charge pressures are desired, and can be achieved by turbocharging.

5. Scavenging can be improved due to an improved pressure ratio between intake and exhaust manifolds

During intake and exhaust valve overlap when the piston is near TDC, a high pressure ratio between the intake and the exhaust manifolds is desirable to drive fresh charge into and displace any products of combustion from the cylinder. Poor scavenging leads to more hot residual gases remaining in the cylinder which decreases the volume available for fresh charge. These hot residuals also raise cylinder temperatures, which in spark ignition engines can increase the likelihood of knock. Increasing the intake manifold pressure will help to improve or give a positive engine scavenging pressure ratio providing the increased exhaust manifold pressure caused by the turbine is not excessive.

2.3.2 Challenges

1. Exhaust pumping work can be increased due to the exhaust restriction of the turbine

As described previously an exhaust event contains two distinct portions of gas flow; blowdown and displacement gases. By placing a turbine in the exhaust system the manifold pressure the cylinder is exhausting to is increased. This decreases the amount of gases that leave the cylinder during the blowdown pulse (assuming an ideal event where these gases are allowed to expand to the manifold pressure), leaving more gases to be displaced by the piston during the displacement pulse. Not only does the piston need to displace more gases, but it needs to drive these gases through the restriction the turbine is presenting.

This could lead to worse cylinder scavenging; however, this is generally negated by the improved scavenging through higher intake manifold pressures as mentioned previously.

2. Turbocharged spark ignition engines have a higher propensity to knock due to the increased charge pressure

A higher pressure charge in a turbocharged engine, for a fixed compression ratio, will be compressed to a higher pressure than that of a naturally aspirated engine. With increased pressure comes increased temperature, both of which will advance the onset of knock. Commonly the compression ratio of turbocharged engines is decreased to compensate for this; however, this leads to decreased combustion efficiency.

3. Complexity is increased from turbocharger cooling, packaging and thermal management

A turbocharger is generally mounted as close to the engine exhaust ports as possible for an optimised pulse turbocharging system (as discussed in section 2.2.2). However, the intake manifold is typically located on the other side of the engine. Routing pipework around the engine bay will always therefore be a compromise between performance and packaging; the best performing pipework may not be able to be packaged into a vehicle.

Turbochargers consist of a compressor connected to a turbine by a shaft, supported in the centre by a bearing housing. These bearings require lubrication, and commonly use engine oil to minimise extra complexity. The oil leaving the turbocharger is commonly highly aerated; as such the drain back to the engine must be as unrestrictive as possible. This limits placement of the turbocharger and the orientations it can operate in.

Most turbocharger systems include a charge air cooler for reducing the temperature of the intake air before it enters the cylinder. Some are air to air heat exchangers which reject heat to the ambient air, others are air to coolant heat exchangers which use a secondary coolant circuit in the vehicle with associated coolant to air heat exchangers to reject the heat to ambient. Lumsden *et al* (2009) use such a heat exchanger for a small packaging solution, but make no mention of a secondary coolant loop. Furthermore, the heat in the secondary coolant circuit must still be rejected, thus the cooling drag of the vehicle will be increased by both air to air and air to coolant heat rejection methods.

The turbocharger itself can also become significantly hot under certain operating conditions. Depending on the type of turbocharger used the oil supply for the bearings may be sufficient

to cool it otherwise a coolant supply may be required, typically the engine coolant, and this heat must then be rejected by the vehicle radiator.

Also, turbine volutes tend to have a high heat capacity and as such they retain heat for much longer than an exhaust manifold would. This can pose a problem for locating components in the engine bay, requiring modification of the under bonnet airflow and sometimes shielding of other components.

4. Increased time to catalyst light off due to the increased thermal mass of the exhaust system

Catalyst light off is the point at which the catalyst becomes hot enough to begin reacting and converting harmful combustion products into less or non-toxic gases. It is important to minimise the time taken to achieve catalyst light off for emissions testing. The New European Drive Cycle (NEDC) requires the test to be started from cold; faster catalyst light off means that the catalyst begins minimising harmful emissions earlier, reducing the total amount of emissions for that drive cycle.

Typically the exhaust gases themselves are used to heat the catalyst to light off temperature; a result of this is that most powertrains are now developed with the catalyst mounted as close to the exhaust port as possible to maximise the exhaust gas temperatures at the catalyst face.

For turbocharged engines time to catalyst light off has been longer than naturally aspirated engines due to the heat capacity of the turbine volute and sometimes the manifolds used; for example, a cast iron manifold has a substantially higher heat capacity than a tubular manifold.

One technology that has been investigated recently is that of pre-turbine catalysts. This involves placing a catalyst, or a pre-catalyst element upstream of the turbine (Konieczny *et al* 2008). Traditionally catalysts are located in the exhaust after the turbine as it is desirable to maximise turbine inlet pressure for performance, but it is argued by the authors that in the context of diesel compression ignition engines it is worthwhile making use of higher exhaust temperatures pre-turbine. However, they only make brief mention of the negative effect this has on turbine and engine performance, concentrating mainly on the emissions analysis. It would also still require a catalyst post turbine, albeit smaller and less restrictive than that commonly used.

In a similar vein, Diesel Particulate Filter (DPF) placement in compression ignition engines has been challenged, and Payri *et al* (2011) have investigated placing this and the Diesel Oxidation Catalyst upstream of the turbine. They found that the higher temperatures favour passive regeneration, but can lead to a 3.3% increase in pumping work.

5. Extracting energy from the exhaust gas leaves less energy for energy recovery systems such as thermoelectric or rankine cycle and after-treatment systems.

Whilst it is true that turbocharging removes a substantial portion of the exhaust gas energy (Carberry *et al* 2005), it can do so more efficiently than other technologies. As previously discussed thermoelectric devices need to absorb a large amount of thermal energy from the exhaust gas but then need to reject this to ambient. It will always be a concern as to what the order of energy recovery from the exhaust system should be, but this will vary depending on the total amount of energy available in the exhaust stream, packaging limitations and emissions requirements.

2.3.3 Turbocharging and Downsizing

Turbocharging and downsizing is an increasingly common method of improving the fuel efficiency of a powertrain. The term downsizing refers to decreasing the cylinder volume; the two main benefits of this are:

1. Pumping work benefit. For a comparable load condition a downsized engine operates with a more open throttle than a non-downsized equivalent. This leads to decreased pumping work on the intake stroke, and when combined with turbocharging positive work can be achieved on the intake stroke.
2. Reduced powertrain frictional losses. The smaller capacity means smaller components can be used with reduced frictional surface area.

However, reducing the cylinder volume for a fixed charge pressure will result in a lower power output. To compensate, it is necessary to pressurise the charge air, and this is commonly achieved by turbocharging.

The Mahle downsized demonstrator (Lumsden *et al* 2009) is a 1.2 L twin series turbocharged engine, designed to replace a 2.4 L V6 engine from a class C or D vehicle. This equates to a 50% downsize, which they estimated would equate to a 25-30% benefit in fuel economy, with better torque across the whole engine speed range. Careful attention had to be paid to cylinder pressure limits, but they found their demonstrator engine had sufficient durability even operating up to 35 bar BMEP.

Han *et al* (2007) show up to 17% improvement in fuel economy for a 40% downsized and turbocharged engine, whilst Shahed and Bauer (2009) state 40% downsizing with turbocharging to restore the baseline torque curve should give a 20% improvement in fuel economy. Common to all of these approaches is the inclusion of a variable valvetrain (VVT) system and Direct Injection (DI). Turner *et al* (2005) state the importance of VVT and DI systems, allowing the elimination of throttles in gasoline engines and further improving pumping work.

Further work by Turner et al (2014) on the Ultraboost project shows that 60% downsizing can result in up to a 23% reduction in tailpipe CO_2. They postulate that increasing this to 70% downsizing could lead to a further 6% reduction in CO_2.

With efficiency benefits as great as those mentioned above, this author considers that the popularity will only increase and that most, if not all, future gasoline powertrains will be downsized and turbocharged. Thus, any further developments in air systems for fuel efficiency must be compatible with turbocharging and downsizing.

2.3.4 Conclusions

As emissions legislation tightens and customer expectations increase with time more internal combustion engines are likely to include turbocharging systems for the benefits outlined in this section. However, there are some challenges in implementing turbocharging systems which may limit their introduction. Largely, these have been overcome and most passenger cars with compression ignition engines are turbocharged and an increasing number of gasoline engines are becoming downsized and turbocharged.

2.4 Turbo-Compounding

The definition of the verb to compound is to put together, combine, construct or compose (Oxford English Dictionary 2013). Turbo-Compounding refers to any turbocharger arrangement where work is taken from the turbomachine unit and is transferred by some means to the crankshaft, or offsets some loss such that crankshaft work increases. This concept originates from the work of Alfred Büchi's 1905 patent where any excess energy extracted by the turbine is transferred to the engine crankshaft through a series of linkages and a gearbox.

There are three main types of technology that turbo-compounding systems can be grouped into; Turbo-Generators, Mechanical Turbo-Compounding (MTC) and Electric Turbo-Compounding (ETC). These will now be discussed in more detail.

Turbo-Generators

More recently Turbo-Generators have been applied to engines. This is where a turbine is attached to a generator which creates electricity. This offsets the use of the vehicle alternator, improving fuel economy by 3-10% (Tennant and Walsham 1989). However, since that paper was published their use has been sporadic. Ryder and Sharp (2010) identify the reason as lack of compatibility with some emission control architectures. Furthermore, their use will likely be superseded by Electrical Turbo-Compounding as this can achieve both the function of a turbocharger and turbo-generator.

Mechanical Turbo-Compounding

Increasingly MTC systems are being investigated, such as the Superturbocharger (VanDyne 2011). This combines a turbocharger with a mechanical linkage, allowing energy transfer both to and from the crankshaft. At low engine speed, the turbocharger absorbs some of the crankshaft work, spinning the compressor faster than it is able to from just turbine power, giving improved transient response. At high engine speed and load, the linkage is able to work in the opposite manner and transfers excess energy from the turbocharger shaft to the crankshaft. The manufacturers claim 25-30% improvement in fuel economy over a naturally aspirated engine, but provide no comparison for a conventional turbocharged engine. It is the author's opinion that this system is capable of providing a better transient response than a conventional turbocharging system, but will offer only a small improvement in efficiency. Also

the complexity of the mechanical linkage will likely inhibit its appeal to automotive manufacturers.

Electric Turbo-Compound

Electric Turbo-Compound (ETC) systems comprise a turbocharger with a motor-generator attached to the shaft. At low speed electrical energy is supplied to the unit, driving the compressor to provide pressurised intake air, aiding transient response of the powertrain. At high engine speed and load, excess energy is extracted from the shaft by the generator. This could be stored in batteries as part of a mild hybrid system, or transferred via electric motor back to the vehicle crankshaft.

Zhuge *et al* (2011) optimised a system that combined a turbocharger with a VNT controlled Turbo-Generator. This produced a 4.74% benefit over US06 and 1.86% over FTP75 drive cycles.

Tavčar *et al* (2011) investigated three different topologies of an ETC system; an electrically assisted turbocharger, a turbocharger with a separate electrically driven supercharger and an electrically split turbocharger. The electrically assisted turbocharger is similar to that used by Zhuge *et al*, whilst the electrically split turbocharger is a system combining a separate turbo-generator and electric supercharger. The result of this study is that the electrically assisted turbocharger and the turbocharger with separate electric supercharger made no significant different to the fuel efficiency of the engine over the NEDC, whereas the electrically split turbocharger increased fuel efficiency by 10.8%. This improvement in efficiency is largely due to the fact the compressor could be largely bypassed during the drive cycle, and the turbine (VGT) could be tuned to provide minimal restriction compared to the baseline and other systems. Thus, the benefit comes largely from reduced pumping work of the engine, rather than improvements by the turbomachines themselves.

One issue with electric turbomachines is the difficulty in powering them with the common vehicle 14 V supply; electric machines capable of providing the performance required by the turbomachines tend to be large and present packaging and weight detriments. Wang and Yuan (2008) investigated using 42 V electric machines in a turbocharged diesel engine; this would allow the use of smaller electric machines and may enable this technology, however, until electric machines are improved or a common change in the standard 14 V electric supply of a vehicle is made, the use of electrically assisted turbomachines will likely be limited to larger diesel engines or hybrid vehicles with secondary electrical power circuits.

2.5 Turbo-Discharging

An opportunity exists for another method of translating energy extracted from the exhaust system back to the crankshaft. Turbocompounding systems extract energy from the exhaust gas and transfer it to the engine crankshaft through a variety of means described previously. Turbochargers transfer turbine energy to a compressor such that intake air is compressed. The compressed air will transfer energy to the crankshaft during the intake stroke if the air pressure is higher than that of the crankcase, exerting work on the crankshaft. However, the turbine extracting energy from the exhaust will cause a restriction during the exhaust stroke, leading to a higher pressure in the cylinder throughout the exhaust stroke. This extra work required during the exhaust stroke, depending on the engine operating condition, can minimise or completely negate any pumping benefit gained by raising the intake pressure.

A new and novel method of energy transfer from the exhaust gas to the crankshaft is that used in Turbo-Discharging where a vacuum, or a reduction in pressure, is created in the exhaust. Energy is extracted from the exhaust gas with a turbine during the part of the exhaust stroke where the piston is largely stationary. The pressure in the cylinder is then reduced whilst the piston is travelling from BDC to TDC. Any reduction in pressure in the cylinder during the exhaust stroke will result in a pumping work benefit. If the pressure in the cylinder can be reduced to below that of the crankcase whilst the piston is moving from BDC to TDC work will be done on the crankshaft. A patent on this concept was granted to Andrew Williams in 2011 (Williams 2011).

It should be noted that Turbo-Discharging will not significantly affect air pressure during the intake stroke as the only potential for energy transfer is through the cylinder during intake and exhaust valve overlap. Therefore, unlike turbocharging, any cylinder pressure reduction during the exhaust stroke will directly improve engine pumping work.

The separated manifold concepts which are utilised in Turbo-Discharging will now be discussed, whereupon the entire concept will be discussed in more detail.

2.5.1 Blowdown Gas Separation

For an ideal Turbo-Discharging system the exhaust event is split into two discrete events. The first, known as the High Pressure (HP) event, releases the blowdown energy from the cylinder which can be captured by a turbine. The second, known as the Low Pressure (LP) event, exposes the cylinder to the low pressure.

Similar split exhaust event concepts have been investigated by two parties, and will be described in detail before exploring the Turbo-Discharging concept in more depth.

Divided Exhaust Period

The Divided Exhaust Period (DEP) concept (Elmqvist-Möller *et al* 2005), (Ekenberg 2002) was the first to apply a split exhaust event to a modern engine. This exhaust arrangement originates from a 1924 patent (Societe Rateau 1924) where the combustion gases are divided; the blowdown and displacement gases flow through two distinct routes in the exhaust system. The blowdown gases flow through one of the exhaust valves which opens first, flowing through a turbine before re-combining and flowing through the rest of the exhaust system. The first exhaust valve shuts and the second opens, through which the displacement gases then pass. These gases bypass the turbine, passing through a close coupled catalyst before recombining with the blowdown gases post-turbine.

The benefit of this system is that the gases which are desirable to extract energy from, the blowdown gases, pass through the turbine whereas the displacement gases do not. The displacement gases flow through a path of less resistance, minimising the increase in pumping work normally associated with turbocharging.

As described previously catalyst light off is important in minimising emissions over a drive cycle and the time to catalyst light off is typically increased when using a turbocharger due to the thermal capacitance of the turbine housing as well as the gas expansion over the turbine. In the DEP concept Elmqvist-Moller et al (2005) located a catalyst in the exhaust path that bypasses the turbine, which all of the exhaust gas flows through when the engine has just started. This reduces the exhaust flow area by 50%; however, it is argued that torque demand in the first few minutes of starting a vehicle is minimal as per the EC2005 cycle. When tested it was found that the engine produced a similar power to a 1.6 naturally aspirated engine

without the use of the turbocharger, more than sufficient for low speed driving whilst the engine comes up to temperature.

They make no mention of how the transition back to using the turbocharger would be managed; light off of the primary catalyst downstream of the turbine would be required before this is possible, but again they do not measure how long this takes.

The other main benefit of the DEP system is that of reduced Residual Gas Fraction (RGF). Reducing RGF offers a performance advantage for several reasons:

1. Exhaust residuals, even after expansion, are significantly hotter than the charge air entering the cylinder. Once combined the in-cylinder temperature is higher than that of the charge air in the intake manifold; this increases the temperature at the end of compression and the peak cylinder temperature. This also increases the cylinder pressure, both of which increase the likelihood of knock in SI gasoline engines. Knock can be seriously detrimental to engine component durability, NVH and performance, and must be avoided. For a given knock margin removing in-cylinder residuals allows for more spark advance, increased compression ratio or for higher intake charge pressure, all of which can be desirable to optimise combustion efficiency.
2. Commonly exhaust gas residuals are used to control emissions of NO_x from combustion by limiting the peak temperatures achieved. By removing the hot residuals, it is possible to further replace these hot residual gases with cooled EGR, decreasing the peak cylinder temperature and further mitigating NO_x emissions.
3. Removing hot gases from the cylinder also offers more space for fresh charge to enter the cylinder. As the residuals are also hot, they will occupy more cylinder volume than the cold charge that could replace them. More air is desirable as it allows more fuel to be burned, but can also lead to more complete combustion especially in compression ignition engines.

The DEP system offers the potential to reduce in-cylinder residual gas by reducing exhaust back pressure during the displacement part of the exhaust stroke. This is achieved due to the turbine bypass flow which does not experience the restriction of the turbine and therefore incurs less of a pressure drop to atmosphere. It was stated that the reduction in residual gases was as much as 60% at low engine speeds and loads, but decreased at higher speeds and loads due to the increased valve restriction.

Valve Event Modulated Boost System

Roth *et al* (2010) utilise the same DEP concept but combine the divided exhaust period with a cam phasing system. As identified by Möller *et al* (2005), this allowed them to use the valve events to control the energy available to the turbine, thus the power transferred to the compressor and therefore boost pressure. In turn this eliminates the need to wastegate, in effect using the exhaust valves as the wastegate to bypass exhaust gas around the turbine. This was proven using One-Dimensional (1-D) modelling and engine testing.

Moreover, they observed increased boost and power at low to medium engine speed, whilst still achieving equal power at rated engine speed. The increase in engine power was not solely due to the increased boost pressure, but also included the benefit from reduced pumping work. This improvement in pumping work, plus optimisation through spark timing allowed for a 4.5% improvement in brake specific fuel consumption (bsfc) at a high part load condition.

2.5.2 Turbo-Discharging Concept

As previously mentioned, Turbo-Discharging uses a similar divided exhaust manifold to that of the DEP and VEMB concepts. Figure 2-5 is a schematic of one potential Turbo-Discharging system configuration on a four cylinder gasoline engine.The HP valve opens first, allowing the blowdown gases to flow from the cylinder through the turbine. However, in a Turbo-Discharging system the energy extracted by the turbine is transferred to a compressor further downstream in the exhaust. The compressor exit is ideally at ambient pressure, therefore when it does work the gas at the compressor inlet becomes depressurised. This is in contrast to a normal turbocharging system where the compressor increases the intake charge pressure; the compressor in a Turbo-Discharging system only has exhaust gas passing through it, and the system does not increase the intake charge pressure.

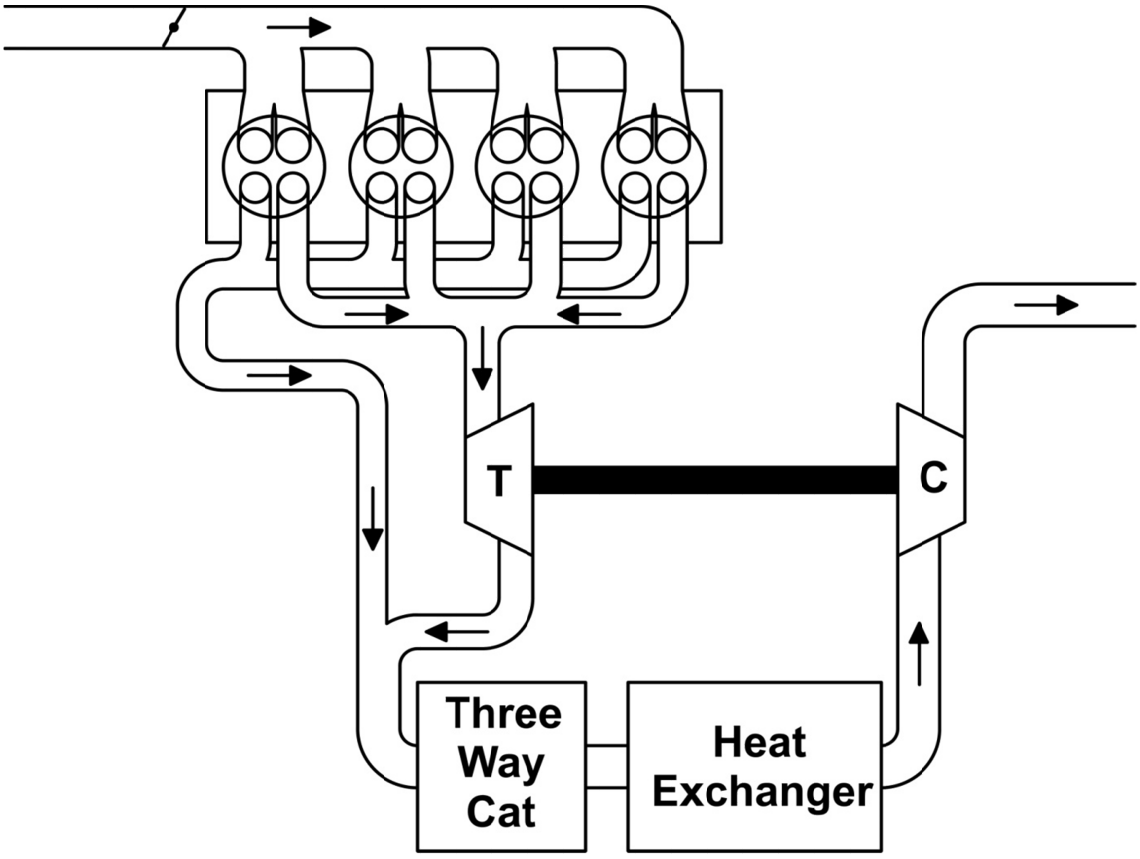

Figure 2-5 - Example Turbo-Discharging System Diagram

This depressurisation from the compressor translates back through the exhaust system to the cylinder via the LP branch of the divided manifold. If the depressurisation is effectively transmitted into the cylinder such that the piston is exposed to it whilst travelling from BDC to TDC, then the pumping work can be further minimised or even reversed completely, allowing positive work to be extracted from the exhaust stroke.

Furthermore, the turbine outlet will also be exposed to the depressurisation generated by the compressor. This has the effect of increasing the pressure ratio across the turbine, which could allow it to extract more work from the exhaust gas.

A schematic of a typical Turbo-Discharging arrangement is shown in Figure 2-5. Also shown in the schematic is a three way catalyst and a heat exchanger. The heat exchanger rejects heat from the exhaust gas before the compressor, increasing the density and allowing the compressor to operate with a higher pressure ratio for a given amount of shaft energy. This, along with aftertreatment options, will be explored later in this thesis.

It is important to note the temporal difference in the valve events. Ideally, the HP valve opening would happen instantaneously; however, this is not realistic. The solution is to open the HP valve before the LP valve to promote the initial flow of gas through the turbine, and once the blowdown gas has gained momentum the LP valve can be opened to expose the rest of the gas in the cylinder to the depressurisation. The degree of overlap required will depend on numerous factors which are investigated in this thesis.

A further significant benefit is that of decreased in-cylinder residuals. Exposing the cylinder to a depressurisation will aid scavenging; the effectiveness of this needs to be investigated in order to quantify this second benefit, along with the primary benefit of Turbo-Discharging.

2.6 Closing Comments

This chapter has reviewed methods of improving IC engine fuel conversion efficiency by recovering energy that would otherwise be wasted, focusing on the energy in the exhaust system. It has looked at ways in which this is currently recovered and translated into a fuel economy benefit, and has suggested a new manner in which this could be achieved. The Turbo-Discharging concept provides a novel system which transfers energy extracted from the exhaust gas back to the crankshaft to achieve a fuel economy benefit.

The following chapter will analyse the concept from a thermodynamic perspective, defining absolute thermodynamic benefits and justifying the inclusion of certain key components in the system, whilst also identifying any operational limits of the system.

3. Energy Analysis

This chapter will describe thermodynamic analysis of the Turbo-Discharging system, with the aim of defining the maximum thermodynamic potential of Turbo-Discharging. It will also identify parameters Turbo-Discharging is fundamentally sensitive to as a foundation for discussion throughout the rest of this thesis.

The theoretical maximum level of depressurisation calculated using this method will be used as a basis to calculate the efficacy of modelled and practical Turbo-Discharging systems later in this thesis.

3.1.1 Thermodynamic Derivation

It is possible to evaluate the primary benefit of Turbo-Discharging as a function of conditions at exhaust valve opening by considering only the exhaust process of a four stroke engine cycle allowing comparison of different engine types, fuels and operating conditions.

Figure 3-1 shows a schematic simplified to show one cylinder in the thermodynamic model. It may be possible to scale the calculation, however, the ideal calculation would take no account of the interaction of the pulses from individual cylinders. The calculation assumes there are no valve flow losses and the exhaust manifold (duct A) is of zero volume. With no volume to expand into the pressure and temperature of the gas at the turbine entry is equal to that in the cylinder.

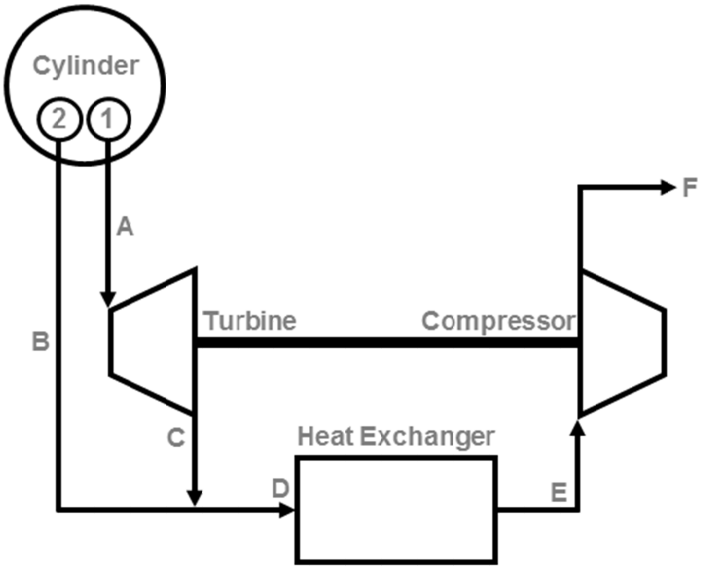

Figure 3-1 - Schematic of thermodynamic model

In this arrangement the turbine will only extract energy from the blowdown portion of the exhaust gas. The proportion of the cylinder contents that flow from the cylinder as blowdown gases will be dependent upon the initial pressure and temperature in the cylinder, and the pressure and temperature downstream of the turbine.

The maximum energy available to the turbine from the exhaust gas at the end of expansion, equal to the internal energy change during an expansion to the exhaust system pressure, is identified for both a Turbo-Discharged and Naturally Aspirated engine in Figure 3-2 by the area enclosed by the dashed line. The total amount of this energy is only available if the gas is

expanded isentropically to atmospheric pressure, which cannot be achieved with a real turbine.

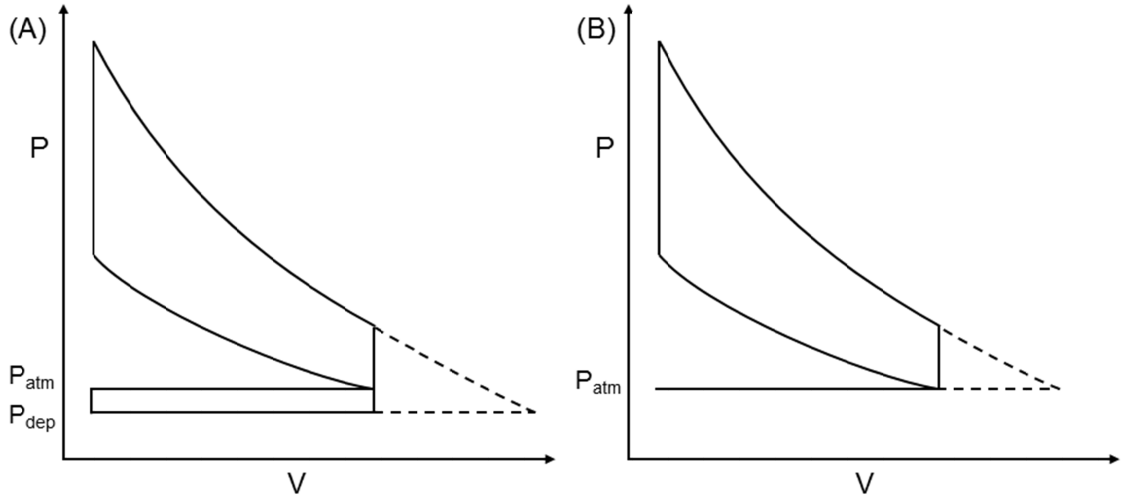

Figure 3-2 – Pressure – Volume diagrams for (A) Turbo-Discharged engine and (B) Naturally Aspirated engine at full load

It can be seen that Turbo-Discharging, by virtue of the depressurisation, gives potential for more energy to be extracted from the turbine as the exhaust gas can expand to a depressurised pressure (P_{dep}) less than atmospheric pressure (P_{atm}).

The initial mass in the cylinder was calculated from the initial values of pressure and temperature assuming the contents to be air as an ideal gas. From the point of exhaust valve opening, variable specific heats were assumed and that the composition of the gas remains constant throughout the exhaust system. The blowdown expansion process was discretised with regular intervals in cylinder mass until the pressure in the cylinder equalled the turbine downstream pressure. The temperature in the cylinder was calculated from the previous step's conditions by

$$T_{i+1} = T_i \left(\frac{v_i}{v_{i+1}}\right)^{k-1} \qquad \textbf{3-1}$$

where T_i and T_{i+1} are the temperatures and v_i and v_{i+1} are the specific volumes before and after the iterative expansion step respectively and k is the ratio of specific heats evaluated at T_i. For an initial pressure and temperature of 500 kPa and 1500 K the difference in the ratio of specific heats between steps was less than 0.02%, thus it proved acceptable to assume the ratio of specific heats was constant over one step. The value of the ratio of specific heats was

calculated using a sixth order curve fit of data from Heywood (1988) for fixed composition burned gases.

From each step, the mass exiting the cylinder was used to calculate the turbine work using

$$\delta W_T = \dot{m}_T c_p \Delta T_T \qquad \textbf{3-2}$$

where δW_T is the turbine work, $\dot{m}_T$ is the mass flow through the turbine, c_p is the specific heat at constant pressure of the exhaust gas passing through the turbine and ΔT_T is the temperature difference of the exhaust gas across the turbine.

The change in temperature across the turbine was calculated from the pressure differential and turbine inlet temperature for a given isentropic turbine efficiency using

$$\Delta T_T = T_{T\,in}\,\eta_T \left(1 - \left(\frac{P_{T\,out}}{P_{T\,in}}\right)^{(k-1)/k}\right) \qquad \textbf{3-3}$$

where $T_{T\,in}$ is the turbine inlet temperature, η_T is the turbine efficiency, $P_{T\,out}$ is the turbine outlet pressure and $P_{T\,in}$ is the turbine inlet pressure. The turbine inlet pressure was assumed to be the same as the cylinder pressure, whilst the outlet pressure was initially estimated. The output of the set of calculations was a revised depressurisation which then replaced the estimated depressurisation. The entire process was then repeated until the estimated and calculated turbine downstream pressure converged.

The result of no valve losses and a zero volume manifold is that the pre-turbine pressure rises immediately to its maximum at EVO. The total cycle compressor work was then assumed to be equal to that of the work done on the turbine over the entire blowdown process.

The displacement pulse from valve 2 was assumed to happen at the constant low pressure manifold pressure. The mass flow from the cylinder in this period was calculated by decreasing the cylinder volume from BDC to TDC in 30 equal volume steps. The mass in the cylinder at each step was calculated by

$$m_{i+1} = m_i \left(\frac{V_{i+1}}{V_i}\right) \qquad \textbf{3-4}$$

where m_i and m_{i+1} are the mass of cylinder contents and V_i and V_{i+1} are the geometric cylinder volumes before and after each displacement step respectively. This also gave an

estimated residual mass fraction at the end of the exhaust event, in this case entirely dependent on the level of depressurisation achieved.

The combined blowdown and displacement exhaust gas flow then passed through an ideal heat exchanger with no pressure drop before being compressed. The compressor inlet temperature, compressor work and mass flow were known. From this the outlet temperature, and in turn the inlet pressure or depressurisation was calculated.

The volume of the heat exchanger and adjoining pipework was considered sufficiently large such that the pressure upstream of the compressor remained steady.

3.1.2 Maximum Achievable Depressurisation

The thermodynamic model was run for a range of given initial pressures and temperatures. The absolute depressurisation achieved is shown in Figure 3-3.

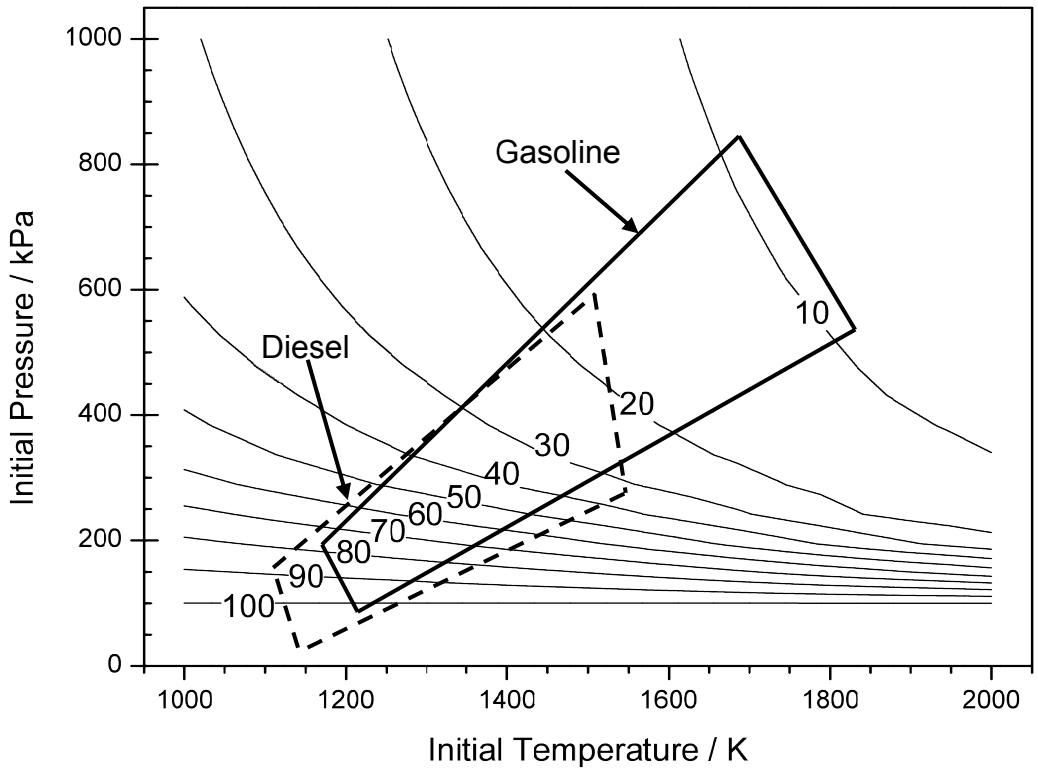

Figure 3-3 – Contours of minimum achievable absolute exhaust system pressure in kPa from a turbo-discharging system for given initial pressure (abs) and temperature. Highlighted regions show typical cylinder conditions at exhaust valve opening for passenger car naturally aspirated gasoline and diesel engines.

The depressurisation achieved increases with both initial pressure and temperature. This is due to the amount of energy the turbine is presented with; a higher pressure and temperature presents the turbine with more energy so more is transferred to the compressor which can do more work on the exhaust gas creating a larger depressurisation.

Figure 3-3 shows much more dependence on initial cylinder pressure than temperature up to 400 kPa, whereupon initial cylinder temperature becomes the more important factor.

Also shown in Figure 3-3 are two regions indicating typical pressures and temperatures at exhaust valve opening for turbocharged diesel compression ignition and gasoline spark ignition engines operating at part load.

Due largely to the increased expansion ratio of the diesel engine and the amount of excess air commonly used in diesel combustion compared to gasoline engines the temperatures and pressures at exhaust valve opening tend to be lower. This means there is less energy available during the blowdown pulse per unit mass.

Due to the way the system is modelled, the compressor and turbine efficiencies combine directly to form a turbomachine efficiency. Altering one will affect the turbomachine efficiency as much as altering the other by the same amount, thus it is only necessary to consider the system sensitivity to the turbomachine efficiency with respect to the level of depressurisation. In practice the split of irreversibilities between the turbine and compressor will affect the amount of heat rejected in the exhaust heat exchanger.

Figure 3-4 shows the same curves of maximum achievable depressurisation for a 64% efficient turbomachine (80% turbine and compressor isentropic efficiencies). The trends in results are similar to that of a 100% efficient turbomachine; a dependence on initial cylinder pressure up to 400 kPa, beyond which there is a much stronger dependence on initial cylinder temperature.

The absolute values of depressurisation achieved with lower turbomachine efficiencies are of course less. For an equivalent amount of exhaust gas energy a less efficient turbine will be able to extract less energy, transferring less energy to the compressor. This in turn means less depressurisation can be created, decreasing the pressure ratio across the turbine reducing the amount of energy that can be extracted.

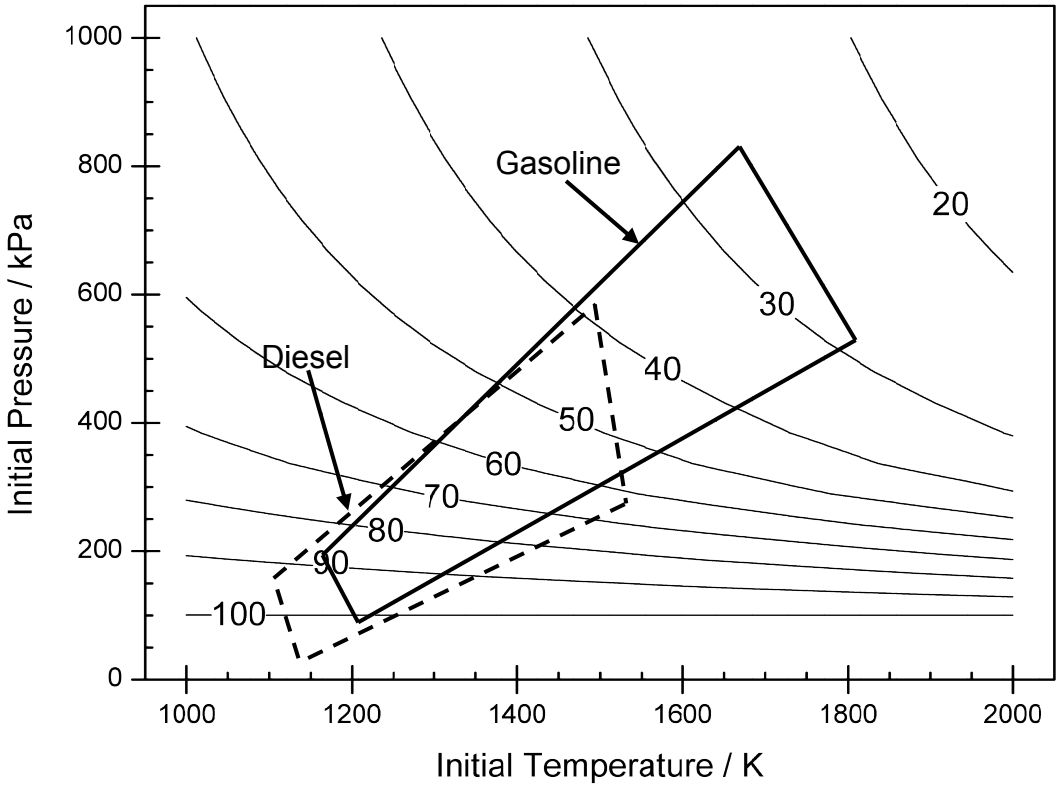

Figure 3-4 – Minimum achievable exhaust system pressure in kPa from an ideal Turbo-Discharging system with 80% turbine and compressor efficiencies

80% efficiencies were chosen as these tend to represent typical achievable turbine and compressor efficiencies of small rotating turbomachinery operating at its design point. However, it is unlikely either the turbine or compressor could operate at this efficiency given the range of conditions they need to be optimised for (they could if they were optimised for a single speed and load point). As such, Figure 3-5 was created with 65% turbine and 70% compressor efficiency giving a 45.5% efficient turbomachine to give a more representative idea of what may be achievable.

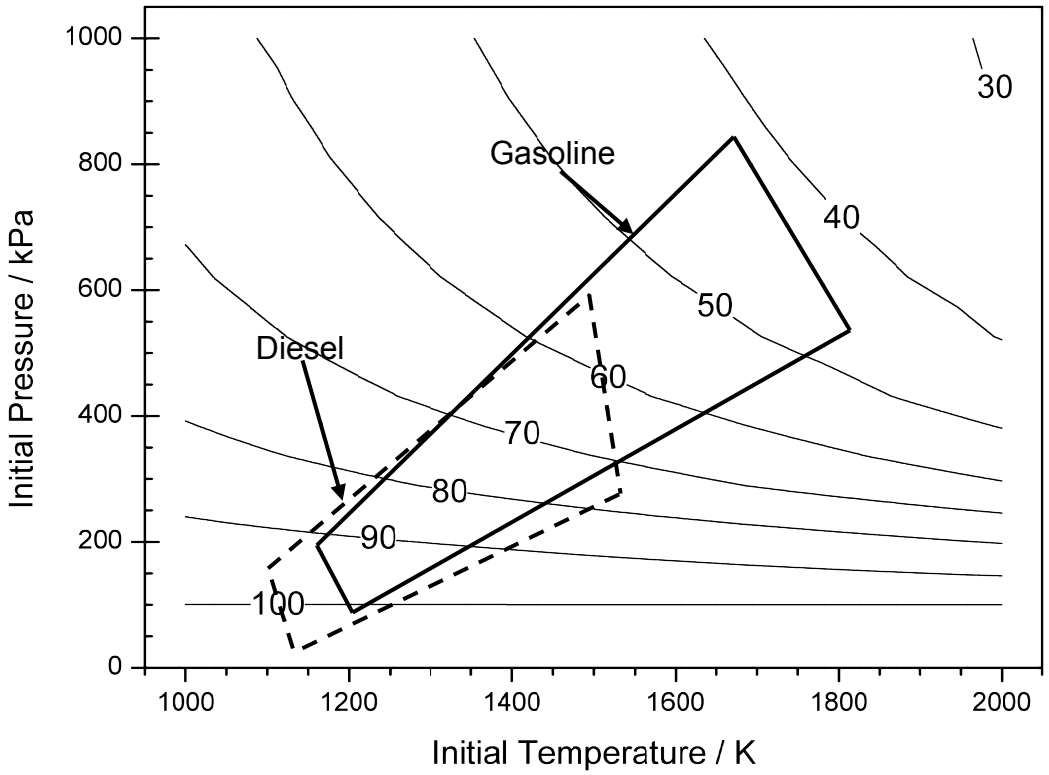

Figure 3-5 - Minimum achievable exhaust system pressure in kPa from an ideal Turbo-Discharging system with 65% turbine and 70% compressor efficiency

This shows that the minimum achievable pressure for a gasoline engine with reasonable turbomachine efficiencies is around 43 kPa, compared to less than 10 kPa for a perfectly efficient turbomachine. This indicates the importance of optimising the turbomachine efficiency for achieving maximum depressurisation.

3.2 Model Sensitivity

There are other parameters which a Turbo-Discharging system, and therefore the model will be sensitive to. These will be discussed now.

3.2.1 Heat Rejection from Exhaust Gases

It is important to assess the level of heat rejection required from the exhaust gas as this will help to define the size and type of heat exchanger required, and the impact this would have on the vehicle.

This was investigated simply by altering the compressor inlet temperature. It is important to note that this will give an indication of the importance of heat rejection, but should not be used to size an actual heat exchanger. A more comprehensive approach is identified later in this thesis considering fixed geometry heat exchangers by using 1-D modelling.

For this sensitivity analysis both 100% (ideal) and 80% (optimal real-case) efficient turbomachines were considered, with the result shown in Figure 3-6.

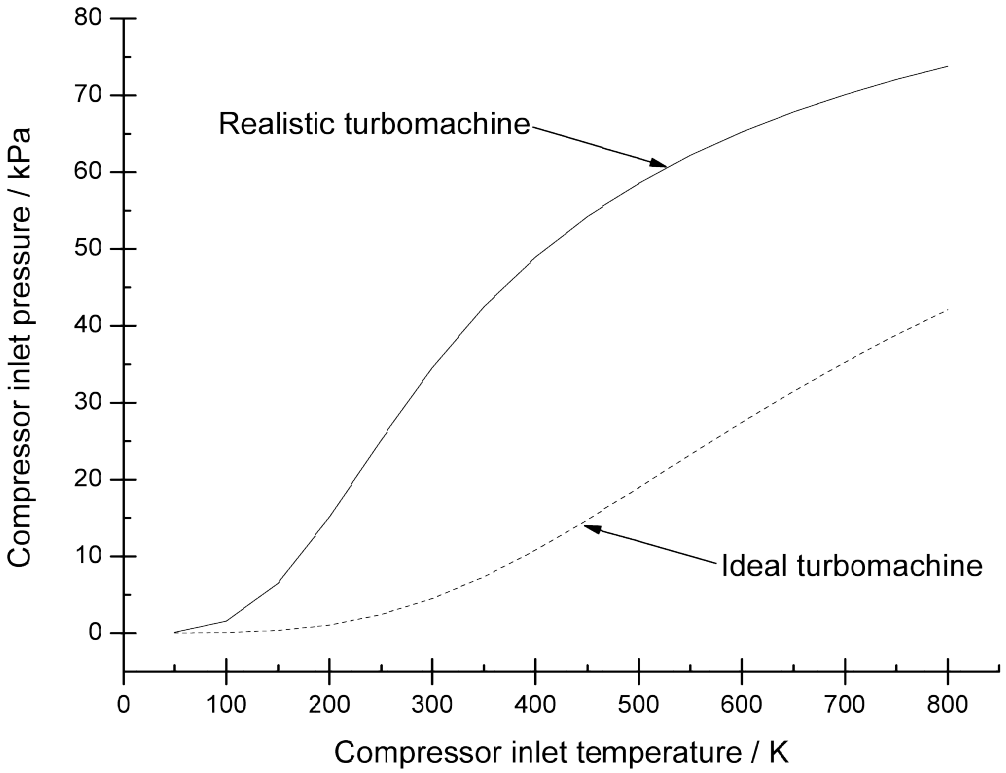

Figure 3-6 - Effect of compressor inlet temperature on achievable depressurisation for 100% and 80% turbomachine efficiencies for fixed initial cylinder temperatures and pressures

For a lower intake temperature at a fixed mass flow the exhaust gas would be more dense. Increasing the density of the gas allows the compressor to create a larger pressure ratio for the same amount of shaft work, and as such a larger depressurisation is created.

The realistic turbomachine is more sensitive at compressor inlet temperatures between 2-400 K than above 400 K. This is interesting when you consider the type of heat exchangers that could be used. An exhaust gas to engine coolant heat exchanger would only be able to cool the exhaust gas to the temperature of the coolant, which in most passenger cars is around

370-380 K. An exhaust gas to air heat exchanger may be able to cool the exhaust gas further to temperatures approaching ambient, allowing for a 15 kPa greater depressurisation.

3.2.2 Depressurisation versus Turbomachine Efficiency

As has been identified previously, turbomachine efficiency will affect the energy extracted from the exhaust gas, and thus the depressurisation generated by the Turbo-Discharging system. Figure 3-7 shows the effect of turbomachine efficiency on the depressurised pressure achieved with a Turbo-Discharging system for three exhaust gas energy cases, varying the exhaust gas energy by the pressure and temperature at EVO. For a turbomachine efficiency of almost zero the achieved depressurisation tends towards zero of course. As the turbomachine efficiency improves the depressurisation achieved improves for all cases.

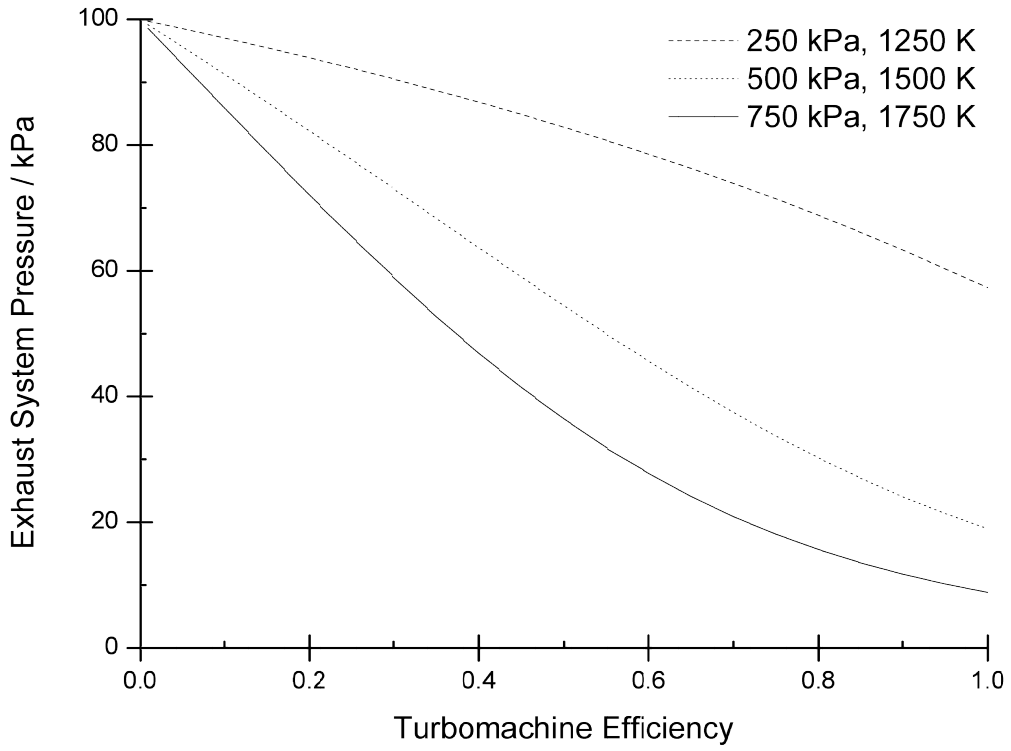

Figure 3-7 - Effect of turbomachine efficiency on depressurisation for three exhaust gas energy levels

For the region of realistic turbomachine efficiencies, 0.25 to 0.64, the lowest exhaust gas energy level is least sensitive to turbomachine efficiency although it generates the least depressurisation. With this insensitivity it may be favourable to increase the amount of energy

in the exhaust gas by altering the ignition or exhaust valve timing, at which point the depressurisation achieved becomes larger and more sensitive to turbomachine efficiency. However, the low energy case may represent a part load case where a small benefit in exhaust system depressurisation may constitute a larger percentage engine efficiency benefit as the engine MEP is lower.

3.2.3 Exhaust Back-Pressure

One practical consideration of the Turbo-Discharging system is the requirement of exhaust noise management and the increased prevalence of exhaust gas aftertreatment systems. Both emissions aftertreatment systems and exhaust gas silencers function by passing the gas through a medium or a volume, both of which restrict flow and will contribute to increased pressure in the upstream exhaust system (back pressure).

In a Turbo-Discharging system increasing the downstream pressure on the compressor for a fixed pressure ratio will increase the upstream pressure. Figure 3-8 shows how the compressor absolute pressure rise, or depressurisation, varies with exhaust system back pressure for three exhaust gas energy levels with a turbomachine efficiency of 0.8.

For a higher exhaust system back pressure, the compressor intake air will be more dense, and thus the compressor can operate more effectively. This is visible most for the highest exhaust gas energy case where the compressor is able to create a larger pressure differential at the highest exhaust back pressure where the effect somewhat counteracts the reduction in available energy with increasing back pressure.

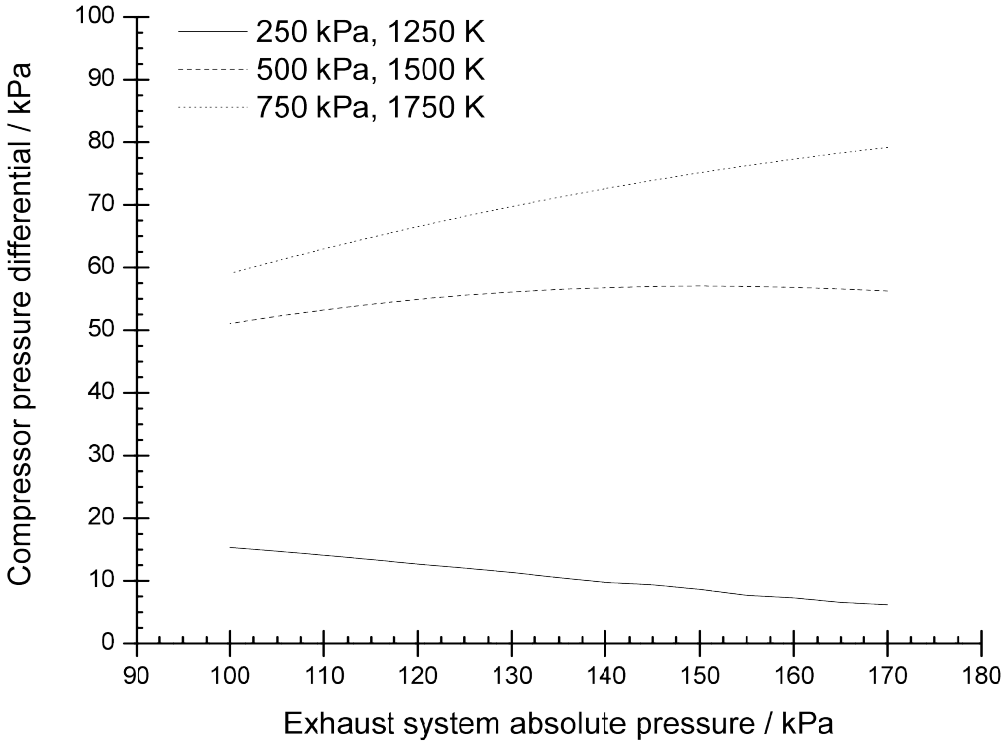

Figure 3-8 – Pressure differential across the compressor for a varying exhaust system back pressure and three exhaust gas energy cases with a turbomachine efficiency of 0.8

The curves shown in Figure 3-8 can be considered to approximate a low, medium and high exhaust gas energy case. The exhaust mass flow rate for the low exhaust gas energy case will be low, therefore reducing the pressure loss across the exhaust system. In this condition, it can be seen that the pressure differential across the compressor is the largest point on the curve for the low energy case. This is significant as the compressor pressure differential can be considered as, for a highly effective Turbo-Discharging system, the improvement in engine pumping work. As an example, for a part-load condition of 3 bar BMEP an improvement in engine pumping work of 15 kPa at an exhaust pressure of 105 kPa would result in a 5% improvement in engine pumping work.

Similarly for a higher part-load and full load condition of 8 and 12 bar BMEP and exhaust pressures of 135 and 170 kPa respectively, the compressor pressure differentials would result in a 7% decrease in pumping work for both conditions. The graph above still shows that it is beneficial to reduce exhaust back pressure as much as possible to maximise engine performance. However, for an engine with high exhaust back pressure Turbo-Discharging may be able to offer a larger proportional benefit in engine pumping work.

3.2.4 Residual Gas Fraction

Gasoline engine performance can be limited by the presence of hot RGF in the cylinder at the end of the exhaust stroke. There are a number of mechanisms by which these hot residual gases limit engine performance which will be discussed in more detail in chapter 7. Most significant is the increase in temperature of the trapped charge, increasing the temperature and pressure at the end of compression promoting auto ignition of the cylinder contents.

The quantity of hot residual gases is partly governed by the pressure the cylinder is exposed to throughout the exhaust stroke, assuming the contents of the cylinder expand fully to that pressure. In a turbocharged gasoline engine the cylinder is exposed to the exhaust back pressure plus the pressure drop across the turbine. When Turbo-Discharging is applied to an engine the cylinder is exposed to the low pressure created by the compressor in the exhaust such that the residual contents are expanded further. For a given cylinder volume, a lower pressure at EVC will result in a lower residual mass.

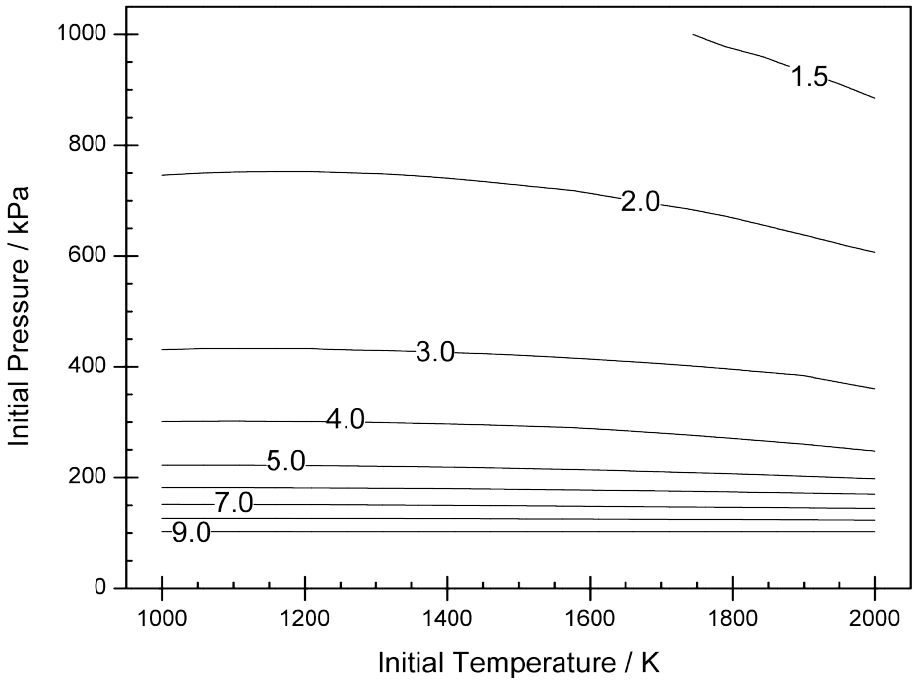

Figure 3-9 – Predicted residual fraction (%) for an NA engine

Figure 3-9 shows the calculated RGF for an NA version of the engine used in this thermodynamic model. The residual fraction is largely dependent on the initial cylinder

pressure, with a small positive effect with cylinder temperature for higher initial cylinder pressures.

The proportion of cylinder mass left in the cylinder following the blowdown pulse increases with increasing initial cylinder pressure and temperature as shown in Figure 3-10.

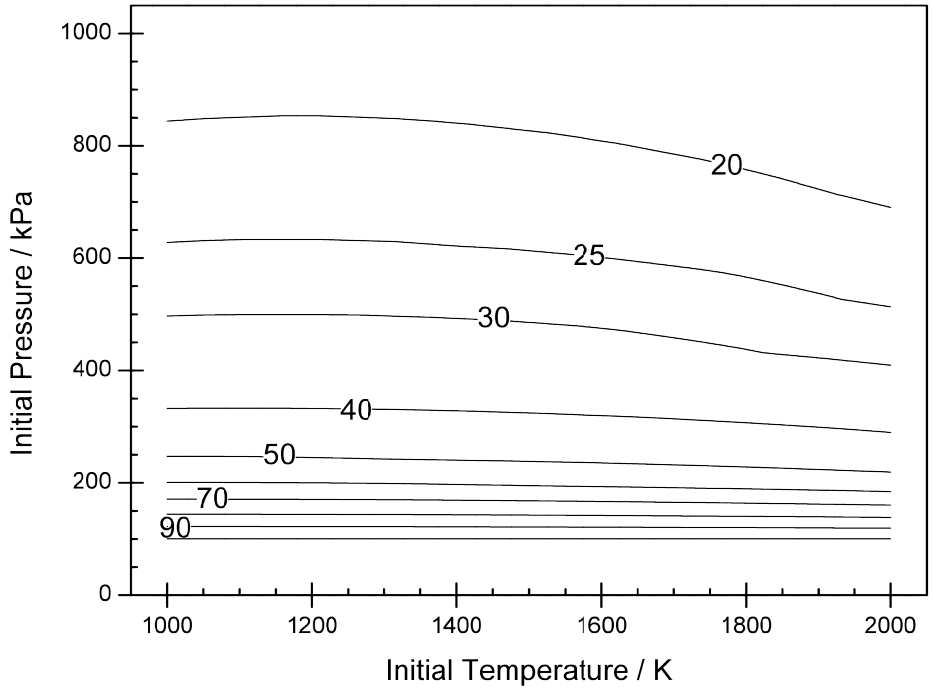

Figure 3-10 - Percent mass at the end of the blowdown pulse for an NA engine

For all cases the amount of mass left in the cylinder after the blowdown pulse decreases with increasing initial cylinder pressure. The initial cylinder temperature only has an effect at higher initial cylinder pressures where it further reduces the mass in the cylinder after blowdown. This effect is largely due to the decreased density of the gas at the end of blowdown due to the higher temperature; for the same expansion ratio a case with a higher initial temperature will have a higher temperature at the end of blowdown. Thus, the gas will have a lower density, and so for a fixed pressure there will be less gas in the cylinder. This then follows through the displacement pulse, which is assumed in the cylinder to be isothermal, such that the gas temperature post-displacement pulse remains higher. Whilst it is true in this model that a higher initial cylinder temperature for a fixed pressure will result in less mass in the cylinder, and therefore the expanded gas would be expected to be less dense, this is isolated in Figure 3-10 plotted as the percentage of the initial cylinder mass.

It should be noted that despite the mass of residual gases being decreased the increased temperature of the gases may counteract any expected benefit in knock resistance.

Figure 3-11 shows the calculated residual mass fraction in percent for an ideal Turbo-Discharging system. As the initial pressure and temperature increase the depressurisation increases. This exposes the cylinder to a lower pressure throughout and most crucially at the end of the exhaust stroke, and as such the residual mass fraction at EVC is less.

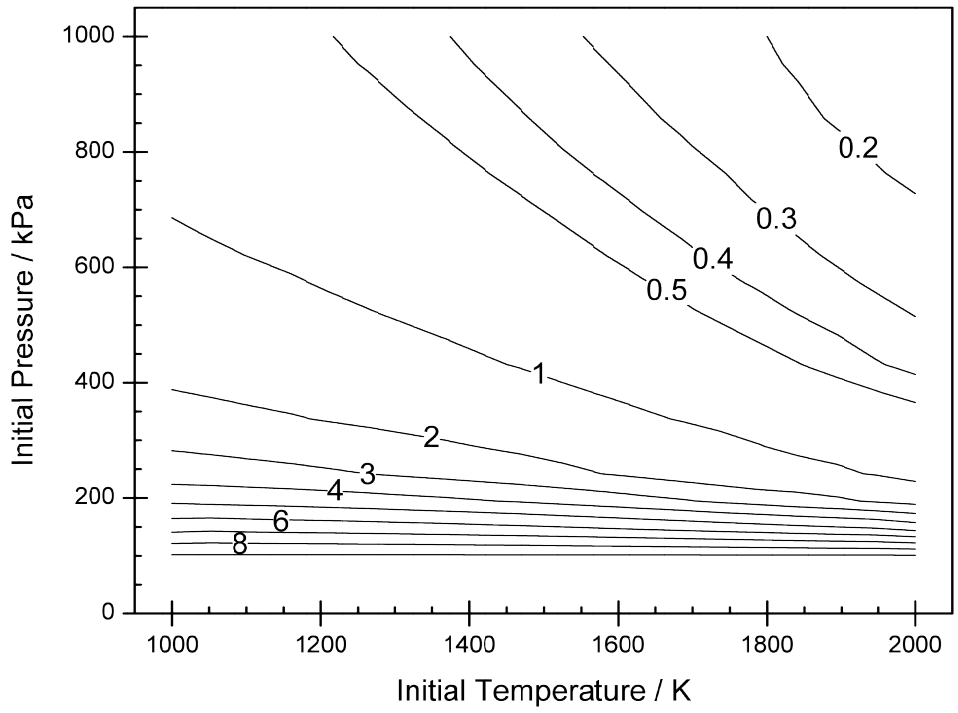

Figure 3-11 - Calculated residual mass fraction in percent for a 100% rotor efficiency Turbo-Discharging system

It can be seen that the residual fraction is a strong function of initial cylinder pressure below initial cylinder pressures of 300 kPa. This reflects the level of depressurisation achieved by the Turbo-Discharging system, as shown in Figure 3-3. As such, for a more realistic turbomachine efficiency, and therefore Turbo-Discharging system efficiency, you would expect to achieve less depressurisation and have higher residual gas fraction. This is demonstrated in Figure 3-12 which shows the case for turbine and compressor rotor efficiencies of 80%.

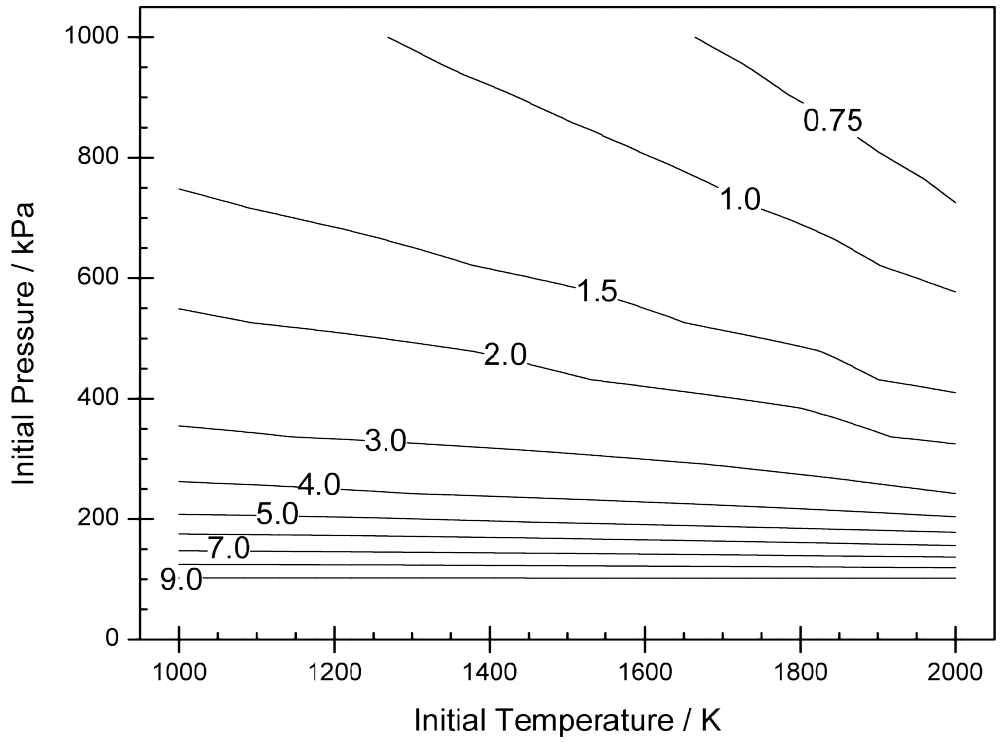

Figure 3-12 - Minimum achievable residuals with 80% rotor efficiencies

The level of depressurisation achieved for a more realistic Turbo-Discharging system efficiency is lower than that of the ideal system, and therefore it is realistic to expect the residual fraction to be higher. Figure 3-12 reflects exactly this; the residual fraction is higher across the entire plot with an absolute minimum residual fraction achieved of 0.54% as opposed to 0.14% with the ideal Turbo-Discharging system efficiency. However, when considering an NA engine the level of residual fraction is still significantly lower as shown in Figure 3-9, the minimum of which is 1.37%.

For a Turbo-Discharging system, an increase in initial cylinder temperature for a given initial cylinder pressure will present the turbine with more energy. This in turn is extracted and transferred to the compressor such that it can create a larger depressurisation. In this model, it is assumed that the lower pressure translates back through the turbine to the cylinder, such that the pressure at the end of blowdown is consistent throughout the entire exhaust system. This leads to a larger proportion of the cylinder mass flowing through the turbine such that less work has to be done by the piston during the displacement stroke, which also occurs at the reduced pressure.

The prior residual fraction investigation was carried out at a fixed exhaust back pressure of 100 kPa. Figure 3-13 shows a comparison of residuals in a NA engine compared to the same engine with a Turbo-Discharging system for the same exhaust back pressures.

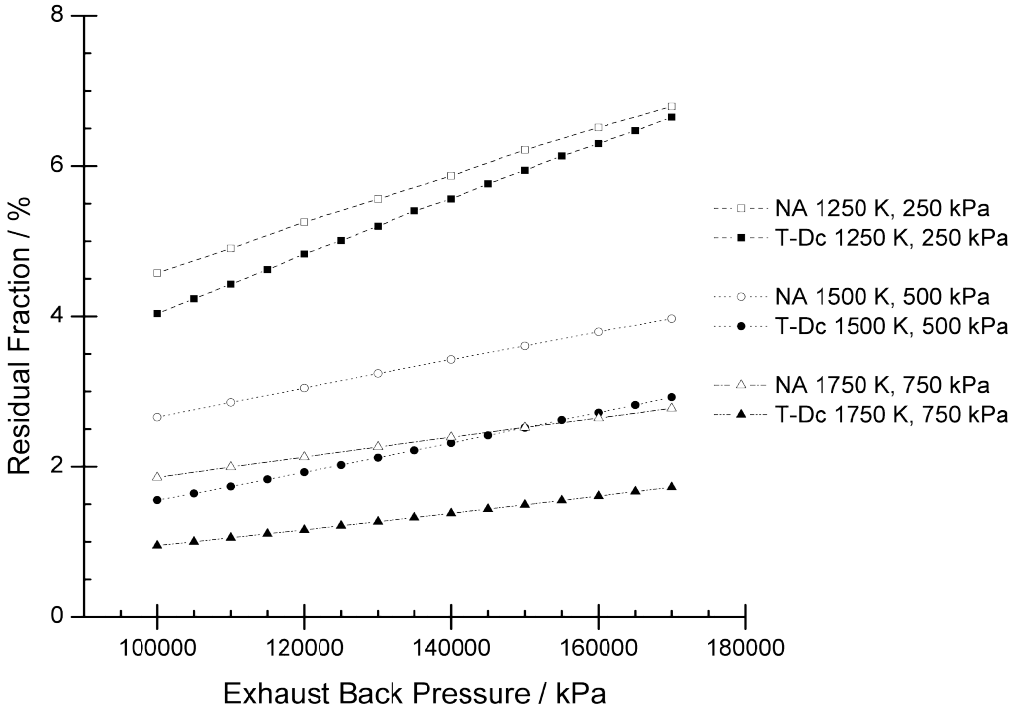

Figure 3-13 - NA and Turbo-Discharging residual fraction for three exhaust gas energy cases over a range of realistic exhaust back pressures

It can be seen that for the lowest exhaust gas energy case, increasing exhaust back pressure reduces the ability of the Turbo-Discharging system to reduce residual gas fraction. The same is true for the middle of the three cases but to a lesser extent, providing around a 1% point reduction in residual gas fraction over the NA engine.

In an actual Turbo-Discharging system this will mean the system is less effective at lower engine speeds and loads, only providing a residual gas fraction benefit at higher exhaust gas energy levels. This is still significant as reducing residual fraction at peak load is arguably more important than part load as under these conditions, spark advance (and therefore closed cycle efficiency) is more limited, enabling the engine to produce more power for a fixed amount of fuel.

3.3 Efficacy Calculation

Efficacy is the power or capacity to produce an effect (Oxford English Dictionary 2013). It is possible to calculate a Turbo-Discharging efficacy by comparing the actual depressurisation achieved to the maximum depressurisation achievable with an ideal Turbo-Discharging system.

If it is assumed that the pressure and temperature at EVO define the energy available to the Turbo-Discharging system, the resultant maximum depressurisation will be an over-prediction. The magnitude of this error will increase as EVO advances due to the increased expansion of the cylinder contents from the expanding cylinder volume. Also, the proportion of expansion due to cylinder geometry will depend on the flow coefficient of the exhaust valve or valves, and how quickly after EVO the pressure decreases. An exhaust valve and port with a high flow coefficient will allow the pressure in the cylinder to reduce more quickly, and as such the change in cylinder volume will have a smaller overall effect.

It is recommended that the Turbo-Discharging efficacy is defined by the conditions at EVO for both the actual system and the ideal model. For the ideal model this defines the absolute maximum energy that could be available to the Turbo-Discharging system, and as such will produce the greatest possible depressurisation. The Turbo-Discharging system efficacy can therefore be defined as

$$E_{T-Dc} = \frac{P_{C,i\ (Max\ theoretical)}}{P_{C,i\ (Actual)}} \qquad \textbf{3-5}$$

where E_{T-Dc} is the Turbo-Discharging efficacy and $P_{C,i}$ is the absolute compressor inlet pressure. This predominantly shows the effect of valve and turbomachine irreversibilities.

3.4 Turbo-Discharging Gasoline and Diesel Engines

Diesel engines tend to have higher compression (and therefore expansion) ratios than gasoline engines. As such, the exhaust gas is more expanded at exhaust valve opening than a gasoline engine, reducing the energy content in the exhaust gas. Figure 3-3, 3-4 and 3-5 all show that due to the increased pressure and temperature of a gasoline engine at exhaust valve opening a larger depressurisation can be achieved over a diesel engine.

Furthermore, diesel engines operate with excess air. This means that any energy extracted from the exhaust can be transferred to a compressor on the intake side which can then do work on the piston during the intake stroke. Turbo-discharging may be able to provide some benefit to pumping work, however, this would be to the detriment of any other turbomachine fitted and as such it would be beneficial to use this excess energy to improve pumping work on the intake stroke.

For these reasons, this thesis will now only consider Turbo-Discharging on gasoline engines. Its applicability to diesel engines should be considered in further work, as there may be applications where Turbo-Discharging may become favourable such as in stationary power engines.

3.5 Closing Comments

Turbo-Discharging has been investigated from the perspective of fundamental thermodynamics to identify the bounds of system performance. Results for a range of initial cylinder pressures and temperatures were presented. These results are used throughout the remainder of this thesis to calculate the Turbo-Discharging system efficacy. Justification has also been made to focus this thesis on Turbo-Discharging gasoline engines due to the larger potential benefits over diesel engines.

The following chapter will discuss the engine test setup and measurement method for the baseline naturally aspirated engine, and some instrumentation that is common to the experimental Turbo-Discharging system in chapter 6.

4. Engine Testing and Measurement Method

This section will describe the base engine and the measurement methods used to gather experimental data for both the baseline and Turbo-Discharging engines.

The engine chosen for this project is a 1.4 L Ford Sigma four cylinder port fuel injected (PFI) spark ignited gasoline engine originating from a 2005 Ford Focus. Some major engine parameters and performance data are included below in Table 4-1.

This engine utilises well established IC engine technologies compared to some more modern or research engines incorporating more advanced fuel saving technologies. The benefit of this is that it allows for easier isolation of the effects Turbo-Discharging may have on the engine as there are less variables to optimise for any given operating condition.

Displacement	1.388	L
Bore	76	mm
Stroke	76.5	mm
Connecting Rod length	136.3	mm
Cylinders	4	
Valves per Cyl	4	
Compression Ratio	11:1	
Firing Order	1-3-4-2	
Max Speed	6200	rpm
Max Power	59.1	kW @ 5700 rpm
Max Torque	124	N·m @ 3500 rpm

Table 4-1 - Ford Sigma Parameters and Performance Data

The engine was attached to a Froude-Consine Model AG150 eddy current dynamometer to provide and control load. The dynamometer is a trunnion-mounted type, where the dynamometer is supported by bearings and the torque is measured using a load cell on a lever arm. The load is provided through electromagnetic induction; as the shaft rotates magnetic fields are cut generating eddy currents in the loss plates, creating heat. This heat is then dissipated by plant coolant pumped through the dynamometer.

The engine speed and load are requested individually on the dynamometer controller. The dynamometer load is controlled by altering the current to the coils generating the magnetic field; a larger current leads to a stronger magnetic field and thus larger eddy currents in the loss plates. The dynamometer controller also controls the engine throttle pedal angle signal, which allows for adjustment in load when maintaining a constant engine speed or adjustment in engine speed whilst maintaining a constant load.

The engine control system and instrumentation will now be described in more detail.

4.1 Engine Speed and Load Control

As mentioned previously, the engine was attached to a Froude-Consine AG150 eddy current dynamometer allowing control of engine load. However, letting the ECU run in closed loop operation led to an inability to accurately control the engine load. The reason for this is the dynamometer was controlling the pedal angle, and for a given pedal angle the spark advance, injection timing, injection duration and throttle angle could change, resulting in fluctuations in torque.

Control of the standard Ford ECU was achieved using Accurate Technologies Incorporated (ATI) hardware and software, also giving the ability to record measured parameters from the engine sensors. To reach a particular set point the pedal angle was adjusted on the dynamometer then the throttle angle was fixed using the ATI software. The ignition timing was in turn fixed and finally the fuelling was adjusted to reach stoichiometric operation according to the wideband lambda sensor which will be discussed in section 4.3. Depending whether the mixture was rich or lean the torque would change as the fuelling was adjusted, however, the throttle position could be adjusted until the desired load was reached.

4.2 Data Acquisition

Most of the signals from the instrumentation used was logged by a National Instruments Compact DAQ (cDAQ-9178) using a bespoke Labview program.

All of the measurement equipment, with the exception of the fuel flow and lambda sensor was connected to the Compact DAQ. One module was used to actuate the exhaust pressure transducer cooling jacket when a measurement is to be taken. This will be explained more thoroughly in section 4.4.

A diagram illustrating the instrumentation and data acquisition for the Turbo-Discharging system is included later in this thesis in section 6.7.

4.3 Engine Fuelling

In order to ensure the engine maintained λ=1 or stoichiometric operation a wideband lambda sensor was used to measure the air-fuel ratio. The sensor used was an ECM NO_x 5210 sensor that is capable of measuring NO_x, lambda and O_2. The controller and display for the sensor gave a visual output, but also had a USB connection to allow connection to a PC for data logging. The signal from this was read into the Labview VI.

At λ=1 the sensor is accurate to ± 0.008, and for $0.8 \leq \lambda \leq 1.2$ it is accurate to ± 0.016.

Three methods of fuel flow measurement were identified, the first a coriolis fuel flow meter. Within the fuel flow meter the fuel flows through twin tubes parallel to the main axis of flow, which are vibrated. In a no-flow condition the vibration imparted onto these tubes causes them to move in equal, opposite directions. When flow is passed through the flow meter, the parallel tubes twist an amount that is proportional to the mass flow through them. This twist of the tubes is measured such that the mass flow can be determined.

The second method used was a volumetric flow meter. A series of optical sensors and a digital timer measured the time to consume a known volume of fuel. This has the obvious disadvantage of being sensitive to temperature. There was no control of the temperature of the incoming fuel.

Thirdly the ECU calculated mass fuel flow rate was recorded. The ECU calculates this based upon the injection time and maps of measured fuel temperature and pressure, and intake manifold temperature and pressure.

The three measurement methods were used over the entire engine speed and load range. From the measured fuel flow rate a lambda value was calculated using the ECU measured air mass flow rate. The resulting lambda values are plotted against engine mass air flow in Figure 4-1. For all of these points the engine was controlled to operate at λ=1, however, the measured error on the lambda sensor increased noticeably with air flow. The error bands for the lambda sensor are also plotted for comparison.

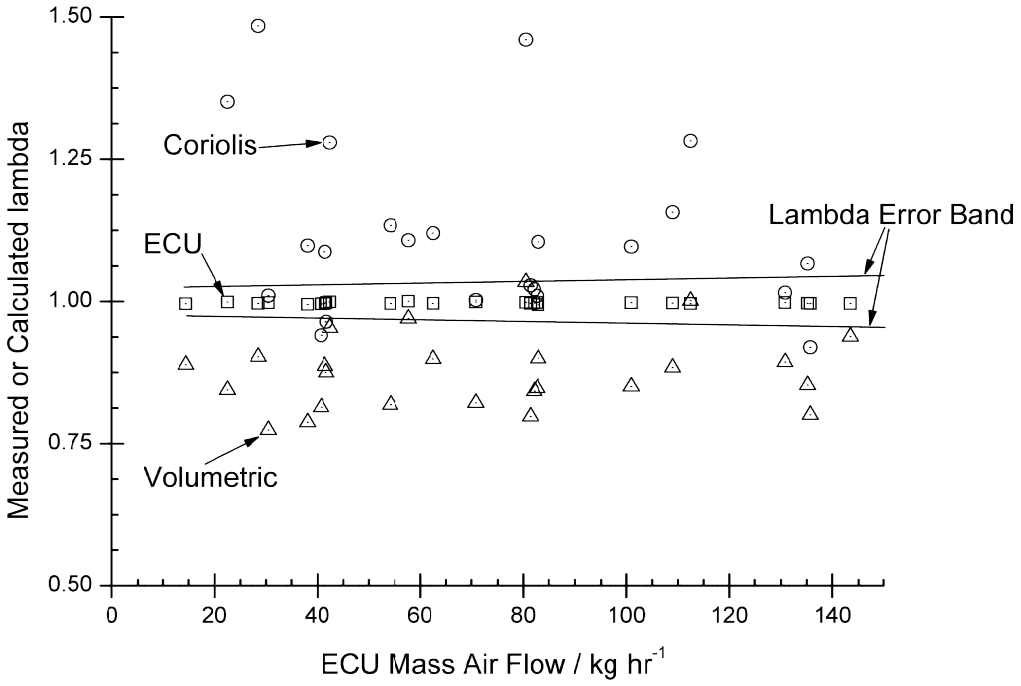

Figure 4-1 – Lambda calculated by various fuel flow measurement methods versus engine mass air flow over the full engine speed and load range

It can be seen that the lambda calculated from the engine fuel mass flow rate is substantially more consistent than either the coriolis or volumetric fuel flow meters. The coriolis fuel flow meter consistently under-read whilst the volumetric consistently over-read the fuel mass flow rate. Thus, it was decided that the ECU measurement would be used in preference to the fuel flow meters.

4.4 Pressure Measurement

In-Cylinder Pressure Measurement

In-cylinder pressure was measured using a Kistler 6117B spark plug with integrated pressure transducer. This allows the pressure transducer to be mounted into the cylinder without significant modification to the engine. The signal from the pressure transducer was amplified then sent to a National Instruments DAQ to allow processing in a bespoke Labview virtual instrument.

The signal from the in-cylinder pressure transducer is a relative measurement, thus it needs to be referenced from a known pressure. The method chosen was to match the intake manifold pressure at 10°CA after TDC. This was chosen as it takes time for the pressure in the cylinder to equalise across the intake valve, and 10°CA gave a reasonable accuracy when calculating the BMEP from the cylinder pressure trace.

Gasoline engines are particularly susceptible to cycle-to-cycle variation in the cylinder pressure trace, commonly defined by a Coefficient of Variation (CoV) which can be applied to any measurement such as maximum cylinder pressure or IMEP. CoV in spark ignition engines is largely caused by differences in charge motion around the spark plug, the amount of fuel and air in the cylinder and varying residual gas fraction between cycles (Heywood 1988). All of these factors cause differences in the fuel burn rate, peak pressure generated by combustion and thus the work generated per cycle. This leads to differences in cylinder pressure from cycle-to-cycle, and as such it is necessary to average many cycles to achieve an acceptable average. Figure 4-2 shows four cycles of measured cylinder pressure overlaid, compared to the average of 200 cycles.

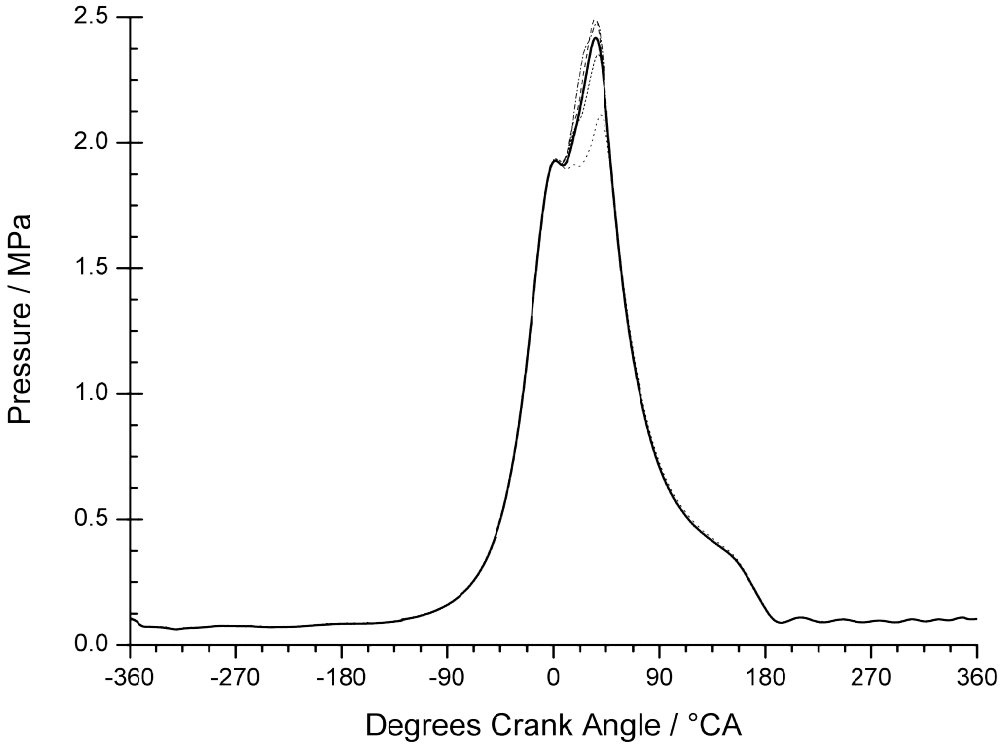

Figure 4-2 - Example of variation in cylinder pressure from cycle to cycle over four cycles at 1500 rpm, 6 bar BMEP with the average shown as the thicker weight line

To illustrate the typical variance in cylinder pressure from cycle to cycle 200 cycles were recorded for a range of engine loads at 3000 rpm. From this data the CoV was calculated for the 0-10%, 0-50% and 0-90% burn durations, IMEP and peak cylinder pressure. The burn durations were calculated with a Heat Release Rate (HRR) calculation using equation 4-1 from Heywood (1988)

$$\frac{dQ_{CH}}{d\theta} = \frac{\gamma}{\gamma - 1} P \frac{dV}{d\theta} + \frac{1}{\gamma - 1} V \frac{dP}{d\theta} \qquad \textbf{4-1}$$

where dQ_{CH} is the gross heat release rate, and P and V are the cylinder pressure and volume respectively. The CoV values calculated are shown in Figure 4-3.

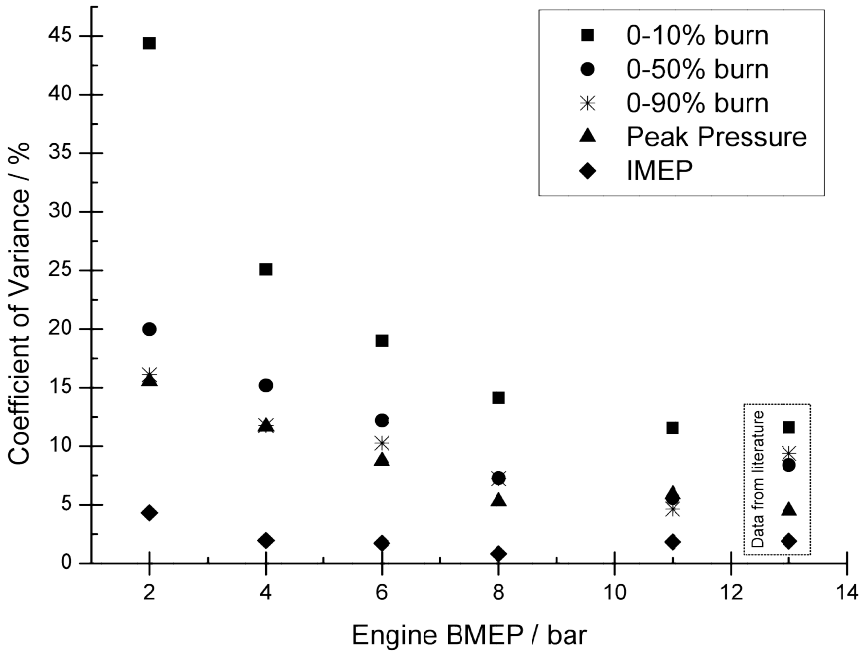

Figure 4-3 - Measured COV for a range of engine loads at 3000 rpm compared with data reproduced from (Stone 1985)

The measured COV improved with increasing load. One factor that improves this is the increased mass flow of air. This increased mass flow increases charge momentum, making it less susceptible to external inputs and gives rise to a more repeatable gas exchange and in-cylinder charge motion. Higher pressures and temperatures also create a faster flame in the cylinder and give less scope for variability.

Also shown in Figure 4-3 is data from Stone (1985) for a fast burn gas engine operating at 1500 rpm, wide open throttle, a fuel-air ratio of 1.12 and minimum advance for best torque (MBT) ignition timing. He also states that the CoV in engine IMEP should be no more than 5-10% for good driveability. The measured values are reasonable for both this criteria and for the data provided.

Unsteady Exhaust Pressure Measurements

Measuring the pressure pulsations in the exhaust system required the use of fast pressure transducers. Those chosen were Kistler type 4007B, a piezoresistive transducer capable of continuous operation in temperatures up to 200°C and over a pressure range of 20 bar.

These were equipped with Kistler type 7553A cooling jackets which provide a cooled housing to mount the pressure transducer in as well as shielding the transducer from the exhaust gas when a measurement is not being taken. This has the added benefit of preventing the transducer from being over-exposed to exhaust soot. Using this with the transducer allows intermittent measurement of exhaust gas up to 1000°C.

The cooling jacket required cooling water, which was supplied from a Kistler temperature conditioning unit type 2621E, and also required compressed air to actuate the jacket to expose the transducer. The air actuation was triggered by a Labview program; a pneumatic valve provides the jacket with the required air pressure when actuated via a digital I/O signal from the NI 9403 module. When no actuating signal is provided, the jacket air supply line is exposed to atmospheric pressure to ensure it stays closed.

The unsteady exhaust pressures and cylinder pressure measurements were referenced to pulses from an encoder attached to the crankshaft. This encoder provided a pulse for every TDC and 720 pulses per revolution of the crankshaft, thus one complete engine cycle was 1440 samples. The pulse from the TDC marker was used to trigger the start of each measurement cycle. This was aligned to actual engine TDC by disconnecting the spark plug from cylinder 1 and then aligning the peak measured cylinder pressure to 1°CA before TDC. The peak cylinder pressure does not occur at TDC due to heat transfer from the compressed charge to the cylinder walls; 1°CA was considered optimum for this work based on prior experience.

The signal from the transducer was sent to a Kistler amplifier which was calibrated in conjunction with the transducer and compensated for ambient temperature. The output from the amplifier was 0-10 V, which fed into the 16-Bit simultaneous analogue input 0-10 V module of the DAQ system.

A simultaneous sampling module was necessary to capture data from both sensors at exactly the same time; regular analogue input modules use a multiplexer to sample each input

channel sequentially, which is unacceptable when measuring more than one unsteady exhaust pressure for direct comparison.

Mean Pressure Measurements

As described previously, each piezo-resitive transducer needs to be referenced to a pressure transducer that can measure absolute pressure. These, along with other steady transducers that were used are identified in Table 4-2.

Measurand	Measurand Range / Bar abs	Sensor	Range / Bar abs
Intake Air	0.05 – 1	GE Unik 5000	0 – 1.6
Turbine Inlet Gas	0.05 – 6	Delta Ohm HD9408T	0 - 10
Turbine Outlet Gas	0.05 – 6	Delta Ohm HD9408T	0 - 10
Low Pressure Manifold Gas	0.05 – 4	Delta Ohm HD9408T	0 - 10
Combined Exhaust Gas	0.05 – 5	Delta Ohm HD9408T	0 - 10
Compressor Inlet Gas	0.05 – 3	Delta Ohm HD9408T	0 - 10
Turbocharger Oil Inlet	0.5 - 4	Delta Ohm HD9408T	0 - 10
Turbocharger Oil Outlet	0.5 - 3	Delta Ohm HD9408T	0 - 10

Table 4-2 - Steady Pressure Summary

Both types of sensor provide a 4-20 mA current output which was fed into the NI 9203 module of the compact DAQ, whose input range was ±20 mA. The conversion between current output and pressure was performed in the Labview VI such that the data logged was the measured pressure in bar.

Intake Pressure

A 0-1.6 bar absolute pressure GE Unik 5000 piezo-resistive transducer was specified to measure intake air pressure. There are three different accuracies available, and the one chosen was the most accurate, varying by up to 0.04% over the full scale of the sensor. This transducer was mounted in the intake manifold after the throttle body before it split into individual runners.

Exhaust Gas Pressure

The average exhaust gas pressure was measured in 5 locations; the turbine inlet, turbine outlet, low pressure manifold, the point at which the low and high pressure manifolds combine and the compressor inlet. This was done to allow the transient pressure transducers to be pinned to the correct absolute value as well as to give an indication of system effectiveness.

The transducers used were Delta Ohm HD9408T series with a 0 – 10 bar absolute pressure range. Further specifications can be found in Table 4-3.

Output	4-20mA current signal
Accuracy	±0.3% of reading at 20°C
Response time	0.5 seconds
Physical connection	1/4 in BSP parallel
Over pressure limit	twice the rated value
Electrical connection	via supplied connector to DIN 41524
Ambient operating temperature	-10°C to +70°C

Table 4-3 - Delta Ohm steady pressure transducer data

The temperature of the exhaust gas that these sensors were required to measure exceeded their safe operating temperature. As such, the transducers were all mounted remotely; a 300 mm minimum length of stainless steel pipe was connected to the exhaust using Swagelok fittings, which was then connected to a length of nylon hose which in turn was connected to the pressure transducer. The only transducer that was mounted directly onto the exhaust was the compressor inlet transducer as the temperature at this point had to be controlled to less than 150°C so as not to overheat the compressor wheel, so remote mounting was not necessary.

4.5 Exhaust Gas Temperature

Measuring the temperature of exhaust is somewhat more difficult than measuring exhaust pressure. The most common method of measurement, thermocouples, have a trade off in that if they are thin enough to react to transient exhaust gas temperature fluctuations they are generally not able to survive in the environment of high temperature, pulsing and corrosive exhaust gases. For the purpose of this work steady exhaust gas temperatures were considered sufficient to validate the model, and as such 1.5 mm Chromel-Alumel k-type thermocouples were used with an accuracy of 0.75% up to 1250°C.

The exhaust gas temperature measurement locations are shown in the overall instrumentation diagram Figure 6-14. They were inserted perpendicular to the direction of flow with the tip of the thermocouple centrally located in the duct. Each thermocouple was mounted in a 1/8" BSP compression gland to ensure no gas leakage.

The signal from each thermocouple is processed by the NI 9213 thermocouple input module in the compact DAQ.

4.6 Turbomachine Speed Sensor

To measure the rotational speed of the turbomachine a Picoturn PT2G eddy current sensor was used. This sensor, when fitted to the Turbo-Discharger compressor, switches the output signal between 0 and 5 V when a blade passes. This produces a pulsation frequency of half that of the blade passing frequency from which, for a specific compressor wheel with a known number of blades, the shaft speed was calculated.

It is important that the sensor is mounted securely, as close to the compressor wheel as possible, in the compressor housing. The maximum clearance is limited to 1 mm, beyond which the sensor is not guaranteed to function. The sensor relies on the passing blades to disrupt a generated field, in doing so switching the CMOS signal from high to low or vice-versa, therefore both mounting depth and angle are important to ensure a good quality signal.

The signal from this sensor is fed into the high speed TTL module of the DAQ system. It is a 5V CMOS square, symmetrical signal that was processed by the NI 9401 high speed TTL module and Labview.

4.7 Closing Comments

This chapter has described the baseline engine experimental test system and justified the equipment and methods used to gather data.

The following chapter details the development of 1-D models for a naturally aspirated engine and a Turbo-Discharged engine including the validation of the naturally aspirated engine model with measured engine data.

5. One-Dimensional Model Development

This chapter will describe the assumptions that were made in the development of the one-dimensional gas dynamics engine model in Ricardo WAVE that is used throughout this thesis.

The purpose of this chapter is to show how the model was developed and quantify the confidence in its predictions.

The three objectives of the 1-D modelling in this thesis are to:

1. Generate a baseline model that sufficiently accurately represents the NA engine to allow for comparison of gas dynamic behaviour between NA and Turbo-Discharging systems.
2. Modify this baseline model with a Turbo-Discharging system to aid development of the experimental Turbo-Discharging experimental rig.

3. Enable a more complete investigation into the potential of Turbo-Discharging beyond the experimental hardware limitations.

5.1 One-Dimensional Engine Model

One Dimensional engine models solve pipe or duct flows by solving one-dimensional compressible flow equations coupled with sub models. The pipe networks are discretised into control volumes. For each control volume changes in energy and mass are calculated and at each control volume boundary momentum of the gas is calculated (Ricardo plc 2009). The model is created through a graphical user interface (GUI) where junctions, orifices and sub-models are connected with ducts defined as arrows. Values for relevant variables are entered against each element of the model along with desired operating conditions. The model is then run using a solver, iterating until all elements have achieved the input convergence criteria. The output can then be explored using a post-processing programme.

It is important to highlight that the purpose of this model is to provide a baseline against which to compare the relative benefits of Turbo-Discharging. It will not be used to predict absolute values of fuel economy.

The convergence criteria used to control solver accuracy was 5 consecutive cycles with a variance of 1% for solved pressures, velocities and wall temperatures, whilst the PID controller used to control BMEP was set to a variance limit of 0.005 bar.

Figure 5-1 is a schematic of the 1-D baseline engine model. Air enters the system from a fixed pressure ambient element. The inducted air passes through an orifice and a butterfly type throttle valve before splitting into the four branches of the intake manifold. Fuel is injected in the intake ports before the air passes through the intake valves into the cylinder. Following the compression, combustion and expansion processes the burned gases are exhausted from the cylinder flowing into the exhaust manifold runners. They combine in the exhaust manifold, pass through a catalytic converter and silencer before finally exhausting to atmosphere.

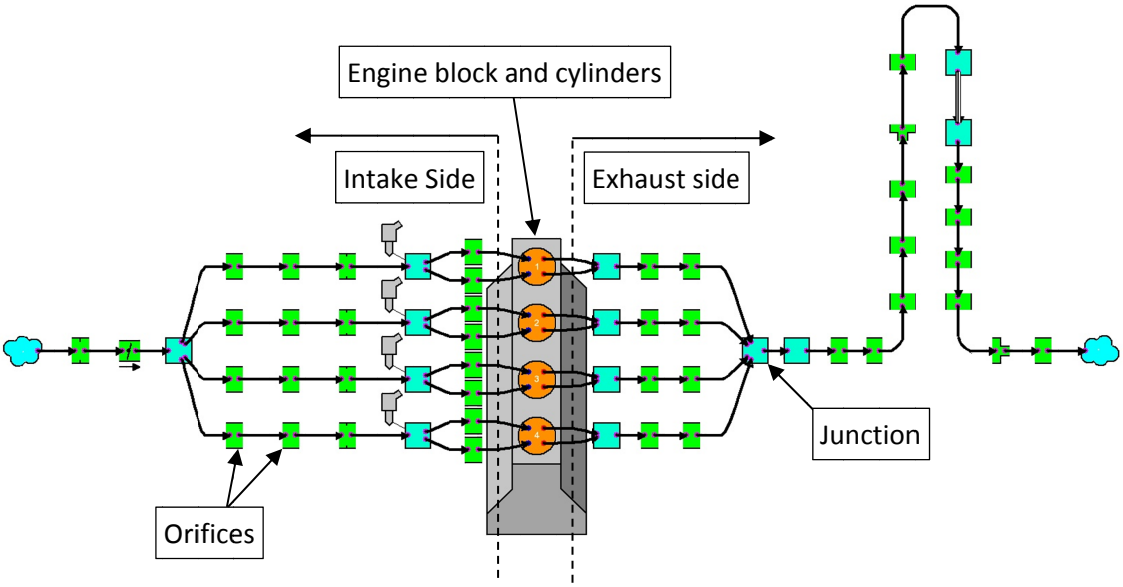

Figure 5-1 - Schematic of baseline 1-D engine model

An orifice was included upstream of the throttle valve to simulate the flow losses experienced by the air cleaner and associated pipework. Flow coefficients for the throttle valve were assumed to allow control of the mass air flow, but no correlation is made to throttle angle throughout this work.

The ducts downstream of the throttle valve and in the exhaust manifold were first geometrically modelled as per the pipework on the baseline engine, and then loss coefficients were modified to replicate the pressure losses and heat flows as accurately as possible.

The heat transfer external to the cylinder was calculated for the exhaust side and the intake ports only. The wall temperature of the intake ports was fixed to 373 K; a reasonable assumption as the engine was only tested in warm steady state operating conditions. A wall conduction model was used to calculate the temperature of the exhaust pipework based on the gas temperature, the temperature of the wall elements adjacent to it, ambient temperature, material thickness and heat capacity.

The fuel used in the model was Indolene (C 7.3, H 13.9) which was selected as a close match to the 95 octane fuel used in the engine test facility. This was found to give good correlation to heat release rates which will be shown later in this chapter.

The fuel-air ratio of the model was controlled using proportional injectors. These inject fuel at a rate proportional to that of the air mass flow rate to achieve the specified air-fuel ratio. 10% of the fuel was considered vaporised and 90% of the fuel mass liquid immediately after

injection. A further 30% of the liquid fraction was evaporated following the injection. The air-fuel ratio was adjusted to that measured from the engine in the test cell for each operating point, which was typically stoichiometric.

5.1.1 Closed-Cycle Cylinder Calibration

The term closed-cylinder calibration refers to the part of the cycle where the intake and exhaust valves are shut. For this work, the Wiebe combustion model was chosen.

The Wiebe function is an approximation of the heat release generated by combustion. It is a mathematical function which approximates the burn profile from input parameters either estimated or measured and calculated from a cylinder pressure trace. The function is

$$W_n = 1 - exp[-a(\theta_i - \theta_o)^{m+1}] \quad \textbf{5-1}$$

where W_n is the non-dimensional cumulative burn rate, θ_i is the engine crank angle, $\theta_0$is the crank angle at the start of combustion, $\Delta\theta$ is the combustion duration and a and m are adjustable parameters to allow the function to be matched to the measured burn profile.

Adjustable parameter a is modified to allow the combustion duration to instead use the 10-90% burn duration. This is beneficial as there can be significant variance in the first and last 10% of the burn profile, resulting in an incorrectly modelled burn profile.

The other user adjustable parameter m is then used to control the bias of the burn profile; a value of 2 leads to an even burn profile, values less than 2 lead to a faster burn of fuel before the 50% burn point, whilst values greater than 2 lead to slower burn of fuel before the 50% burn point. This skewing of the burn profile may be necessary to compensate for charge motion around the spark plug to account for fast or slow flame propagation. For the purposes of this investigation the exponent was not varied as sufficient accuracy to measured results was obtained without variation.

The burn profile in WAVE was then used to calculate the cylinder pressure and temperature. The appropriate portion of fuel is burned as the model progresses through the cycle according to the burn profile, mass flowrate of air and the specified air-fuel ratio.

The sensitivity of the mass air flow to the 50% burn point and 10-90% burn duration is shown for two engine operating points in Figure 5-2. The engine mass airflow is critical in predicting engine performance, and it can be seen that varying the 10-90% burn duration by up to 5° CA has no significant effect on mass airflow. Varying the location of the 50% burn point has more influence on the mass airflow, up to 5% at 1500 rpm, 6 bar BMEP. This has a direct influence on the fuel mass flow rate due to the proportional injectors and fixed air-fuel ratio.

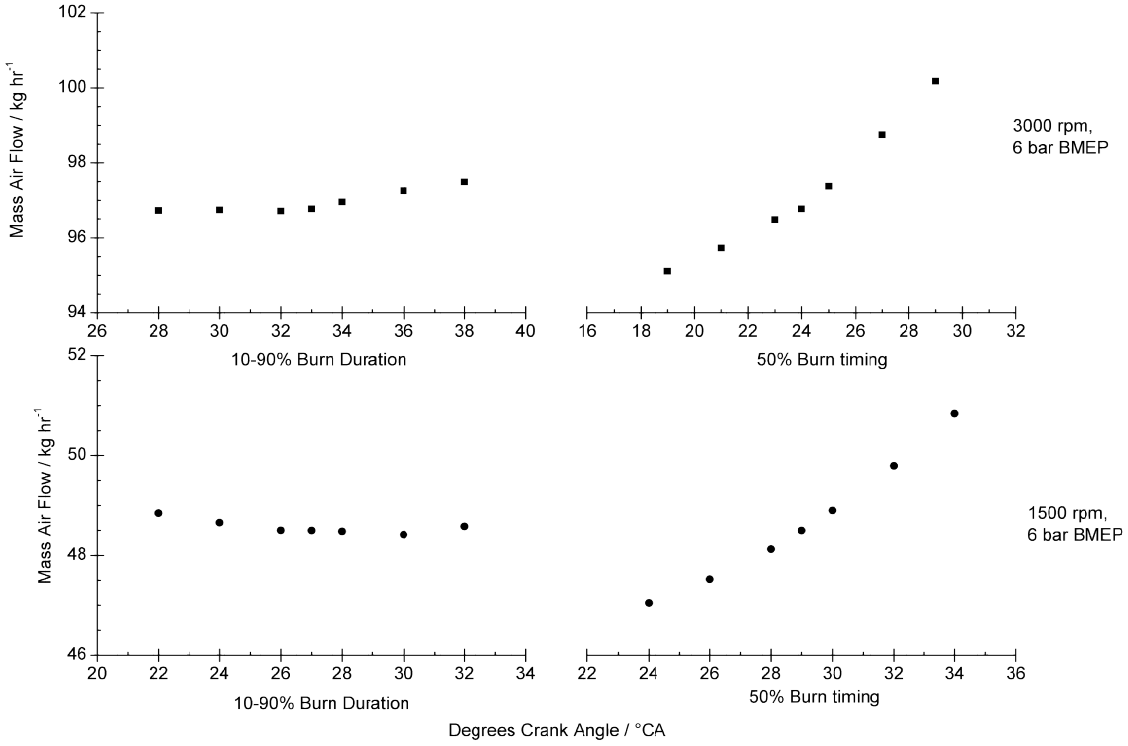

Figure 5-2 – Modelled variance in engine mass airflow through varying 10-90% burn duration and 50% burn point at 1500 rpm and 3000 rpm, 6 bar BMEP where positive crank angle values are after TDC

Speed sweeps from the model at various engine loads show that the time to the 50% burn point from the engine ignition timing varies by up to 2.5°CA for a particular engine speed. Therefore it is acceptable that the offset to the 50% burn point from ignition, and the 10-90% duration will be fixed for each speed, and are shown in Figure 5-3.

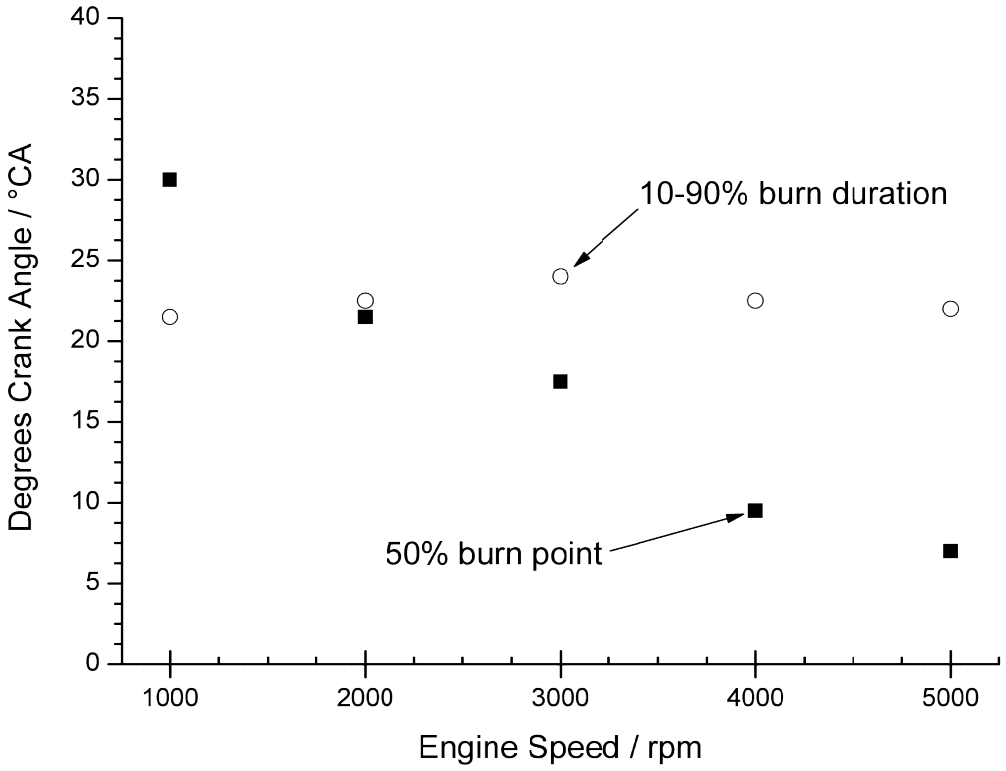

Figure 5-3 - 50% burn points and 10-90% burn durations used in the Wiebe combustion model correlated against experimental data

Heat Transfer

For the in-cylinder processes the Woschni (1967)heat transfer model with load compensation was used. The equation to calculate the heat transfer is

$$h_W = 0.0128 D^{-0.02} P^{0.80} T^{-0.53} {v_c}^{0.8} C_{enht} \qquad \textbf{5-2}$$

where h_W is the heat transfer coefficient, D is the cylinder bore, P is gas pressure in the cylinder, T is the gas temperature in the cylinder, v_c is a characteristic velocity and C_{enht} is a variable.

The characteristic velocity, for the load compensated model, is calculated as

$$v_c = max\left[\left(c_1 v_m + c_2 \frac{V_D T_r}{P_r V_r}(P - P_{mot})\right), \left(c_1 v_m (1 + 2\left(\frac{V_c}{V}\right)^2 IMEP^{-0.2})\right)\right] \qquad \textbf{5-3}$$

where v_m is the mean piston speed, V_D is the cylinder displacement, T_r is a reference temperature, P_r is a reference pressure, V_r is a reference volume, P_{mot} is the motored cylinder pressure, V_c is the cylinder clearance volume and V is the instantaneous cylinder volume. The reference pressure, temperature and volume were all assumed to be atmospheric in the 1-D model. The constant c_1 is equal to 6.18 during scavenging and 2.28 when the valves are closed, and c_2 is equal to 3.24×10^{-3} during combustion and 0 before combustion and during scavenging.

The first part of equation 5-3 is Woschni's original correlation which calculates the characteristic velocity as the sum of the mean piston speed and an additional velocity that is dependent on combustion and the difference in pressure between a motored and firing condition (Ricardo plc 2009). The second correlation is still a function of mean piston speed but includes cylinder volume and IMEP terms. The maximum value of these two terms is used to calculate the characteristic velocity.

The heat transfer model was important in achieving the correct cylinder pressure at the end of compression. An adequate balance between the 'valves closed' and 'valves open' heat transfer coefficient multipliers was found, the result of which is shown below in Figure 5-4 for 1500 rpm, 6 bar BMEP.

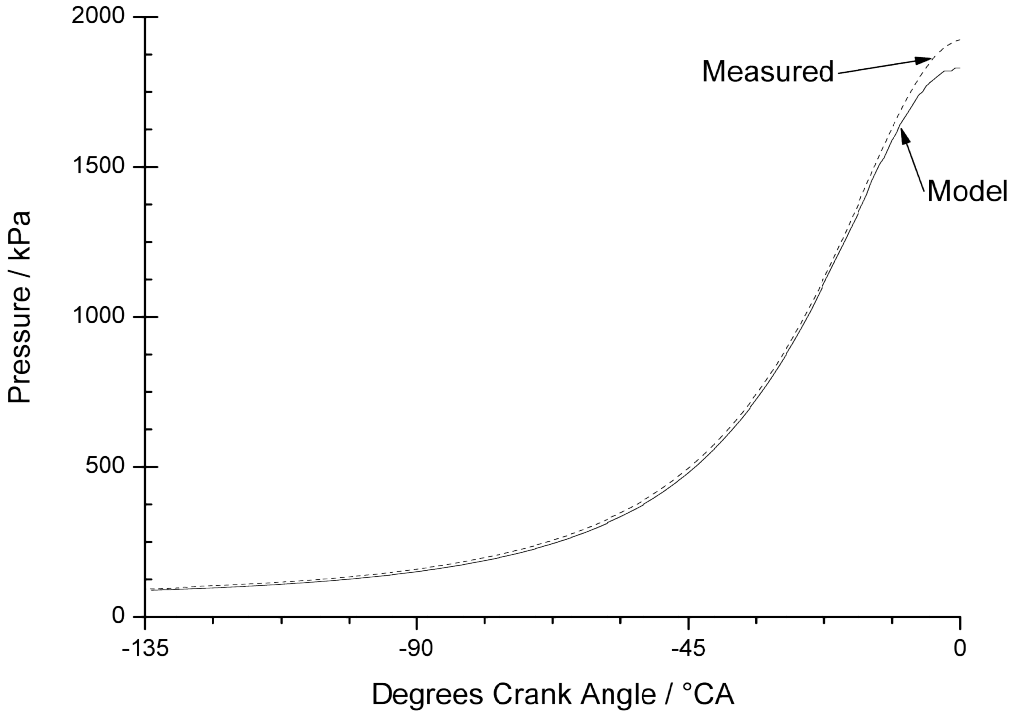

Figure 5-4 - Cylinder pressure trace showing the end of the intake and compression strokes for the NA engine at 1500 rpm, 6 bar BMEP

5.1.2 Gas Exchange Process Calibration

The intake process is crucial for accurately predicting engine performance as it governs the charge air admitted to the cylinder, from which most other engine parameters result.

Although flow rig measured valve flow coefficients were available they proved inadequate, in agreement with previous reports by Blair and Drouin (1996).

There are a number of sources of error when measuring flow coefficients on a steady state flow rig that could account for the tuning necessary when using measured values in a 1-D model. One of the most important differences is the lack of a piston on most steady flow rigs. The piston will have a significant effect on the flow into or from the cylinder when close to TDC, changing the angle the gas approaches or exits the valve. The author suggests that further work could help identify the effect of piston to valve proximity on flow coefficient, which may help improve 1-D model calibration in the future.

Thus, it was decided to tune valve flow coefficients based on those supplied within Ricardo WAVE to match the cylinder pressure trace during the intake and exhaust strokes over the engine operating speed and load range. The final intake flow coefficients used are shown below in Figure 5-5.

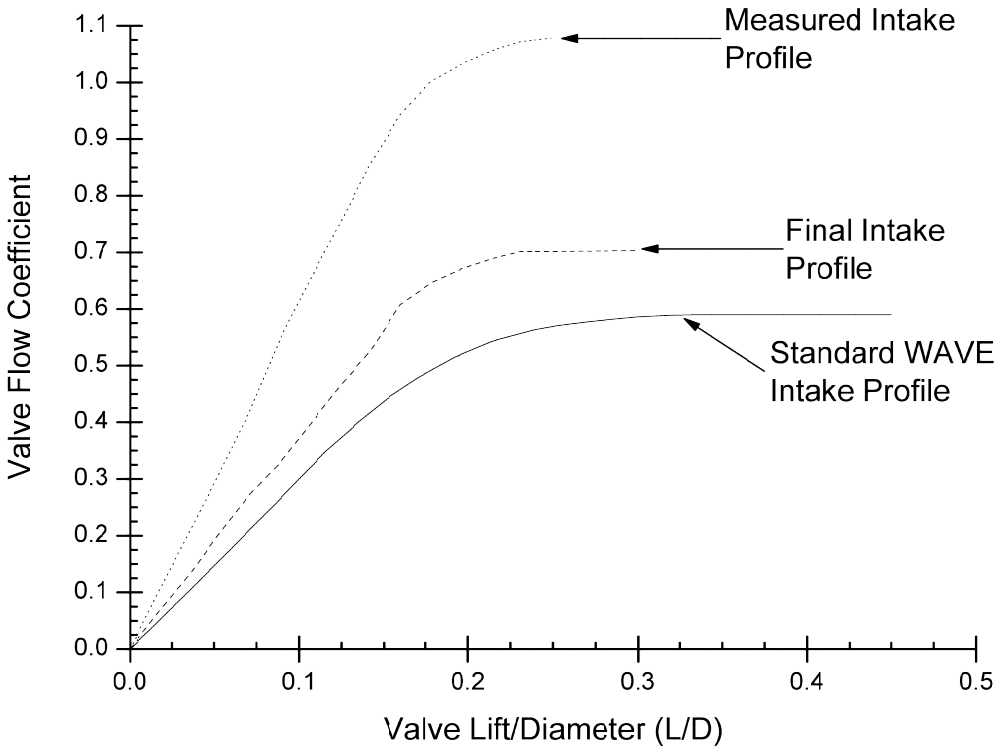

Figure 5-5 - Valve flow coefficients from NA engine 1-D model plotted against valve lift divided by diameter (L/D)

The result of the calibrated intake valve flow coefficient is shown in Figure 5-4, and the modelled charge airflow is presented in section 5.1.3.

Accurate definition of the exhaust valve flow coefficients was also important to ensure the exhaust gas contains the correct amount of energy. This was especially important when the model was modified to include the Turbo-Discharging system, which will be discussed further in section 7.4.

To assess the gas exchange process the cylinder pressure trace generated by the model was assessed against that measured from the engine. This was done for several speed and load points, an example of which is shown below in Figure 5-6.

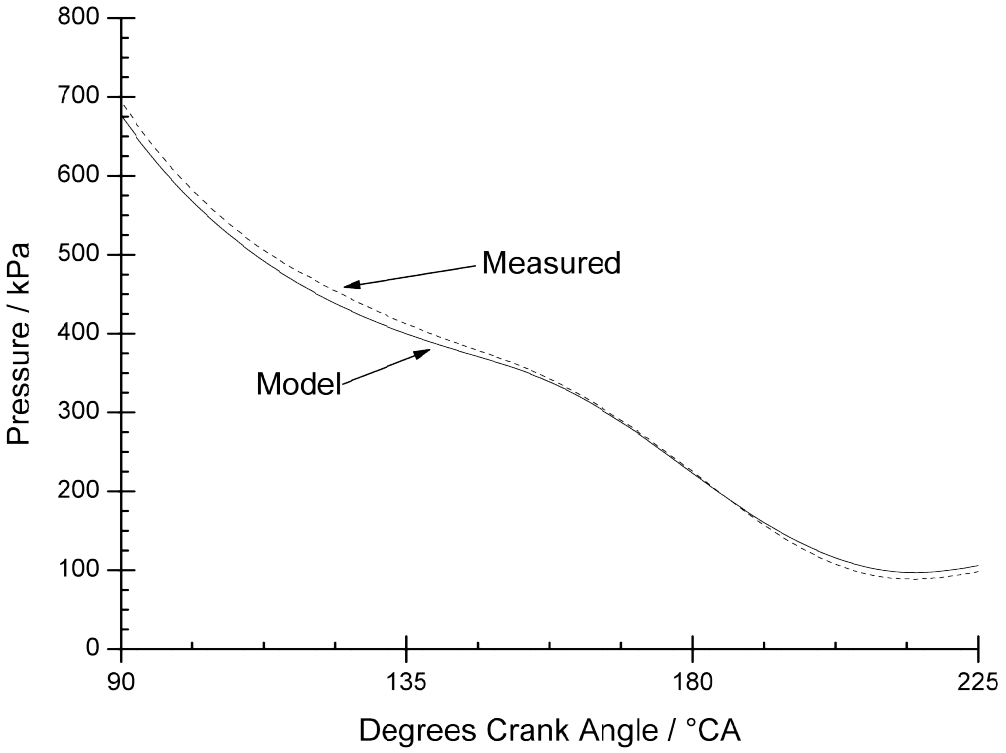

Figure 5-6 - Cylinder pressure during the exhaust process of the NA engine operating at 1500 rpm, 6 bar BMEP

This data, and other cylinder pressure traces at different speeds and loads all sufficiently accurately matched that of the measured data both in terms of absolute values and pressure profiles. It was therefore decided that, for the NA engine model, the standard WAVE valve flow coefficients without additional tuning were sufficient.

5.1.3 Full Load Calibrated Model Performance

It is important to show that the modelled airflow behaves accurately in the limit condition, i.e. at full load. A good correlation of airflow in the limit condition of full load generally means that the behaviour of the model at part load should be acceptable.

Figure 5-7 shows the volumetric efficiency of the model versus that measured from the engine. There is a similar general trend of the model compared to the measured data, however, there is a variance of up to 12% at 1000 rpm. The explanation for this may be that the intake pressure and temperature were measured in the intake manifold before the gas diverged into the individual intake runners. The actual pressure in the individual intake runners may be lower, and the temperature may be higher, resulting in a lower density. This would lead to an increased volumetric efficiency, more similar to that of the model.

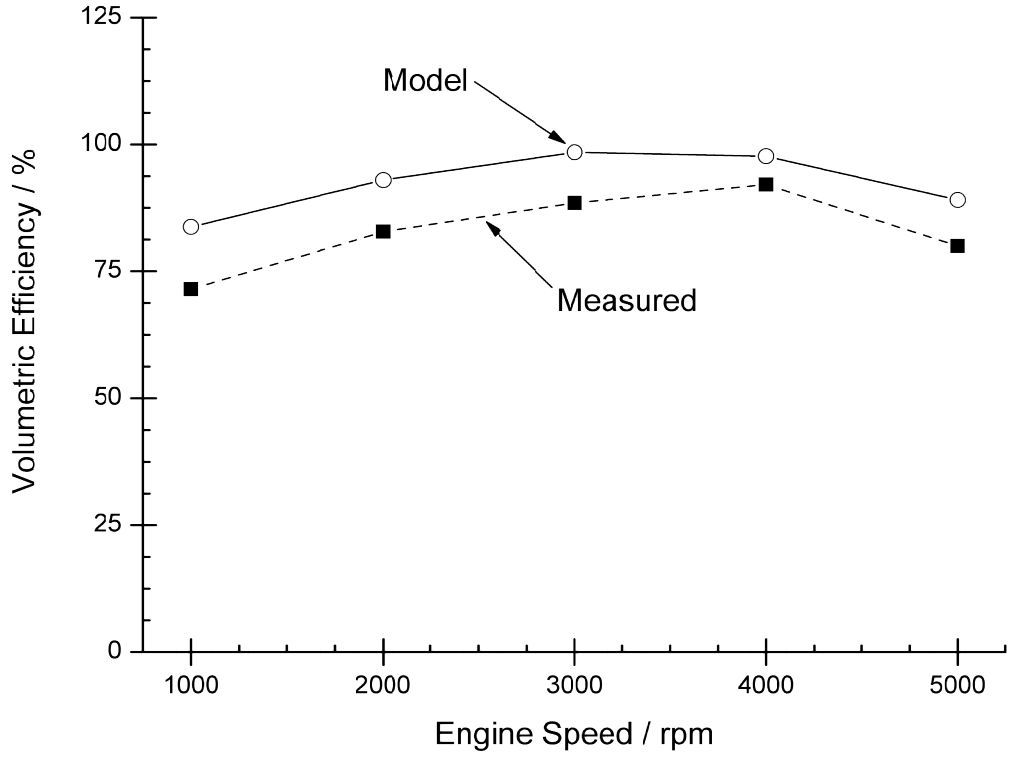

Figure 5-7 - Measured and modelled volumetric efficiency at WOT over the engine speed range

To prove whether the discrepancy in volumetric efficiency was due to measurement error, Figure 5-8 shows the modelled intake air mass flow versus that measured on the engine. It can be seen that these show good agreement throughout the engine speed range, thus it is likely

that there is some error in measurement accuracy in the calculation of the volumetric efficiency.

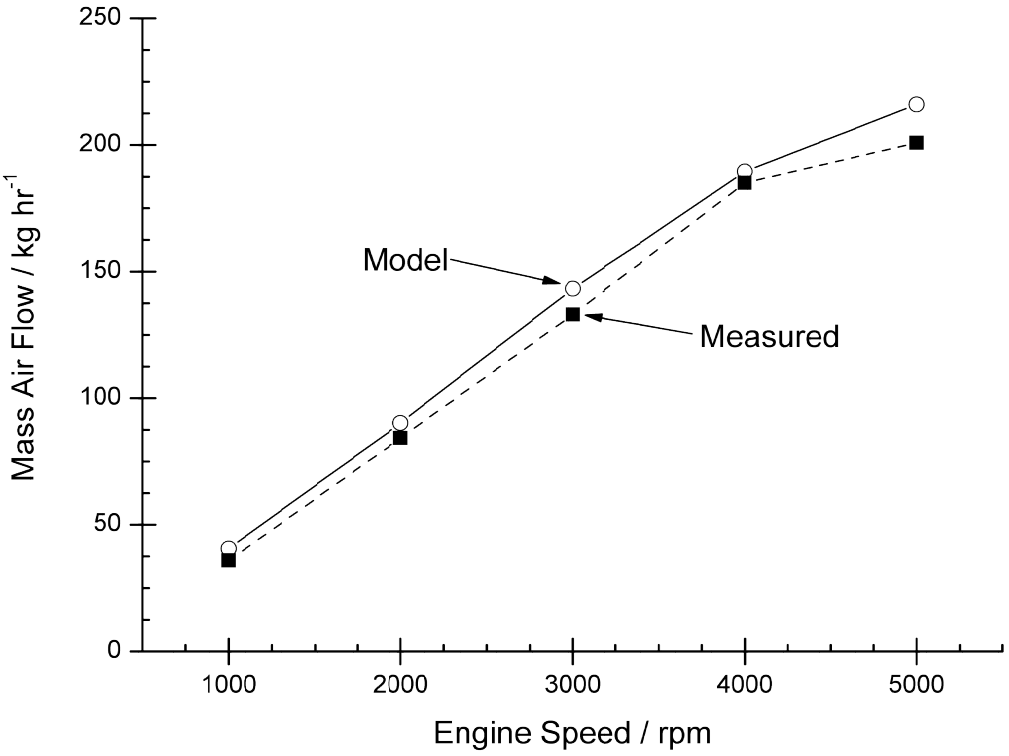

Figure 5-8 - Intake mass airflow of the model compared to the measured value

To further improve the accuracy of the modelled mass air flow to that measured from the engine it would be necessary to tune the heat transferred to the intake air, the intake and exhaust valve lashes and intake runner loss coefficients across the engine speed and load range. To enable this model to be compared to those used later in this thesis, the aforementioned variables were left fixed and the level of accuracy acceptable.

The engine load achieved at WOT for both the modelled and testbed engine are shown in Figure 5-9. It follows that as the intake mass airflow is a good match to the measured value, the modelled BMEP will also correlate well.

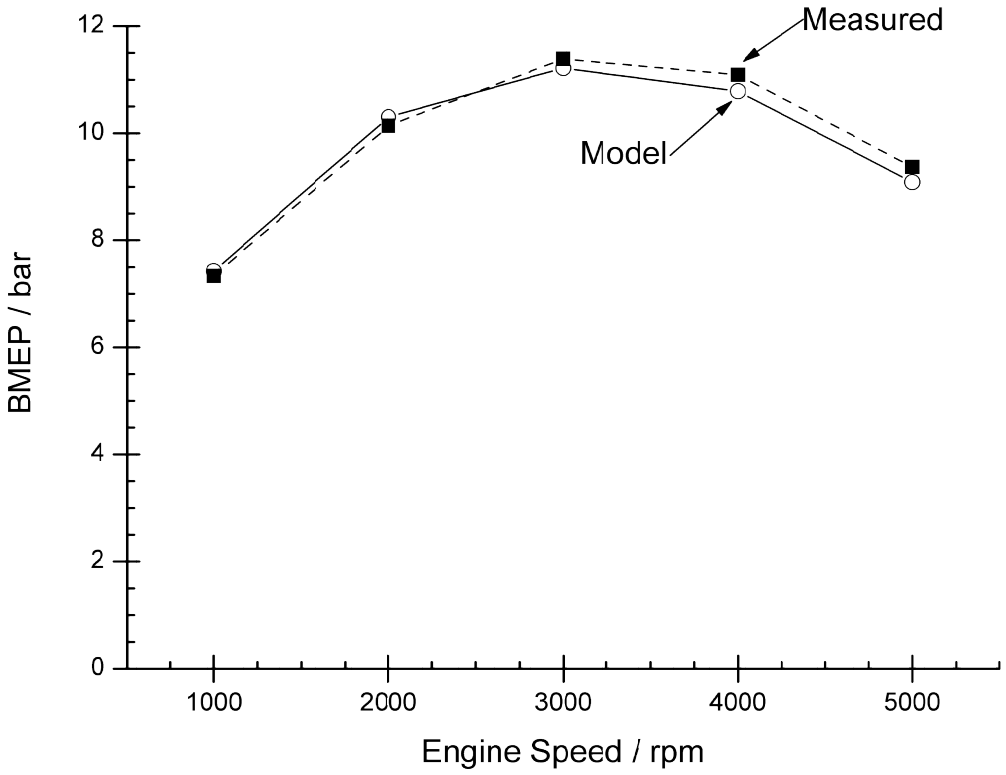

Figure 5-9 - WOT engine BMEP for the engine and model

Thus, the performance of the model at WOT can be considered adequately calibrated for the purposes of this investigation.

5.2 Part Load NA Model Validation

To confirm part load performance of the model a load sweep at 3000 rpm was completed. Figure 5-10 shows a comparison between the measured and modelled engine volumetric efficiency.

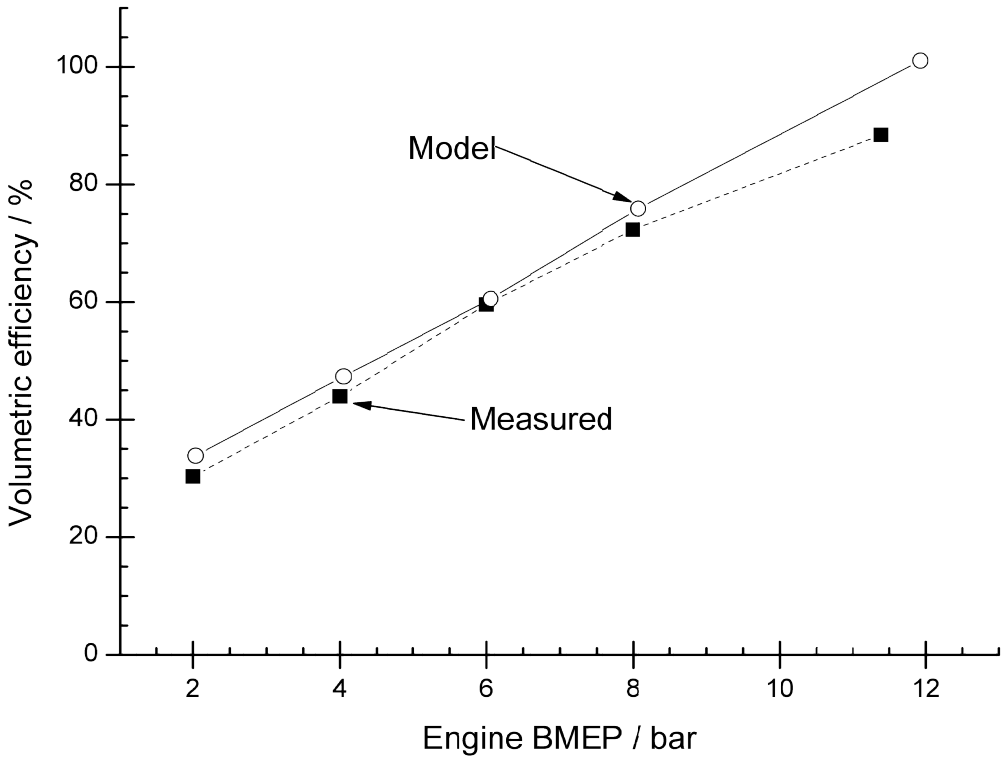

Figure 5-10 - Volumetric efficiency vs Engine BMEP comparison between measured data and 1-D engine model at 3000 rpm

The model shows acceptable correlation to the measured data. This is confirmed by the engine mass air flow, presented in Figure 5-11.

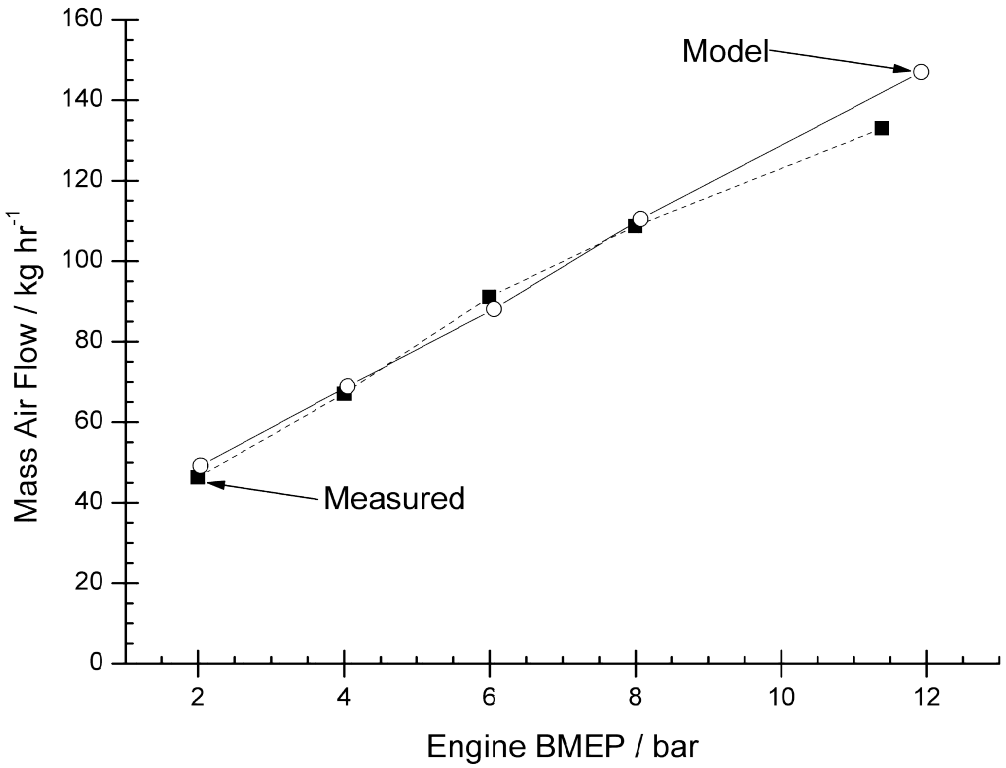

Figure 5-11 - Modelled and measured engine mass flow at 3000 rpm

It should be noted that the model can achieve a slightly higher peak load at WOT. This is likely the result of a slightly higher volumetric efficiency at higher engine air mass flows. With further tuning of the intake manifold runner lengths and loss coefficients it may be possible to more accurately replicate the measured engine performance. However, the focus of this model is to provide a baseline to compare Turbo-Discharging against, and if the same intake manifold geometry is used then the Turbo-Discharging model will have the same limitations in volumetric efficiency. Thus, this is sufficient for this investigation.

5.3 Turbo-Discharging Model Construction

The validated naturally aspirated engine model was modified to include the Turbo-Discharging system by integrating a turbomachine and heat exchanger into the exhaust, as well as modifying some other important components and parameters. These changes will be detailed in this section.

5.3.1 Turbomachine Implementation

The turbine and compressor elements in Ricardo WAVE use experimentally measured compressor and turbine performance maps to represent the real compressor or turbine. The data for this is typically taken from the maps created by the manufacturers on steady flow gas stands, which is then interpolated and extrapolated within WAVE to create a lookup table.

The implementation of the compressor and turbine elements into the model will now be discussed. The turbomachine matching for the experimental rig will be discussed in section 6.2, and the turbomachine matching method will be discussed in more detail in section 9.2.

Compressor

For the compressor, there are three methods available in the software for extrapolating the measured data to create these maps; classic physics, momentum physics and momentum physics with reversed flow. The classic physics model assumes the flow through the compressor behaves in a quasi-steady manner. This requires that the lines of constant speed on the compressor map always retain a negative gradient (there is an option within WAVE to force this). The limitations of this model are that it cannot be used to model reversed flow or surge through the compressor.

The momentum physics option uses a model developed by Greitzer (1976) and subsequently Fink *et al* (1992). This method has significant advantages over the classic physics method including allowing the use of positive-gradient constant speed lines on a steady state compressor map, the elimination of time step size dependant oscillations when the compressor is operating left of the surge margin and an improvement in dynamic behaviour which improves prediction of pulsations over the whole compressor map.

The final compressor model option includes extrapolation into the reverse flow region.

The model chosen was the momentum physics without reverse flow for the reason that reverse flow should not be required for the modelling work being undertaken. This is due to the high compressor mass flow and comparatively low shaft powers; high mass flow will drive the compressor operating point away from the surge line. Also, some of the compressors being considered for this work had positive speed line gradients within the main body of the compressor map, therefore the classic physics model was not applicable.

The moment of inertia for the turbomachine used is not known, however, all of the simulations for this part of the project are steady state. Inertia is important for transient simulations but it should not substantially affect a steady state result provided there are negligible rotor speed variations during a single crank revolution.

Compressor maps tend to have little or no data at low speed, mass flow or pressure ratios. The thermodynamic calculations demonstrated that only low to moderate pressure ratios can be expected across the Turbo-discharging compressor such that it will be operating almost exclusively in the low speed portion of the map. With further work it may be possible to measure this area of the map more accurately and thus improve the accuracy of the simulation in this area. However, this is a necessary limitation at this time as there is no data available.

Turbine

The turbine map is generated in the same manner as the compressor map in that measured values from the gas stand are interpolated and extrapolated to produce sufficient data to run the model.

However, there was an issue with the turbine compared to the compressor. There was only limited data available for the turbine in that the one line provided was that of highest mass flow and was made up from the peak mass flow from every constant speed line. This is not enough data to accurately reconstruct a turbine map, so an existing turbine map was scaled to fit the limited data provided by Garrett using the mass flow and speed scaling factors in the turbine settings panel. The accuracy of this solution will be discussed in the model calibration section 7.1.

5.3.2 Other Engine Model Modifications

Manifold Geometry

The first major modification of the model was to construct a manifold with divided exhaust paths for the high and low pressure gases, as per the schematic in Figure 2-5.

The high pressure exhaust gases exit the cylinder into a small volume exhaust manifold. The flow paths from each cylinder combine before passing through the turbine. The low pressure gases exit the cylinder via short runners into a log type manifold constructed from zero-length ducts linking junctions. This is a comparatively large diameter exhaust manifold with significant length, giving a large volume. The two exhaust paths then re-combine before passing through a heat exchanger, modelled by a multiple count duct of 600 4 mm diameter ducts. This provides significant cooling to the gases before they pass through the compressor, and finally exhaust to ambient.

To allow for accurate prediction of material temperatures in the exhaust manifold the global conduction and heat transfer model was enabled. This, given the thickness, heat capacity and thermal conductivity of the material, along with the gas and ambient temperature allows for condition specific calculation of the manifold temperature. This allows the potential for a much more accurate prediction of exhaust gas temperatures by taking into account the heat transfer to and from the surroundings.

Valve Timing

The second significant modification for Turbo-Discharging is the split exhaust period with independent operation of each exhaust valve. This was achieved by specifying two different types of exhaust valve per cylinder, and assigning each valve a custom profile as shown in Figure 5-12.

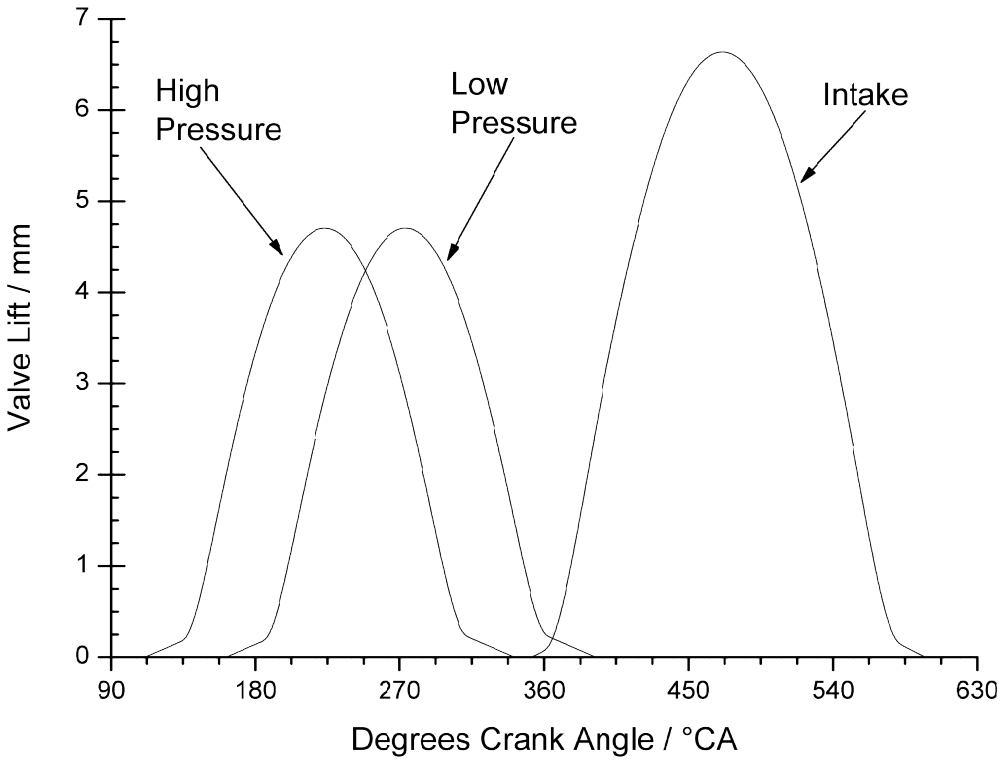

Figure 5-12 - Valve lifts chosen for Turbo-Discharging

The profiles used were developed from the standard Ford profile. The reason for this is WAVE provides a simple method of altering the duration and lift of a profile by use of multipliers, so it is possible to run the model varying the valve profile for each case to ascertain which performs best.

One limitation of these profiles is that the engine uses a flat follower, therefore the camshaft cannot have any indentation or negative change in profile gradient; this will be explained more thoroughly under valve events in chapter 6. Also taken into account were the valve velocity and acceleration limits.

The consequence of this is that the choice in valve profiles was more limited than it may be with more modern variable valve systems such as Fiat Multiair (Fiat Powertrain Technologies S.p.A 2009).

5.4 Closing Comments

This chapter has shown how a baseline 1-D model of a NA engine was developed, calibrated and validated, beginning with measuring values from the baseline engine and then explaining how these were incorporated into the model.

It was then explained how this initial model was modified into a Turbo-Discharging model, both in terms of component addition and other engine parameters that had to be altered to accurately represent a Turbo-Discharging model. Optimisation of these variables is covered in Chapter 7.

The next chapter will introduce the Turbo-Discharging experimental system which will be used to calibrate and validate the Turbo-Discharged engine model.

6. Turbo-Discharging Experimental System Design

This chapter will present experimental objectives, and then explain in detail how the naturally aspirated test engine was modified and instrumented to include a Turbo-Discharging system.

6.1 Experimental Objectives

The two main objectives for the experimental testing portion of this research were:

1) To gather sufficient data to validate the model elements specific to Turbo-Discharging such that it could be used for further investigation of the concept
2) To help identify and quantify hardware limitations and technological risks associated with Turbo-Discharging.

6.2 Turbomachine Matching

It is important for a conventional turbocharger to be sized, or matched, appropriately to an engine for maximum performance and efficiency, but also for transient response. Similarly it is important that the Turbo-Discharging turbomachine is matched correctly to the engine, however, there are significant differences that mean standard matching procedures will not lead to an optimal match.

In contrast to a conventional turbocharging system the Turbo-Discharging arrangement considered here makes use of all the available exhaust gas energy all the time; energy extraction from the turbine is not managed using a wastegate or a VGT. As such it is prudent to begin the matching procedure with the turbine, optimising the amount of energy it can extract.

All of the exhaust gas in a conventional turbocharged engine flows through the turbine. This means that both the blowdown and the displacement portions of the exhaust gas impart work on the turbine. The Turbo-Discharging system is designed such that only the blowdown gases impart work on the turbine. Thus the turbine is exposed to higher magnitude pulsations and less net mass flow than on a conventional turbocharged engine, as can be seen from the modelled data in Figure 6-1.

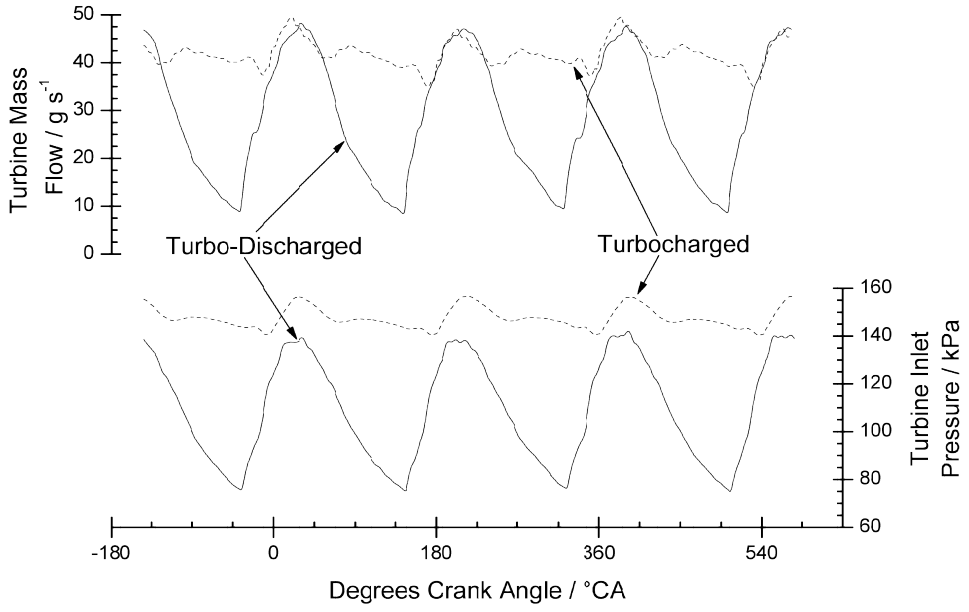

Figure 6-1 – Turbine mass flow and inlet pressure for a turbocharged and Turbo-Discharged engine at 3000 rpm WOT

The fact the mass flow through the turbine is decreased would, from conventional turbocharger steady state matching procedures, prescribe a smaller turbine. This means the efficiency of the turbine over the average mass flow will be higher, however, the efficiency at the point at which the turbine extracts the most energy is most important. This is particularly important for Turbo-Discharging because of the magnitude of pulsations. Equally, at some points, the mass flow through the turbine drops to almost nothing, and the efficiency at this point is of no interest at all. This can be seen in Figure 6-2, especially so for 2000 rpm where there is less energy in the cylinder at EVO.

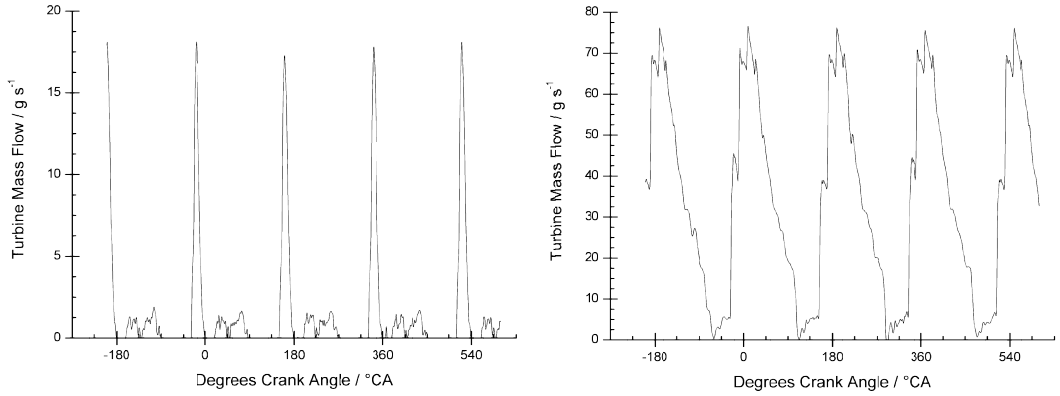

Figure 6-2 - Turbine mass flow versus crank angle at WOT for 2000 rpm (left) and 5000 rpm (right)

Thus, it is suggested that to select a turbine for Turbo-Discharging the mass flowrate needs to be averaged against the energy extracted. This was done using the 1-D engine model, calculating and summing the energy extracted per degree crank angle step. This gives the modified curve as shown in Figure 6-3.

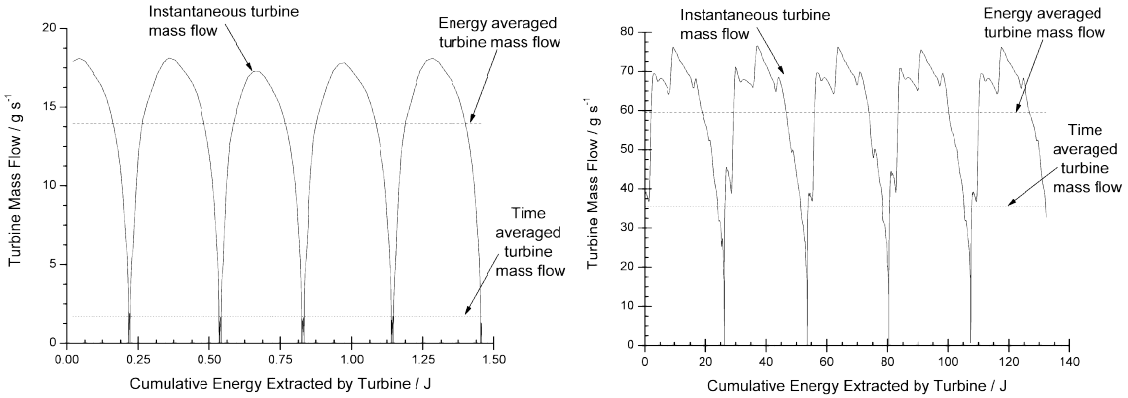

Figure 6-3 - Cumulative energy extracted by the turbine vs Mass flow rate, including time and energy averaged mass flow rates at WOT for 2000 rpm (left), 5000 rpm (right)

It is clear from this graph that the points at which most energy is extracted by the turbine are higher than both the time and energy averaged mass flow rates. However, the energy averaged mass flow rate is almost ten times greater than the time average for the 2000 rpm case which suggests the use of a larger turbine.

This works for the turbine operating in a steady state condition. However, it is currently unclear as to how much of an effect the increased turbine size and inertia will have on the engine and Turbo-Discharging system during a transient manoeuvre. The author realises this is very important in conventionally turbocharged engines, however, in this case the torque benefit due to Turbo-Discharging is much smaller and may not even be perceptible to the driver of the vehicle. This means initially less emphasis can be put on optimising the turbomachine sizing for transient, but should be the subject of further work.

The turbine model was approximated by scaling an existing turbine map to match the choke line provided by the supplier. This data is shown in Figure 6-4, where turbine pressure ratio and mass flow are plotted with lines of constant speed, and data points are shown for the raw data used to generate the full map as well as the data available from the aftermarket turbocharger supplier. It can be seen that the scaled turbine map is a reasonable approximation for the data provided.

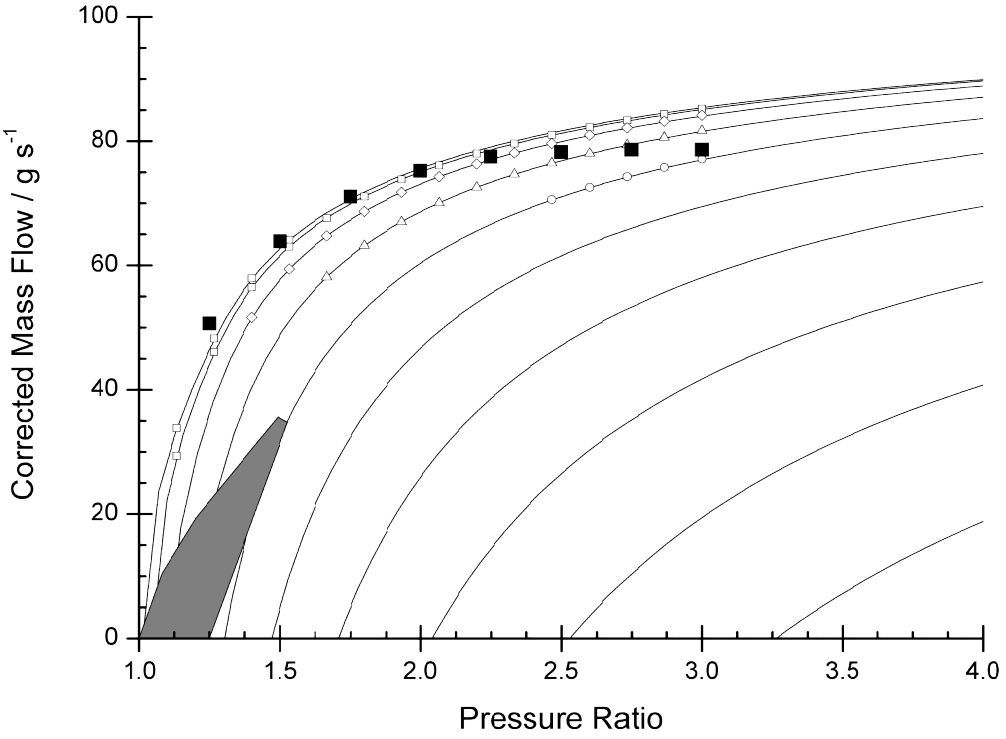

Figure 6-4 – Garrett GT2056 turbine pressure ratio versus mass flow with lines of constant speed where the hollow points represent measured data used to generate the map, solid points represent data used to scale the map and the shaded area shows the operating conditions of the Turbo-Discharging system

The requirement of the compressor is to generate the maximum pressure ratio for a given shaft power. For a conventional turbocharger, engine WOT conditions are generally used to show the operating range over the compressor map, as these conditions define the largest mass flows through and pressure ratios generated by the compressor.

For a Turbo-Discharging system where there is no pressure ratio control the WOT operating curve is more simple. Figure 6-5 shows a Garrett GT2056 compressor map with operating points from Turbo-Discharging shaded in grey.

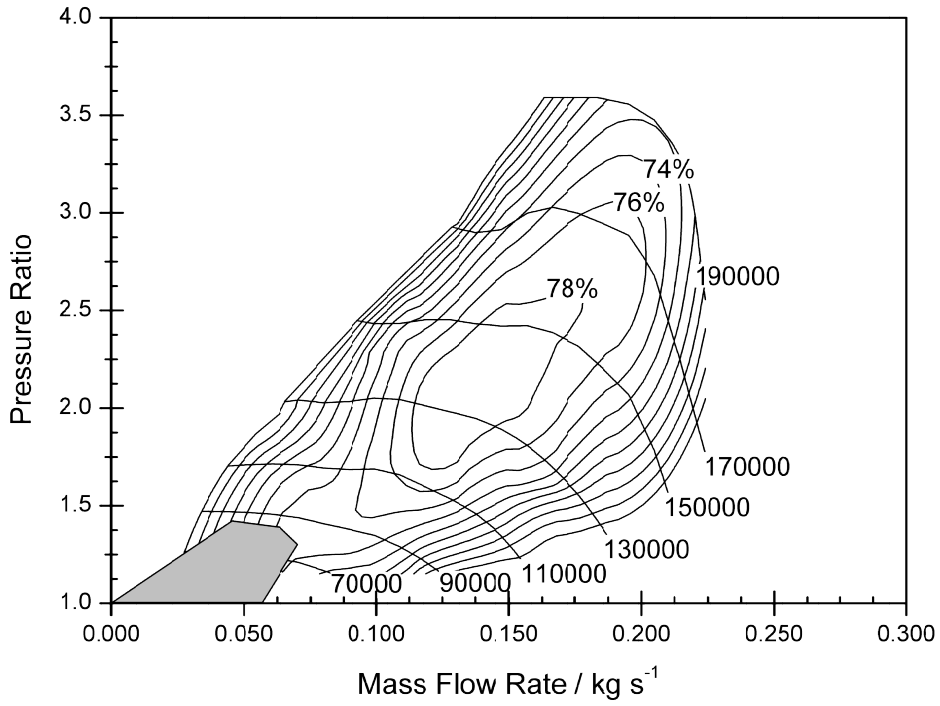

Figure 6-5 - Garrett GT2056 compressor map with lines of constant compressor speed and efficiency, with modelled operating points from Turbo-Discharging shaded in grey

The plotted operating range of Turbo-Discharging only makes use of a small portion of the compressor map. However, for a peak pressure ratio of 1.4, an absolute pressure of 0.7 bar can be generated in the exhaust system. This could be improved upon by choosing a smaller compressor, however, for the purposes of this initial investigation the turbomachines available to use on the experimental system were limited to available aftermarket turbocharger units. The turbochargers considered are shown in Table 6-1.

Type	Bearing type	Compressor			Turbine		
		Wheel Diameter	Trim	A/R	Wheel Diameter	Trim	A/R
		mm	%		mm	%	
1548	Journal	48	60	0.48	41.2	72	0.35
2052	Journal	52.2	48	0.51	47	72	0.5
2056	Journal	56	55	0.53	47	72	0.46
2252	Journal	52	60	0.51	50.3	72	0.67
2259	Journal	59.4	52	0.42	50.3	72	0.56
2554R	Ball	54.3	60	0.8	53	62	0.64
2560R	Ball	60.1	60	0.6	53	62	0.64

Table 6-1 - Available turbochargers for the Turbo-Discharging experimental engine test (Honeywell International Inc 2010)

Similarly to the compressor, the mass flows and pressure ratios generated through the turbine only mean a small portion of the operating range is used for all of the available turbomachines. Therefore, the decision was made to use a GT2056 turbocharger as this was the smallest turbocharger available with common interfaces to other components, allowing it to be swapped easily with other turbomachines in the future.

Optimisation of the turbomachine matching given complete freedom of turbomachine scale is presented in section 9.2.

6.3 Exhaust System

To conserve the kinetic energy in the blowdown gas a small manifold is required. This is so for two reasons:

1. Small manifolds maintain the gas at a higher pressure, decreasing the pressure drop across the exhaust valve which helps to conserve the exergy in the gas.
2. A larger manifold volume has a larger surface area for heat transfer, decreasing exhaust gas enthalpy.

Thus the high pressure manifold was designed to be as small as possible; the distance of the turbine inlet flange from the cylinder head was minimised, the inner-most exhaust ports were chosen to minimise gas path length and 22.2 mm internal diameter tube was used. The finalised manifold design is shown in Figure 6-6.

A compromise was made in that bosses for both fast pressure transducers and thermocouples were included in the manifold. Including these meant the length of each runner was effectively doubled, giving scope for reduction of manifold volume and improvement in system performance in future systems.

Conversely the low pressure manifold was designed to have a relatively large volume to help maintain a steady pressure. If the manifold volume is small it takes less time to depressurise but the gas entering it from the cylinder could significantly raise the pressure, whereas if the volume in this manifold is large compared to the cylinder volume the gas entering it from the cylinder won't increase the pressure significantly.

It may be possible to tune the manifold lengths to give a similar or lower pressure with a small volume, however, for this initial study where transient performance was not a major concern it was appropriate to have a larger volume. The depressurised exhaust volume from the LP exhaust valve to the compressor including the downstream pipework from the turbine was around 80 L.

6.3.1 Exhaust Port Isolation

The Ford Sigma engine, as with most modern 4-valve engines, combines the flow from both exhaust valves for each cylinder within the cylinder head. For Turbo-Discharging it is a requirement to separate and keep separate the flows from each exhaust valve. Therefore, to use the Sigma engine, modifications had to be made to prevent the flows from mixing within the cylinder head.

The method chosen to achieve this was to fabricate and hand finish stainless steel inserts with a contact fit into the cylinder head. The surface roughness of the internal surfaces of the cylinder head was significant due to the gravity sand casting process and also the internal geometry of each exhaust port varied depending on the core shift of that particular casting. Production solutions could clearly be simpler.

The design of these is shown in Figure 6-6. The dividers were attached to a circular base which was located by a flange (divider locator plate), with a keyway to prevent rotation of the divider. A second flange to which the manifold was attached then fitted over the top. This compressed the dividers into the cylinder head to ensure a seal. In between the divider and the manifold an H-section seal was used, fabricated from 0.7 mm stainless steel (port bridges). This provided a labyrinth seal between the back of the divider and the manifold.

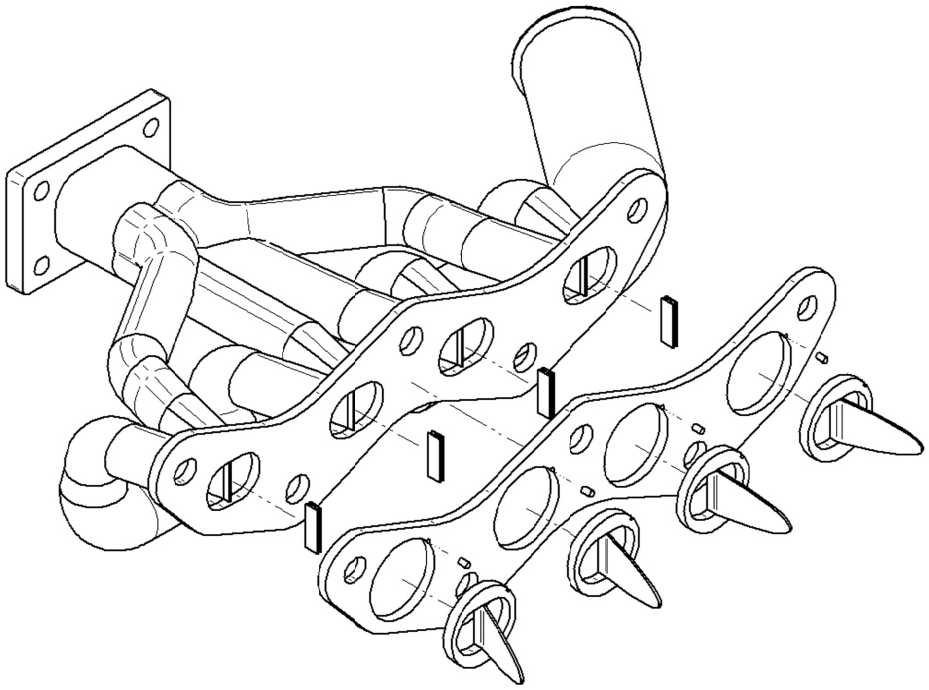

Figure 6-6 – From left to right the components shown are the exhaust manifold, port bridges, divider locator plate and port dividers (gaskets not shown)

In order to ascertain the magnitude and impact of any leakage between the high and low pressure manifolds, an experiment was undertaken to measure the total manifold leakage.

The high pressure side of the manifold was sealed and pressurised using a regulated air line to pressures of up to 4 bar, whilst the low pressure manifold was left open to atmosphere. The only flow path from one side of the manifold to the other was through either the manifold to divider or the divider to cylinder head joints. The flow of gas from the low pressure manifold was measured using a hot wire anemometer traversed across the exit flow area.

To quantify the representative leakage orifice diameters a WAVE model representing the leakage test rig was created. Two ambient elements, one at high pressure and the other at low pressure represented the driving pressure differential. The two halves of the manifold were replicated, joined by ducts with an orifice in the centre. The diameter of this orifice was then varied until an appropriate diameter was found that matched the leakage shown in the experiment. The results are shown in Figure 6-7.

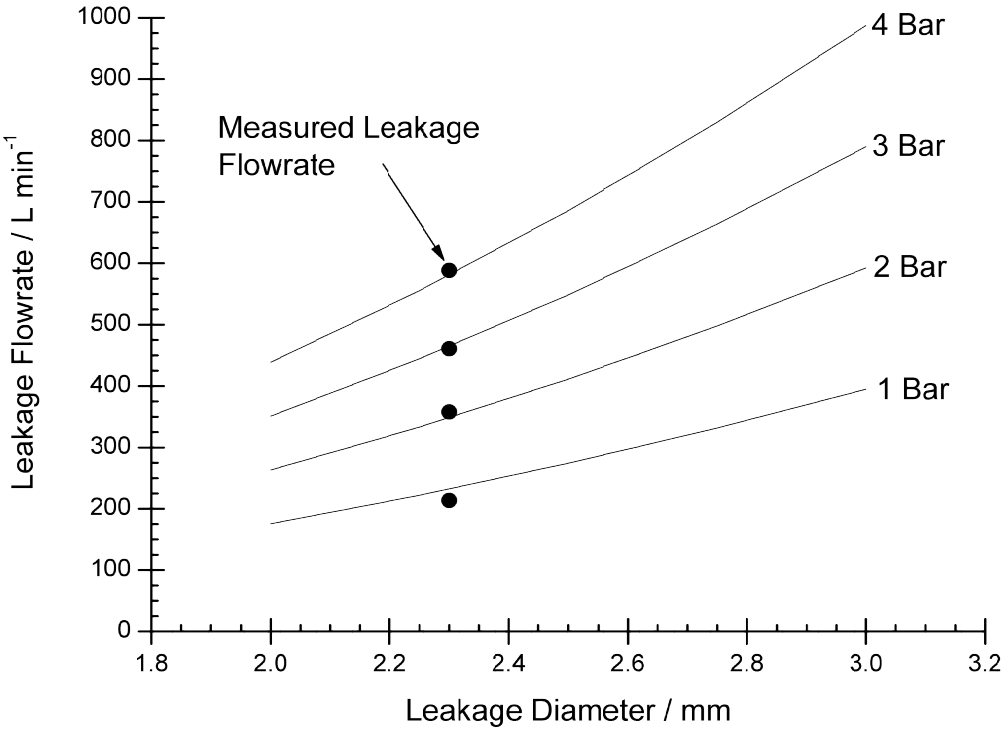

Figure 6-7 - Comparison between measured manifold leakage flowrate and simulated leakage in Wave for 4 pressure differentials from 1 to 4 bar

It was found that an orifice size of 2.3 mm was required to replicate the flow rates from the experiment. An example of the flow through this duct at 3000 rpm, 6 bar BMEP is shown in Figure 6-8. It can be seen that the net mass flow is from the HP to the LP manifold, although the flow is very oscillatory. Overall at 3000 rpm, 6 bar BMEP the net leakage flow from the HP to the LP manifold is less than 1% of the total mass flow through the HP manifold. The effect of port-to-port leakage on Turbo-Discharging system performance will be discussed further in chapter 9.

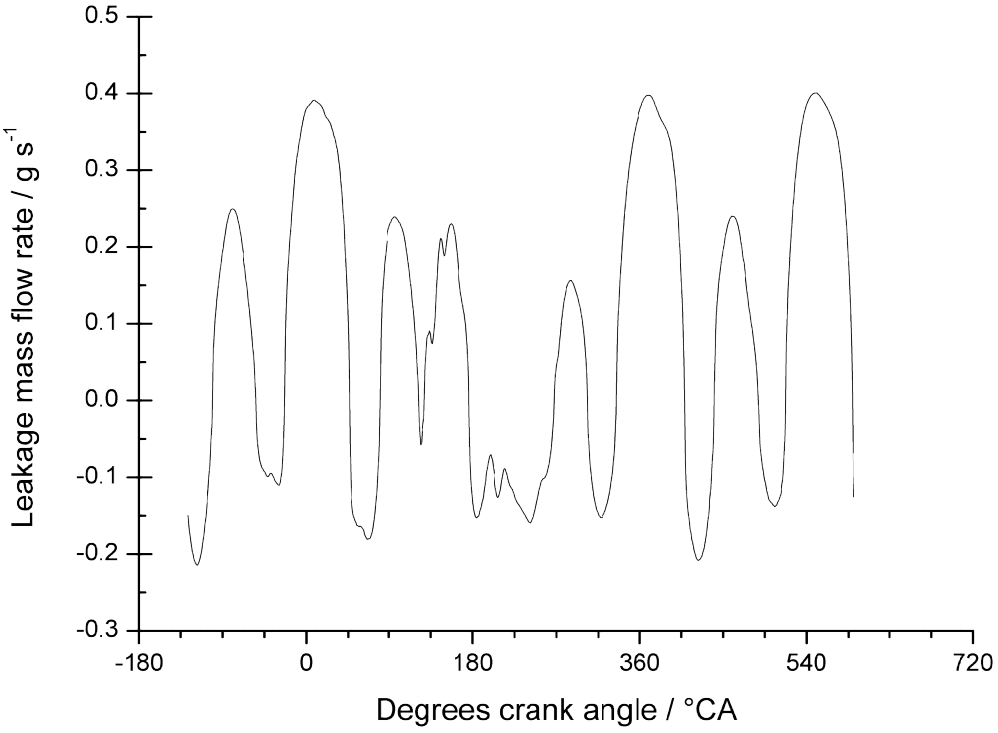

Figure 6-8 - Leakage from HP to LP manifold paths over one engine cycle at 3000 rpm 6 bar

Other Considerations

Another aspect to consider is that the flow path through the port has been altered. Around 5% of the port area is occupied by the divider, but more importantly the flow through the port is no longer as direct as without the divider. Consider the low pressure manifold flow from the cylinder on the right side of Figure 6-6. The flow passes through the port then turns through more than 90° to flow down the exhaust, required due to the construction of the port divider. Arduous gas routing such as this will create a pressure drop in the manifold limiting the cylinder depressurisation for a given depressurised exhaust pressure.

Furthermore, the port has a larger wetted surface area. This is likely to adversely affect pressure losses through the port and manifold.

Production solutions could benefit from a redesigned cylinder head, with individual exhaust ports for each valve. These are rare within modern engines, with research being undertaken into exhaust manifolds incorporated into the cylinder head, with only one port to the exhaust (Turner *et al* 2010). However, it would be possible for this type of manifold to be incorporated into the cylinder head or monoblock of an engine in a similar manner to that currently being researched. This inefficiency will be mentioned later in chapter 9 where an optimised model is considered.

6.3.2 Exhaust Gas Heat Exchanger System

An exhaust gas heat exchanger was required to remove heat from the exhaust not only for exploration of compressor efficiency with respect to gas temperature but to maintain compressor inlet temperature within material limits. The solution developed is shown in Figure 6-9.

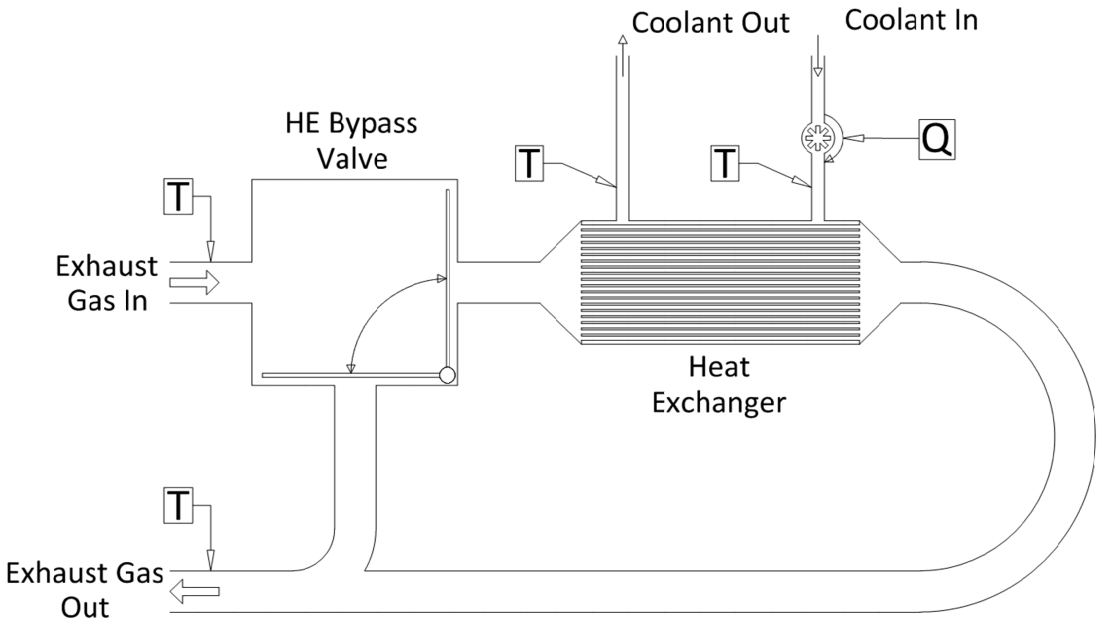

Figure 6-9 – Exhaust Gas Heat Exchanger Rig, T = temperature measurement, $\dot{Q}$ = flowrate measurement

Heat was removed from the exhaust gas using a Bowman 8-40-3742-6 exhaust gas shell and tube water cooled heat exchanger. Rather than vary the coolant flow rate and risk boiling the coolant in the heat exchanger the exhaust gas temperature was controlled by a bypass valve upstream of the heat exchanger such that a portion of the gas could be bypassed and when mixed with the cooled gases the desired temperature was achieved. The bypass valve was PID controlled and used a linear actuator to control the valve position. There were also bosses throughout the system for allowing thermocouple insertion for measuring exhaust gas temperature.

One key specification of the heat exchanger rig is that the pressure drop should be small maximising the depressurisation translated to the cylinder. The heat exchanger chosen had a substantially large flow area of 0.06 m^2 compared to 0.002 m^2 for the pipework such that there was no measurable pressure drop across the rig during engine part-load operation and only up to 40 mbar in WOT operation.

6.4 Valve Events

As discussed previously the performance of a Turbo-Discharging system is heavily dependent on valve timing as this controls the energy flows between the high and low pressure sides of the manifold.

The possible profiles for Turbo-Discharging were limited by two main factors:

1. The velocity and acceleration of the valve must be maintained such that the follower does not detach from the surface of the cam.
2. The curvature of the profile on the cam must never become concave, i.e. if there was an indentation on the surface of the cam the flat follower would bridge this giving an incorrect lift, velocity and acceleration profile and potential wear problems.

The acceleration limit imposed was 1.6 times greater than that of the original Ford profile. This was possible due to the safety factor imposed upon the valve accelerations on the standard engine and by limiting the engine operating speed to 5000 rpm instead of the engine design limit of 6250 rpm.

The profile curvature was discretised in 1 cam degree intervals and corrected accordingly. The resulting profiles are shown in Table 6-2 which were used in the WAVE model.

Cam profile duration multiplier	Lift multiplier	Max Lift incl. 0.3 mm lash	Max Velocity	Max Acceleration	% Increase in Acceleration
		mm	mm/deg	mm/deg^2	
0.5	0.223	1.05	0.04	1.75E-02	34.6
0.6	0.336	1.8	0.055	2.00E-02	53.8
0.7	0.485	2.8	0.07	1.90E-02	46.2
0.8	0.675	4.2	0.08	1.70E-02	30.8
0.9	0.9175	5.8	0.11	1.45E-02	11.5
1	1	6.4	0.1	1.30E-02	0

Table 6-2 - Acceptable valve profiles according to change in gradient of cam profile

It can be seen that the relationship between the reduction in the lift multiplier with the duration multiplier is not linear. This means that for a valve event of half that of the original, the maximum lift attainable is only 22.3% that of the original at 1.05 mm. This gives this profile very limited use.

From the model, equal profiles for the high and low pressure valves were chosen with a duration multiplier of 0.8 and lift multiplier of 0.675 giving a 179° cam angle valve event of 4.82 mm lift. Figure 6-10 shows these profiles compared to the original Ford profile; the high pressure valve opens 16.75° $C_{am}A$ ahead of the original profile, while the low pressure valve opens 30.2° $C_{am}A$ after the high pressure valve.

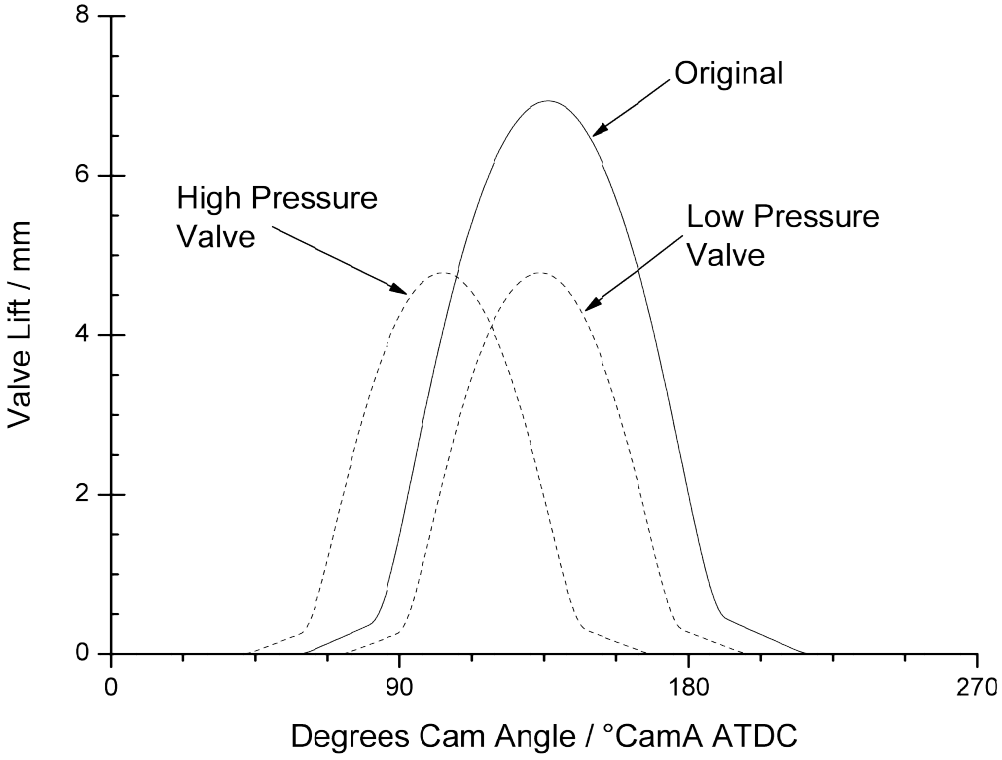

Figure 6-10 – Modified Exhaust Camshaft Profiles Compared to the Original Ford Profile

Valve lash was adjusted on the Turbo-Discharging experimental setup by specifying the correct size of graded follower. This was important as, with scaling down the rest of the profile, the ramp included to compensate for valve lash decreased. The lash when cold was controlled to less than 0.3 mm.

6.5 Turbomachine Lubrication

The primary benefit of Turbo-Discharging is realised through exhaust system depressurisation. The depressurisation of exhaust gas could under certain engine operating conditions lead to increased oil carry over from the turbomachine lubrication circuit due to increased pressure differentials over the oil seals.

6.5.1 Oil Transfer

It is important to eliminate or minimise oil transfer from the turbocharger lubrication system into both the exhaust and air paths. Oil transfer into the exhaust system can lead to damage of after-treatment resulting in increased engine emissions and poor engine performance as well as the oil partially burning in the exhaust and being emitted from the exhaust pipe of the vehicle as white smoke. This is significantly less dangerous than leaking oil into the air path of a compression ignition engine, where it is possible for the engine to 'run-away'. This occurs when sufficient oil is leaked for the engine to begin operating uncontrollably on the engine oil and as the lubrication oil is consumed component damage occurs through insufficient lubrication and overheating at which point components fail or the engine seizes. This is less of an issue for spark ignition engines where it is possible to starve the engine of oxygen with the intake throttle, however, it can still pose a significant emissions risk.

For a compressor in a conventional turbocharging system the turbomachine oil pressure and boost pressure generally increase with increasing turbomachine rotational speed for a given mass flow as they are both a function of engine speed. This means that the air pressure should, in steady state, always be greater than the oil pressure and there should be no oil carry over into the compressor air path.

The compressor inlet pressure in a Turbo-Discharging system could be as low as 0.6 bar absolute whilst the maximum pressure of the outlet is limited by the back pressure of the exhaust system which could vary up to 1.7 bar absolute depending on engine speed and load, exhaust system design and aftertreatment requirements. The compressor seals are exposed to this fixed compressor outlet pressure throughout the whole range of operation even whilst the engine oil pressure increases with increasing engine speed. Given engine oil pressures can be in excess of 5 bar absolute during normal operation there is a significant risk that oil could be driven from the bearing housing into the air path.

The turbine is also susceptible to oil carry over due to the highly pulsated blowdown pulses experienced in a Turbo-Discharging system. During the blowdown part of the pulse the instantaneous pressure could be as high as 5 bar absolute. However, depending on the time between pulses, the effectiveness of the compressor and the design of the exhaust system it may be possible for the pressure in the high pressure manifold to decrease to that of the low pressure part of the system. This could again lead to an unfavourably large pressure differential across the oil seals leading to oil carry over into the exhaust.

Figure 6-11 illustrates the potential leakage paths that could be observed on both sides of a turbomachine in a Turbo-Discharging system. As explained previously oil carry over could be expected on both sides of the turbomachine. The important value is the static pressure on the gas side of the oil seal. Unfortunately this could not be measured directly; the steady pressure transducers were mounted in the gas paths up and downstream of the turbine and compressor.

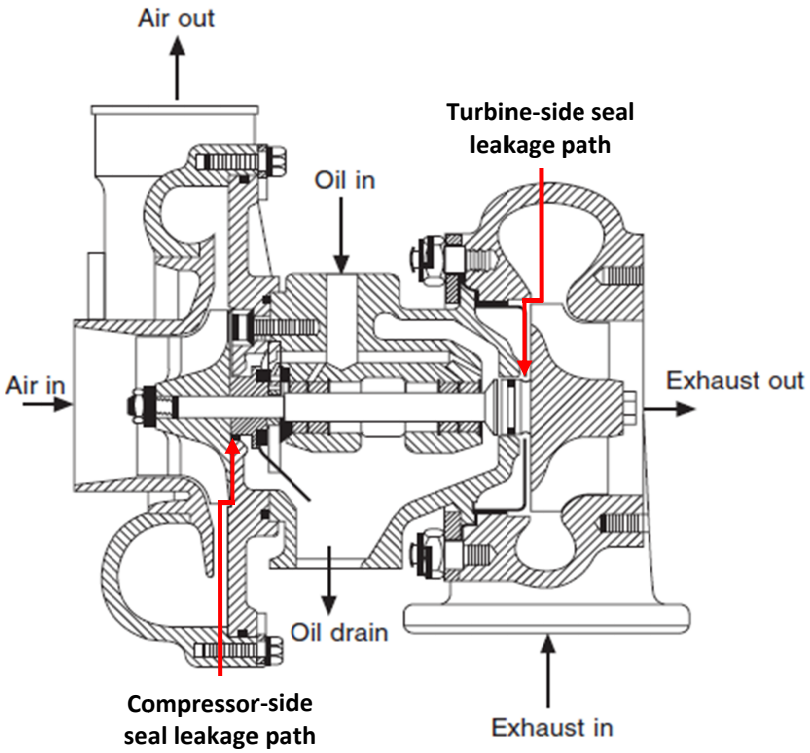

Figure 6-11 - Turbocharger Cut-Away Drawing Reproduced from Garrett *et al* (2001)

For the compressor it is likely the static gas pressure at the oil seal will be most similar to the compressor outlet pressure. It may be slightly less due to the large volume of gas moving past the closed volume behind the compressor wheel creating a slight vacuum. However, it can be

assumed that this pressure at the oil seal will be in the region of the exhaust back pressure over the entire operating range of the compressor.

The gas pressure at the turbine-side oil seal is likely to be influenced more by the exhaust gas pulsations as the gas flows radially inwards into the turbine. Thus, the gas flow will act to increase the static pressure at the oil seal on the turbine side.

However, depending on the operating condition the depressurisation in the exhaust system may translate through the turbine decreasing the pressure at this point. The minimum static pressure at this point, ignoring any effect of gas flow, will be equal to the low pressure manifold static pressure. Thus it is important to mitigate oil transfer on both the compressor and turbine side of a Turbo-Discharging system.

Attard *et al* (2007) observed oil transfer through the compressor on their turbocharged Formula SAE engine. Formula SAE rules require that a restrictor is placed in the air intake upstream of the compressor to restrict the air mass flowrate. However, when the flow through the restrictor chokes and more work is provided by the compressor the volume between the restrictor and the compressor inlet becomes depressurised. They found this depressurisation drew oil through from the turbocharger bearing housing detrimentally affecting combustion through plug fouling and increased propensity to pre-ignition or knock.

Their solution was to modify the turbocharger to provide improved sealing through the use of redesigned piston ring seals and a vent to atmosphere between the piston rings. The vent between the piston rings is key to this concept; any vacuum leakage past the first compressor side piston ring would draw air into the compressor rather than oil from the turbocharger core. However, they make no comment on any oil leaking through the first seal and venting to atmosphere.

One method to avoid oil transfer could be to depressurise the oil return from the turbomachine enabling the same mass flow rate of oil to be achieved for a lower oil inlet pressure reducing the risk of oil transfer. However, the capability of this method had to be proven so an investigation was undertaken on a turbocharger test rig to identify the conditions at which oil transfer occurs and the possible safe extension of operating range by depressurising the oil return.

6.5.2 Depressurised Oil Return Capability

The turbocharger test rig used to conduct this investigation had an oil conditioning system that could provide oil at a given flowrate, pressure and temperature. The oil reservoir was depressurised by a variable air vacuum pump connected to the air volume at the top of the reservoir such that the oil return depressurisation from the turbomachine can be varied.

The turbine was driven by cold compressed air supplied by a steady pressure of up to 6 bar, the outlet of which was open to atmosphere. The compressor outlet was connected to an intercooler, the air from which then passed back into the compressor inlet. The purpose of this was to maintain a steady pressure through this sealed loop across a range of operating conditions. This compressor side gas path was connected to the turbine inlet to ensure the air pressure at both oil seals was as similar as possible. Given a similar design of oil seal this means both seals should have the same leakage characteristics and should begin to leak at the same pressure differential.

This setup would not allow for control of the turbomachine speed independent of the turbine inlet pressure and there was no control over the turbine outlet pressure. Similarly, due to the closed-loop air circuit, the compressor inlet pressure was governed by the work input by the turbine. Control of the oil return pressure was possible by adjusting the flow rate through the vacuum pump.

To observe the presence of air carry over into the oil, i.e. no oil carry over into the air, an observation window was installed in the oil return from the turbocharger. If air carry over into the oil occurs the oil should be aerated. Conversely, substantial oil carry over into the gas paths could be observed by examining the turbine outlet, and within the compressor outlet pipe.

Steady gas pressures were measured using the same Delta Ohm steady pressure transducers as used in the engine tests and logged via a NI 9203 compact DAQ card. Steady gas and oil temperatures were measured using K-type thermocouples connected to a NI 9213 compact DAQ card. Turbocharger speed was measured using the same eddy current type Picoturn turbocharger speed sensor as used in engine testing. The output of these was logged using a bespoke NI Labview program.

6.5.3 Results

The turbocharger was run over a range of turbine inlet pressures and thus rotational speeds. The operating conditions and results are shown below in Table 6-3.

Turbo speed	Oil Return Pressure	Compressor Air Inlet Pressure	Oil Seal Differential Pressure	Visible Aeration
rpm	Bar abs	Bar abs	Bar abs	
12000	1	1.03	0.03	No
12000	0.6	1.03	0.43	Yes
35000	0.68	1.115	0.435	Yes
35000	1	1.13	0.13	No
35000	0.93	1.125	0.195	Marginal
35000	0.9	1.13	0.23	Yes
35000	0.85	1.13	0.28	Yes
35000	0.8	1.128	0.328	Yes
60000	0.6	1.345	0.745	Yes
90000	0.6	2.01	1.41	Yes
90000	0.55	2.27	1.72	Yes

Table 6-3 - Operating conditions and aeration results from the depressurised oil return rig

It was possible to vary the oil return pressure to enable investigation of acceptable oil seal pressure differentials for lower speed conditions, however, for higher speed conditions a high oil return pressure could not be generated and therefore oil aeration was always observed. Examples of oil aeration and lack of aeration are shown below in Figure 6-12.

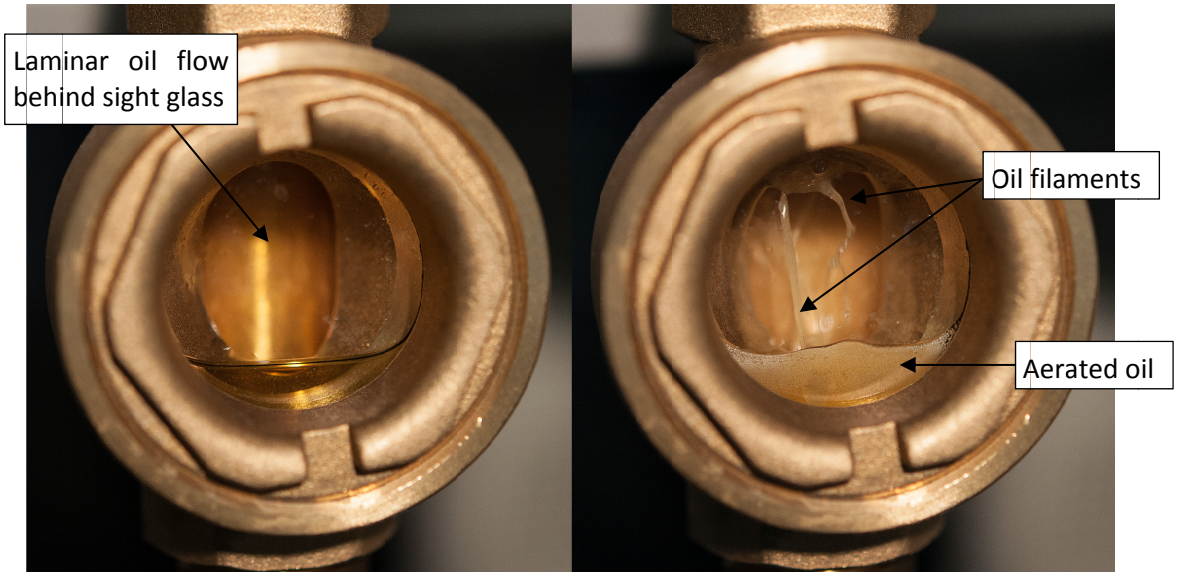

Figure 6-12 - Examples of observed lack of oil aeration (left) and oil aeration (right) at 35000 rpm turbomachine speed

The left image shows oil flow from the turbomachine where no gas is entering the oil system. This does not guarantee oil transfer to the gas path, however, it gives an indication that it might be occurring. The image on the right shows typical oil flow from the turbomachine when there is gas entering the oil system. Filaments of oil can be seen indicating that the flow of oil from the bearing housing is turbulent, and aeration can be observed at the base of the inspection glass indicating gas must be entering the oil circuit. The oil inlet pressure and temperature and turbomachine speed for both these conditions was constant; the only alteration was the oil return pressure.

From the results in Table 6-3 a limit value of pressure differential across the seals of 0.2 bar was defined. This meant that the oil pressure in the turbomachine should never be greater than 0.8 bar absolute for an exhaust pressure of 1 bar absolute to inhibit oil transfer.

The engine oil pump is specified to deliver oil throughout the engine at pressures dependent upon engine speed. The crankcase pressure, which would be the oil return pressure, is controlled by the engine breather system to a value close to 1 bar absolute. As engine speed rises the oil pressure rises in unison, whilst the crankcase pressure remains constant. To utilise the solution identified a larger depressurisation would be required at higher engine speeds.

The solution identified was to design and fabricate a bespoke oil conditioning and supply rig for the Turbo-Discharging turbomachine. This will be described in more detail in section 6.6.

Alternative solutions

An alternative solution to depressurising the oil return system would be to increase the effectiveness of the shaft seals. This may be possible with the introduction of face seals.

Face seals work by applying a force over a comparatively large surface area between the shaft and the seal. A conventional piston ring seal will never seal completely due to the gap required in the ring that allows it to expand and contract. In comparison the face seal maintains a positive contact over the entire sealing face, eliminating any potential leak path (Simon *et al* 2010). These are in series production on the BMW triple turbocharger system due to the fact one of the high pressure stages remains stationary for prolonged periods of engine operation whilst supplied with high engine oil pressure.

However, there are two major downsides of face seal utilisation in turbomachine applications. The first is they result in an increase in shaft friction compared to a piston ring type seal. This is

a function of the positive contact and the large surface area of the seal. Turbo-Discharging may be more sensitive to turbomachine friction than conventional turbocharging applications due to lower shaft powers resultant from the turbine only capturing blowdown energy.

The second downside is the result of the friction between the rotating shaft and the stationary seal. The high rotating speed of the shaft will generate a significant amount of heat and also wear. The sealing material must therefore be able to withstand high temperatures, be wear resistant and low friction. It is generally not possible to satisfy these three requirements in one material and as such any potential material suitable for this application will be expensive.

6.6 Turbomachine Lubrication System

Turbomachine lubrication is an important aspect of the experimental setup for two reasons:

1. Accurate control and monitoring of the condition of the lubricating fluid is essential to maintain consistent values of turbomachine friction;
2. To mitigate oil transfer into the gas paths as described previously.

A schematic of the turbomachine lubrication system is shown in Figure 6-13. To achieve the inlet pressures required by the turbomachine a GMP 600M 370 W gear oil pump was selected. This has an internal bypass to allow control of the oil flowrate through the turbomachine and an overpressure valve for safety. The oil to this is gravity fed from a reservoir into the pump from which it travels through an automotive oil filter before entering the turbocharger.

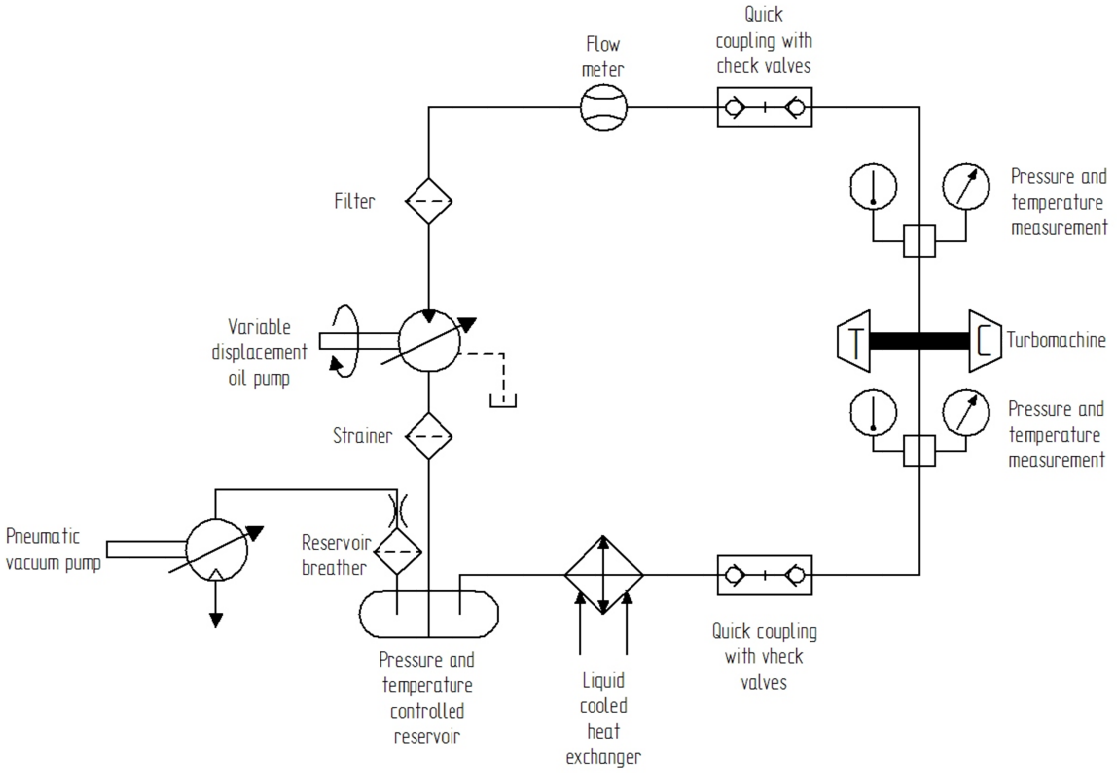

Figure 6-13 - Schematic of the turbomachine lubrication system

From the turbomachine the hot oil flows through a Bowman EC-120 heat exchanger before returning to the reservoir. This is required due to the heat transfer from the exhaust gas to the turbomachine and the turbomachine to the oil.

The oil is then heated in the reservoir by electric heaters which maintain the desired supply temperature of the oil. This has the benefit of being able to raise the oil temperature before the engine is started.

Pressure transmitters described in Table 6-4 and K-type thermocouples either side of the turbomachine were used to record the oil pressure and temperature.

Measurand	Measurand Range / Bar abs	Sensor	Range / Bar abs
Turbocharger Oil Inlet	0.5 - 4	Delta Ohm HD9408T	0 - 10
Turbocharger Oil Outlet	0.5 - 3	Delta Ohm HD9408T	0 - 10

Table 6-4 - Transducers used to measure lubricating oil pressure

Oil transfer across the turbomachine seals is dependent upon the pressure differential between the gas and oil. Reducing the oil pressure in the turbomachine reduces the gas pressure required to prevent oil transfer. However, reducing the oil supply to the

turbomachine, for a fixed return pressure, will reduce the oil flow rate through the turbomachine. To alleviate this a pneumatic vacuum pump was attached to the reservoir, powered by compressed air. This lowered the oil return pressure to ~0.6 bar absolute which transmitted back through the system to the turbomachine in turn reducing the oil pressure at the shaft seals to less than atmospheric pressure. This allowed testing of **T**urbo-Discharging mitigating significant oil carry over.

6.7 Data Acquisition

Figure 6-14 shows a diagram of all the instrumentation used in the experimental rig and how the data from each measurement device is captured. Each P or T symbol within a circle represents a pressure transducer or thermocouple measurement point respectively. Solid lines with arrows represent the flow of a liquid or gas whilst dashed lines represent a flow of data.

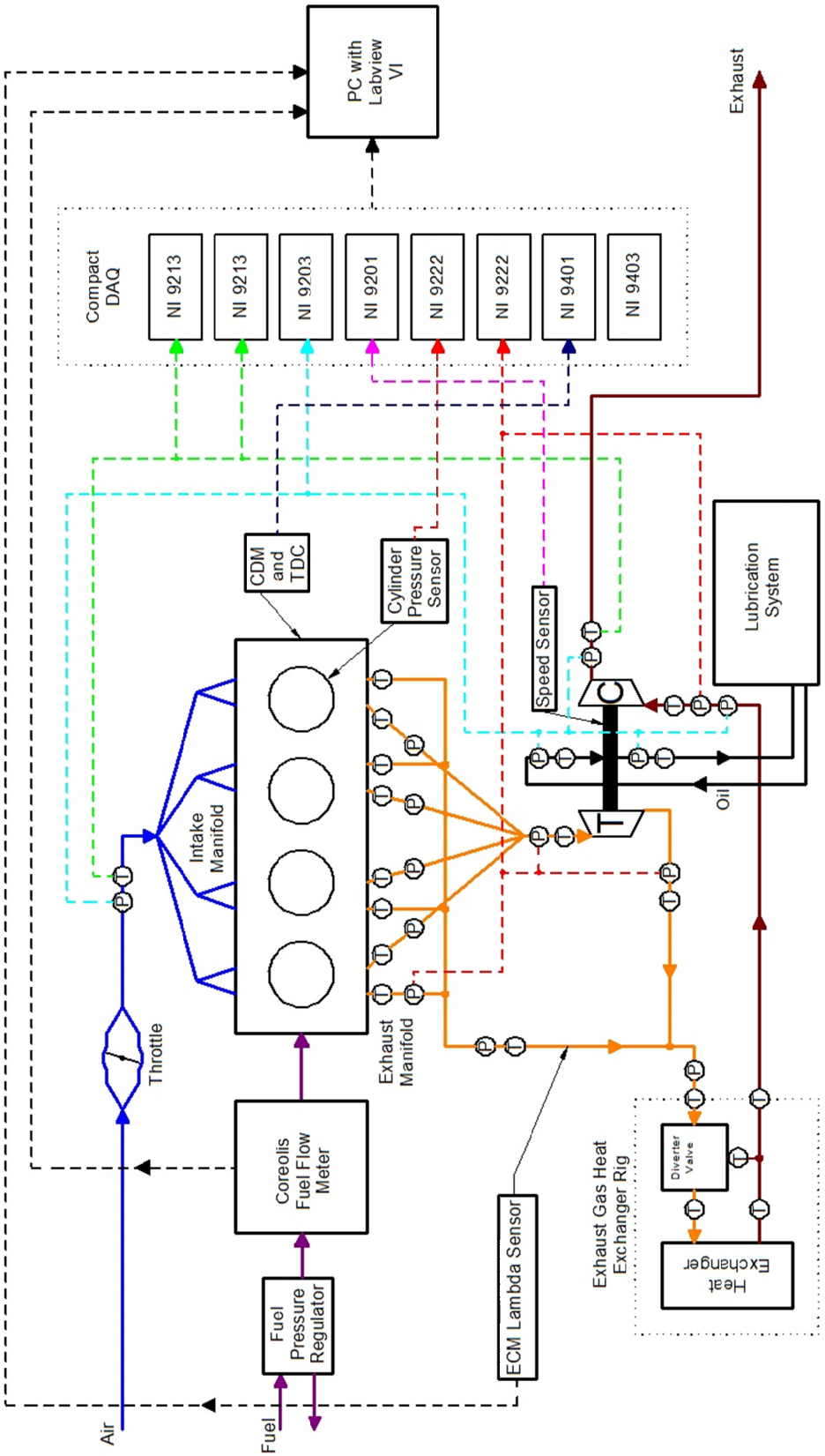

Figure 6-14 - Schematic of Experimental System Showing All Instrumentation for Data Capture (some wiring not shown for clarity)

6.8 Closing Comments

This chapter has explained how the experimental test rig hardware was designed and components specified and installed to modify the standard NA engine into a Turbo-Discharged engine system.

Information has been given on, for example, how the exhaust manifold was designed to maintain separate flows from each exhaust valve. This, combined with the benchmark leakage data of this separation method, may be useful for those wishing to utilise exhaust port separation in the future.

The next chapter will present the measured data from the engine and will discuss the results. It will explain how the one-dimensional model was calibrated using the measured data and will then discuss the primary benefit of Turbo-Discharging.

7. Turbo-Discharging a Naturally Aspirated Internal Combustion Engine

This chapter will show the Turbo-Discharged engine model validation and then explore factors affecting the Turbo-Discharging system both using modelling and experimentation.

The purpose of this chapter is to show the reader how the model was validated and then how it was used in conjunction with the experimental rig to further explore aspects of Turbo-Discharging. An output of this chapter will be some optimised performance parameters for the Turbo-Discharging model and suggested methods for designing the system to overcome some of the technical challenges described previously.

7.1 Turbo-Discharging Model Calibration

The purpose of the model is to allow further exploration of the Turbo-Discharging concept and as such the focus of this calibration is on engine breathing, fuel economy and performance, with the focus on replicating correct engine behaviour rather than tuning the model to reproduce absolute values.

The first step of calibration was to match the in-cylinder processes by tuning the combustion and heat transfer models. This was conducted in the same manner as in the baseline engine model as described in section 5.1.1. The air intake hardware remained unchanged from that of the standard engine including valve events. Therefore there was no need to calibrate this further than previously described in 5.1.2.

For ensuring correct energy extraction from the turbine there were several parameters that had to be calibrated:

1. Exhaust gas flow restrictions upstream of the turbine;
2. The turbine model;
3. The leakage rate between the HP and LP manifolds;
4. Heat transfer upstream of the turbine.

Measured valve flow coefficients typically describe the flow of exhaust gas from the cylinder through the exhaust port of the cylinder head. In the case of the WAVE models in this work a short duct is included to simulate the gas path in the cylinder head. For the Turbo-Discharged model the same valve flow coefficient was retained from the baseline model and the change in exhaust port geometry was input as ducts and junctions. The geometry plus loss coefficients at the ends of the ducts were tuned to match the cylinder pressure and turbine inlet transient pressure traces. An example of the match achieved is shown in Figure 7-5.

The turbine model was already tuned as described in section 6.2. Similarly the manifold leakage had already been identified experimentally and modelled as described in section 6.3.1.

Finally the heat transfer from the manifold was calibrated to match the turbine inlet temperature and the combined exhaust temperature measured during testing. This was achieved by adjusting the wall transfer coefficients of the exhaust system such that more or less heat was transferred to the ambient upstream of the turbine. The largest amount of heat

transfer from the exhaust gas upstream of the turbine tends to be to the cylinder head. This was managed by controlling the wall temperature of the cylinder head and varying the wall heat transfer multiplier. The rest of the exhaust system was modelled as a homogenous structure with axial conduction and it was found that only controlling the heat transfer to the cylinder head was sufficient to match the turbine inlet temperature. Figure 7-2 shows an example of the match achieved in turbine inlet and outlet temperatures at full load.

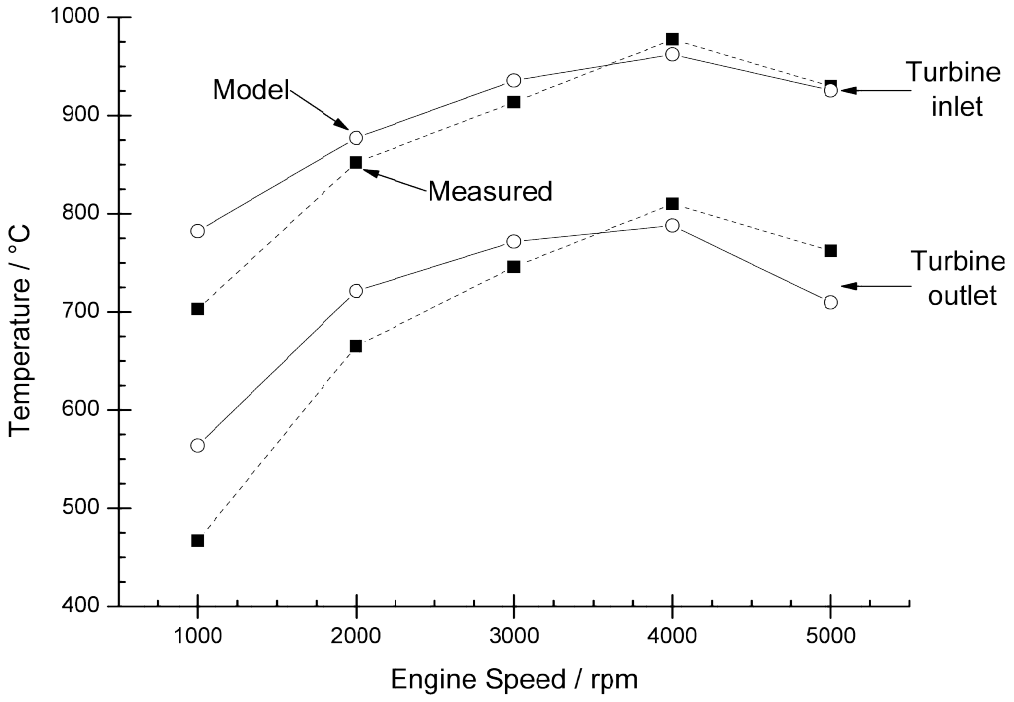

Figure 7-1 - Cycle averaged Turbo-Discharging turbine inlet and outlet temperatures at full load

7.2 Turbo-Discharging Validation

This section will present the calibrated model results and compare them to the measured data from engine testing. It consists of two main sections; full load and part load validation.

7.2.1 Full Load Validation

As previously described in the NA model calibration full load engine performance gives a good indication into the accuracy and behaviour of the engine model. Key to the behaviour of the model is the engine airflow, and engine volumetric efficiency is significant in governing this. Figure 7-2 shows the model and measured total volumetric efficiency values. The model in this case is a closer match to the measured values than the baseline engine and displays good accuracy in the trend of volumetric efficiency over the engine speed range. The result of the good match in volumetric efficiency is a good match in engine mass air flow, also shown in Figure 7-2.

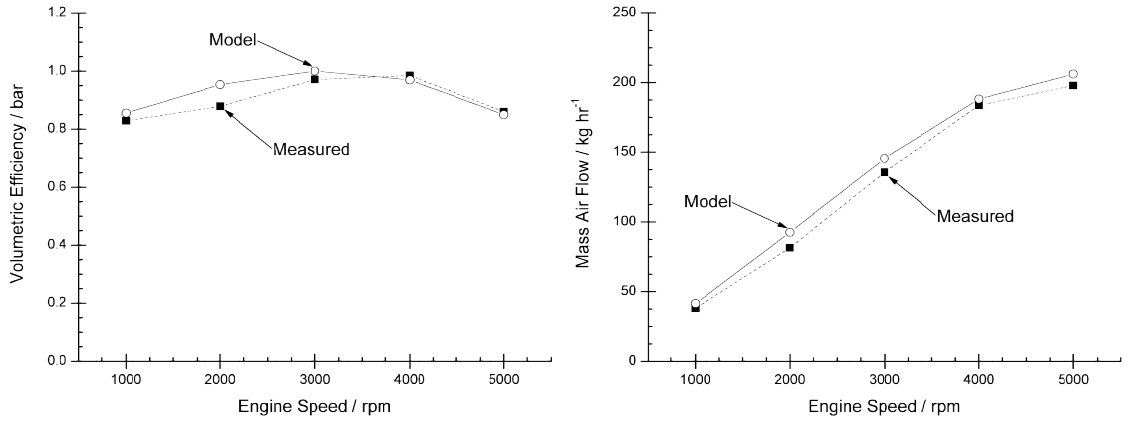

Figure 7-2 - Turbo-Discharging model and measured total volumetric efficiency (left) and mass air flow (right) at full load

Maximum modelled and measured engine BMEP is presented in Figure 7-3. The trend is similar to both that of the engine mass air flow and volumetric efficiency; a good match in terms of the shape of the maximum BMEP curve with reasonable accuracy at each point.

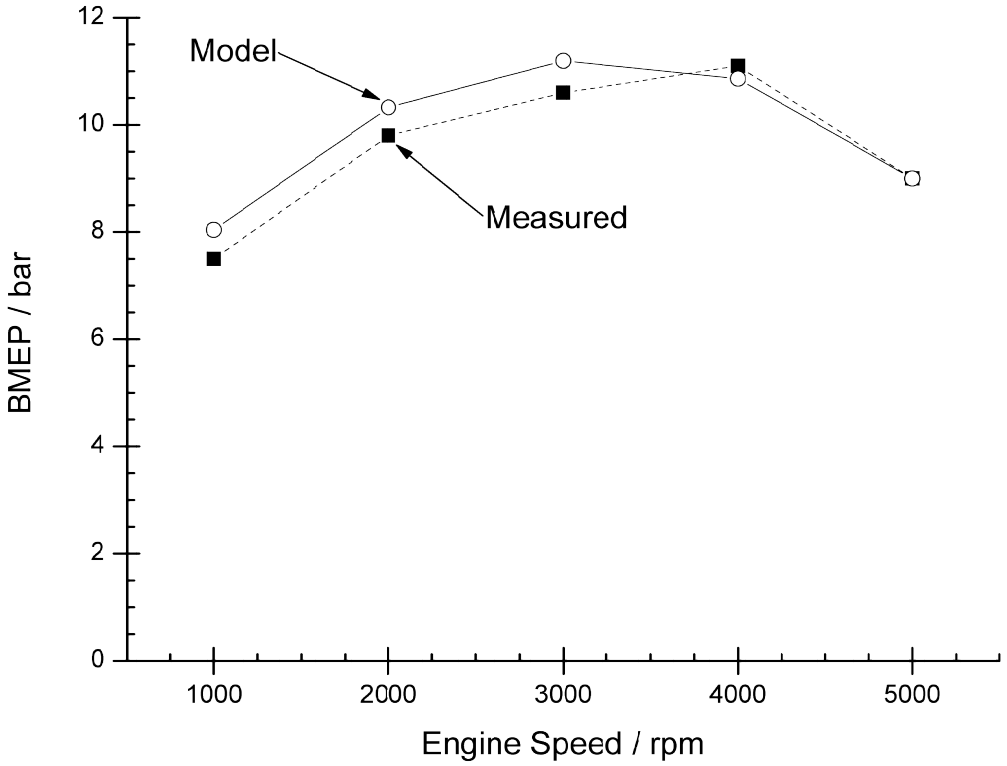

Figure 7-3 - Turbo-Discharged modelled and measured engine BMEP at full load

Figure 7-4 shows compressor inlet pressure and turbomachine speed for the Turbo-Discharging system. The turbomachine speed is an important indicator of the accuracy and behaviour of the turbine and compressor maps.

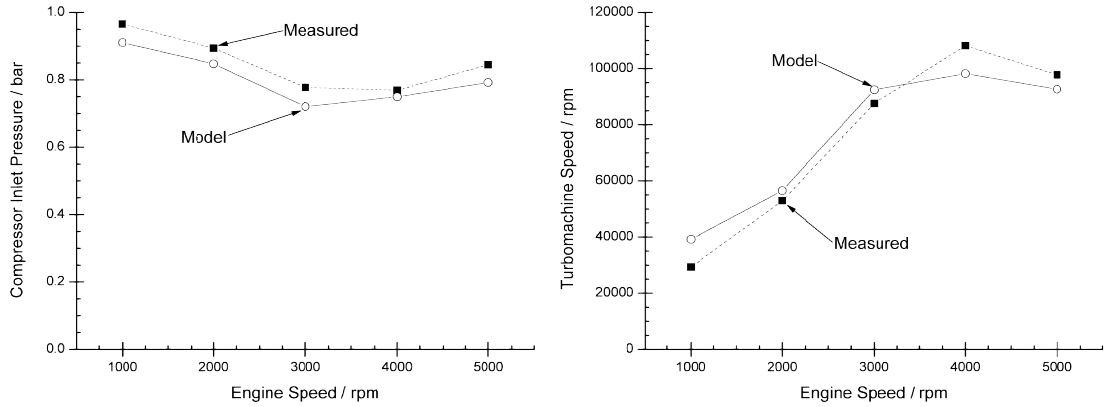

Figure 7-4 - Modelled and measured Turbo-Discharging compressor inlet pressure (left) and turbomachine speed (right)

It can be seen that the turbomachine speed exhibits the same trend as the measured data with peak speed occurring at 4000 rpm engine speed. The trend of compressor inlet pressure against engine speed in the model is very close to that measured on the experimental rig but the model predicts around 50 mbar lower depressurisation than was measured, which is still within 10% of the measured values for each point.

Figure 7-5 shows transient turbine inlet and outlet pressures at 3000 rpm, WOT. The modelled turbine outlet pressure exhibits a similar lower value to the cycle-averaged compressor inlet pressure. The turbine inlet pressure rise rate shows good correlation indicating the cylinder conditions at EVO, gas path and gas transfer to and through the turbine and turbine sizing are well calibrated. However, the pressure decay throughout the blowdown pulse is slower in the model than was measured on the engine. This would account for extra shaft energy in the turbomachine which would in turn create a larger depressurisation.

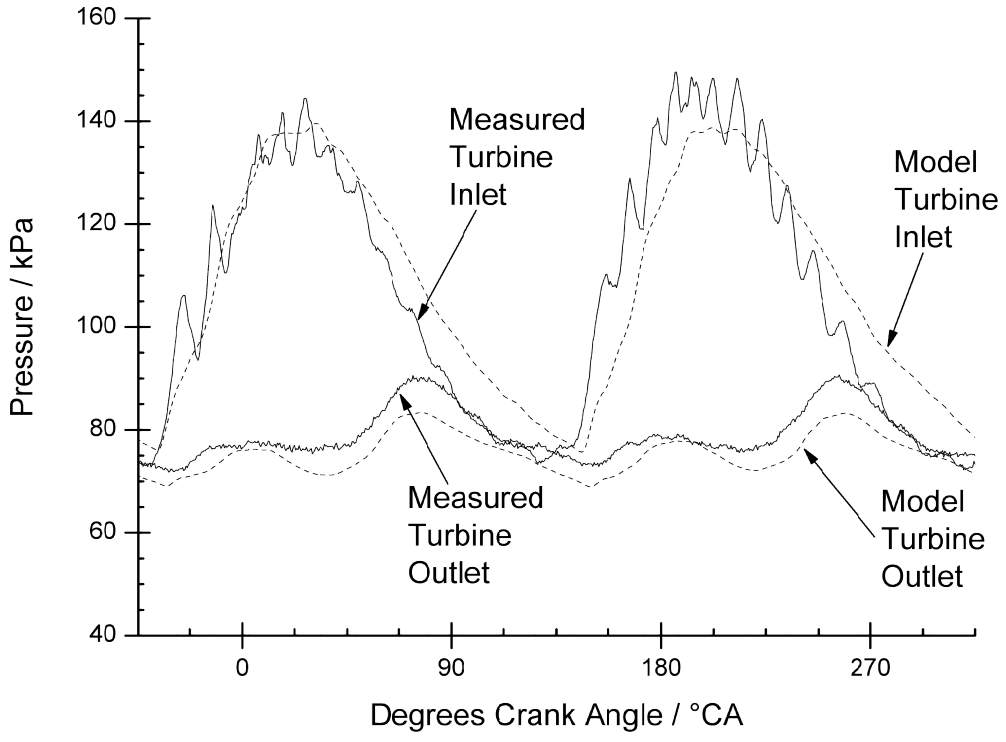

Figure 7-5 - Comparison of Turbo-Discharging measured and modelled turbine inlet and outlet pressures at 3000 rpm WOT

Figure 7-6 shows turbine inlet and outlet pressures at 5000 rpm WOT. The difference in achieved depressurisation is again evident in the turbine outlet pressures, but the turbine inlet pressure still shows a good match in terms of the pressure rise rate and absolute values and the overall trends of pressure fluctuations are a good match.

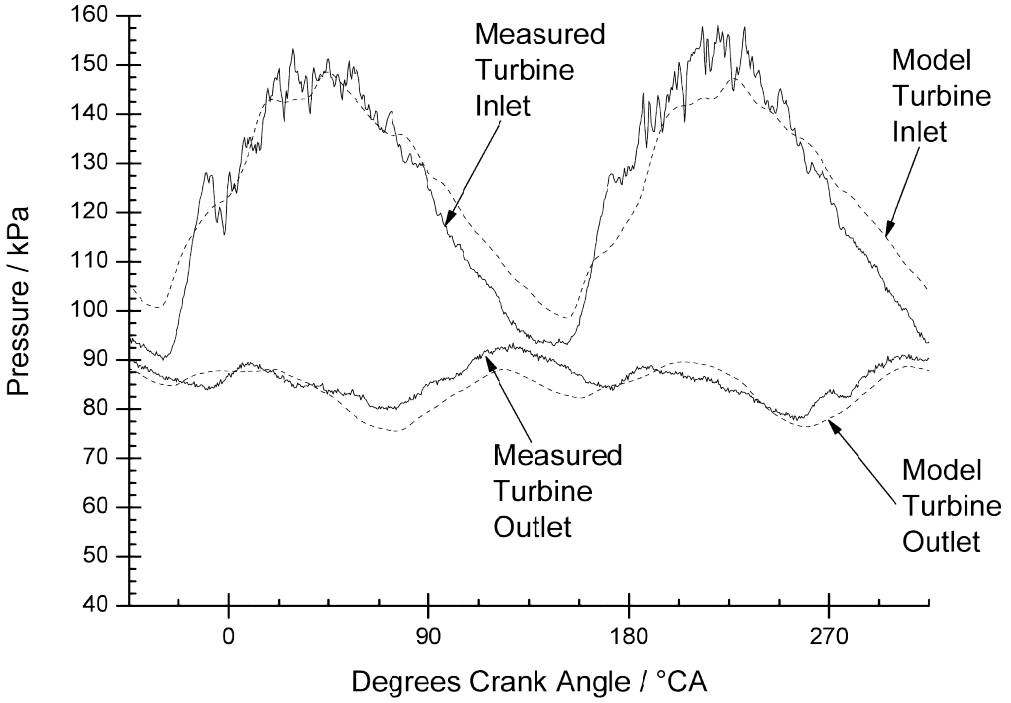

Figure 7-6 - Comparison of Turbo-Discharging measured and modelled turbine inlet and outlet pressures at 5000 rpm WOT

Alternatively the difference in depressurisation may have arisen due to error in the measured value of compressor inlet temperature which was then input into the model; too low a temperature would allow the compressor to operate more efficiently in the model and thus create a lower depressurisation. These points considered, and given the good match of the overall trends without further tuning at different engine conditions, the behaviour presented is acceptable for the purposes of this investigation.

7.2.2 Part Load Validation

Similarly to the NA model, a load sweep at 3000 rpm was completed to validate the part load performance of the 1-D model.

The volumetric efficiency and mass air flow show good correlation as shown in Figure 7-7. This is to be expected as the engine intake system has remained identical to the NA model and the Turbo-Discharged model at WOT also showed good correlation.

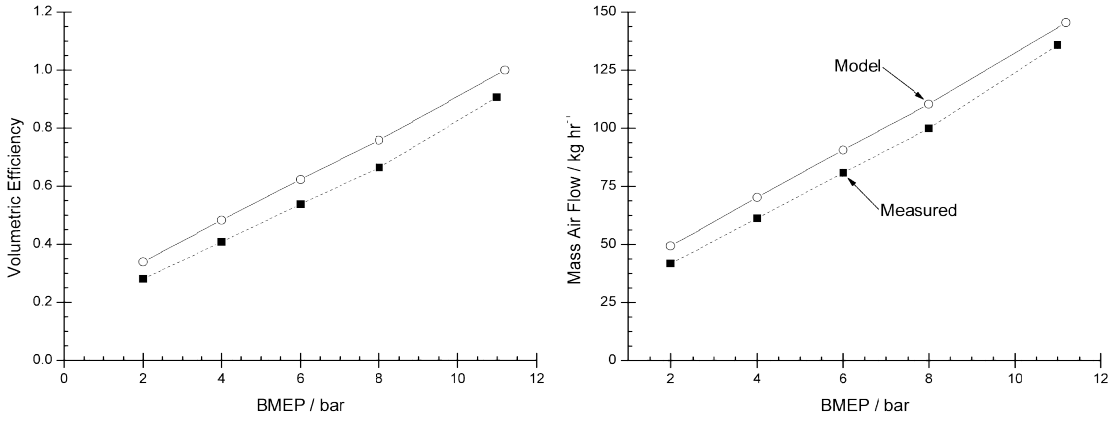

Figure 7-7 - Comparison of measured and modelled volumetric efficiency (left) and mass air flow (right) at 3000 rpm with varying load

Focussing on the Turbo-Discharging system the compressor inlet pressure and turbo speed also show good correlation as shown in Figure 7-8. Similarly to full load the model slightly over-predicts the depressurisation caused by the compressor. The turbomachine speed shows a good match varying by less than 5%.

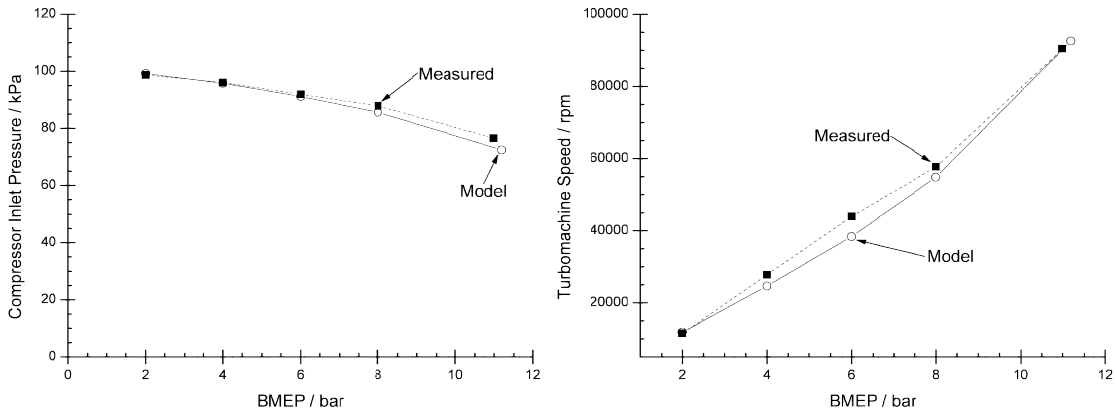

Figure 7-8 - Comparison of measured and modelled compressor inlet absolute pressure (left) and turbomachine speed (right) at 3000 rpm with varying load

Figure 7-9 shows a comparison of the measured and modelled turbine inlet and outlet pressures at 3000 rpm 6 bar BMEP. A good correlation can be observed in the turbine outlet pressure and the rise in turbine inlet pressure. Similarly to the full load transient pressures the modelled turbine inlet pressure does not decay as quickly as that measured on the engine. At part load the increased shaft energy offered by the higher turbine inlet pressure is not enough to cause significant difference in the level of depressurisation generated.

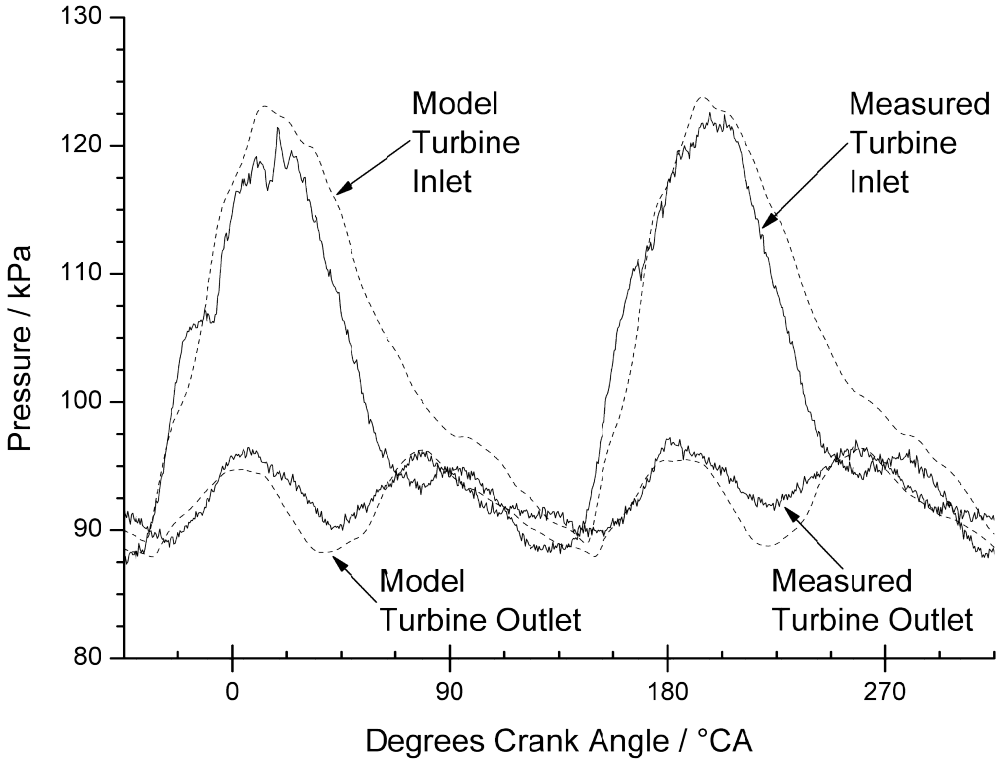

Figure 7-9 - Comparison of Turbo-Discharging measured and modelled turbine inlet and outlet pressures at 3000 rpm 6 bar BMEP

Figure 7-10 shows the same transient pressures for 3000 rpm 2 bar BMEP. Again a good correlation is observed, both in pressure magnitude and pulsation fluctuations of both the inlet and outlet.

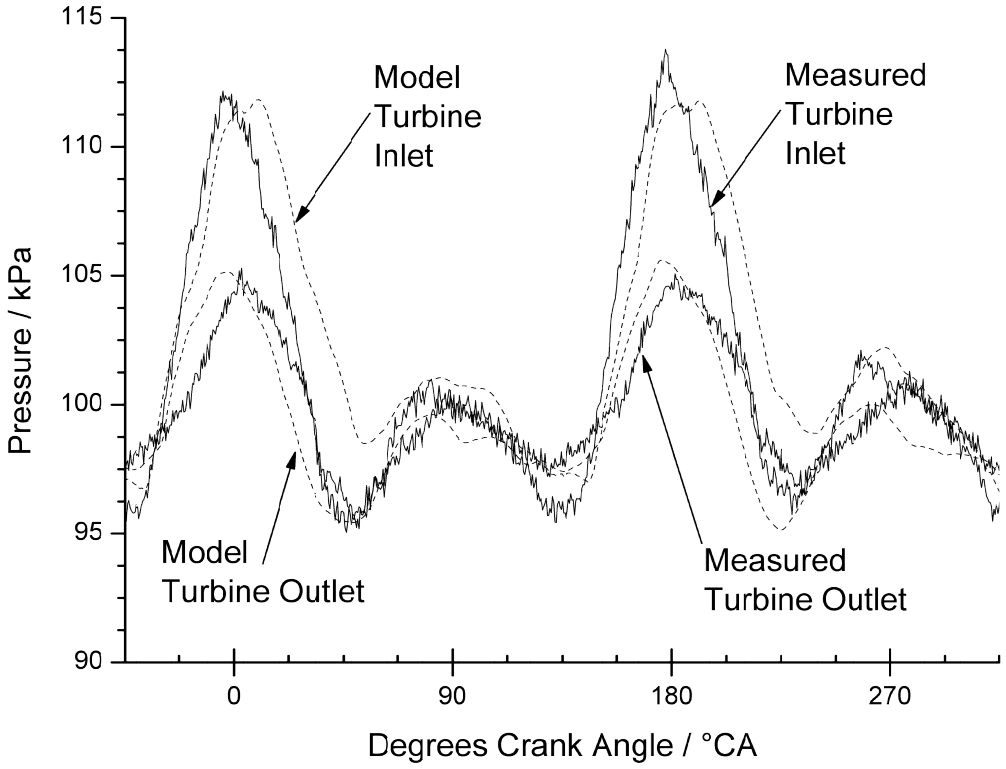

Figure 7-10 - Comparison of Turbo-Discharging measured and modelled turbine inlet and outlet pressures at 3000 rpm 2 bar BMEP

The modelled data presented shows good correlation to the data measured on the engine. Some inaccuracies have been observed but the data trends of the model are representative of the real Turbo-Discharging system. This satisfies the requirement of the model which was to create a representative model to allow for further investigation of Turbo-Discharging.

7.3 Modelled Energy Flows

7.3.1 Efficacy

Turbo-Discharging efficacy as described in section 3.3 is defined as the ratio of the maximum theoretical depressurisation defined by the thermodynamic model to the achieved depressurisation.

The cylinder pressure at EVO was taken from the measured and modelled data. However, the cylinder temperature at EVO was taken from the model for both the measured and modelled efficacy calculation. Typically it is difficult to measure in-cylinder temperature as measurements tend to be intrusive and may adversely affect combustion, and the thermal mass of a thermocouple (for example) that will endure cylinder conditions is too high for it to react fast enough to the changing cylinder conditions.

The thermodynamic model was then re-run to the measured and modelled conditions at EVO and a minimum theoretical compressor inlet pressure generated. The efficacy was then calculated from this and the measured or modelled compressor inlet pressure. The resultant efficacies are plotted in Figure 7-11 for a load sweep at 3000 rpm.

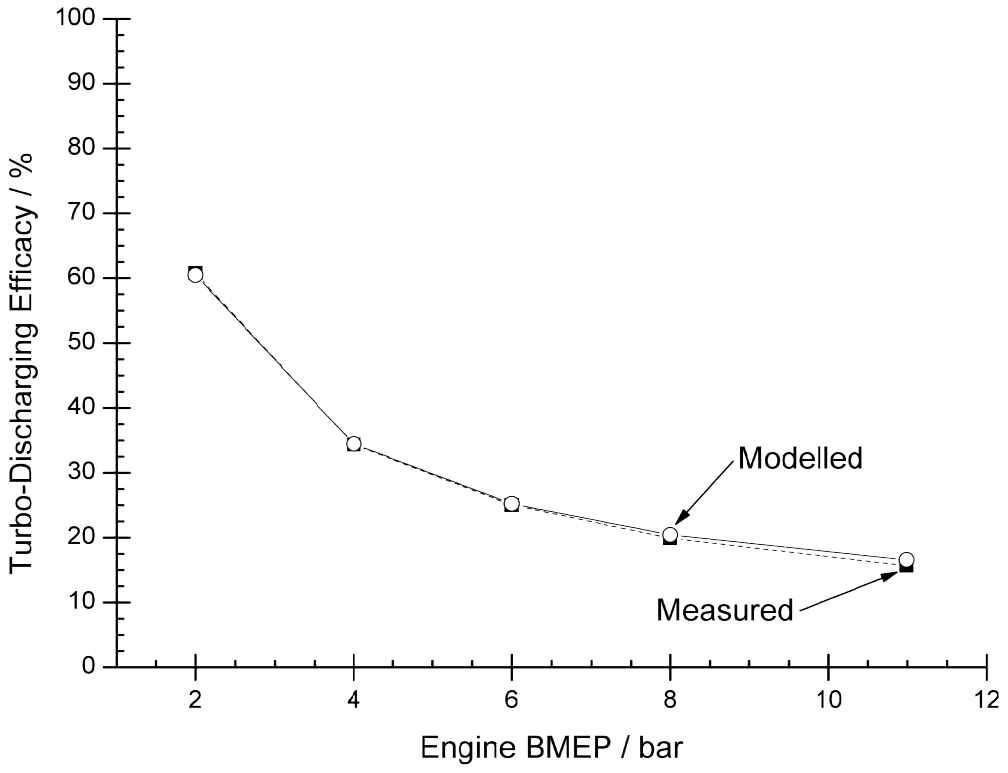

Figure 7-11 – Calculated Turbo-Discharging efficacies from measured and 1D modelled data at 3000 rpm

Figure 7-11 shows that the efficacy of the measured and modelled Turbo-Discharging system decreases with increasing engine load. This is confirmed by Figure 7-12 where Turbo-Discharging efficacy is plotted for a speed sweep at full load. Neither measured nor modelled efficacies exceed 20% across the engine speed range. The modelled efficacies are slightly over-predicted due to the greater depressurisation achieved in the model for reasons described previously.

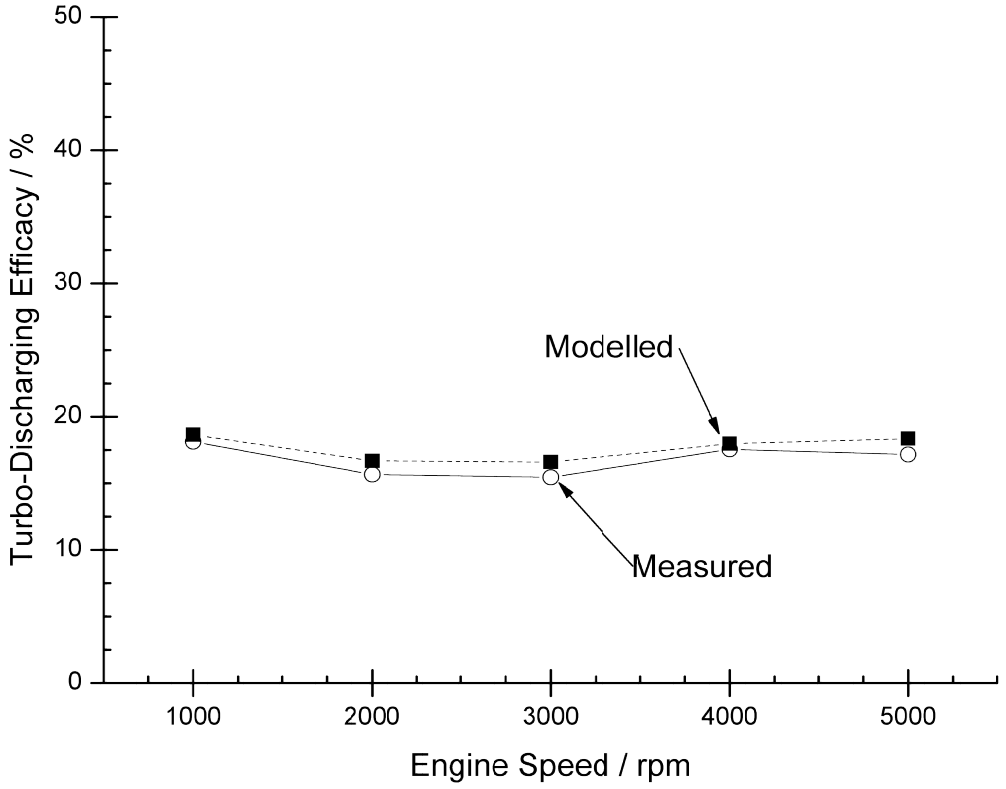

Figure 7-12 - Measured and modelled Turbo-Discharging efficacy at full load

Turbo-Discharging efficacy considers the ability of the system to extract energy from the exhaust gas and convert this into a depressurisation. Sources of inefficacy include entropy generation across the exhaust valve, heat transfer upstream of the turbine, turbine and compressor irreversibilities and flow losses through any of the gas paths. These have been explored in the optimisation of the 1-D model in chapter 9.

7.4 Pumping Work Benefit

The primary benefit of Turbo-Discharging is defined as the improvement in the pumping work of the engine through depressurising the exhaust system which in turn improves fuel economy. This section will quantify using modelling and experimental investigation the achievable pumping work benefit on a naturally aspirated port fuel injected spark ignition engine.

The level of improvement in pumping work achievable through Turbo-Discharging is dependent on two factors:

1. Turbo-Discharging system efficacy;
2. The energy available in the exhaust gas.

The energy available in the exhaust gas is largely dependent on the engine operating condition. The overall benefit of Turbo-Discharging will largely depend on the amount of energy it is presented with and how effectively the system can convert it into a pumping work benefit. This section will show through experimental data and modelling what the maximum pumping work benefit would be for a naturally aspirated, port fuel injected spark ignition engine.

7.4.1 Measured Turbo-Discharging Performance

Figure 7-13 shows the compressor inlet pressure measured experimentally. At low engine speed and low load there was insufficient energy transferred to the turbine such that the compressor could not create a significant depressurisation. The depressurisation is largely a function of engine load, affecting the amount of available energy. Engine speed effects are secondary and arise from pipe and valve losses.

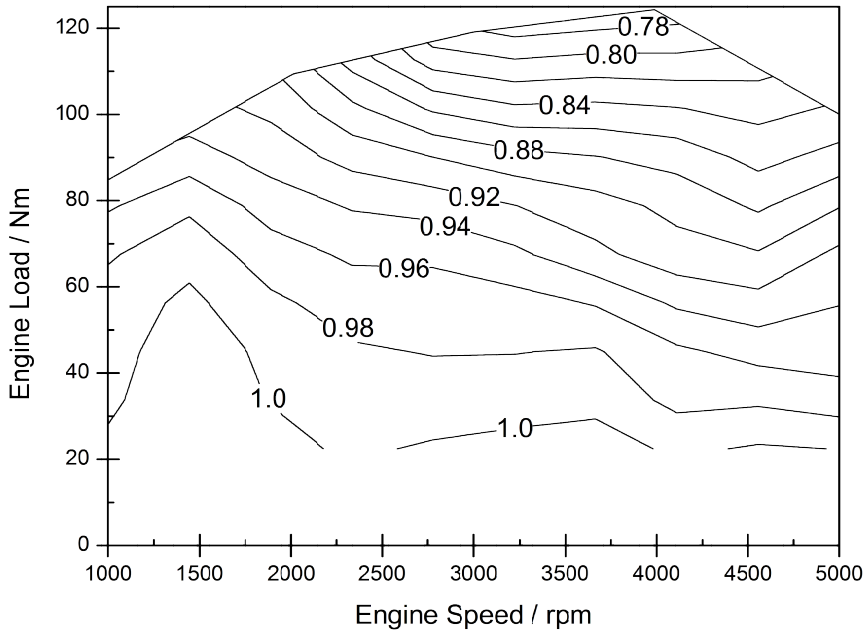

Figure 7-13 – Contours of compressor inlet pressure (bar absolute) from Turbo-Discharging engine test data

Figure 7-14 shows contours of turbine inlet temperature and air mass flow rate versus engine speed and load. For given intake and exhaust valve timing the energy available to the turbine is dependent on these two factors. The split of mass flow between the high and low pressure manifolds will depend on the engine operating condition and the pressure and temperature of the gas at EVO. Both the turbine inlet temperature and air mass flow rate increase with both engine speed and load although it can be seen the turbine inlet temperature is more of a function of load than speed whereas the air mass flow is affected almost equally by both.

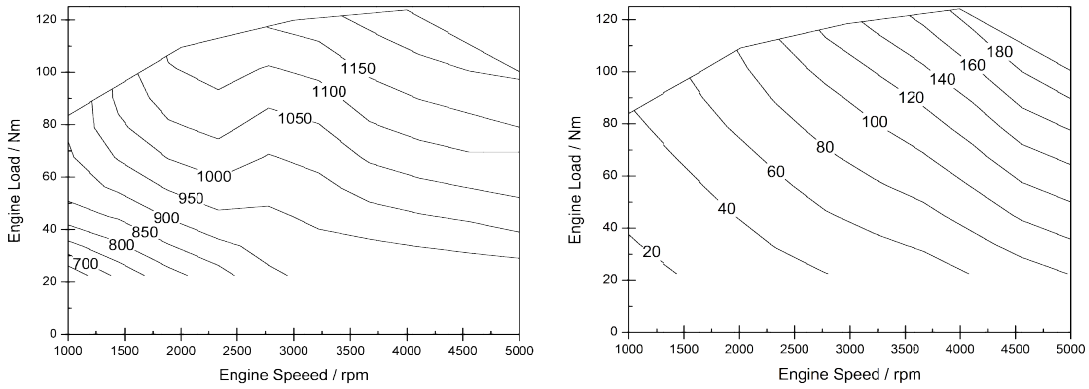

Figure 7-14 - Contours of turbine inlet temperature in degrees Kelvin (K, left) and air mass flow rate in kilograms per hour (kg/hr, right) for the Turbo-Discharging engine test

These plots highlight the lack of exhaust gas energy at low engine speed and load. This translates into a low turbomachine speed as shown in Figure 7-15. The line of lowest speed on the compressor map is 70000 rpm at which it can achieve a pressure ratio of between 1.2 and 1.25. Comparing this to the turbomachine speed values in Figure 7-15 illustrates just how little of the compressor map is being utilised for the majority of the engine speed and load map. The range of actual operating points from the engine test is plotted on the compressor map presented earlier in Figure 6-5.

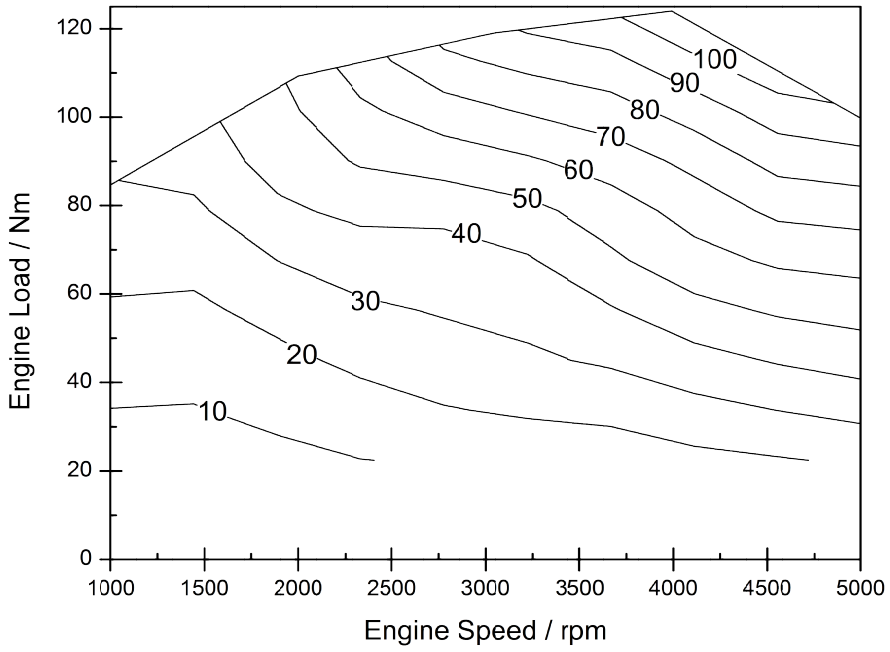

Figure 7-15 - Contours of turbomachine speed (kprm) from the Turbo-Discharging engine test

This illustrates quite clearly that the compressor, for this particular system, is capable of flowing far more exhaust gas than is required and with a smaller compressor it would be possible to align the operating range with the island of peak efficiency. The significant effect of this would be an increased pressure ratio across the compressor for a given energy input in turn creating a larger depressurisation.

It is possible to calculate a maximum equivalent pumping work benefit from the level of depressurisation achieved. This is done by dividing the depressurisation by the BMEP to give a percentage maximum pumping work benefit. This assumes there are no losses in the translation of the low pressure from the compressor inlet back to the cylinder and does not consider any secondary benefits such as RGF reduction or gas dynamics. The result is shown in Figure 7-16.

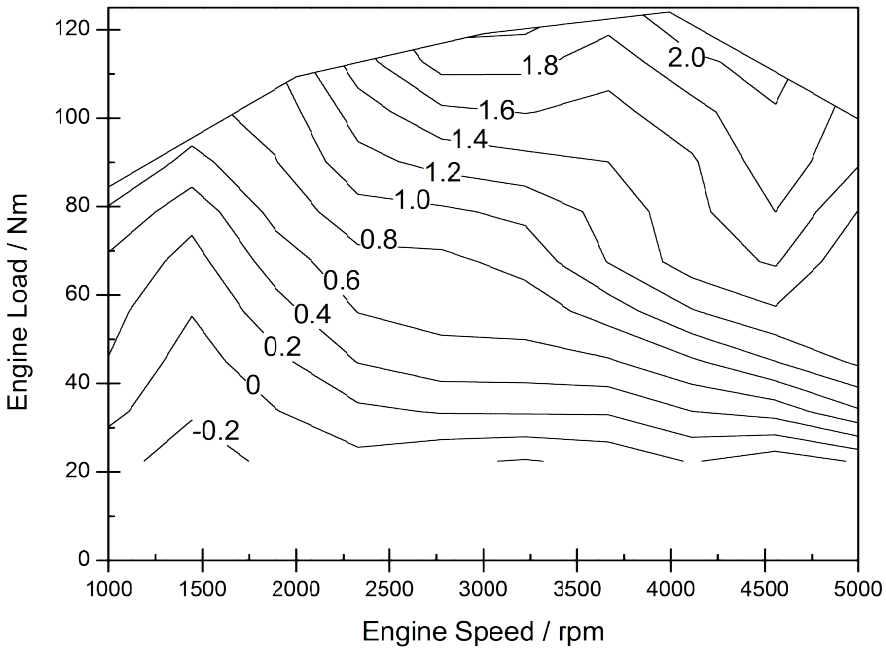

Figure 7-16 - Contour lines of maximum primary Turbo-Discharging percentage benefit

The maximum pumping work benefit is observed at high engine speed and load and achieves a 2% benefit in pumping work.

Minimising PMEP during the exhaust stroke requires the blowdown pulse to happen in as short a period as possible whilst the piston is stationary around BDC, the depressurisation to be as large as possible and to transmit back through the low pressure manifold into the cylinder with as few losses as possible.

To achieve an instantaneous blowdown pulse the HP valve and manifold must have as little pressure drop as possible and the turbine should be large such that it offers as little back pressure on the engine as possible (i.e. it restricts the flow as little as possible). There is obviously a trade off with turbine size as well as packaging restrictions limiting the manifold geometry, material mechanical and thermal limits and valvetrain design governing the flow capacity of poppet valves.

7.4.2 Valve Timing

The primary performance gain from a Turbo-Discharging system is dependent on the energy content of the exhaust gas and how effective the system is at transferring that energy back to the crankshaft. It is possible to trade off exhaust gas energy with crankshaft work by altering the exhaust valve timing. There are limits on how far the exhaust valve timing can be varied which will be described below, but with a Turbo-Discharging system it is also important to individually consider the variability of the HP and LP exhaust valve events.

Conventional Valve Event Constraints

The ideal EVO occurs when the maximum amount of expansion work has been extracted from the gas in the cylinder. This is limited by the geometry of the engine where peak cylinder volume occurs at BDC. However, it may be possible or desirable for EVO to occur before BDC. This may be beneficial when the cylinder contains more mass as it gives more time for this mass to exit the cylinder. Also, as the piston approaches BDC it slows, and for a given crank angle period the piston does less expansion work. Thus EVO can occur before BDC without significant effect on the energy extracted by the crankshaft.

This is beneficial when utilising an exhaust gas energy extraction system such as turbocharging or Turbo-Discharging. The reason for this is even though the gas in the cylinder is not undergoing much expansion it is still transferring thermal energy to the cylinder walls, effectively losing energy that would otherwise be available to the turbine.

If the exhaust valve is opened before the exhaust gas is fully expanded the deficit in crankshaft work may be compensated by the increased performance of the turbocharging or Turbo-Discharging system. There is a trade-off between higher energy exhaust gas and increased expansion work in the cylinder which will be investigated in this chapter for Turbo-Discharging.

Discharging system. There is a trade-off between higher energy exhaust gas and increased expansion work in the cylinder which will be investigated in this chapter for Turbo-Discharging.

The other main consideration of valve timing in a regular engine is the overlap between exhaust and intake valves for cylinder scavenging. The overlap period is included to flow intake air through the cylinder and reduce RGF, as well as increasing the length of the intake event to maximise the quantity of charge trapped in the cylinder. There is a limit on how early the intake valves can be opened; if the intake valves open too early the cylinder and exhaust pressure may be too high such that exhaust gases flow from the cylinder into the intake manifold. The flow of hot residual gases into the intake manifold is undesirable as it will increase the charge air temperature which can induce knock.

For Turbo-Discharging air flowing through the cylinder is undesirable as it will increase the mass flow through the compressor without increasing the energy available to the turbine, reducing the depressurisation generated and limiting the pumping work benefit of the system. The baseline chosen was for the exhaust event to end at TDC which with the standard intake cam means there is less than 10° CA of valve overlap.

Turbo-Discharging Specific Valve Event Constraints

One feature required by Turbo-Discharging is the individual operation of the two exhaust valves. However, for this modelling study it is assumed the HP and LP valves can be phased and the duration and lift varied individually. This would represent a system such as the Mahle Cam-in-Cam (Taylor *et al* 2011) or Borg Warner (Roth *et al* 2010) systems combined with a variable lift mechanism such as that of BMW Valvetronic (Luttermann *et al* 2006).

7.4.3 LP Valve Event

As described previously, the LP valve closing time is effectively fixed if maximum exhaust depressurisation is desired. Thus varying the LP valve opening will vary the duration and lift of the valve.

Varying the LP valve duration at 3000 rpm and 6 bar BMEP leads to more mass bypassing the turbine as shown in Figure 7-17. Should the engine be operating at a point where there is no blowdown or the blowdown pressure equalises before the LP valve event, the same is still true

as the gas will begin to be forced through the turbine by the piston displacing from BDC to TDC.

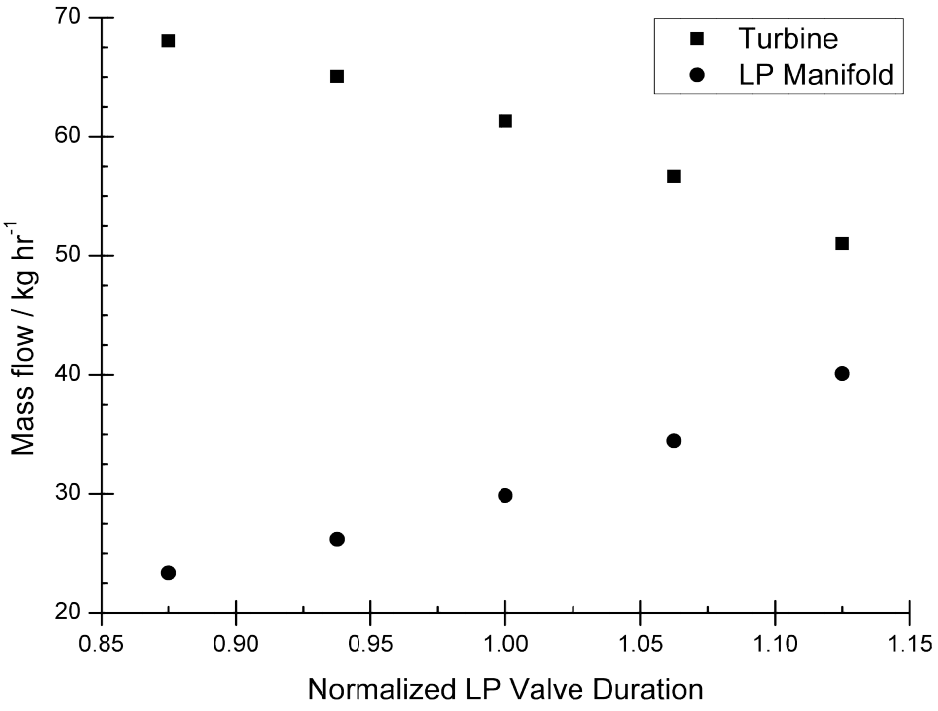

Figure 7-17 – Simulated effect of LP valve duration on exhaust mass flow split at 3000 rpm 6 bar BMEP

Decreasing the mass flow through the turbine will decrease the energy extracted by the turbine and therefore the compressor will not achieve as great a depressurisation. This, and the result of reduced turbine power is shown in Figure 7-18.

Compressor inlet pressure is a direct result of the shaft work supplied by the turbine. With decreasing compressor inlet pressure a reduction in RGF would be expected. This case is complicated by the fact the LP valve duration is decreasing with the compressor inlet pressure giving less time for the lower pressure to act on the cylinder.

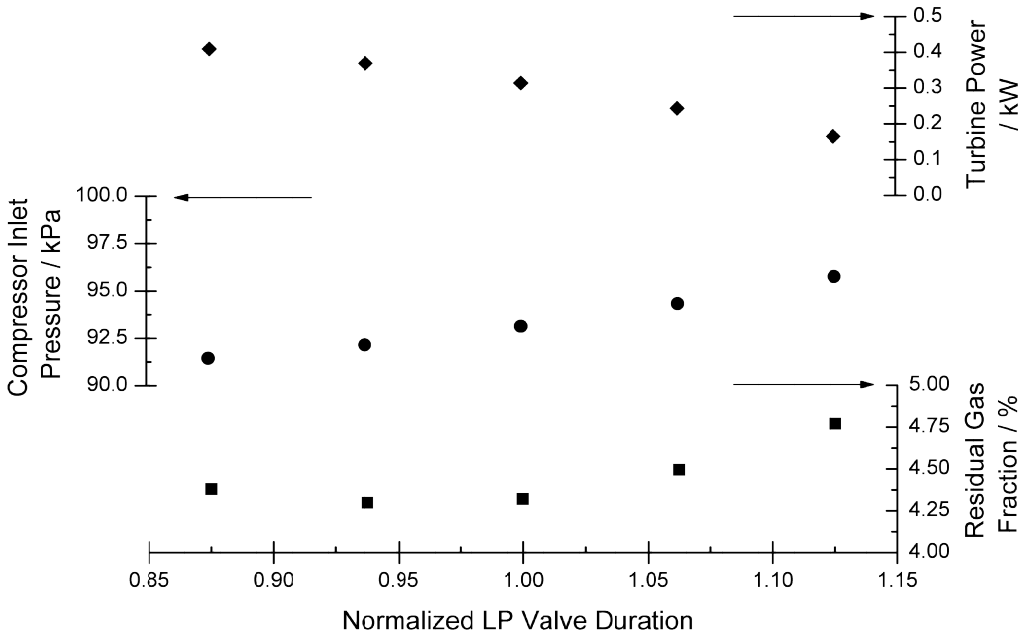

Figure 7-18 - Simulated effect of LP valve duration on turbine power, compressor inlet pressure and residual gas fraction at 3000 rpm 6 bar BMEP

The benefit of exhaust system depressurisation on PMEP with fixed exhaust valve timing has been identified previously. In this case, reducing LP valve duration increases the depressurisation but increases the engine PMEP as shown in Figure 7-19.

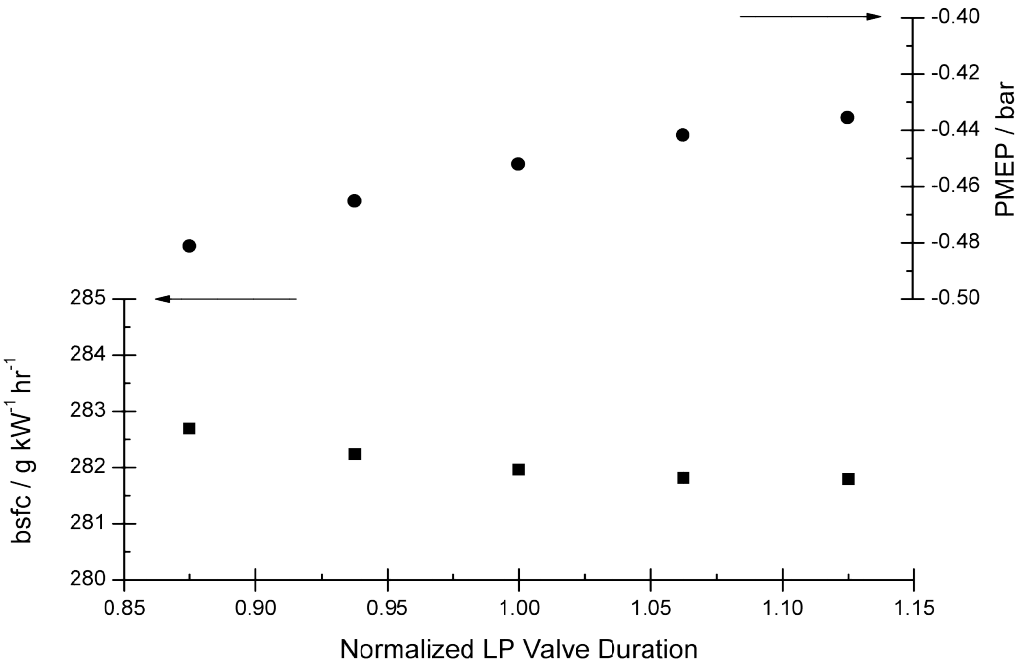

Figure 7-19 – Simulated effect of LP valve duration on PMEP and bsfc at 3000 rpm, 6 bar BMEP

The reason for this is the reduction in LP valve duration reduces the proportion of mass flow through the LP manifold, increasing the proportion of gas flowing through the turbine. This exposes the engine to a higher back pressure and thus increases PMEP. The result of this increase in PMEP is an increase in bsfc, also shown in Figure 7-19.

Figure 7-20 shows the mass flux split for the 0.875 and 1.125 normalized LP valve duration cases shown in the previous figures where positive is mass flowing into the cylinder and negative is mass flowing from the cylinder. It is clear that increasing the LP valve duration, in turn advancing the LP valve opening, increases the proportion of the mass flux through the LP manifold and decreases the total mass flow through the turbine. However, the peak flux from the blowdown pulse remains similar, indicating that the valve is either choking or the HP valve is still capable of allowing the majority of the blowdown gases to exit the cylinder before the LP valve opens.

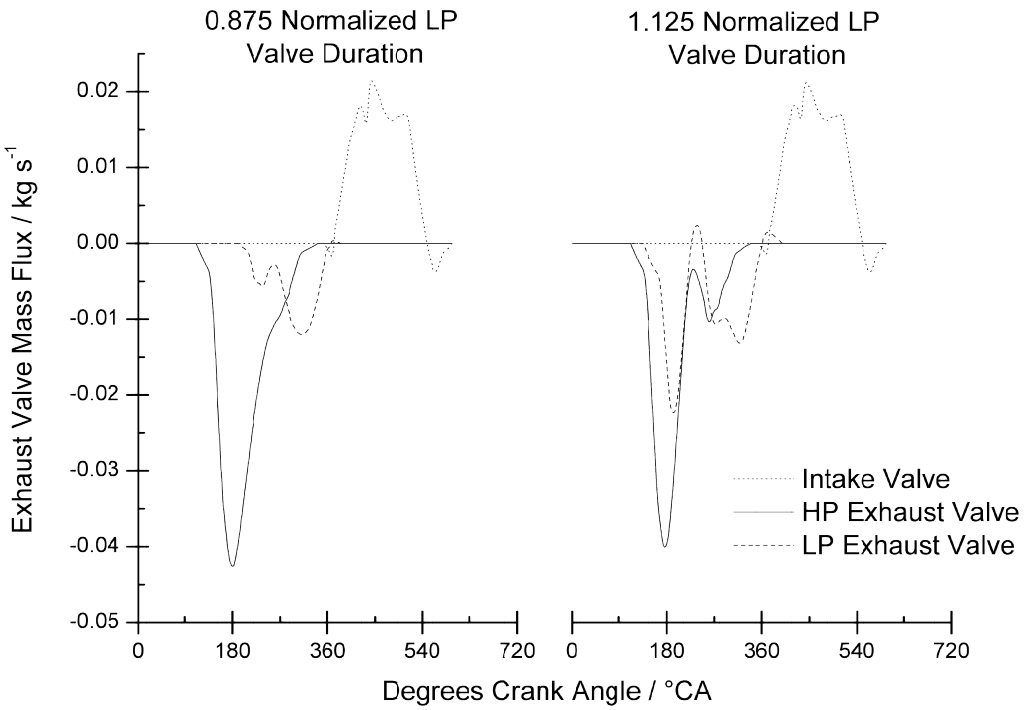

Figure 7-20 - Two simulated extreme cases of LP Valve duration showing the mass flux split between each exhaust branch at 3000 rpm, 6 bar BMEP

From the mass flux through the LP valve, it is more likely that HP valve is choking. For the longer LP valve duration, a mass flux spike can be seen as the valve opens, indicating that the gas in the cylinder will still expand through the valve into the exhaust.

At 4000 rpm 11 bar BMEP varying the LP valve duration for a higher speed, higher load case results in the same trade-off in mass flow split in the exhaust as for the lower load case, as shown in Figure 7-21.

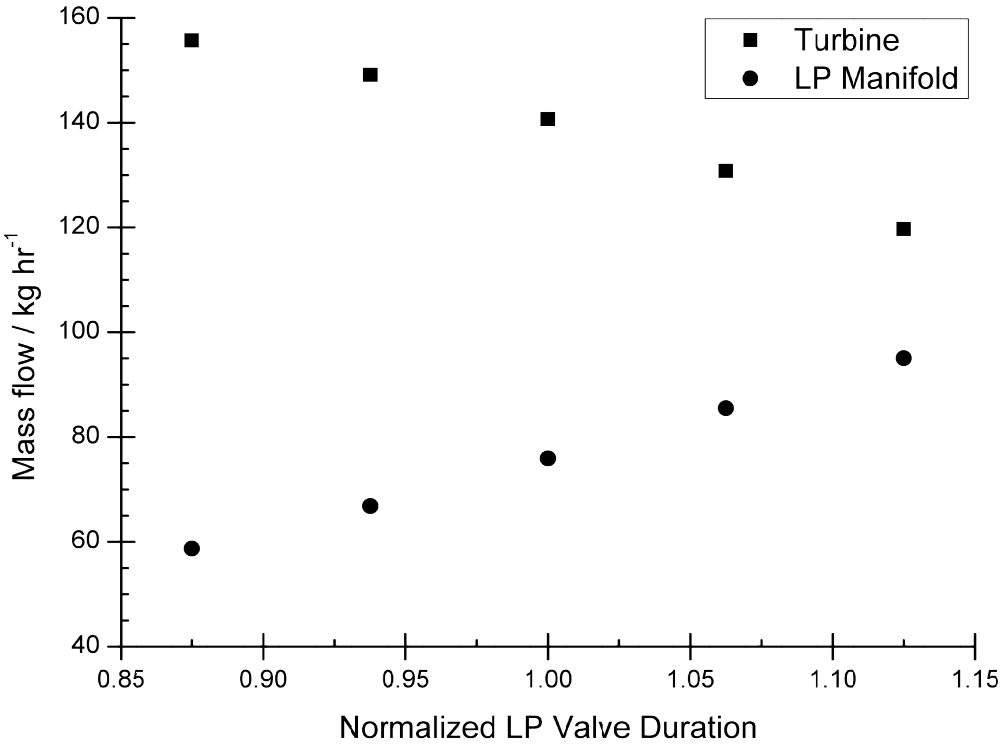

Figure 7-21 – Simulated effect of LP valve duration on exhaust mass flow split at 4000 rpm 11 bar BMEP

Decreasing the LP valve duration increases the flow through the HP valve and turbine. The increased flow leads to increased turbine power and exhaust system depressurisation. In this case the turbine power is particularly sensitive to LP valve duration with a change of 2.5 kW which leads to a difference in depressurisation of almost 20 kPa.

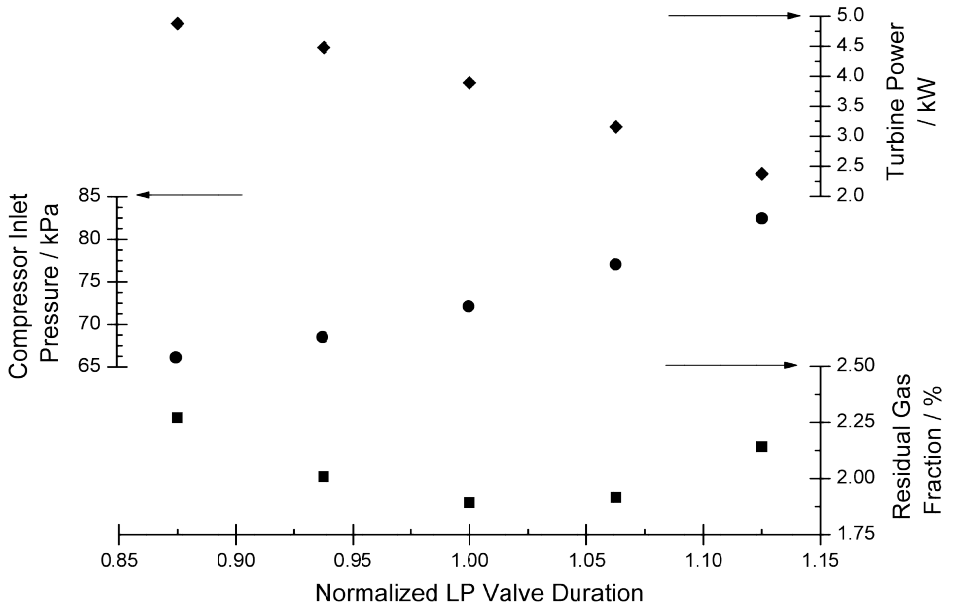

Figure 7-22 - Simulated effect of LP valve duration on turbine power, compressor inlet pressure and residual gas fraction at 4000 rpm 11 bar BMEP

The minimum residual gas fraction again does not occur for the maximum depressurisation. Instead this occurs around the original valve duration. This is likely due to the pressure as the LP valve is closing.

Similar to the previous speed and load case the lowest PMEP value is for the longest LP valve event. The reason for this is the longer valve event leads to increased valve flow area throughout the exhaust event and decreasing the flow area at high load and therefore high mass flow rates will significantly affect PMEP.

The effect of PMEP on bsfc again is very apparent as shown in Figure 7-23 and is more significant than the effect of depressurisation. It is therefore imperative to maximise valve open area at high speeds and loads, sacrificing the level of depressurisation.

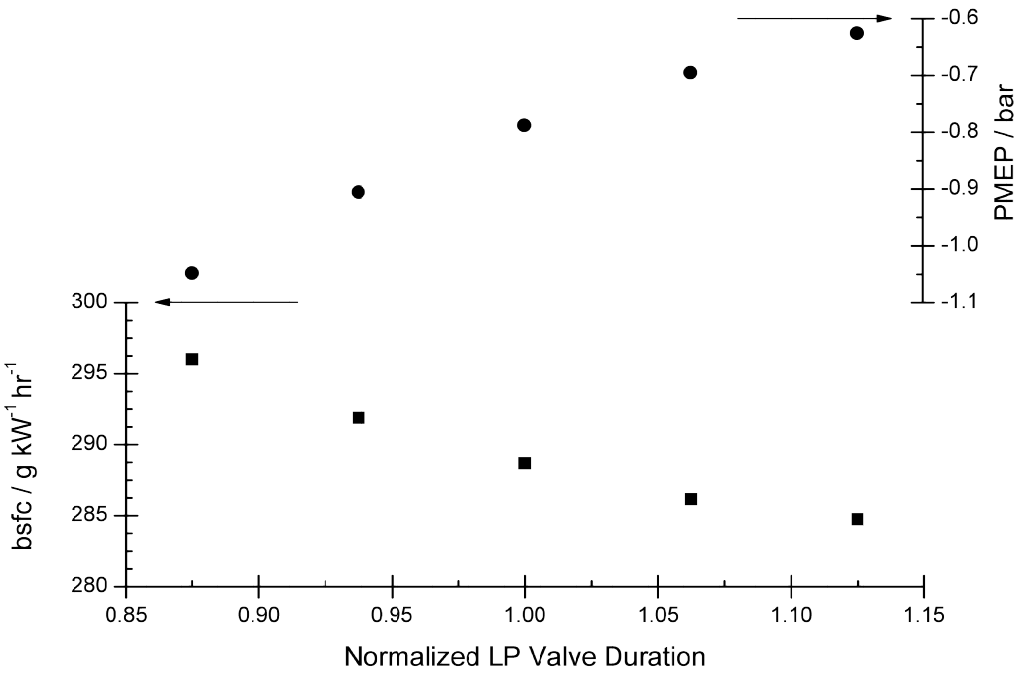

Figure 7-23 – Simulated effect of LP valve duration on PMEP and bsfc at 3000 rpm, 6 bar BMEP

In conclusion, it has been shown that it is important to maximise the LP valve event duration and therefore flow area to reduce PMEP which in turn will improve bsfc. Modulation of the Turbo-Discharging system depressurisation using the LP valve event should be avoided as this has too much effect on PMEP.

The effect of varying the HP valve event will be discussed in the next section.

7.4.4 HP Valve Event

It has been assumed throughout this thesis that the HP valve has to open first. The reason for this is that the blowdown gases need to be directed through the turbine. The effect of advancing the HP valve event for a fixed LP valve event is shown below in Figure 7-24.

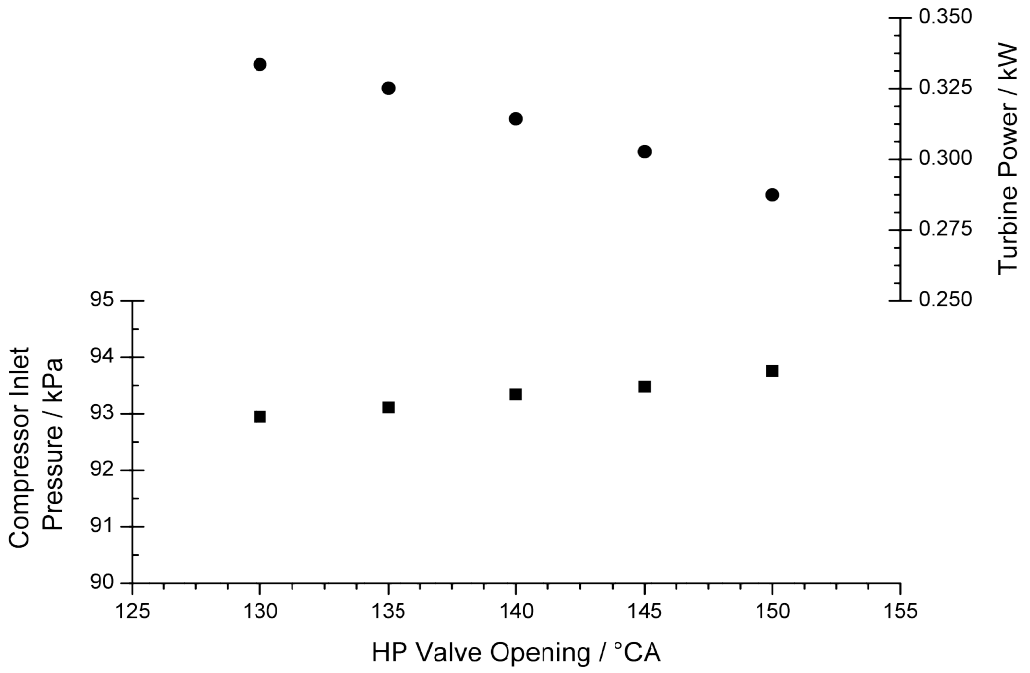

Figure 7-24 – Simulated effect of HP valve opening on turbine power and compressor inlet pressure at 3000 rpm, 6 bar BMEP

It can be seen that advancing the HP valve event allows more energy to be extracted by the turbine and a larger depressurisation generated. This is due to the increase in exhaust gas enthalpy as the exhaust valve timing is advanced.

When considering the LP valve duration it was found that PMEP correlated closely with bsfc. Figure 7-25 shows that when considering the HP valve opening this is not the case. The reason for this is by opening the HP valve earlier in the cycle less energy is extracted by the piston during the exhaust stroke which means the engine needs more air, and therefore fuel, to generate the same power.

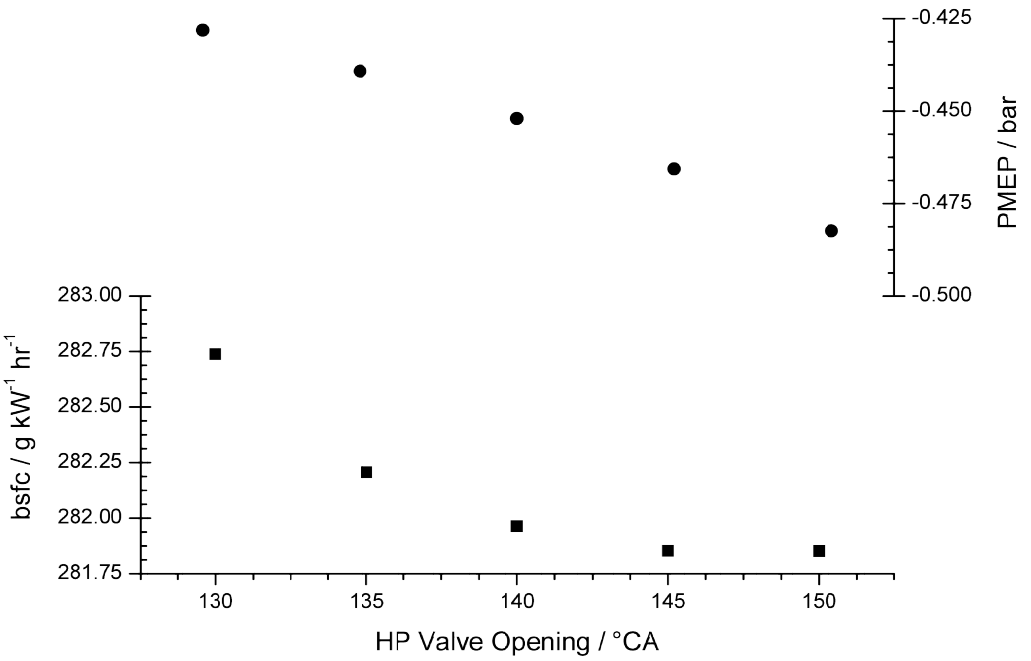

Figure 7-25 – Simulated effect of HP valve opening on PMEP and bsfc at 3000 rpm, 6 bar BMEP

Figure 7-25 also shows there is an optimum point for bsfc at around 145°CA. This is the point at which it becomes more effective to use the remaining energy in the gas in the exhaust system over further expansion of the gas in the cylinder. Thus for this operating case and component configuration, even though the pumping work benefit increases with advancing HP valve opening, it is optimal to open the HP valve around 145°CA.

The effect of HP valve duration is also important. For a given operating condition if the event is too short then not all of the blowdown energy will be presented to the turbine resulting in a lower system depressurisation. If the event is too long there is a risk through cylinder exhaust event overlap that the flow into the HP manifold will reverse as another cylinder begins exhausting. This may cause flow of exhaust gas back into the cylinder giving potential for gas to pass through the cylinder from the HP to LP manifold, reducing the energy available to the turbine through reduced mass flow in turn reducing system depressurisation.

Valve duration was linked to valve lift in the same manner as for the LP valve investigation. It is important to note that a longer valve duration will also mean a larger permissible valve lift which will result in a non-linear increase in effective valve flow area over the entire exhaust event.

Figure 7-26 shows the effect of HP valve duration on turbine power and resultant depressurisation. The relative HP valve duration is a multiplier from the original Ford Cam profile; a number below one denotes a shorter valve event.

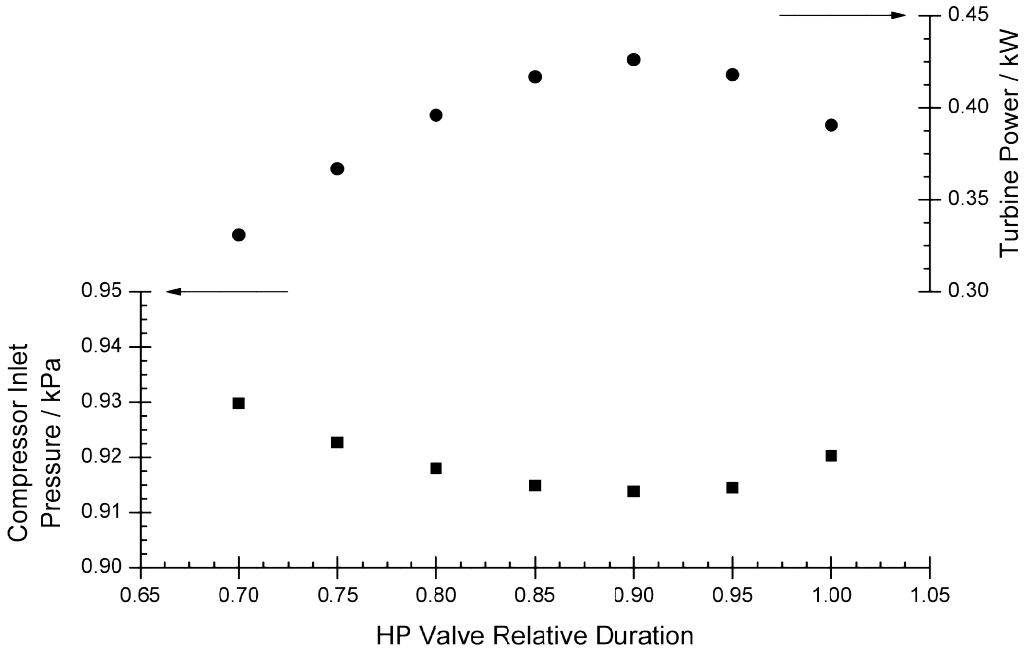

Figure 7-26 – Simulated effect of HP valve duration on turbine power and depressurisation at 3000 rpm, 6 bar BMEP

A peak in turbine power and therefore depressurisation is seen at a relative valve duration of around 0.9. For valve durations greater than this the turbine power decreases due to a drop in inlet pressure and temperature. The reason for this is the valve events between cylinders begin to overlap, as described above, and the blowdown pressure pulse begins to be clipped such that the average pressure is lower.

The reversal of flow back into the cylinder from the HP manifold also, for this simulation, has a positive impact on bsfc. This, along with the effect on PMEP, is shown in Figure 7-27.

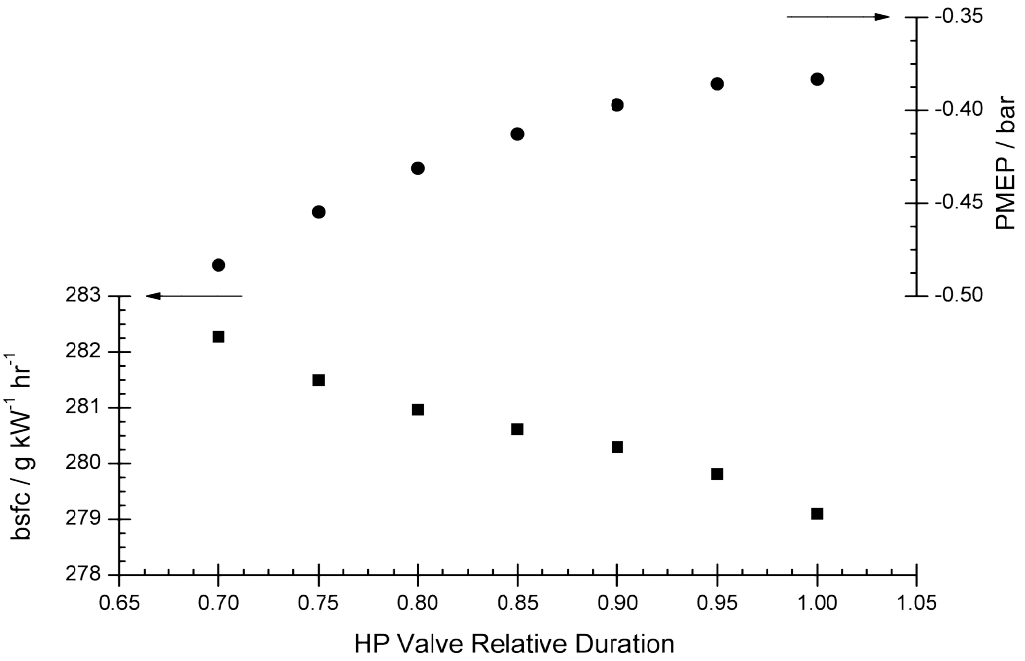

Figure 7-27 – Simulated effect of HP Valve duration on PMEP and bsfc at 3000 rpm, 6 bar BMEP

The figure shows PMEP decreases for an increasing valve duration. This agrees with the LP valve investigation, where increasing the open area of the exhaust valves improves PMEP. The bsfc generally reflects this, however, the longest two valve durations appear to produce an anomalous result in that bsfc further decreases.

The reason for this is the engine is throttled under this condition and as the duration proceeds beyond 0.95 residual gas fraction begins to increase. For the engine to maintain the same load the throttle needs to open further. This reduces throttling losses and increases engine fuel efficiency and is observed as a reduction in bsfc. This will only work in practice to a point; increasing hot residual gases will promote knock which in turn will limit ignition advance or achievable compression ratio and therefore engine fuel conversion efficiency.

A further operating condition will again be considered to indicate how much variability is required to optimise the valve events.

The same sensitivity to HP valve opening was conducted at 4000 rpm, 11 bar. Figure 7-28 shows the effect of valve opening timing on turbine power and the subsequent depressurisation generated.

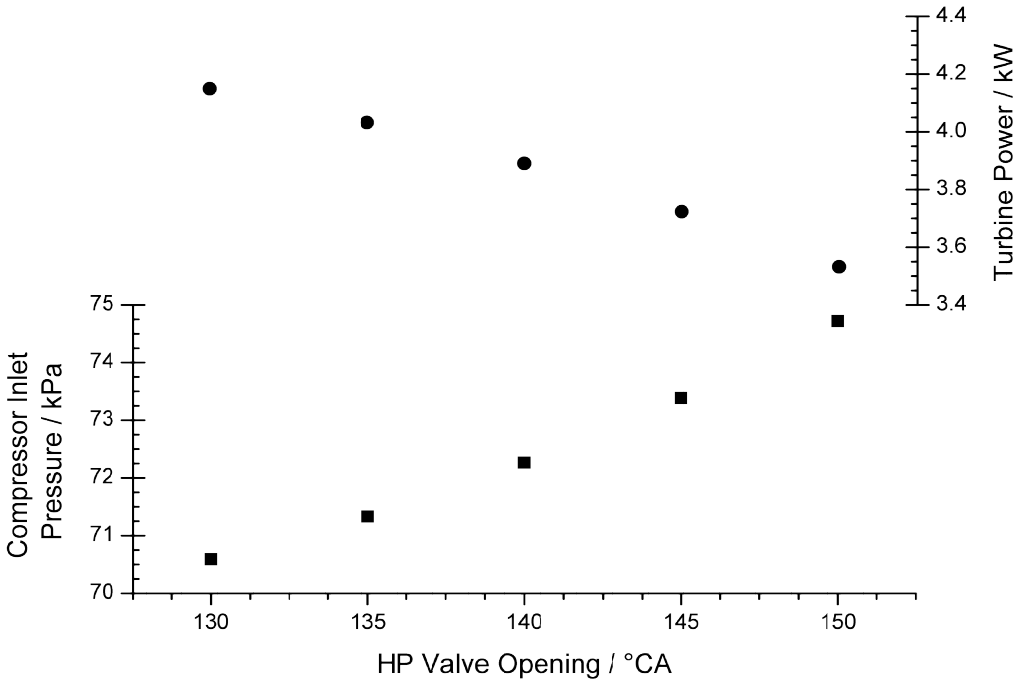

Figure 7-28 – Simulated effect of HP valve opening on turbine power and compressor inlet pressure at 4000 rpm, 11 bar BMEP

Whilst it is clear that the earliest HP valve opening is still desired, the earliest valve opening was not beneficial to engine fuel efficiency at 3000 rpm, 6 bar BMEP. Figure 7-29 shows the reverse in that early HP valve opening is beneficial to engine bsfc and PMEP.

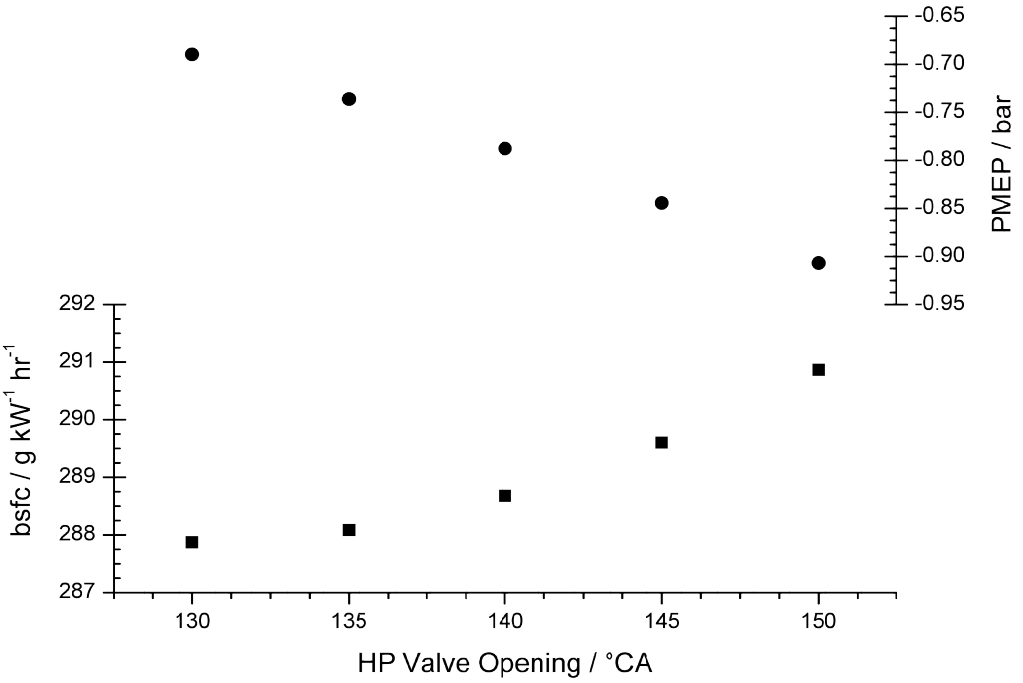

Figure 7-29 – Simulated effect of HP valve opening on PMEP and bsfc at 4000 rpm, 11 bar BMEP

The HP valve opening helps to govern the mass flow split between the HP and LP sides of the Turbo-Discharging system. At lower speeds and loads it may be possible to evacuate all of the exhaust gas which will impart work on the turbine in a shorter period, in which case it is beneficial to maximise the expansion work in the cylinder and open the HP valve as late as possible. Compounding this is the lack of turbine energy at lower speeds and loads such that there is less benefit of Turbo-Discharging.

At this engine speed and load point, however, much more energy is available to the turbine. This leads to a larger depressurisation and therefore a larger benefit of Turbo-Discharging. Furthermore a longer period may be required to evacuate gas through the HP valve to the turbine before the LP valve opens. Advancing the HP valve opening decreases the overlap between the HP and LP valve events leading to more gas passing through the turbine that can impart work on it and less bypassing it through the LP valve and manifold.

It is worth noting that, although not shown in these plots, there will still be a trade-off with in-cylinder expansion and turbine work. Advancing the HP valve opening beyond that shown may lead to reduced in-cylinder expansion and therefore reduced engine fuel conversion efficiency.

Figure 7-30 shows the effect of HP valve duration for a fixed valve opening on turbine power and system depressurisation at 4000 rpm, 11 bar BMEP. As the duration increases from the minimum there is little effect until a relative duration of 0.85 where the turbine power starts to decrease.

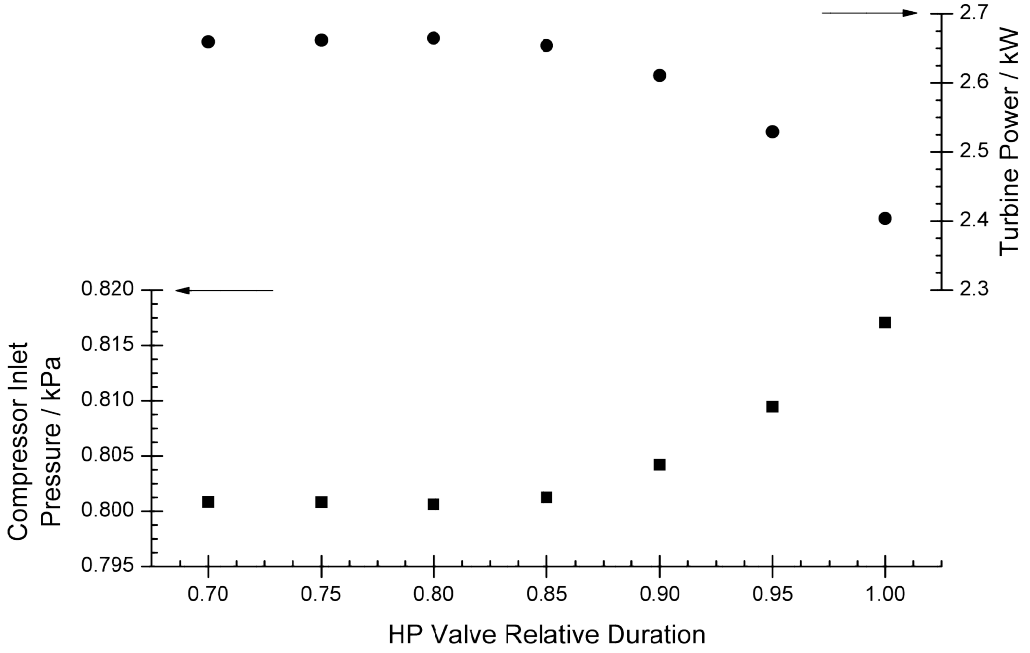

Figure 7-30 – Simulated effect of HP valve duration on turbine power and depressurisation at 4000 rpm, 11 bar BMEP

The reason for this is the manner in which the valve events have been scaled. The entire profile has been stretched from the point of valve opening. This has the effect of shifting the point of peak lift, and the ramp to it, later in the cycle. The slower ramp rate delays the blowdown gases from leaving the cylinder reducing the energy available to the turbine at a fixed point in the cycle. Adjusting the duration in this manner therefore has a similar effect to delaying the exhaust valve opening.

This is also observed in the PMEP and bsfc shown in Figure 7-31. There is a clear optimum in both around a duration of 0.85 whereupon turbine power starts to decrease.

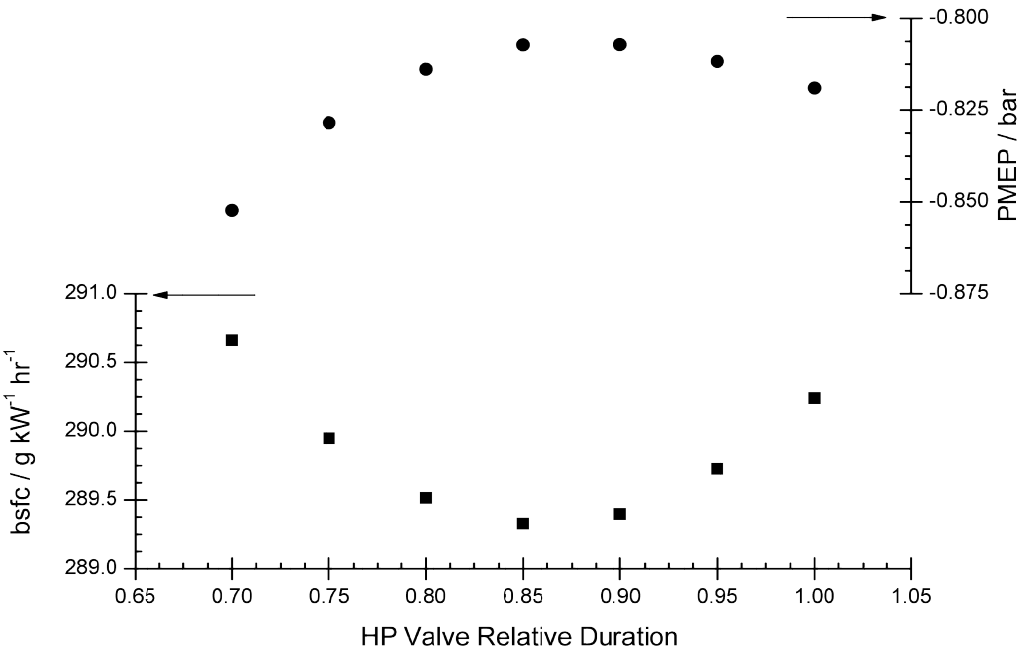

Figure 7-31 – Simulated effect of HP Valve duration on PMEP and bsfc at 4000 rpm, 11 bar BMEP

It is also worth noting that at 4000 rpm, 11 bar BMEP the largest effect on PMEP and bsfc is that of the Turbo-Discharging system whereas for throttled part-load conditions with less depressurisation it is important to balance manageable levels of RGF to de-throttle the engine and turbine power to maximise the depressurisation achieved.

7.5 Observed Fuel Economy Benefit

The fuel economy of both the NA and Turbo-Discharged engines was measured using the ECU calculated fuel flow values described in chapter 4. For each measurement point not at WOT, the throttle position and spark advance were fixed, and the fuelling altered until the mixture was stoichiometric. As such the combined primary and secondary benefits of Turbo-Discharging manifest themselves in the results.

Figure 7-32 is a contour plot of the percentage fuel economy change of the measured Turbo-Discharging engine test data over the baseline engine test data. It can be seen that a maximum benefit of 8% can be observed at low engine speed and load whilst the maximum detriment is limited to around 10% at high engine speed.

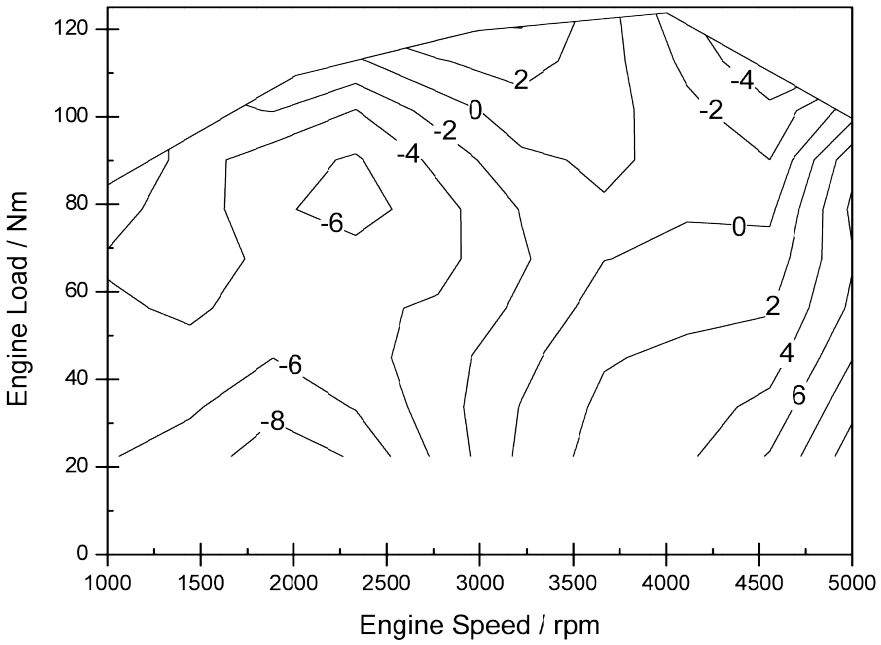

Figure 7-32 - Contour plot of measured Turbo-Discharged engine speed vs engine load with contours of percentage change in bsfc compared to the baseline

There are four main areas on this plot that will be discussed individually:

1. The low speed, low load region of fuel economy benefit;
2. The medium speed, high load fuel economy deficit region;
3. The high speed, high load region of fuel economy benefit;
4. The high speed, low load region of fuel economy detriment.

1. Low speed, low load region of fuel economy benefit

The fuel economy improvement at low load cannot be attributable to the primary benefit of Turbo-Discharging. Figure 7-13 shows the depressurisation measured at the compressor inlet by a steady pressure transducer. There is no depressurisation in the low speed low load region of the engine map as shown; as such there can be no benefit from it. This is also shown in Figure 7-16 which plots the predicted pumping work benefit of Turbo-Discharging; at low speed there is a detriment to pumping work of 0.2%.

The Turbo-Discharging system actively avoids valve overlap as any valve overlap when there is a depressurisation would draw fresh charge through the cylinder limiting the possible level of depressurisation and thus the pumping work benefit of the system. The standard and Turbo-Discharging valve timings are shown in Figure 7-33.

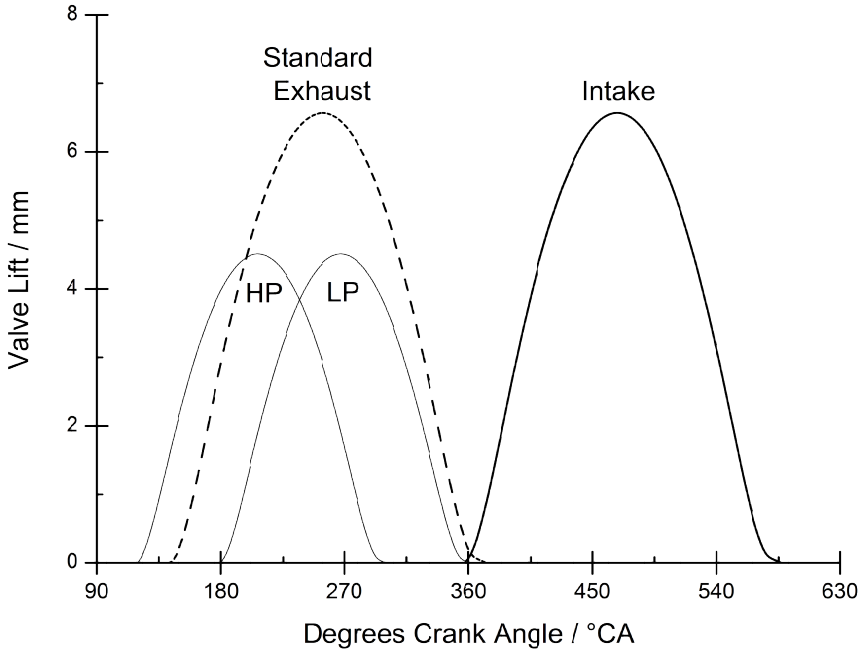

Figure 7-33 - Turbo-Discharging and standard valve timing and lifts

At low speed and low load the baseline engine intake manifold pressure at IVO may be lower than that in the cylinder and the exhaust manifold which, given adequate overlap, would draw burned gases back from the manifold into the cylinder and possibly into the intake manifold. With the Turbo-Discharging valve timing as described there is no overlap between the intake and exhaust events so burned gases will not flow back into the cylinder.

If this is the case the extra RGF would cause a longer burn duration. Figure 7-34 shows mass fraction burned curves calculated from 200 cycles of measured data for the baseline and Turbo-Discharged engines at 2000 rpm, 6 bar BMEP. The 10-90% burn duration for the Turbo-Discharged case is 3 degrees shorter than that of the baseline engine which is clearly visible. A shorter burn duration will give a higher and earlier peak cylinder pressure giving more time for expansion whilst the piston is moving towards BDC and thus more work can be extracted. This means to achieve the same engine load less fuel is consumed, resulting in the low speed and load benefit in Figure 7-32.

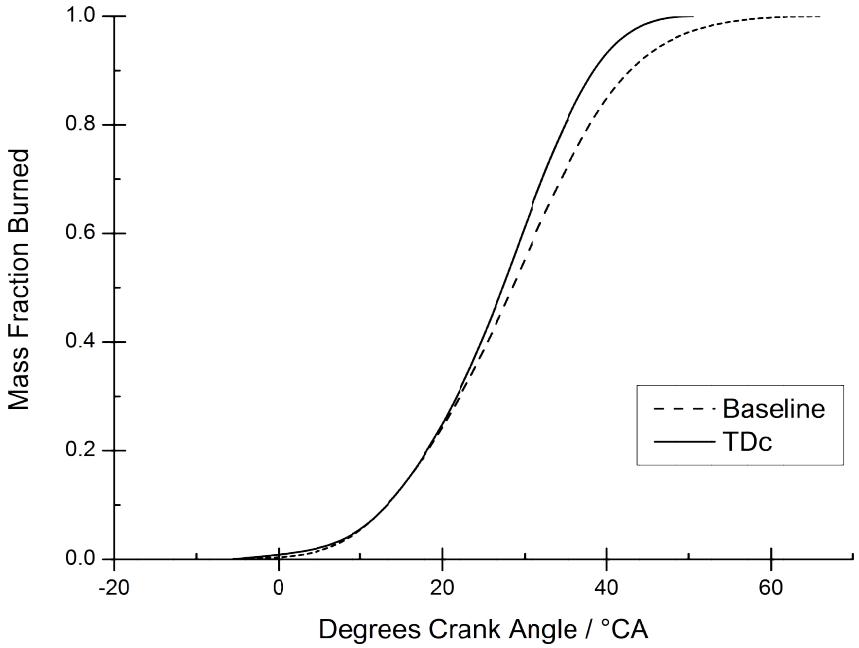

Figure 7-34 - Mass fraction burned curves for the baseline and Turbo-Discharged engines at 2000 rpm, 6 bar BMEP

2. The medium speed, high load fuel economy deficit region

Near peak load between 2500 and 3750 rpm there is a region of fuel economy detriment, i.e. the Turbo-Discharged engine is consuming more fuel than the baseline engine to produce the same torque.

Under these conditions it was noted that the Turbo-Discharged engine was knock limited in that the ignition timing compared to the standard engine had to be retarded to avoid knock. This is likely due to the more restrictive exhaust manifold used in the prototype Turbo-Discharging system and a lack of significant depressurisation to overcome this restriction. In this condition on the standard engine the valve overlap between the intake and exhaust valves would help to drive fresh charge into the cylinder and help to reduce RGF. The Turbo-Discharging system with no valve overlap does not have this mechanism of reducing RGF which may cause it to be higher than the baseline engine in this region. For example, at 3000 rpm full load the BSAC of the baseline engine was 4.032 kg kW^{-1} hr^{-1} as opposed to 3.647 kW^{-1} hr^{-1} for the Turbo-Discharged engine. Further work should be done to optimise valve timing in this region as it has been shown that maximising engine efficiency for different speeds and loads can require significantly different valve events.

3. The high speed, high load region of fuel economy benefit

Between 3750 and 4750 rpm and between 70 Nm and peak load there is an area of fuel economy benefit with a maximum fuel economy benefit of 4%. In this region the exhaust gas contains the largest amount of energy which is available to the turbine. This allows more energy to be extracted and a larger depressurisation to be created.

It is important to note that as the engine speed increases there is less time for knock to occur and as such the engine becomes less knock-limited. This means the engine can run at the same ignition timing as the base engine.

To ascertain if this benefit was entirely due to the pumping work benefit of Turbo-Discharging the level of depressurisation was converted into a predicted proportional primary benefit of Turbo-Discharging by dividing the depressurisation by the engine BMEP. This gave a maximum theoretical primary benefit of Turbo-Discharging as shown in Figure 7-16. In fact, at low engine speed and load there is a predicted detriment of Turbo-Discharging, where the exhaust system

pressure is higher due to the restriction of the manifold, turbine, heat exchanger and compressor.

The peak pumping work benefit in the medium to high speed, high load region from Figure 7-16 is only in the region of 2%. The extra benefit observed in this region could be due to improvements in engine breathing on the intake side from increased charge momentum due to the depressurised cylinder at the start of the intake stroke or reduced residual gas fraction allowing the combustion duration to be shorter.

Figure 7-35 shows the mass fraction burned curves for both engine configurations operating at 4000 rpm, peak load. It can be seen again that combustion in the Turbo-Discharged case is happening faster with a 10-90% burn duration 3°CA shorter than the baseline case. This again will offer a torque improvement, thus to reach the same load requires less fuel to be burned.

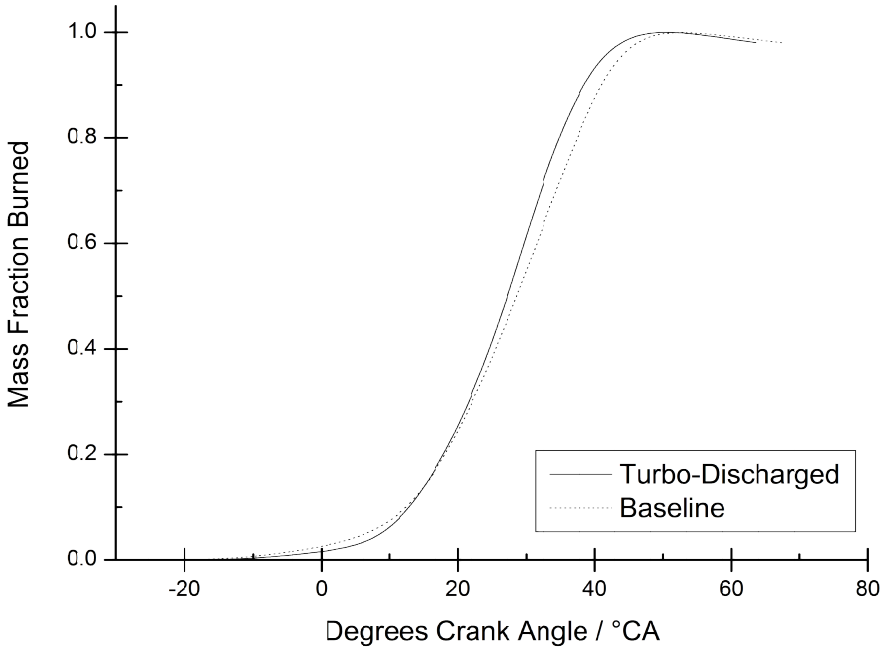

Figure 7-35 - Mass fraction burned curves for the Turbo-Discharged and baseline cases at 4000 rpm, peak load based on experimental data

4. The high speed, low load region of fuel economy detriment

At high speed, and especially low load, a fuel economy detriment can be observed in Figure 7-32. Figure 7-13 shows there is only minimal depressurisation in these conditions, and Figure 7-16 confirms that there could only be up to 1% primary benefit under these conditions. This is due to limits in engine breathing due to the manifold design, turbomachine specification and valve flow limitations.

The split manifold design restricts the flow into the exhaust system, with a 4% reduction in flow area due to the divider design. The flow through the cylinder head into the manifold is liable to cause larger pressure losses due to the arduous gas path compared to the standard manifold. Moreover, due to the offset nature of the high and low pressure events there is a substantial period of the exhaust event where there is only one valve open. Figure 7-36 highlights these areas in grey.

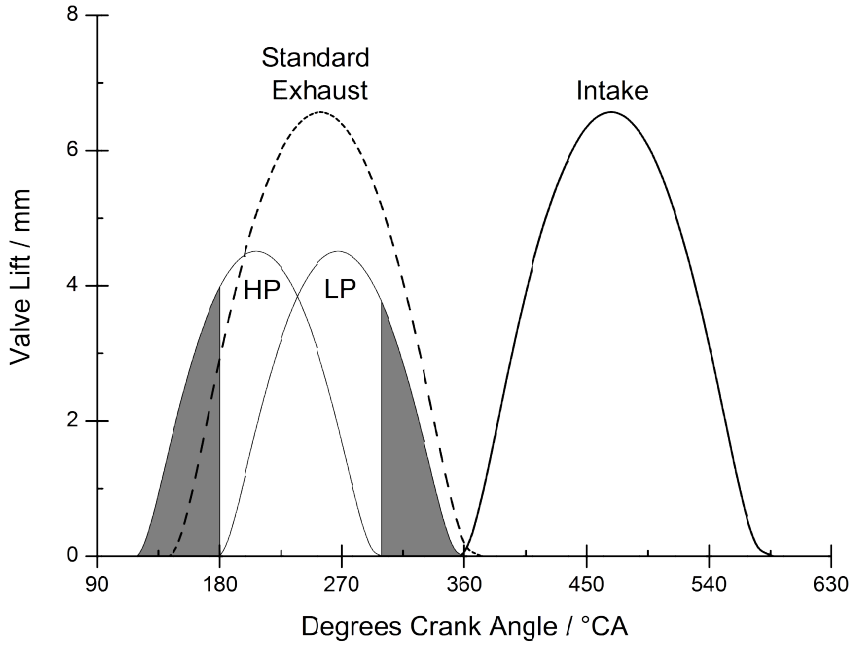

Figure 7-36 - Standard and Turbo-Discharging valve events with area of single exhaust valve operation highlighted

This, combined with the reduced lift and duration of the valve events, amounts to an exhaust event with only 54.8% of the total flow area over the entire event compared to the standard valve event. It is therefore reasonable to expect a reduction in flow capacity at high engine speeds. It would be possible to improve this by increasing the diameter of the valves and redesigning the gas paths through the cylinder head.

7.6 Closing Comments

This chapter has shown how the 1-D Turbo-Discharged model was validated against measured data both at full and part load such that it could be used for further investigation of the technology. The efficacy of the measured and modelled Turbo-Discharging systems was then calculated and the potential improvement was presented.

An investigation into the pumping work benefit was then shown, raising the importance of exhaust valve events on system effectiveness and their effect on engine fuel conversion efficiency. Finally the observed fuel economy benefit measured on the Turbo-Discharged engine was presented and areas of high and low efficiency were discussed.

The next chapter will investigate through modelling and experimentation the secondary benefits of Turbo-Discharging such as the effect of depressurisation on knock margin and charge admittance.

8. Secondary Benefits of Turbo-Discharging

The secondary benefits of Turbo-Discharging are defined as any benefit the system may offer that is not the primary; i.e. any benefit that isn't a reduction in PMEP resulting from the depressurised exhaust.

The two most significant secondary benefits observed from Turbo-Discharging are as follows:

1. A depressurised cylinder at EVC results in reduced RGF which gives more cylinder volume for fresh charge. Increasing the quantity of fresh charge allows more fuel and air to enter the cylinder which when combusted can produce more power. Residual gases from combustion are also significantly hotter than fresh charge. When the quantity is reduced the overall temperature of the cylinder contents is reduced which leads to lower peak cylinder temperatures and pressures. This leads to the later onset

2. Increased intake charge momentum from cylinder depressurisation giving an initial increase in fresh charge acceleration which, subject to tuning effects, can increase the trapped mass of oxygen allowing more fuel to be burned. There is also the potential to draw charge through the cylinder straight into the exhaust to further improve cylinder filling and scavenging.

This section will investigate these secondary benefits and attempt to isolate their effects on engine performance.

8.1 Effect of Depressurisation on Knock Margin

There are several different types of knock, or auto-ignition, which occur in modern gasoline spark ignition engines. This section will focus on spark knock; that which occurs after ignition and can be eliminated by retarding the spark. The depressurisation created by Turbo-Discharging may influence other types of knock and further work should consider the effect of Turbo-Discharging on these.

Spark knock occurs when the pressure and the temperature of the end gas rise as they are compressed by the burned gases expanding in the cylinder. If these pressures and temperatures rise sufficiently then the end gas may auto-ignite (Heywood, 1988). Thus spark knock can be controlled by limiting the pressure and temperature at the end of compression such that the burned gas expansion does not cause auto-ignition. Higher compression ratios are desired for combustion efficiency; for the same fuel addition a higher compression ratio will give a higher cylinder pressure, and so for a fixed expansion ratio more work can be extracted. Knock is therefore a key factor in limiting the efficiency of gasoline IC engines and its mitigation may offer efficiency benefits.

In a similar manner knock also limits the earliest achievable ignition timing. Optimum ignition timing achieves the highest possible cylinder pressure with the smallest amount of spark advance such that the expansion stroke can achieve the largest possible change in pressure to extract as much energy from the gas as possible. However, if ignition timing is retarded to avoid knock less work can be recovered during the expansion stroke. Thus it is desirable to delay the onset of knock as much as possible to allow for maximum spark advance to achieve high combustion efficiencies.

Knock intensity has been shown to be dependent on RGF. Westin (2000) showed that for a 2.1% reduction in RGF the spark could be advanced by 6°CA for a given knock intensity. They stated two reasons why the reduction in RGF allowed for spark advance; the change in chemical composition of the cylinder contents and the high temperatures of the residual gases. Of these, the increase of in-cylinder temperature was defined as having the biggest effect on the propensity to knock. When considering two RGF cases (5.1 and 7.2%) they calculated a 30 K difference in the temperature at intake valve closing. Even with such a small difference in quantity of RGF, its high average temperature in these operating conditions of 1400 K leads to a significant difference in temperature at the start of compression which will then affect peak cylinder temperature, upon which knock is dependant.

It is common in gasoline engines operating in a throttled condition for burned gases remaining in the cylinder at IVO to exit into the intake manifold before being pulled back into the cylinder by the vacuum created by the piston. If the cylinder is left in a depressurised state there will be less of a pressure difference between the cylinder and the intake manifold such that flow out of the cylinder into the intake manifold is reduced. This will have a positive effect on the scavenging and charging of the cylinder, manifesting as an increase in volumetric efficiency as the piston does less work to draw the charge into the cylinder and as a reduction in RGF.

Reduced hot RGF will also result more usable cylinder volume for intake charge or cooled EGR. If RGF can be replaced with cooled EGR the knock margin could be increased further.

It is hypothesised that through depressurisation during the exhaust stroke RGF can be reduced which has been shown in the thermodynamic model used in chapter 3. This was investigated practically and is discussed in section 8.3.

The other most significant secondary benefit of cylinder depressurisation, and therefore Turbo-Discharging, will now be discussed before both are investigated on the engine and using 1-D modelling.

8.2 Effect of Depressurisation on Charge Admittance

If an exhaust depressurisation is applied to an engine cycle with an overlap between exhaust and intake valve events the initial pressure ratio between the cylinder and intake manifold at intake valve opening will again be larger as in the previous case. However, in this case the gas is allowed to flow through the cylinder, not just accelerating faster into a closed volume but gaining more momentum as it flows through the cylinder into the exhaust. When the exhaust valve closes the gas in the intake manifold already has momentum creating a ram or supercharging effect. This may allow the intake event to be extended further into the compression stroke admitting more air to the cylinder allowing for an increase in torque.

There are three potential issues with the effect mentioned above:

1. If the engine is port fuel injected the charge will carry fuel through the cylinder into the exhaust, increasing HC emissions and fuel consumption;
2. Passing air straight through the cylinder increases the mass flow through the compressor without providing the turbine with any extra work. This will decrease the achievable depressurisation, decreasing the primary benefit of Turbo-Discharging;
3. Exhaust aftertreatment may be sensitive to the amount of air in the exhaust gas to the point where it cannot work effectively and emissions may be increased.

The first issue is averted completely on a DI engine operating in a stratified combustion mode. Other engines for markets where there is less emphasis on emissions may also remain PFI, however, it is likely these engines would not be able to justify the extra cost of the components required for Turbo-Discharging.

The second issue needs to be a calculated compromise between fuel efficiency and engine torque. For example, passing more air through the cylinder will give the charge more momentum but it may decrease the level of depressurisation achieved and thus negatively affect the primary benefit of Turbo-Discharging. However, operating with minimal valve overlap will maximise the depressurisation seen by the cylinder during the exhaust stroke and thus maximise the fuel economy benefit but will negate most of this supercharging effect. It may be possible to optimise this with a variable valve control system for a particular vehicle or driving mode and could be varied over the engine speed range to optimise performance on drive cycles.

This supercharging effect of the depressurisation created on charge admission will be investigated using a modified version of the NA baseline engine model and the compromise between engine torque and fuel economy will be investigated.

The third concern of unburned air in aftertreatment systems is one that is commonly experienced in modern pressure charged gasoline engines where scavenging strategies are employed. This involves passing the pressurised air through the cylinder to aid removal of residual burned gases in a valve overlap period. The limitation on this currently arises from emissions legislation where there is a limit on the quantity of unburned air in the exhaust as this effectively dilutes the exhaust gas and improves measured engine emissions. Furthermore excess oxygen (lean spikes) in the exhaust gas may inhibit operation of three way catalytic converters, reducing their conversion efficiencies and increasing exhaust emissions.

One method to avoid this would be to employ the same strategy as above for optimising fuel economy or performance through selectable engine operating modes. Scavenging with large amounts of intake air could be minimised during part load operation where fuel economy and emissions are of interest and it could be increased for high load operation where these are less important.

Both secondary effects will now be investigated experimentally and theoretically using a modified 1-D engine model.

8.3 Experimental Investigation

To investigate the effect of RGF on knock margin and charge admission it was decided to modify the engine test rig to separate some of the effects of the Turbo-Discharging system. This was achieved by removing the Turbo-Discharging system from the baseline engine and attaching a centrifugal blower to the engine exhaust to create a depressurisation. This simulates a Turbo-Discharging system with a high effectiveness of translating the depressurisation back into the cylinder from the utilisation of both the exhaust valves.

The blower used was a Ron Tai Electrical Engineering company RT-3700 centrifugal blower which could create a depressurisation of up to 0.3 bar depending on the exhaust gas flow rate. The exhaust gas first passed through the exhaust gas heat exchanger rig described in section 6.3.2 which was required to cool the exhaust gases before they entered the blower. The depressurisation created by the blower was measured using Delta Ohm HD9408T steady pressure transducers.

The operational range of this test setup was limited by two factors:

1. When gas is compressed it increases in temperature. This led to a maximum blower intake temperature limit such that the outlet temperature did not exceed a safe working level. The blower intake temperature was dependent upon the engine operating condition and the effectiveness of the heat exchanger rig;
2. The pressure ratio created by the blower was a function of mass flow rate; the higher the mass flow rate the less depressurisation was attainable. At higher speeds and loads, even if the intake temperatures were acceptable, the blower would have been unable to create a significant depressurisation.

Both these reasons led to a maximum achievable engine speed of 2500 rpm.

Since the blower only operated at a fixed speed the level of depressurisation generated would have been fixed for a given engine speed and load. To allow this to be varied a gate valve was installed in the exhaust upstream of the blower. This valve was adjusted to vary the exhaust manifold depressurisation and also to allow for increased exhaust back pressure when the blower was switched off.

The engine was controlled using the ATI Vision software. Not only did this allow for control of throttle angle and ignition timing as before, but it allowed for interrogation of the engine knock sensor. As well as displaying the signal from the knock sensor it displayed a logical variable denoting when the ECU identified a cylinder as knocking. This was used to define the onset of knock.

As mentioned previously the knock margin was analysed for a range of exhaust manifold pressure conditions (0.75-1.15 bar) over a range of engine speeds and loads. The dynamometer controller was set to a speed and load whereupon the throttle angle, ignition timing and injection timing were fixed using the ATI software. From this point the ignition timing was advanced until the onset of knock. The advanced ignition gave rise to increased engine torque and the peak torque reached before the onset of knock was recorded. Fuelling was controlled in closed loop by the engine ECU, varying in lambda by a maximum of 3%.

It should be noted that the standard engine valve events overlap by 20°CA. Under certain conditions this overlap will allow for fresh charge to be pulled through the cylinder, further decreasing RGF. Moreover, this may increase charge momentum beyond that achievable with Turbo-Discharging. As such this experiment can be considered an optimistic view of what may be achievable with a Turbo-Discharging system.

The RGF was measured using a Cambustion NDIR500 (Cambustion 2014). This is a fast Non-Dispersive Infra-Red (NDIR) gas analyser which uses a spark plug with an orifice to allow a sample of the cylinder gases to be extracted by the analyser. The analyser measures the CO and CO_2 of the sample gases, CO2 directly reflecting the quantity of burned gases in the cylinder. The volume of the sample line and the analyser are minimised to ensure a fast reaction time, as low as 8 ms to measure from 10-90% range. Measuring the minimum and maximum CO_2 over the cycle then allowed calculation of the RGF.

8.4 Experimental Results

It was only possible to induce knock through advanced timing at loads greater than 55 Nm for any engine speed, and engine speeds less than 2000 rpm showed little difference in how exhaust manifold pressure affected the knock margin due to the inherent knock resistance of the combustion system at these engine speeds and loads. Figure 8-1 shows data for NA and Turbo-Discharging representative exhaust back pressures where the contours represent the maximum amount of spark advance from the base condition before knock was detected. The points outside of the two sets of data have been removed as there is not enough data to sufficiently accurately extrapolate over the entire map. It can be seen that for the same amount of advance with a lower exhaust pressure it is possible to achieve a higher load.

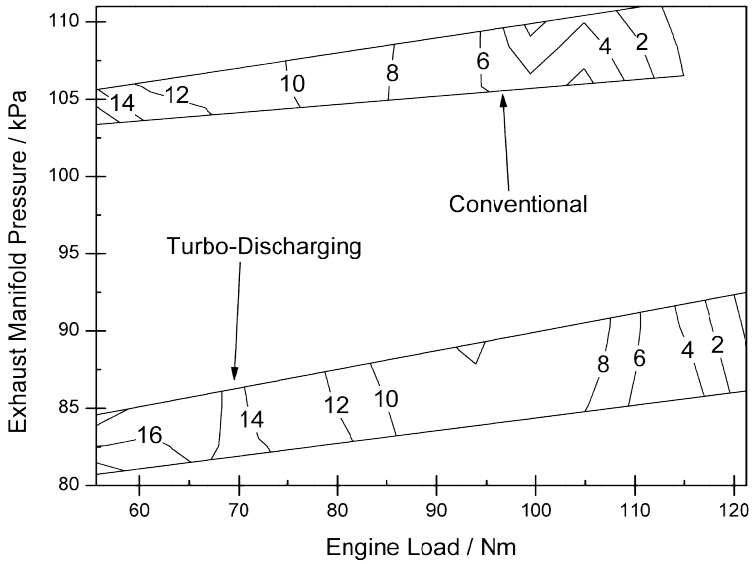

Figure 8-1 - Plot showing contours of maximum possible spark advance from baseline condition vs steady exhaust manifold pressure and engine load at 2000 rpm

Also visible in Figure 8-1 are the peak torque figures before no spark advance is possible. It can be seen that a lower exhaust pressure gives, for no spark advance, a higher peak load. This is attributed to the reduced PMEP through improved breathing during the exhaust stroke and the increased cylinder volume due to reduced RGF.

The values of measured RGF at EVC are plotted in Figure 8-2. Four series of data are plotted; with and without exhaust depressurisation, and with and without spark advance. The square symbols refer to the points with no spark advance, the circular symbols refer to the maximum

amount of spark advance before knock was observed, the solid symbols refer to operating points with no exhaust system depressurisation and the hollow symbols refer to points with exhaust depressurisation.

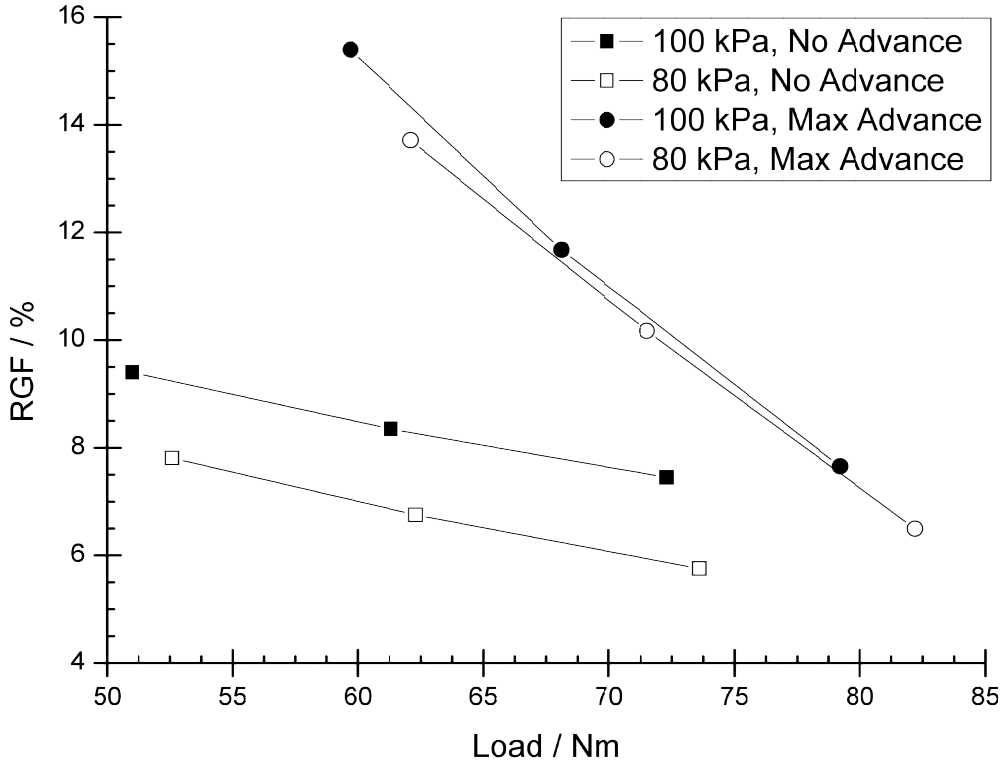

Figure 8-2 - Measured Residual Gas Fraction (RGF) at EVC at 2000 rpm for various loads at 80 and 100 kPa exhaust manifold pressure

As described previously increasing the spark advance significantly increases the engine load for a given engine air and fuel flow, which is reflected above. However, Figure 8-2 also shows that the exhaust depressurisation decreases RGF by between 1.5-2% for every point. This reduction in RGF allows for 1-2 Nm torque benefit for no spark advance, and 2-4 Nm for maximum spark advance.

8.5 Modelling Investigation

The NA baseline engine model was modified to provide a depressurisation in the exhaust and reflect the experimental engine test rig described previously. This was achieved by lowering the exhaust ambient to that of the blower intake pressure and modifying the geometry of the exhaust system to that used in the practical experiment. Significantly for this experiment the valve timing remained at that of the standard engine with 20° of overlap between the exhaust and intake events.

8.5.1 Reduction in RGF

The model was initially run with a fixed throttle angle for two exhaust pressures; 0.8 and 1 bar absolute. As expected, and as measured on engine, a lower exhaust pressure leads to a lower cylinder pressure during the exhaust stroke. This is shown in Figure 8-3.

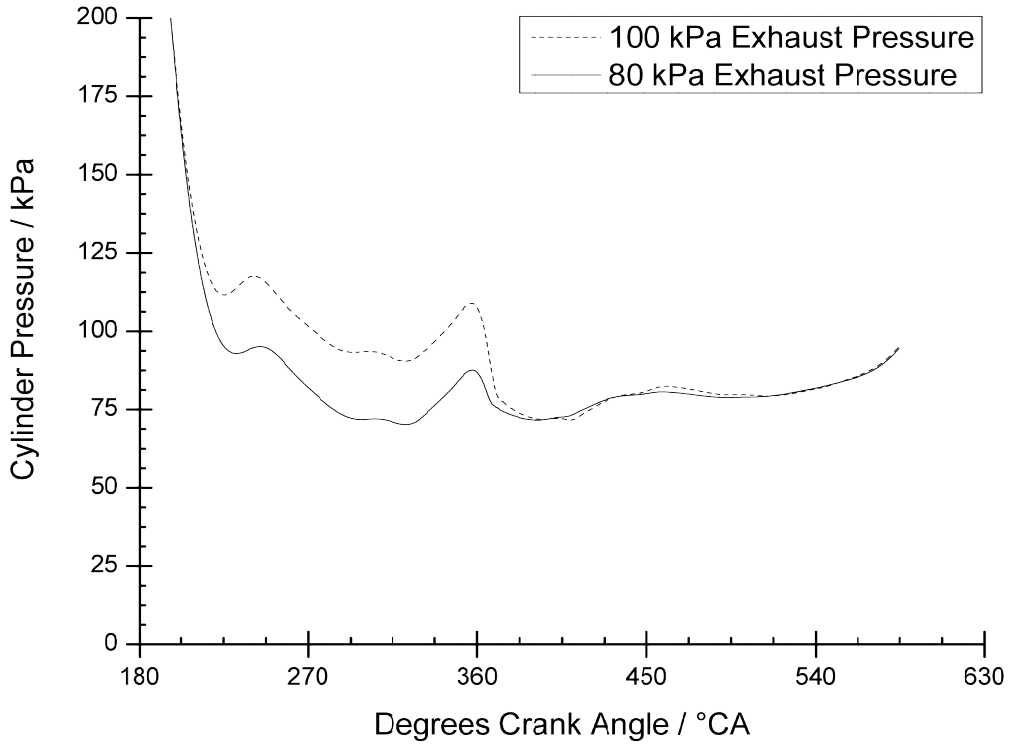

Figure 8-3 – Modelled cylinder pressure during exhaust event for 100 and 80 kPa exhaust back pressure at 2000 rpm, 8 bar BMEP

The reduction of exhaust pressure in the model results in a direct reduction in cylinder pressure during the exhaust stroke. The pressure at the end of the exhaust stroke reduced from 109 kPa to 87 kPa. The corresponding reduction in RGF was 16%, from 4.4 to 3.6% RGF.

This reduction in RGF can be partially explained by the increased expansion throughout the exhaust event as shown in the cylinder pressure in Figure 8-3 and the cylinder temperature shown in Figure 8-4.

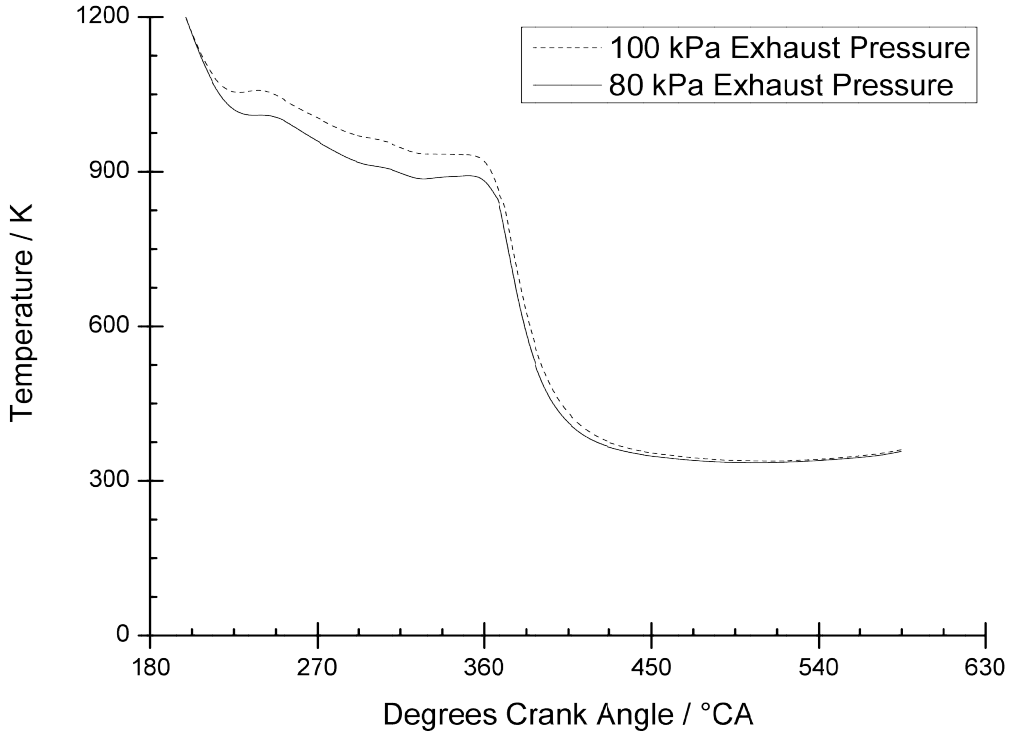

Figure 8-4 - Modelled cylinder temperature for 100 and 80 kPa exhaust system pressure at 2000 rpm, 8 bar BMEP

The cylinder temperature at IVO is 39 K lower for the 80 kPa exhaust case, and is also a result of the increased expansion.

It should be noted that the case with the lower exhaust pressure required less mass air flow to achieve the same BMEP. The reason for this is the reduced work required in the exhaust stroke to evacuate the cylinder. The reduced air flow, combined with the exhaust and intake valve overlap, will have an effect on the cylinder scavenging.

To isolate this effect, the exhaust valve event was reduced in length such that there was no valve overlap. Thus the gas exchange in the exhaust event alone will govern cylinder scavenging and RGF.

Figure 8-5 shows the simulated RGF versus crank angle for the two exhaust pressure cases. It can be seen that the reduced exhaust pressure case has reduced RGF throughout the majority of the exhaust stroke, resulting in a final RGF of 7.68% as opposed to 8.84%.

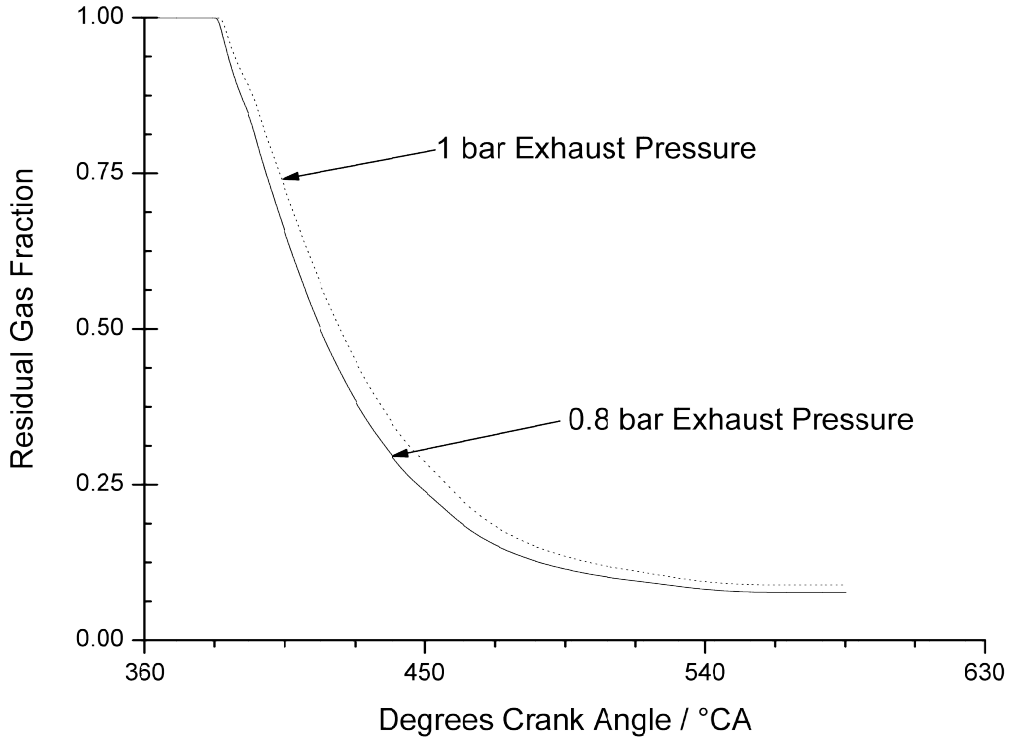

Figure 8-5 - Effect of exhaust pressure on RGF with no valve overlap at 2000 rpm, 8 bar BMEP

The reduction in RGF in this case is less at around 10%, illustrating that the cylinder scavenging during the intake and exhaust valve overlap is improved by lowering the exhaust pressure.

8.5.2 Increased Charge Momentum

The investigation into how cylinder depressurisation affects intake charge motion used the same model as described previously, simulating the modified NA engine with and without the depressurised exhaust.

To investigate the change in charge momentum it was necessary to control the model to a fixed intake manifold pressure, rather than an engine load. This is required as the depressurisation causes a reduction in PMEP; to achieve the same BMEP the depressurised case requires less air and fuel demanding a lower intake manifold pressure. Controlling the intake manifold pressure allows inspection of the cylinder charging process under the same boundary conditions.

The pressure in the exhaust ports was controlled to 0.8 and 1 bar respectively. This was done to highlight the effect of exhaust depressurisation on the reversed flow of burned gases from the cylinder into the intake manifold after IVO. Figure 8-6 shows the difference in mass flux through the intake valve for the two cases, for an intake manifold pressure of 0.8 bar.

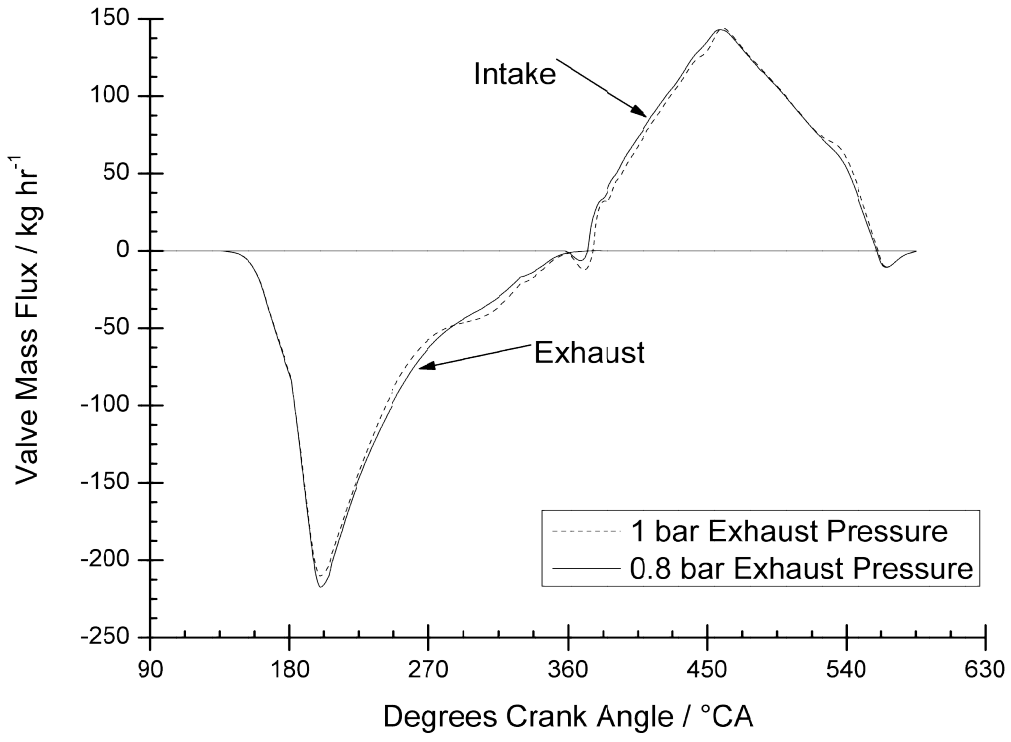

Figure 8-6 - Effect of exhaust depressurisation on exhaust and intake mass flux with no valve overlap

The reverse flow into the intake manifold is practically eliminated during the valve overlap period for the case with the depressurised exhaust. This allows the mass flux through the intake valve to rise earlier, resulting in more charge entering the cylinder. This can be seen in the total engine air mass flow; 163.6 kg hr^{-1} at ambient exhaust pressure versus 166.7 kg hr^{-1} for the depressurised case. There is no mass flow through the exhaust valve during the overlap period shown in Figure 8-6, therefore this increase in trapped air mass allows a higher load to be achieved for a given intake manifold pressure.

In this case the depressurised exhaust pressure was controlled to the same as that of the intake manifold to highlight the reduction in reversed flow into the intake manifold. It is important to consider another two cases; when the depressurised exhaust pressure is significantly higher and lower than the intake pressure.

For an exhaust pressure significantly higher than the intake pressure an exhaust depressurisation will still help to reduce reverse flow into the intake manifold. This has been simulated by operating the engine in a throttled condition and is shown in Figure 8-7.

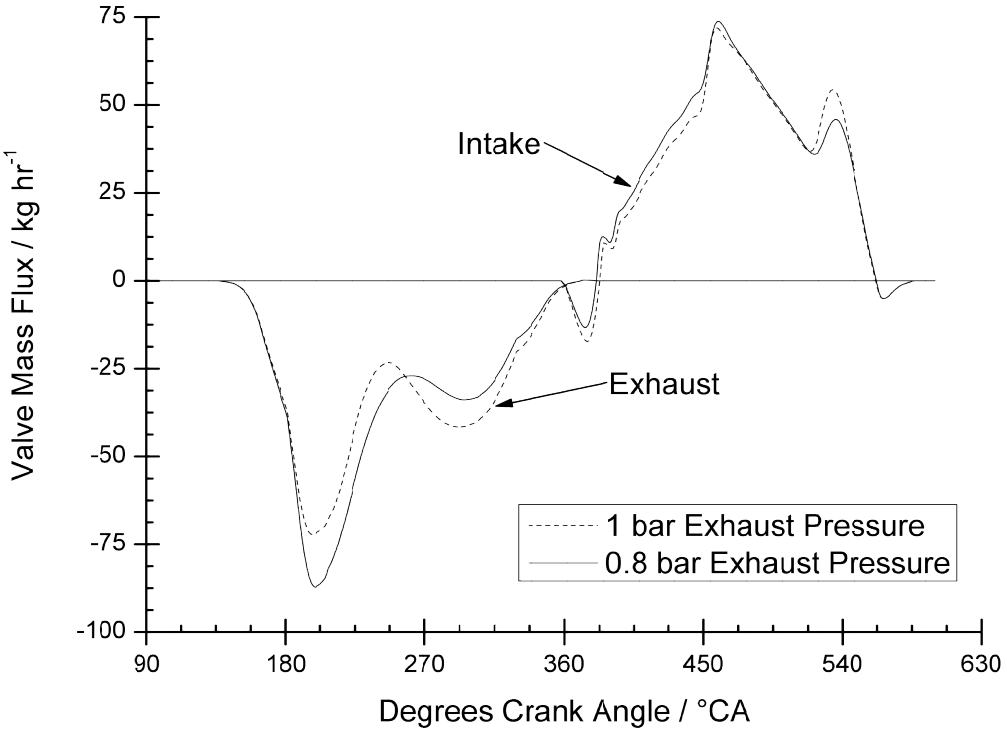

Figure 8-7 - Effect of exhaust depressurisation on exhaust and intake mass flux with no valve overlap with a low intake pressure

With the exhaust depressurisation the initial flow from the cylinder during the exhaust stroke is improved as with the previous case. This requires less flow from the cylinder during the latter stages of the exhaust stroke and as with the previous case the cylinder pressure during the valve overlap period is reduced.

From this low pressure the flow of intake charge into the cylinder is improved. There is less reverse flow through the intake valve and the mass flux through the intake valve immediately after this is increased. The result is an increase in engine mass airflow of 4%. However, the increase in simulated BMEP from 2.7 to 3.1 bar cannot be directly attributed to the increase in mass airflow due to a 0.2 bar reduction in PMEP from the reduced exhaust pressure.

The final case is one where the intake manifold pressure is the same as or higher than that of the exhaust pressure, which should give the best cylinder scavenging. For an NA engine this cannot be achieved for an atmospheric exhaust pressure, but it could be possible with Turbo-Discharging. Figure 8-8 shows the valve mass fluxes at an intake manifold pressure of 1 bar absolute for the atmospheric and depressurised exhaust cases.

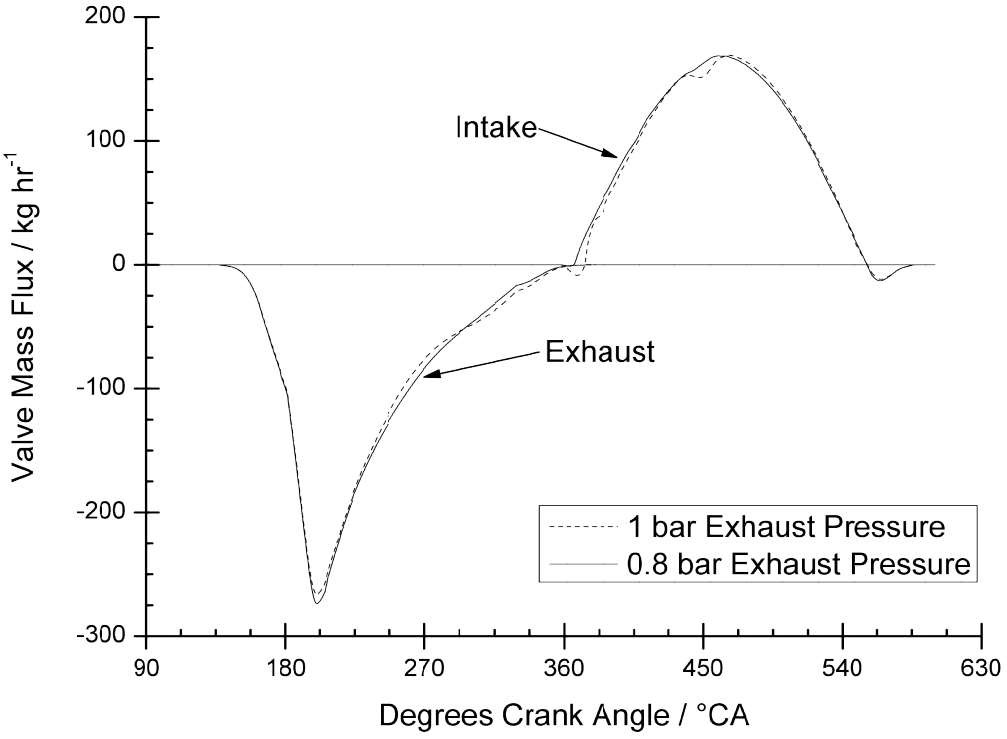

Figure 8-8 - Effect of exhaust depressurisation on exhaust and intake mass flux with no valve overlap for a high intake pressure

Similarly to the two previous cases, the depressurised exhaust case is more effective at evacuating the cylinder contents in the first part of the exhaust stroke. In this case, the high intake manifold pressure combined with the reduced exhaust pressure completely eliminates any reversed flow of burned gases into the intake manifold. The flow of intake charge into the cylinder is again improved, increasing from 204 kg hr^{-1} to 208 kg hr^{-1} for the depressurised case. The change in PMEP is limited to 0.1 bar for this case, however, the moderate increase in engine mass airflow and reduction in RGF from 3.2 to 2.5% allows for a 3.7% increase in BMEP.

It is clear then that for all the intake manifold pressures simulated, it is favourable to depressurise the exhaust system to improve cylinder scavenging and improve cylinder charging. Furthermore, it may be possible to further optimise ignition timing and valve events to take full advantage of the benefit of a depressurised exhaust.

8.6 Closing Comments

This section has identified and investigated residual gas fraction reduction and the increase in charge momentum as the two main secondary benefits of the depressurisation resulting from Turbo-Discharging both experimentally and with 1-D gas dynamics modelling. It has highlighted the potential for further efficiency benefits over the primary benefit of Turbo-Discharging in reducing engine PMEP as well as benefits to engine performance.

The next section will investigate a Turbo-Discharging system with some of the experimental constraints removed and will subsequently identify what may be possible beyond that presented previously.

9. System Optimisation Potential

This chapter will consider the potential for further Turbo-Discharging system benefit over that measured and modelled previously by removing constraints such as turbomachine matching and port-to-port leakage in the exhaust manifold. The system performance will then be compared to that of the NA model to ascertain a total potential benefit.

Further considerations will also be discussed such as the need for exhaust gas after-treatment, and some hardware limitations such as turbine and compressor inlet temperatures and how these may compromise system performance.

The 1-D model generated in this work was designed such that it replicated the experimental rig. There were certain compromises made when designing the experimental rig such as the method of exhaust port separation and the geometry of the exhaust manifold to allow for sufficient instrumentation. With these compromises removed it should be possible to improve

the effectiveness of the Turbo-Discharging system. This section will consider the total depressurisation generated, engine PMEP and bsfc with fixed combustion and fuelling.

Multiple system improvements have been considered individually in this section. This is useful for highlighting aspects that should be changed to improve system performance, but it will also be necessary to collectively assess all improvements as they will have a significant impact on each other. The benefits will be presented cumulatively throughout this section with consideration given at the end for optimisation of all the variables collectively.

9.1 Exhaust Gas Flow

With a cylinder head design optimised for Turbo-Discharging the two exhaust valve flows would be entirely separate with no leakage between them, only recombining downstream of the turbine. This was achieved simply by removing the leakage path in the model.

Figure 9-1 shows modelled cycle averaged absolute pressures for 2000 (hollow data points) and 4000 (solid data points) rpm throughout the exhaust system and identifies where there are significant changes in pressure between neighbouring elements. These are:

A. Effect of manifold leakage on HP manifold;
B. Pressure drop across the turbine;
C. Effect of manifold leakage on LP manifold;
D. Pressure difference across compressor.

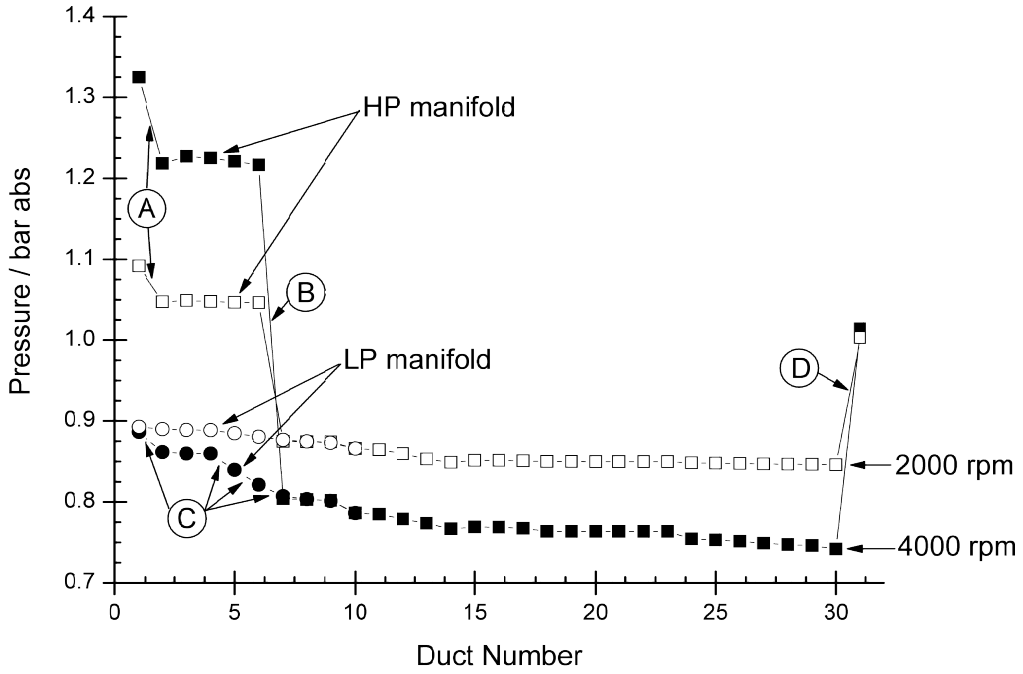

Figure 9-1 – Cycle-averaged absolute pressures in ducts throughout the Turbo-Discharging exhaust system (see text for details)

Figure 9-1 highlights the importance of mitigating leakage between the HP and LP sides of the exhaust manifold. The data for the LP side of the manifold is taken from cylinder 1 and due to the log-type manifold design the level of depressurisation at the exhaust valve is adversely affected by the leakage through the ports of the other three cylinders. The difference in cycle-averaged pressure at the exhaust valves between cylinders 1 and 4 is up to 5 kPa but if leakage is mitigated completely Figure 9-1 shows this could be as high as 9 kPa.

The gas flow in the previous model is limited by the exhaust valve size which can be increased within reason to improve the flow capacity of a single valve. This may allow for more energy to be extracted by the turbine as the exhaust will lose less energy expanding over the HP exhaust valve, or for better transmission of the depressurisation through the LP valve into the cylinder. Both valves were increased from 24.1 mm to 28 mm to match the intake valves considering there will be an upper limit on valve diameter imposed by the combustion chamber geometry.

Within reason it may also be possible to reduce the volume of the HP exhaust manifold. Reducing its volume will help to maintain the dynamic pressure energy portion of the exhaust gas, in turn reducing the energy dissipated in expansion from the cylinder into the exhaust manifold. This was achieved by reducing the length of the exhaust runners from 200 mm to

100 mm keeping the diameter constant. These factors were investigated individually at 3000 rpm, 6 bar BMEP and 4000 rpm, 11 bar BMEP.

Figure 9-2 shows the effect of the above potential improvements for exhaust gas flow on the 1-D model operating at 3000 rpm, 6 bar BMEP. The improvements are shown in the form of floating bars from left to right, each representing the benefit or deficit compared to the previous case. In the case of this graph, improvements will show as a bar below the previous case.

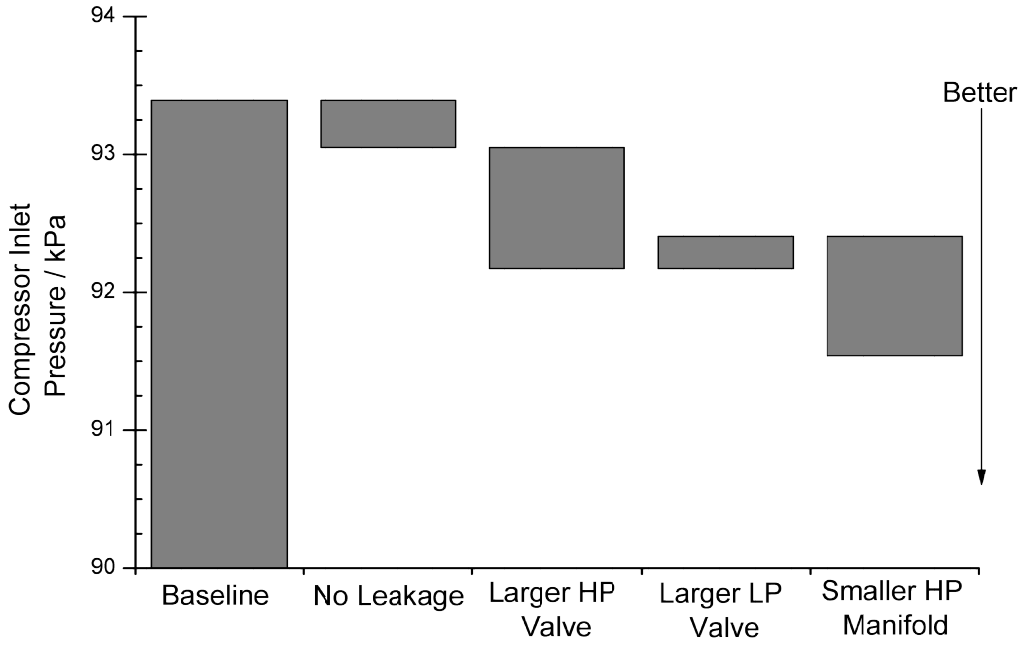

Figure 9-2 - Effect of several exhaust gas flow improvements on compressor inlet pressure at 3000 rpm, 6 bar BMEP

It can be seen that increasing the diameter of the LP exhaust valve reduces the depressurisation created by the compressor. The larger diameter of the valve means that the valve is less choked as it opens leading to more flow bypassing the turbine and reducing the energy transferred to the compressor. This suggests a later potential optimum valve opening to counteract the apparent detriment.

Figure 9-3 shows the effect of the same design changes on engine PMEP where negative values detract from crankshaft work. It can be seen that all of the design changes improve engine PMEP, the most significant of which is the HP valve diameter.

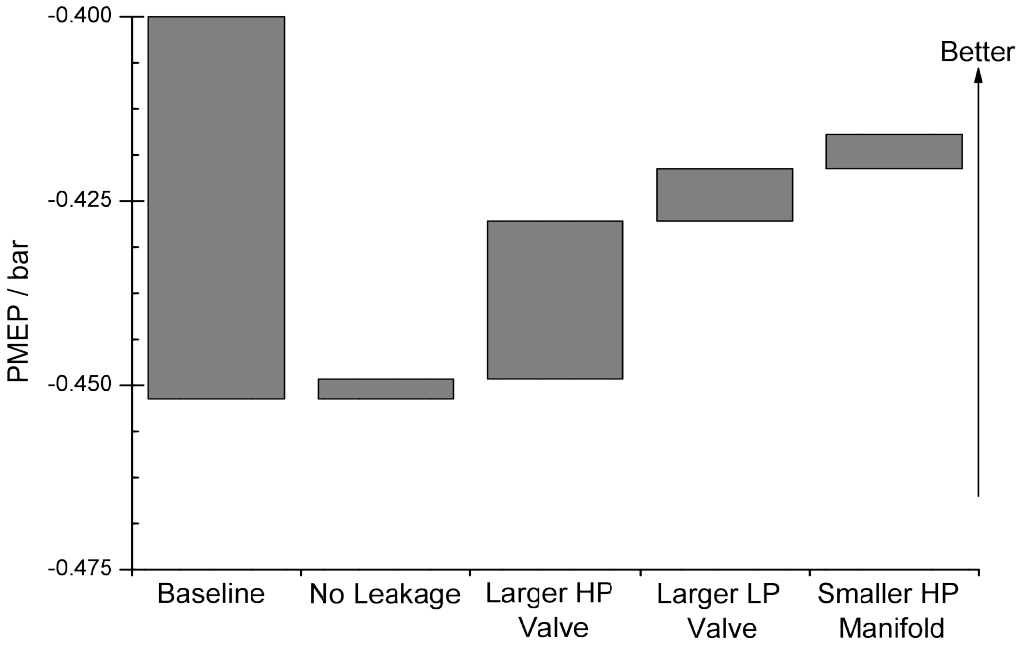

Figure 9-3 - Effect of exhaust flow improvements on PMEP at 3000 rpm, 6 bar BMEP

Finally, Figure 9-4 shows the effect of the exhaust flow design changes on engine bsfc. The model shows that improving PMEP will improve engine bsfc and again the most significant improvement is the increase in HP exhaust valve diameter.

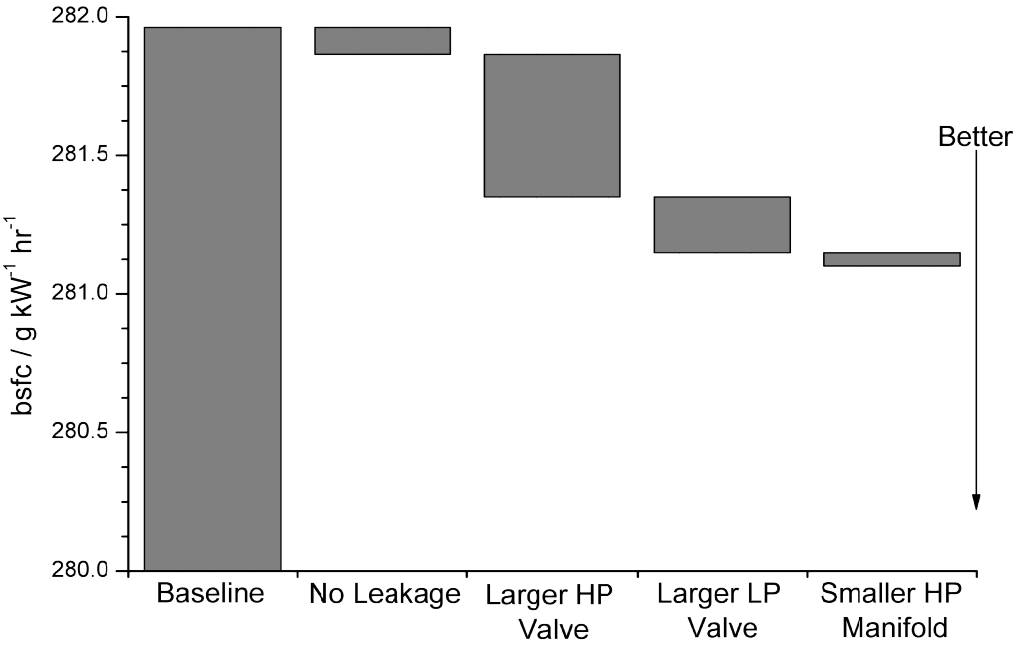

Figure 9-4 - Effect of exhaust flow improvements on bsfc at 3000 rpm, 6 bar BMEP

Increasing the diameter of the HP valve will have two main effects; a higher turbine inlet pressure and reduced mass in the cylinder to be displaced by the piston.

For a larger diameter valve the valve flow area will be larger for the same lift and duration and crucially it will choke at higher flow rates as the valve is opening. This means a higher turbine inlet pressure can be achieved allowing the turbine to extract more energy. This is shown in Figure 9-5.

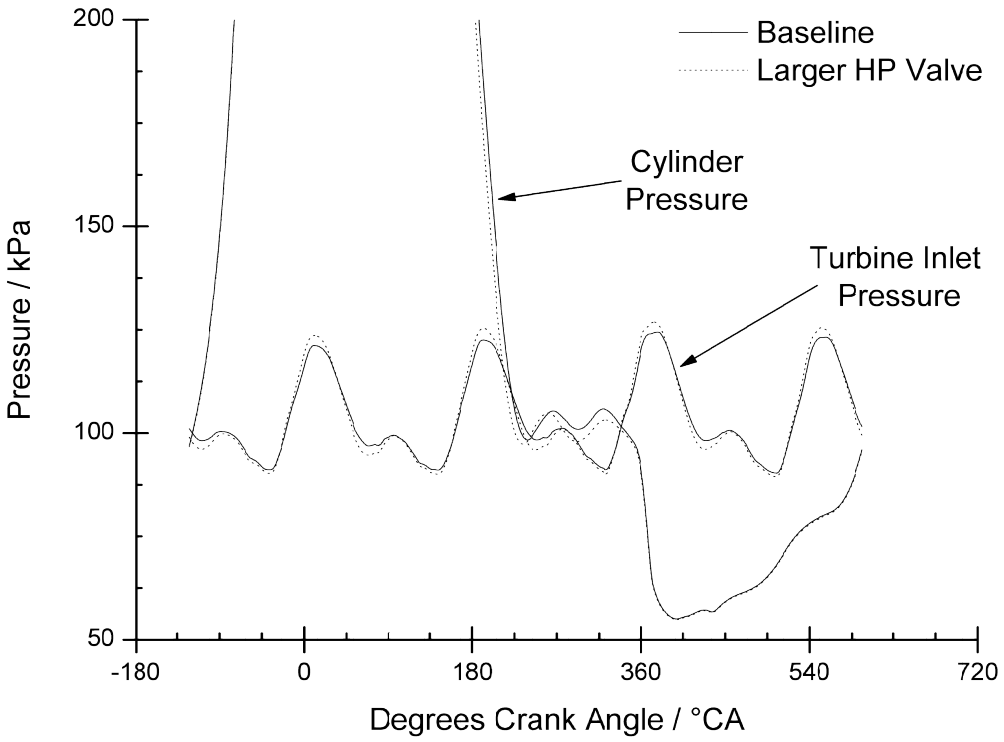

Figure 9-5 – Cylinder and turbine inlet pressure traces for baseline and increased HP valve diameter cases at 3000 rpm, 6 bar BMEP

The second benefit can also be seen in Figure 9-5; following the cylinder blowdown, the pressure in the cylinder is reduced. This is an indication there is less mass in the cylinder that needs to be displaced, reducing PMEP and thus bsfc.

For a higher exhaust gas flow rate, at 4000 rpm, 11 bar BMEP, the two most significant improvements in the depressurisation generated are the increase in HP valve diameter and reduction in volume of the HP manifold as shown in Figure 9-6. Again, increasing the LP valve size led to mass being diverted away from the turbine, the result of which was a decrease in the depressurisation generated.

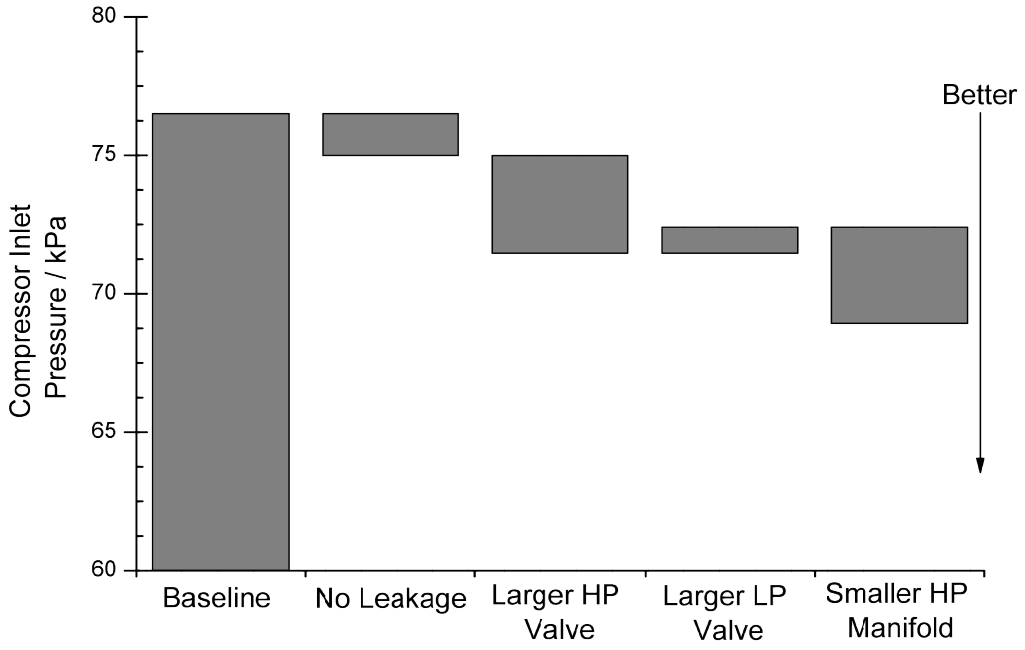

Figure 9-6 - Effect of several exhaust gas flow improvements on compressor inlet pressure at 4000 rpm, 11 bar BMEP

The increase in HP valve flow area has a more significant effect on engine PMEP than the previous case due to the higher exhaust gas flow rate. A smaller valve will spend longer in choke whilst opening and closing than the larger valve diameter, limiting the mass flow from the cylinder and reducing the pressure energy in the gas as it is expanded over the more restrictive valve.

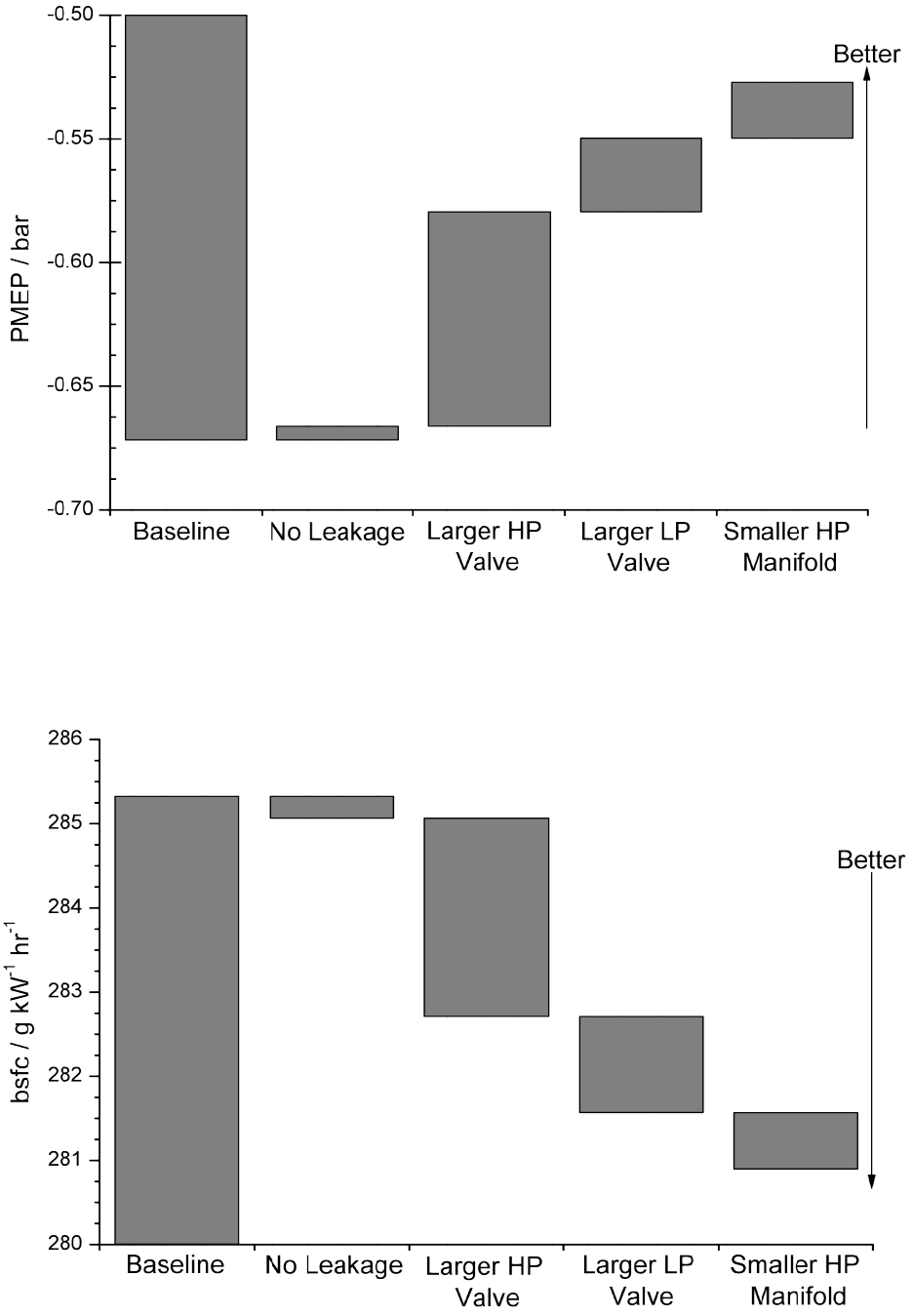

Figure 9-7 - Effect of exhaust flow improvements on PMEP and bsfc at 4000 rpm, 11 bar BMEP

Figure 9-7 again shows the significance of PMEP on bsfc as the largest improvement in PMEP correlates to the largest improvement in bsfc. Increasing the HP valve size decreases the flow losses across the valve and also allows the turbine inlet pressure to rise faster due to a more rapid increase in effective valve area. This leads to increased turbine power, improved exhaust depressurisation, decreased PMEP and lower bsfc.

Summary

For both speed and load cases, the improvement in depressurisation generated between the baseline and best case was around 30%. For the lower load case, this gave only a 0.3 % improvement in bsfc from 281.9 to 281.1 g kW^{-1} hr^{-1}. The higher load case was more sensitive to the exhaust flow capability due to the higher exhaust mass flow rate and a more substantial improvement in PMEP was achieved which resulted in a 2% improvement in bsfc from 285.2 to 281 g kW^{-1} hr^{-1}.

This section has proved that it is important to optimise the flow of exhaust gases from the cylinder through the exhaust valves into the exhaust. It has also highlighted the importance of the valve events in terms of mass flow distribution, as proved previously in sections 7.4.3 and 7.4.4. It has been proven previously that the valve events should be optimised for each engine speed and load condition, and this will be taken into account in the optimised model results shown in section 0.

9.2 Turbomachine Matching

It has already been shown that the compressor used on the Turbo-Discharging experimental test is too large for most engine operating conditions and only generates useful depressurisation towards peak loads and at high engine speed. This section will investigate the optimum size of turbomachines for improving engine fuel conversion efficiency. Three speed and load points were considered for this investigation; 2000 rpm 2 bar BMEP where the exhaust gas contains little energy, 3000 rpm 6 bar BMEP where the gas contains a useful amount of exhaust gas energy and 4000 rpm peak load where the experimental rig has already proven there is sufficient energy to generate a depressurisation.

To vary the size of the turbomachines the turbine or compressor diameter multipliers were used. The mass flows extracted from the performance maps are multiplied by these values squared. This is not a good method of estimating maps of real turbomachines as it does not account for decreasing tip losses with increasing turbomachine size, for example. However, for the purpose of this study it will be sufficient to show the magnitude of improvement in engine efficiency and performance possible with varying turbomachine size.

9.2.1 Turbine Sizing

A sweep was made of turbine diameter at the three speed and load points to identify the optimum turbine diameter for depressurisation, engine PMEP and bsfc.

Figure 9-8 shows the effect of turbine diameter on the energy extracted by the turbine at 2000 rpm, 2 bar BMEP. It can be seen that the turbine does not extract a useful level of energy for any turbine diameter due to the lack of energy in the blowdown portion of the exhaust gas at this engine operating condition. This is an important consideration for the design of a Turbo-Discharging system; if a depressurisation is required at low engine speeds the valve events must be altered such that the exhaust gas is pumped out of the cylinder by the piston through HP manifold and turbine. With an appropriate LP valve event it may still be possible to reduce the residual gas fraction beyond that of an equivalent NA engine operating at the same speed and load point if this is desirable at the expense of engine pumping work. This trade-off of blowdown energy and pumping work should be the subject of further work.

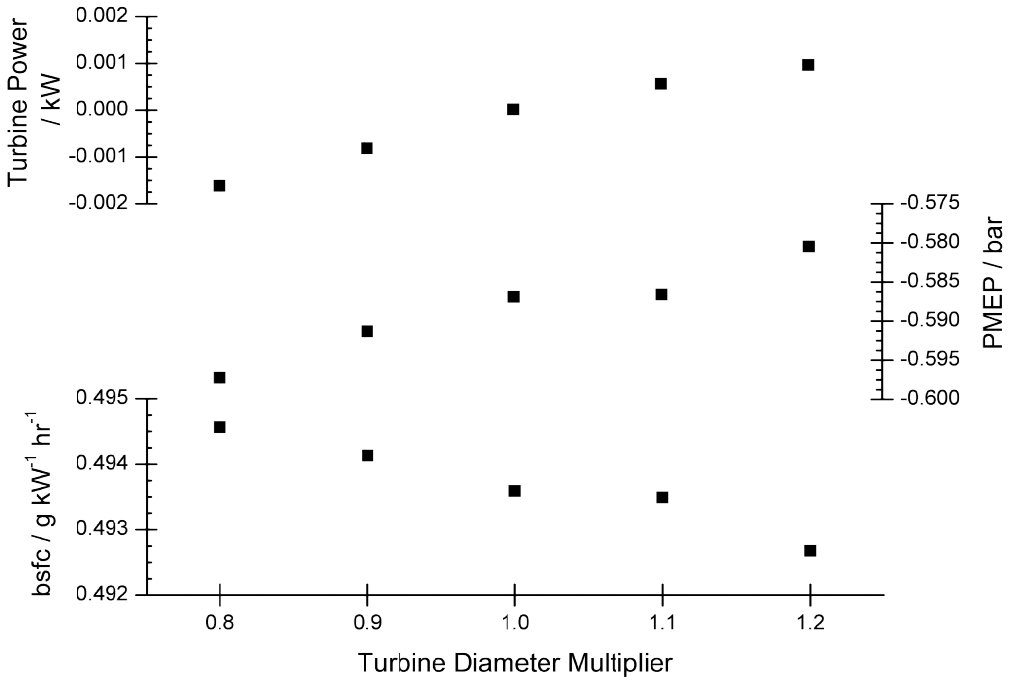

Figure 9-8 - Effect of turbine sizing on turbine power, PMEP and bsfc at 2000 rpm, 2 bar BMEP

Figure 9-8 also shows that a larger turbine will help to reduce pumping work during the exhaust stroke which leads to improved bsfc. As such, for optimum efficiency at low speed and

load conditions where there is insufficient energy in the exhaust gas for a depressurisation to be generated, the Turbo-Discharging system must be designed to create as little exhaust gas flow restriction as possible.

Figure 9-9 shows the effect of turbine diameter on turbine power, compressor inlet pressure and engine PMEP at 3000 rpm, 6 bar BMEP. The optimum turbine sizing for energy extraction from the exhaust gas is with a multiplier of 1.1, however, the optimum size for minimal pumping work is between 1.2 and 1.3.

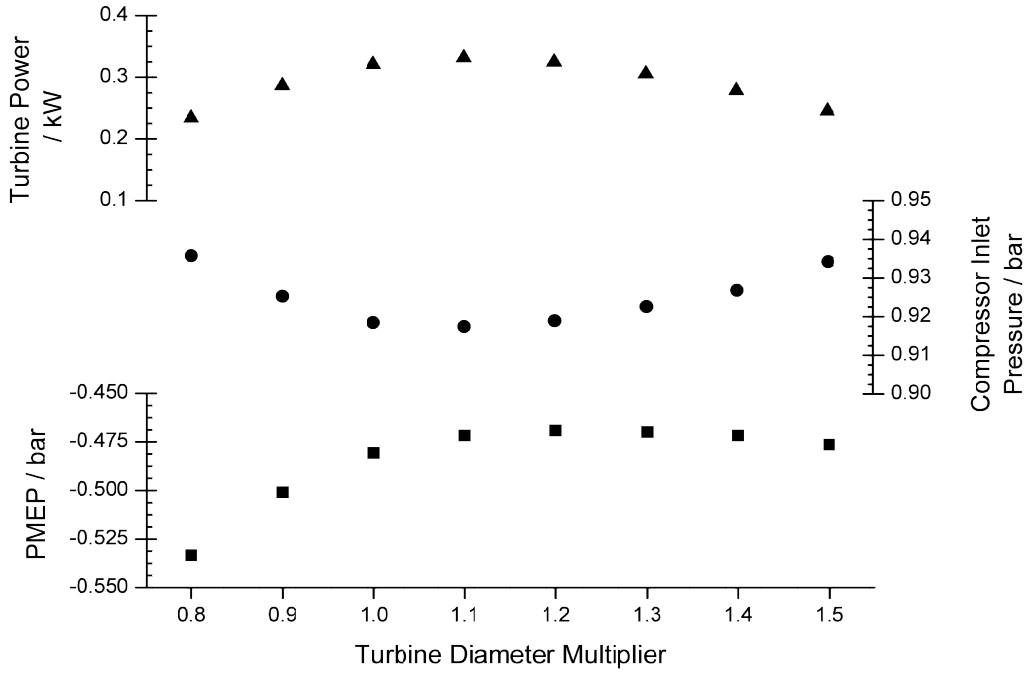

Figure 9-9 - Effect of turbine diameter on turbine power, absolute compressor inlet pressure and PMEP at 3000 rpm, 6 bar BMEP

The turbine diameter effectively controls the proportion of mass flow through each side of the manifold. A smaller turbine may restrict the flow of exhaust gas, so although it may be able to extract more energy for a fixed mass flow, the actual mass flow through it will reduce. It is desirable for more mass to flow through the turbine in the blowdown pulse as it leaves less mass in the cylinder for the piston to evacuate which reduces pumping work. Figure 9-10 shows that increasing the turbine diameter multiplier does increase the proportion of mass flow through the HP branch of the manifold.

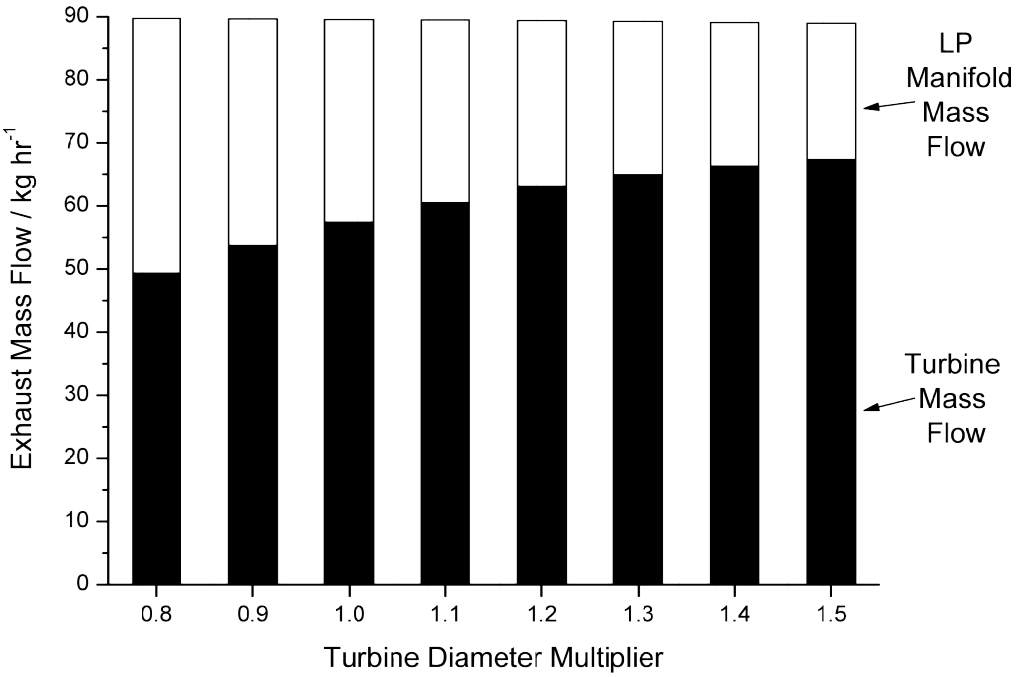

Figure 9-10 - Effect of turbine diameter on HP and LP manifold mass flow proportions at 3000 rpm, 6 bar BMEP

The proportions of mass flowing through or around the Turbo-Discharging turbine help to explain why the point of minimum engine pumping work does not align with the maximum depressurisation generated by the Turbo-Discharging system. However, Figure 9-11 shows that engine bsfc is at a minimum at a turbine diameter of 1.4. It also shows the dependency of bsfc on mass air flow and volumetric efficiency; the point of minimum bsfc occurs when the engine is consuming the least amount of air and therefore fuel, and when it is able to draw that air into the cylinder most effectively.

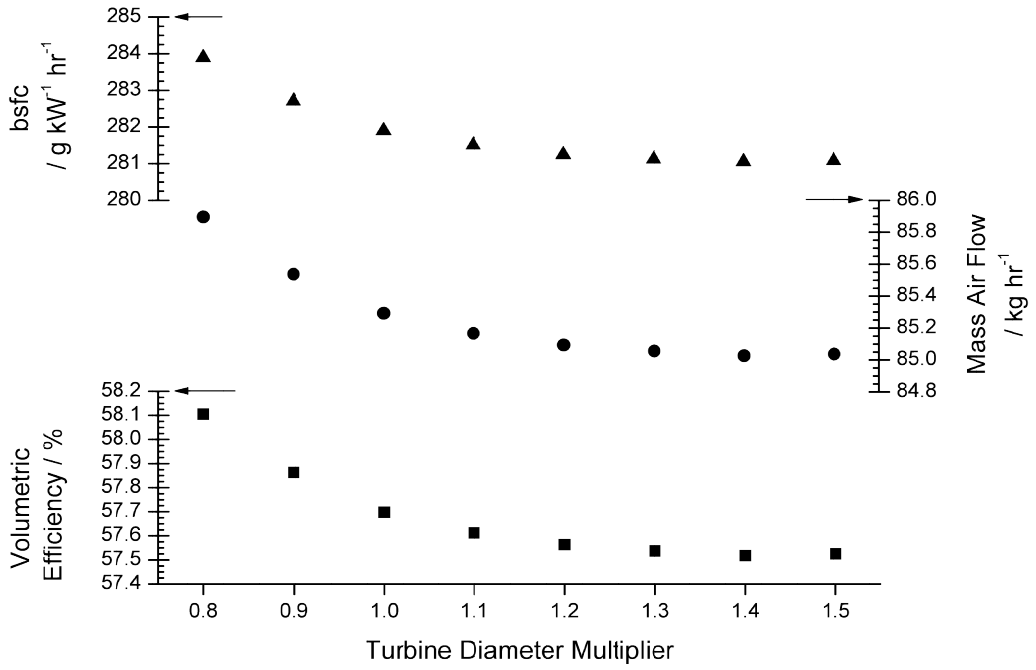

Figure 9-11 - Effect of turbine diameter on bsfc, engine mass air flow and volumetric efficiency at 3000 rpm, 6 bar BMEP

The reason for the optimum bsfc at a turbine diameter of 1.4 is that the cylinder remains at a higher pressure during the latter part of the expansion stroke whilst the exhaust valves are open and as a result the piston recovers more expansion work as highlighted by the shaded area (A) in Figure 9-12. In this case, the extra expansion work recovered is greater than the PMEP benefit offered by the depressurised exhaust.

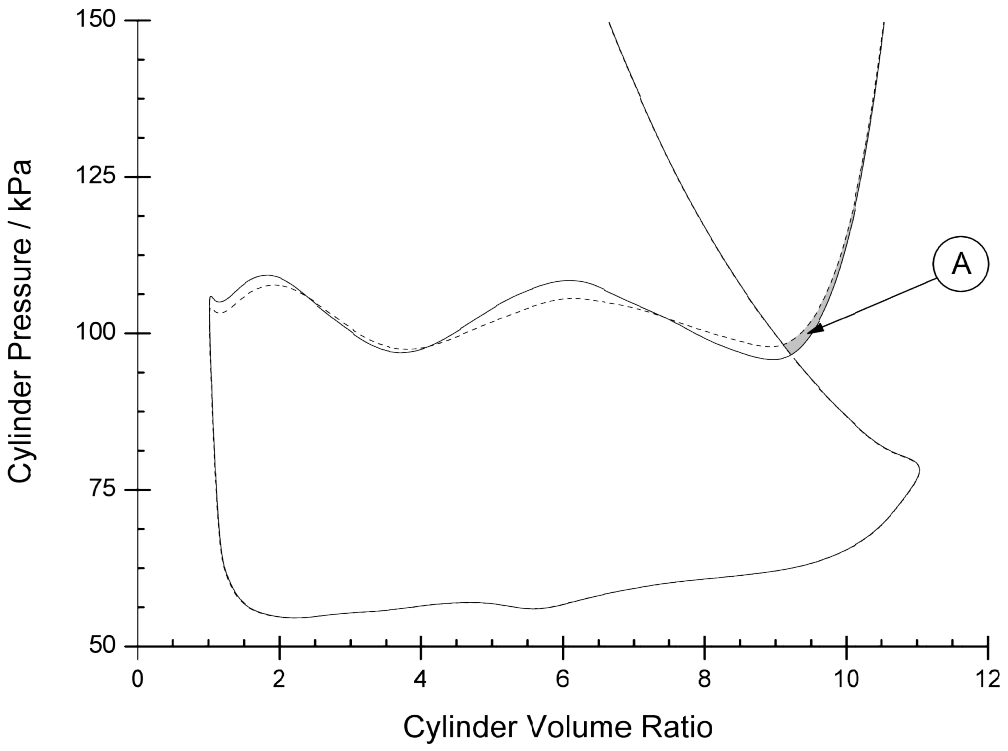

Figure 9-12 - PV diagram for the most depressurised and lowest bsfc cases of turbine diameter variation at 3000 rpm, 6 bar BMEP where point (A) highlights the extra in-cylinder expansion

The investigation at this engine speed and load point has shown how sensitive engine efficiency is to exhaust pressures at part load conditions. It must also be noted that the changes in bsfc between the point of greatest depressurisation and lowest bsfc are small and could well be within modelling or measurement error.

It has been shown previously that the Turbo-Discharging system can, at peak load, produce a significant depressurisation and as such engine performance becomes more dependent upon the performance of the Turbo-Discharging system. Figure 9-13 shows the effect of varying turbine diameter on turbine power, exhaust depressurisation and engine pumping work at 4000 rpm, peak load.

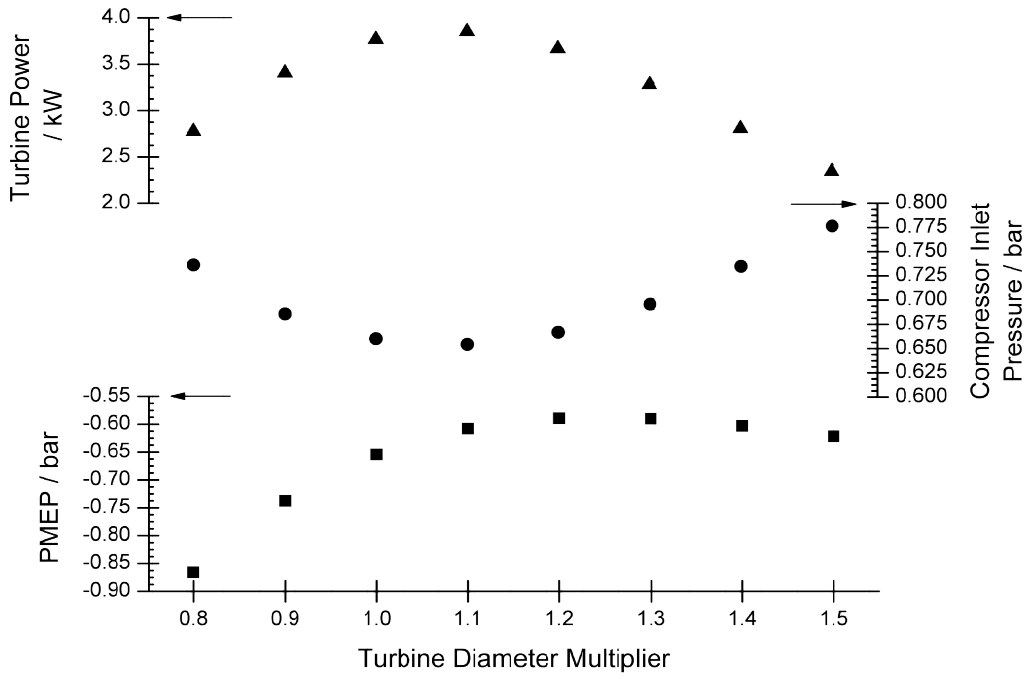

Figure 9-13 - Effect of turbine diameter on turbine power, depressurisation and PMEP at 4000 rpm, peak load

The point of maximum turbine power corresponds with the point of lowest compressor inlet pressure. However, similarly to 3000 rpm 6 bar BMEP the point of minimum PMEP is for a larger turbine. Again, this is due to extra expansion in the cylinder due to the smaller restriction of a larger turbine. Figure 9-14 shows a P-V diagram comparing the two turbine diameters offering the lowest depressurisation (dashed line) and the lowest PMEP (solid line).

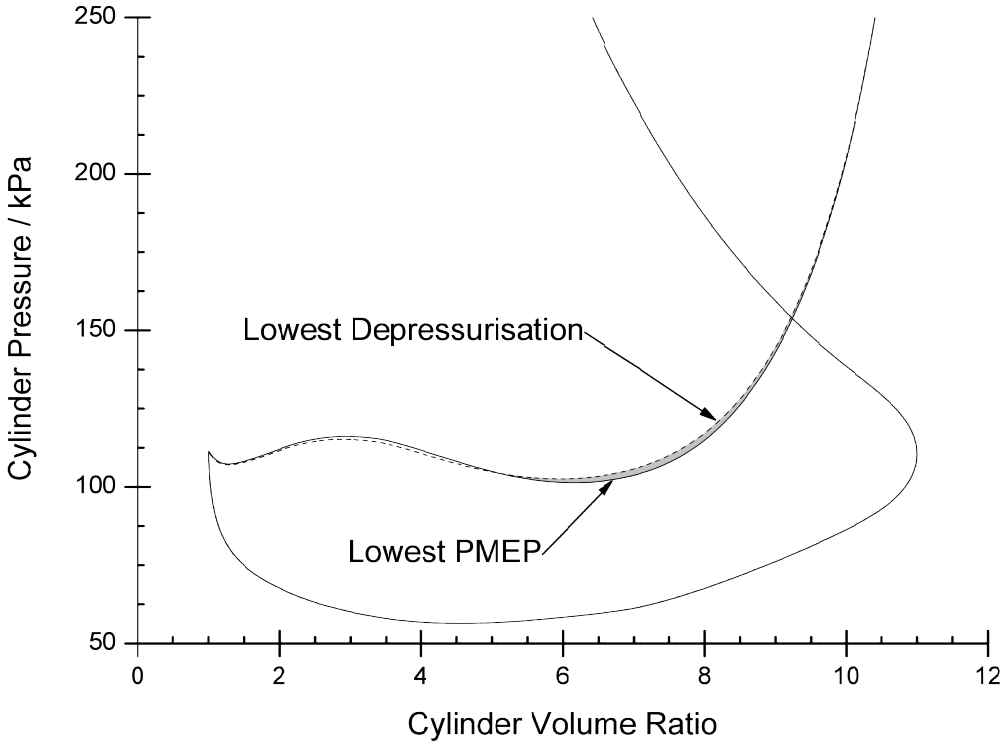

Figure 9-14 - P-V diagrams of turbine diameters with lowest depressurisation (dashed line) and lowest PMEP (solid line) at 4000 rpm, peak load where the grey shaded area shows the benefit of the larger turbine

The turbine from the system which develops the lowest depressurisation allows for less expansion of the gas during the HP portion of the exhaust stroke which leads to a higher cylinder pressure both before and after the crossing point on the P-V diagram. This results in less in-cylinder work and a larger pumping loop.

For this speed and load point the peak load varied depending on the performance of the Turbo-Discharging system. Figure 9-15 shows the effect of turbine diameter on the BMEP generated and the corresponding influence on bsfc.

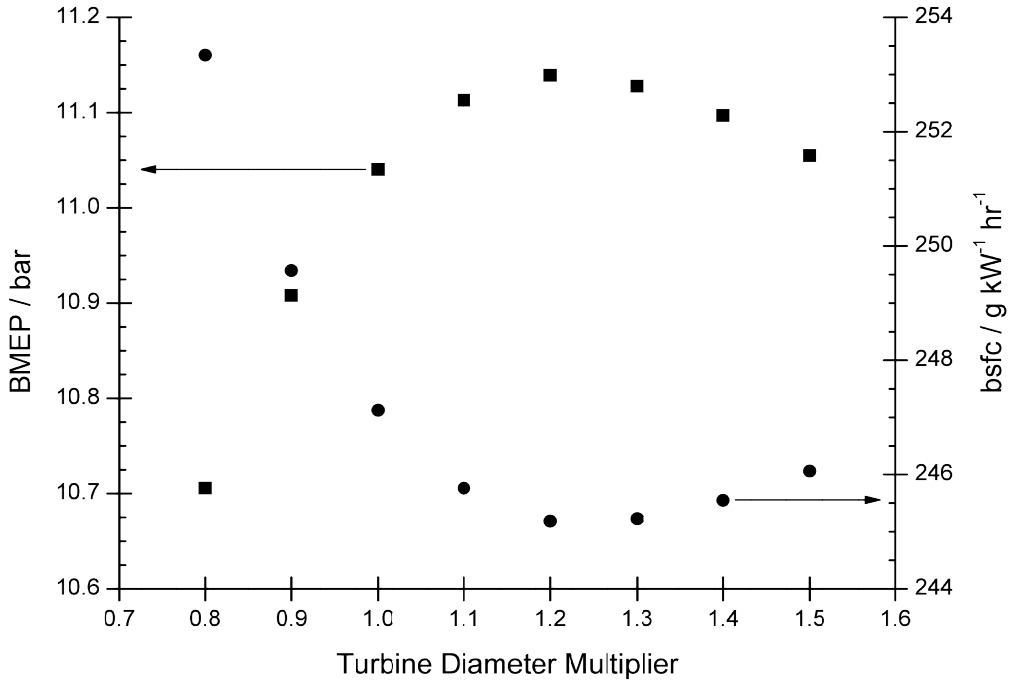

Figure 9-15 - Effect of turbine diameter on BMEP and bsfc at 4000 rpm, peak load

The point of maximum BMEP and minimum bsfc correspond with the turbine diameter which offers the lowest PMEP, not the greatest depressurisation. Therefore it is important to optimise Turbo-Discharging turbine sizing at every speed and load condition for engine pumping work rather than maximising depressurisation.

Summary

The most important considerations for optimal turbine sizing of a Turbo-Discharging system are as follows. For low load conditions where there is insufficient exhaust gas energy to extract, the turbine must be sized such that it causes as little restriction as possible. Reducing engine pumping work in this condition has the most beneficial effect on engine fuel efficiency.

A turbine which extracts as much energy from the exhaust gas as possible does not always offer the largest improvement in fuel efficiency. It is important to consider turbine sizing in conjunction with exhaust valve events to maximise in-cylinder gas expansion whilst the exhaust valves are closed and to minimise pumping work.

9.2.2 Compressor Sizing

A sweep of compressor size was carried out at the same speed and load points to investigate the effect of compressor sizing. For this investigation the turbine size was fixed at the optimum for bsfc identified in the previous section.

At 2000 rpm, 2 bar BMEP the available work is so low that it no useful depressurisation can be created and as such it is not considered further.

Figure 9-16 shows the effect of compressor diameter on depressurisation, PMEP and bsfc at 3000 rpm, 6 bar BMEP. The point of maximum depressurisation corresponds directly with that of least pumping work and lowest bsfc.

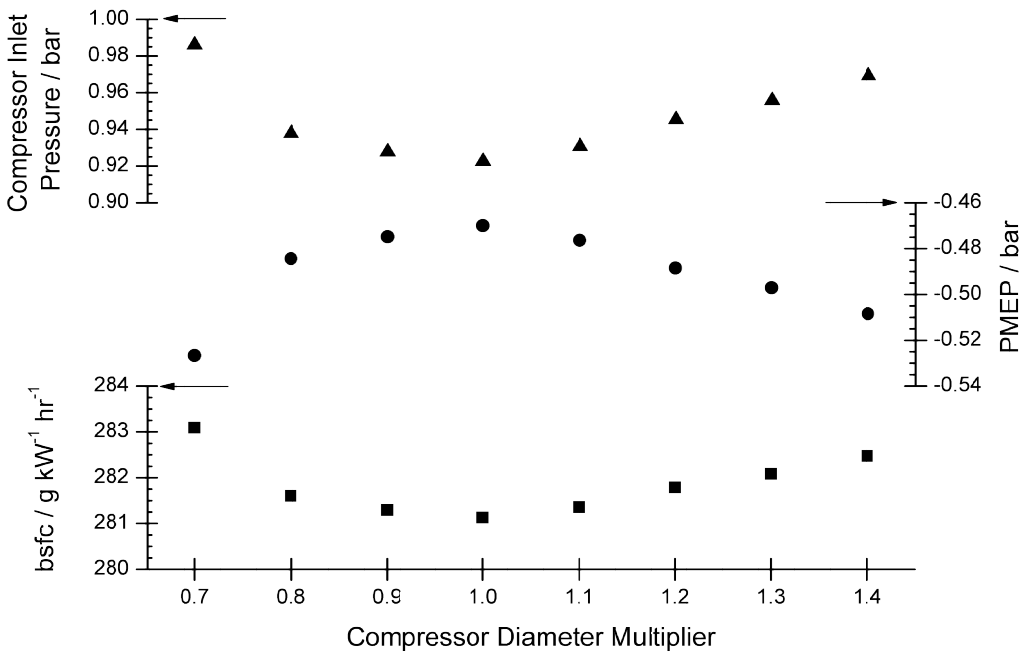

Figure 9-16 - Effect of compressor sizing on system depressurisation, PMEP and bsfc at 3000 rpm, 6 bar BMEP

The relationship between compressor diameter and Turbo-Discharging system performance, and in turn engine performance, is more straightforward than that of turbine diameter. The optimum size compressor for engine fuel efficiency corresponds directly with that which generates the largest PMEP improvement and lowest compressor inlet pressure.

Figure 9-17 highlights that the compressor diameter, and the subsequent depressurisation, can have a significant effect on the power extracted by the turbine. A lower turbine outlet pressure, for a fixed turbine mass flow, will increase the work extracted by the turbine. However, the point of maximum turbine work does not correspond with the greatest system depressurisation.

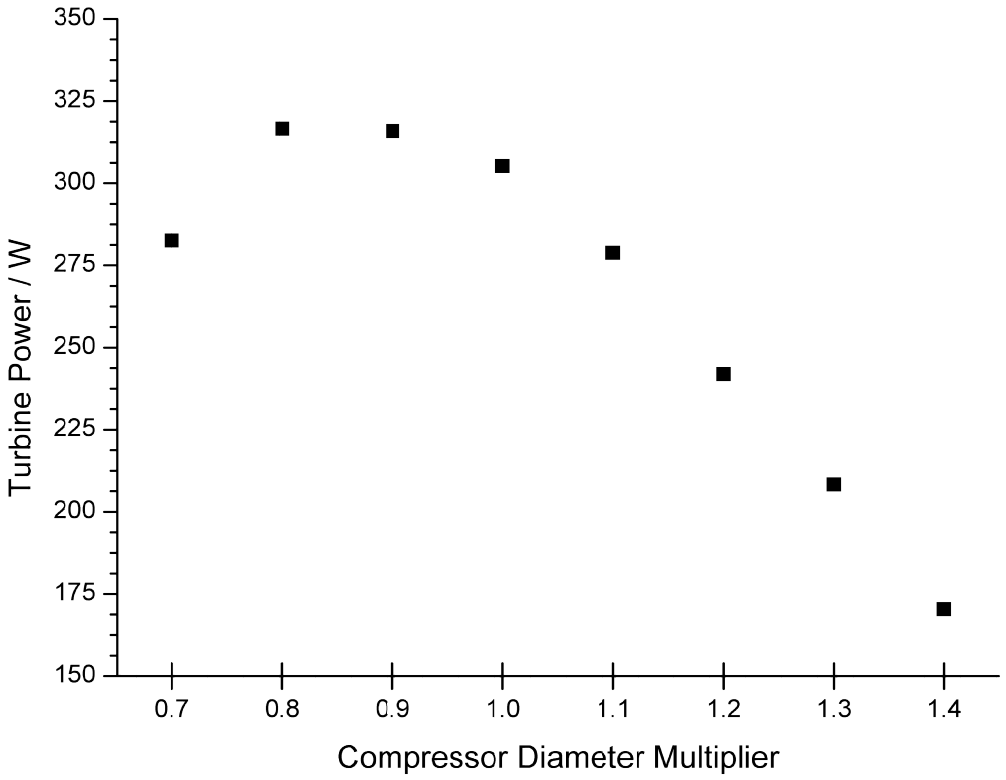

Figure 9-17 - Effect of compressor diameter on power extracted by the turbine at 3000 rpm, 6 bar BMEP

Again, this is due to the exhaust system pressure affecting the mass flow proportions through the HP and LP sides of the exhaust manifold, and thus the energy that can be recovered by the turbine. Increasing the exhaust system pressure, to a point, drives more mass flow through the HP valve and allows the turbine to extract more energy, but at a detriment to engine pumping work.

Thus, for a part load condition where a depressurisation can be achieved, optimum engine fuel efficiency will be achieved for the compressor diameter that achieves the lowest depressurisation.

Figure 9-18 shows the effect of varying compressor diameter at 4000 rpm, peak load. Maximum depressurisation is achieved with a compressor diameter multiplier of 0.9, however, it is likely the real minimum is around 0.95. Corresponding with this point of maximum depressurisation are the points of minimum PMEP and lowest bsfc.

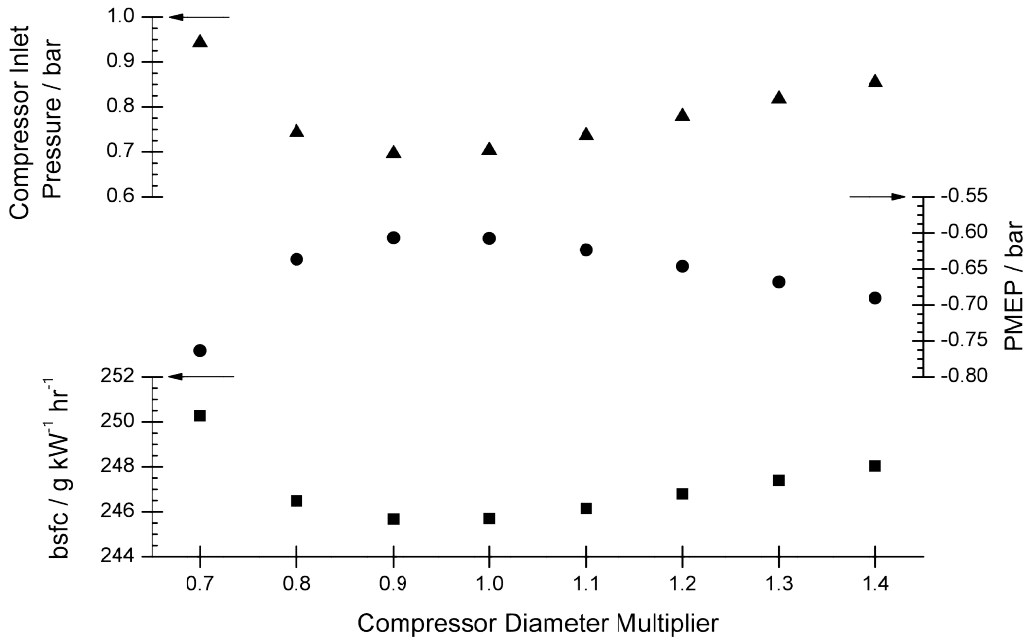

Figure 9-18 - Effect of compressor diameter on depressurisation, PMEP and bsfc at 4000 rpm, peak load

Similarly to the turbine diameter investigation, the maximum BMEP achieved varied with compressor diameter. This is shown in Figure 9-19.

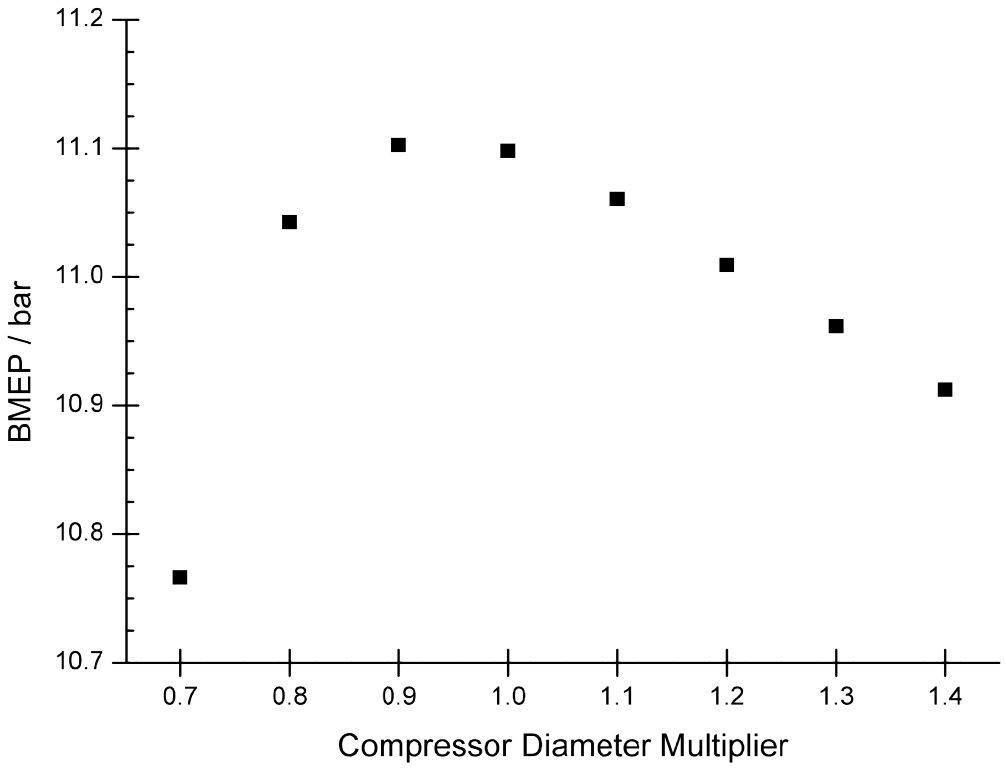

Figure 9-19 - Effect of compressor diameter on maximum achievable BMEP and 4000 rpm

Again, the point of maximum BMEP corresponds to the point of minimum PMEP. It is worth noting the gradient of change in BMEP with compressor size is more favourable for a larger than a smaller compressor. This means that it is less detrimental if a compressor is slightly over-sized than under-sized.

9.2.3 Turbomachine matching conclusions

There is insufficient energy in the exhaust gas at 2000 rpm, 2 bar BMEP for a Turbo-Discharging system to be effective and the sizing of the turbomachines will have little effect on system and engine performance. Given the low mass flows of exhaust gas through the exhaust in this operating condition it is unlikely the Turbo-Discharging system will cause much restriction, but the performance will be compared to the NA engine in section 9.4.

At 3000 rpm, 6 bar BMEP it has been shown that the Turbo-Discharging system can generate a useful depressurisation and as such the size of the turbomachines has a significant effect on the performance of the Turbo-Discharging system and in turn the efficiency of the engine. It is important to note that the turbine sizing affects the mass flow split between the HP and LP manifolds and the turbine size for maximum energy extraction may not be the same size for optimum engine system efficiency. Also the pressure during the initial part of the exhaust stroke needs to be considered as it has been found that too small a turbine can reduce expansion in the cylinder, reducing work recovered by the piston and negatively impacting engine fuel efficiency.

The compressor sizing, however, is more straightforward. The optimum compressor diameter is that which allows the compressor to operate at the point of maximum efficiency and to generate the largest pressure ratio. This has little effect on the mass flow split between the HP and LP manifolds although the pressure ratio across the turbine is increased with decreasing depressurisation which allows the turbine to recover more energy.

At 4000 rpm, peak load the turbine diameter which generates the lowest depressurisation again does not give the best engine fuel efficiency or generate the highest BMEP. The turbine matching must minimise PMEP whilst again considering the mass flow balance between the HP and LP manifolds and maximising in-cylinder work.

Optimum Turbo-Discharging and engine system efficiencies are achieved with a compressor that is sized to best make use of the energy transferred to it from the turbine.

For the operating conditions chosen, it was found that a reasonable optimum could be achieved with a turbomachine of one size. This may not be possible across the entire engine speed and load range, however, it does give a good indication that Turbo-Discharging system effectiveness could be optimised for the majority of engine operating conditions with a single

turbomachine. For turbocharged engines with a wider range of mass flows and exhaust temperatures and pressures it may be desirable to vary turbine energy extraction or to bypass the compressor; these options should be included in any future investigation into Turbo-Discharging turbocharged engines.

9.3 Thermal Management

This section will discuss the thermal hardware limitations which may restrict Turbo-Discharging efficiency and performance.

9.3.1 Turbine Inlet Temperature

Blowdown gases are composed of the highest energy and thus highest temperature portion of the burned combustion gases. Comparatively the displacement gases have been expanded within the cylinder then further expand across the exhaust valves into the exhaust manifold, and as such can be up to 100-200°C cooler than the blowdown gases as measured on the Turbo-Discharging experimental rig. This correlates well with the work by Roth *et al* (2010) where they measured a 100-200 K difference between ports on their VEMB system.

Figure 7-14 shows the measured turbine inlet temperature on the experimental test rig. The maximum temperature observed is around 950°C which is within the limits of common turbocharger turbines. However, this may change if Turbo-Discharging is applied to a turbocharged engine where the temperature of exhaust gases tends to be higher.

Turbine inlet temperature is therefore not a limitation on efficiency of the NA Turbo-Discharging system as tested and modelled.

9.3.2 Compressor Inlet Temperature

The heat exchanger chosen for the experimental rig had a large flow area to minimise the resistance to the flow whilst having a large surface area to maximise heat transfer from the exhaust gas. However, the heat rejection from the gas was still limited by the residence time of the gas in the heat exchanger. It may be possible through design and optimisation to increase the heat rejection from the exhaust gas whilst maintaining a minimal pressure drop upstream of the compressor. Alternatively it may be possible to use materials for the compressor that can withstand higher temperatures, reducing the required heat exchanger capacity.

Figure 9-20 shows the effect of compressor inlet temperature on achievable depressurisation at 3000 rpm, 6 bar BMEP and 4000 rpm, peak load, achieved by varying the wall temperature of the heat exchanger.

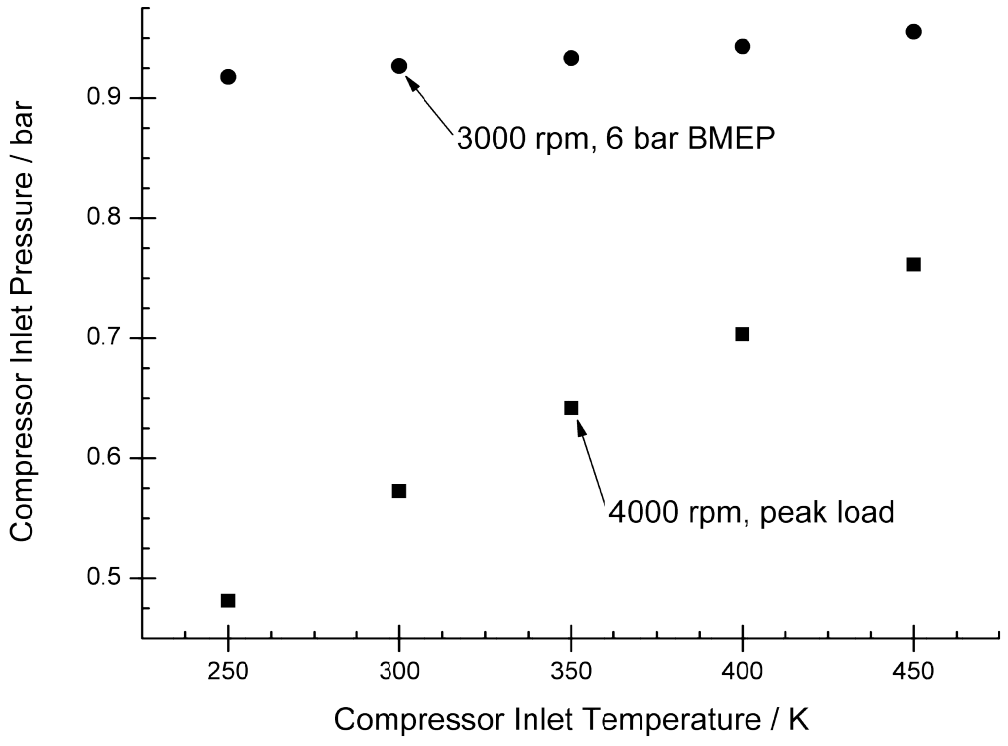

Figure 9-20 - Effect of compressor inlet temperature on achievable depressurisation at 3000 rpm, 6 bar BMEP and 4000 rpm, peak load

It can be seen that the relationship between achievable depressurisation and compressor inlet temperature is relatively linear for both engine operating conditions. Although the benefit of reducing the temperature from 400 to 300 K is only 15 mbar for 3000 rpm 6 bar BMEP, at 4000 rpm peak load it is greater than 125 mbar. For part load conditions considering the implications of real heat exchangers where rejecting more heat causes a larger pressure loss it is not worthwhile rejecting more heat. However, if the system is being optimised for peak power then heat rejection appears to have a significant effect on the achievable depressurisation.

9.4 Benefit of Turbo-Discharging over Natural Aspiration

A model with all the optimised parameters described in this chapter was run such that it could be compared to the validated model and NA engine.

The optimisation process considered each individual factor in series, however, it is clear that some variables will influence each other both positively and negatively. Given the scale of such a task only the HP valve event was optimised beyond that identified in the individual investigation. A full optimisation should be considered in further work investigating the achievable performance with different hardware options such as variable valve systems.

The values used for this study are shown in Table 9-1. The values were constant across the engine speed range except for the HP valve opening, which was retarded by 10°CA at 1000 and 2000 rpm as it was found to be beneficial. The combustion profile and timing was kept constant for all cases.

		Optimised Model	Validated Model
Compressor Diameter Multiplier		0.95	1.05
Compressor Efficiency Multiplier		1	1
Compressor Inlet Temperature	**K**	300	430
HP Valve Diameter	**mm**	28	24.1
HP Exhaust Manifold Diameter	**mm**	22.2	25
HP Valve Duration Multiplier		0.8	0.8
HP Valve Lift Multiplier		0.689	0.689
HP Valve Opening	**°CA**	135	135
Manifold Leakage Diameter	**mm**	0	1
LP Valve Diameter	**mm**	28	24.1
LP Valve Duration Multiplier		0.8	0.8
LP Valve Lift Multiplier		0.689	0.689
LP Valve Closing	**°CA**	365	365
Turbine Diameter Multiplier		1.2	1.05
Turbine Efficiency Multiplier		1	1

Table 9-1 - Values used in the optimised and validated Turbo-Discharging models

Figure 9-21 shows the modelled WOT BMEP curves for the NA engine, validated Turbo-Discharging and optimised Turbo-Discharging models. It can be seen that the performance of the validated Turbo-Discharging model is very similar to that of the NA engine. The optimised model achieves a higher BMEP across the entire engine speed range, increasing the achievable BMEP by 12% at 1000 rpm and 6% at 5000 rpm.

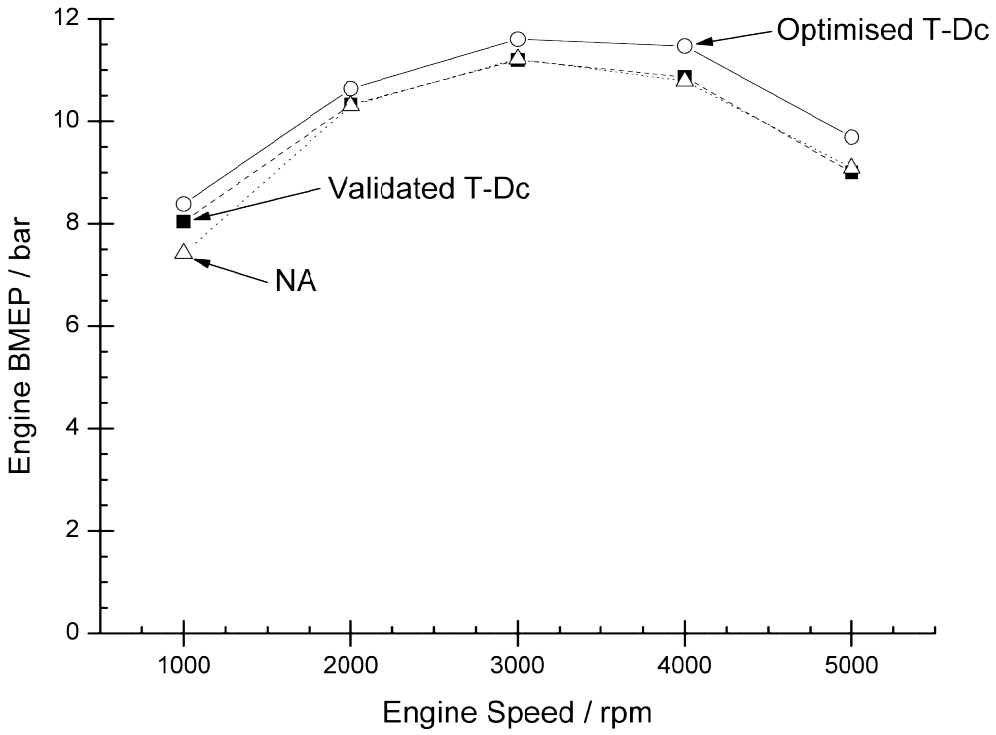

Figure 9-21 - BMEP achieved by the engine model at WOT for the NA, validated and optimised Turbo-Discharging cases with fixed combustion parameters

The benefit in BMEP between the validated and optimised Turbo-Discharging models is partially explained by a reduction in pumping work. Figure 9-22 shows a comparison of PMEP between the NA, validated and optimised Turbo-Discharged models. The Turbo-Discharged models are producing positive pumping work, i.e. net work is being done on the piston during the exhaust and intake strokes. At speeds greater than 3000 rpm, the validated Turbo-Discharged model has worse PMEP than the NA, however, the optimised Turbo-Discharged model is only worse at speeds in excess of 4000 rpm.

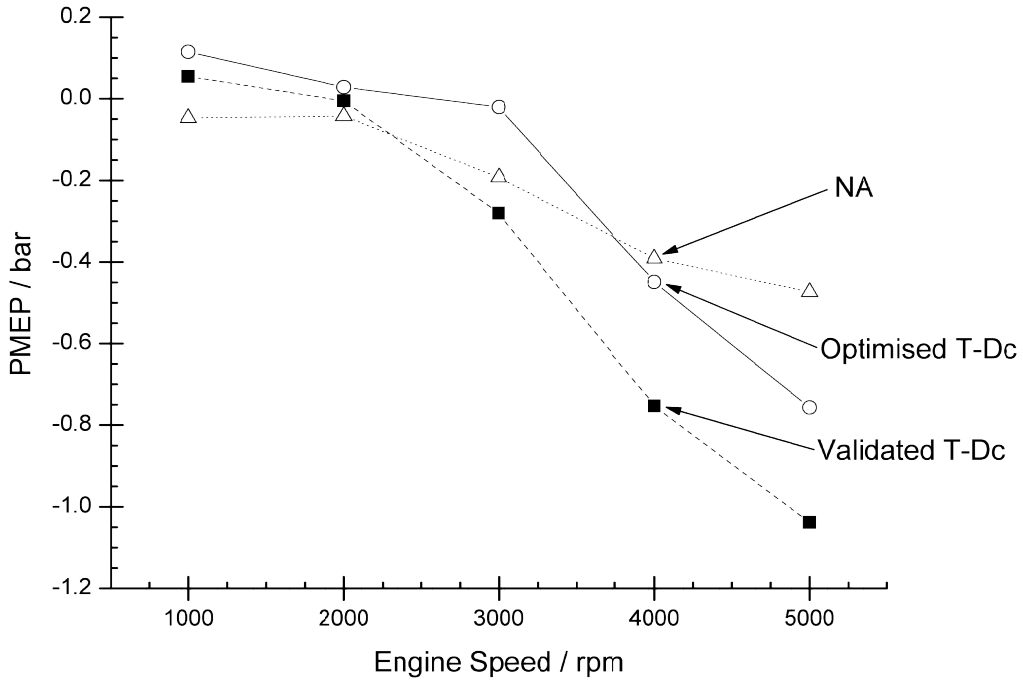

Figure 9-22 - Engine PMEP of the NA, validated and optimised Turbo-Discharging models

The improvement in PMEP of the optimised over the validated Turbo-Discharged model is due to greater achievable depressurisation. This is shown in Figure 9-23.

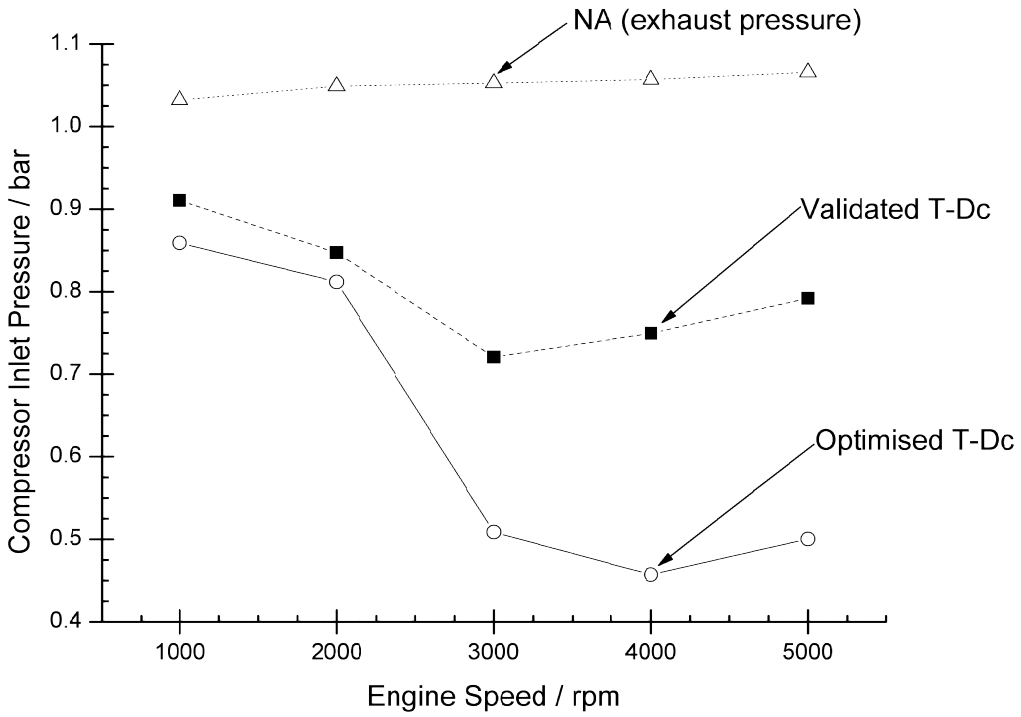

Figure 9-23 - Depressurisation generated at WOT by the validated and optimised Turbo-Discharging systems compared to the exhaust pressure of the NA engine model

The optimised model shows an improvement in the depressurisation achieved across the whole engine speed range. This is likely attributable to the smaller compressor diameter multiplier and the lower compressor inlet temperature.

At speeds over 3000 rpm the optimised model also shows a significant improvement in achieved depressurisation of almost 0.3 bar. However, this does not account for differential in BMEP. Figure 9-24 shows a P-V diagram which compares the validated and optimised models at 4000 rpm, WOT on a log-log scale. The difference in pumping work is evident from the differing size of the pumping loops, however, the validated model also suffers from reduced expansion work during the beginning of the exhaust stroke. This explains the remaining difference in BMEP between the validated and optimised models.

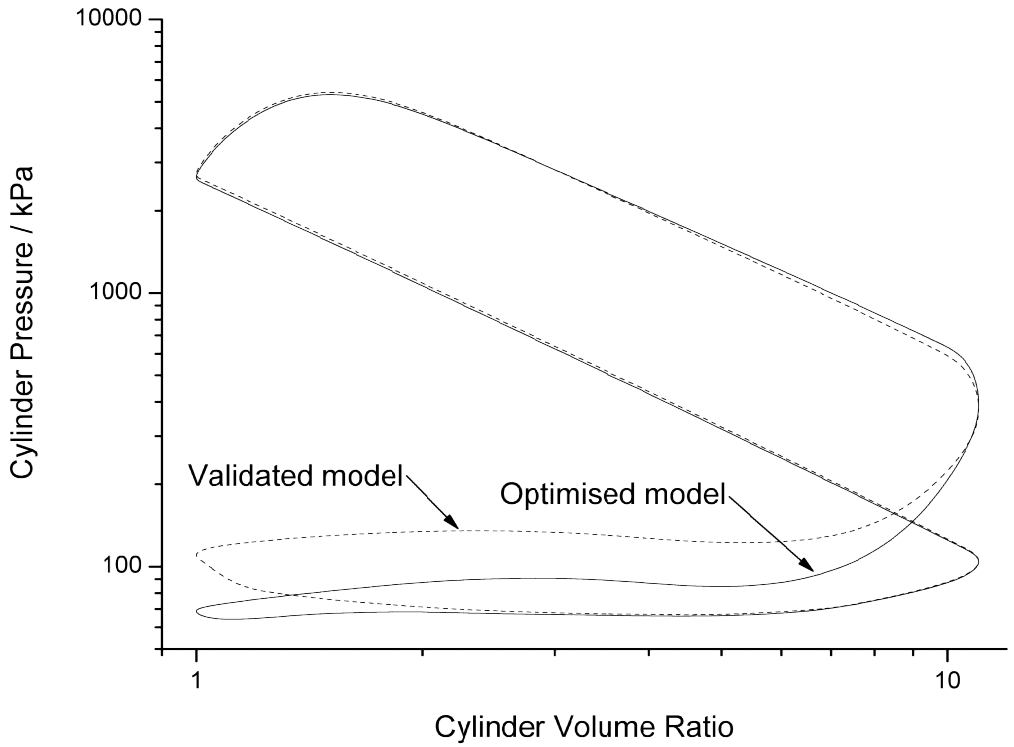

Figure 9-24 - P-V diagram of the validated and optimised Turbo-Discharging models at 4000 rpm, WOT on a log scale

Figure 9-25 shows the bsfc for the NA, validated and optimised Turbo-Discharged models. It can be seen that at full load there is a significant benefit in Turbo-Discharging compared to the NA engine model and again between the validated and optimised Turbo-Discharging models.

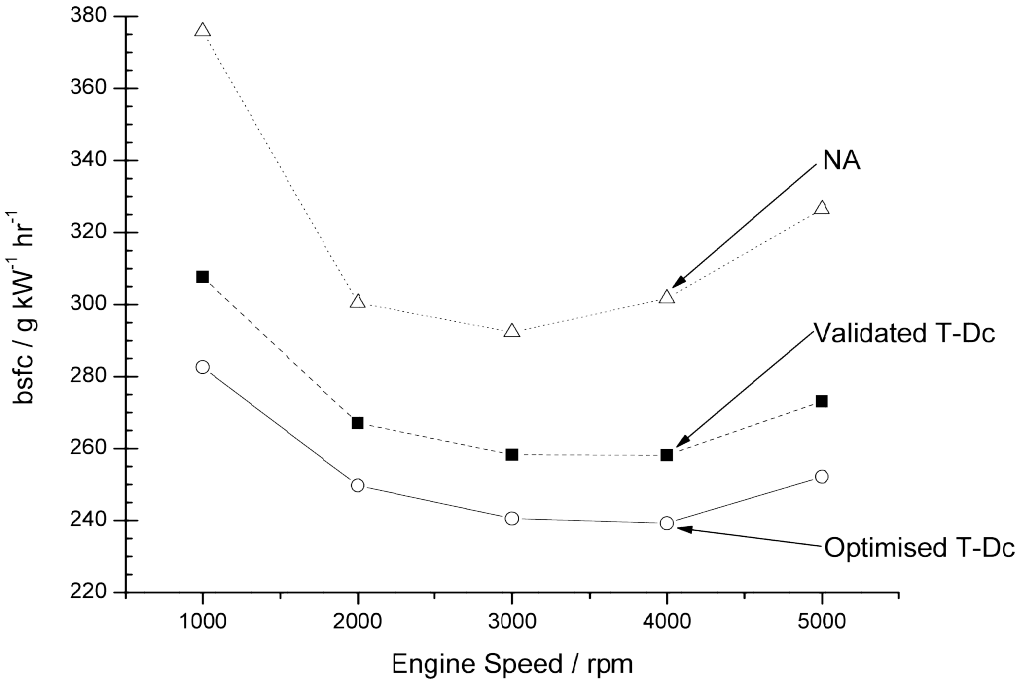

Figure 9-25 - Comparison of NA engine model, validated and optimised Turbo-Discahrging model brake specific fuel consumptions at full load

The optimised and validated cases have similar air and fuel mass flows to within 4%. Therefore, the difference in bsfc observed is that of an efficiency benefit; the optimised case makes better use of the fuel energy, generating a higher BMEP for the same mass flow of air and fuel.

Figure 9-26 shows Turbo-Discharging efficacy versus engine speed for the WOT validated and optimised models calculated from the cylinder pressures and temperatures at EVO. The efficacy for the optimised model is worse at low speed than that of the validated model. This is a result of the higher temperatures seen at EVO for the optimised case; 1800-1900 K compared to 1600-1700 K for the validated case. Higher losses can be associated with the higher temperature case through increased heat transfer upstream of the turbine in turn reducing the energy available to the turbine compared to the ideal case.

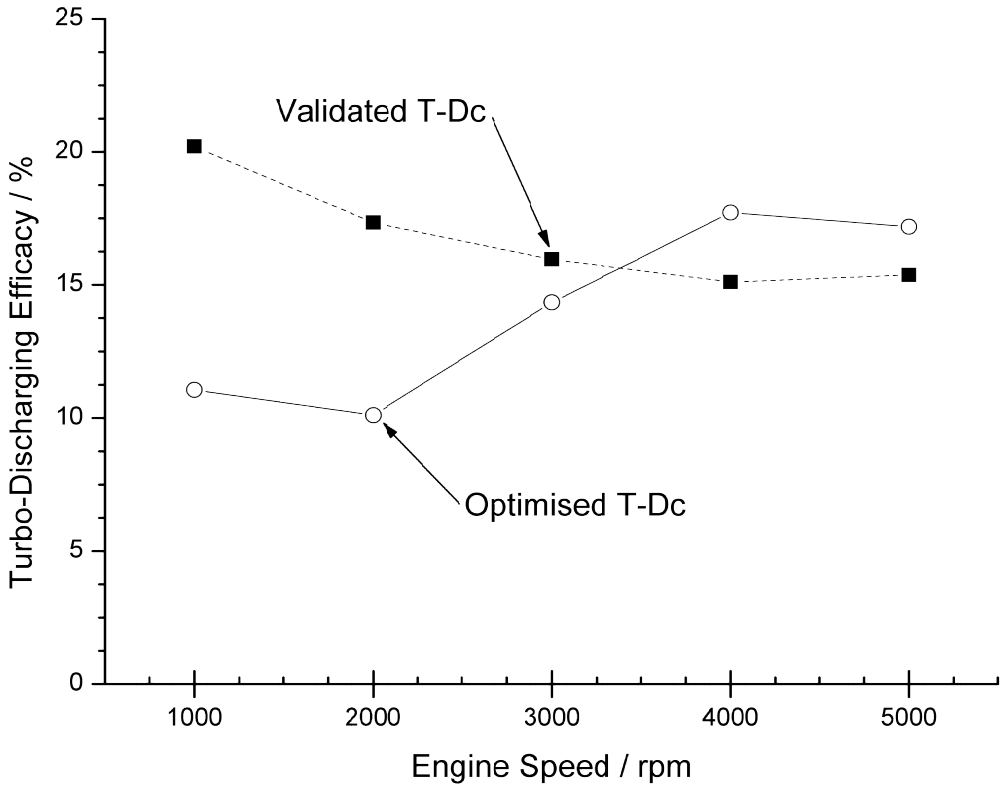

Figure 9-26 - Calculated Turbo-Discharging efficacy at WOT for the validated and optimised models

At 4000 and 5000 rpm the efficacy of the optimised model exceeds that of the validated model. This is due to the increased efficiencies of the turbomachines on the optimum model at these speeds. The turbine efficiency is increased due to the larger turbine diameter multiplier, shifting its point of optimum efficiency towards higher mass flows. The compressor efficiency is increased despite using a smaller compressor diameter due to the reduction in compressor inlet temperature.

9.5 Further Possible Optimisation

This chapter has discussed several variables and their effect on Turbo-Discharging and engine system performance. As mentioned previously it should be possible to further optimise the variables discussed both for full and part load. There are also other variables which could affect Turbo-Discharging system performance and therefore could affect engine fuel efficiency or performance.

The first and possibly most significant variable which has not been discussed is the intake valve event. The assumption throughout this work was for the intake valve events to remain constant at the standard profiles of the experimental engine. As identified earlier in this thesis, it may be possible to positively affect charge motion and create a ram or supercharging effect by increasing the valve overlap with the exhaust. This would have an adverse impact on the achievable depressurisation which could detract from the PMEP benefit achievable during the exhaust stroke. However, it may improve the pumping work required during the intake stroke such that engine fuel efficiency is not affected. The investigation of this was not undertaken due to the experimental engine being port fuel-injected and as such any charge carry over into the exhaust would directly detract from engine fuel efficiency. This effect, therefore, should be investigated in further work with a direct injection engine.

A technology which may be beneficial to Turbo-Discharging effectiveness is that of variable turbine geometry. Turbine and compressor sizing has been discussed and the effect of varying the size has been shown for three load conditions. The sensitivity of pumping work to turbine sizing and mass flow balance between the HP and LP manifold branches has been shown. The use of a VGT would allow for optimisation of energy extraction by the turbine for a fixed HP valve event, increasing the back pressure during the HP portion of the exhaust stroke to increase the pressure ratio across the turbine and extract more energy whilst maintaining a long duration LP event such that the cylinder can be successfully evacuated and pumping work minimised.

Furthermore for a turbocharged engine with a wider operating range of mass flows and exhaust pressures and temperatures it may be desirable to be able to control turbine energy extraction and to manage exhaust gas flow around the turbomachines. A VGT may be beneficial in these circumstances, as well as turbine wastegates or compressor bypass valves. These should be investigated in any subsequent turbocharged engine experiments.

One potential benefit of the exhaust arrangement of Turbo-Discharging, DEP and VEMB systems is that of the ability to de-activate the HP valve during engine cold start and provide fast catalyst light-off. This is possible as the gases pass through the comparatively un-restrictive LP manifold and retain more heat than if they passed through the HP manifold. The turbine reduces the temperature of the exhaust gases as they expand across it whilst the turbine housing has a large thermal inertia and absorbs a significant portion of exhaust gas enthalpy during cold start. The DEP system provided a pre-catalyst in the LP portion of the manifold to enable even faster catalyst light-off (Elmqvist-Möller *et al* 2005) and this is something that could be considered in Turbo-Discharging systems. The most significant difference between the two systems is the depressurisation of Turbo-Discharging and care should be taken in specifying the catalyst to ensure minimal pressure drop and to maximise the translation of the depressurisation to the cylinder. Furthermore, operation of the catalyst under low pressure conditions should be considered.

9.6 Closing Comments

This chapter has identified how the calibrated and validated model and the experimental system could be modified to further improve the effectiveness of the Turbo-Discharging system, in turn increasing the efficiency of the internal combustion engine. An optimised Turbo-Discharging system can offer a 12% torque advantage over an NA engine and a reduction in bsfc at part load conditions of 7% at 3000 rpm, 6 bar BMEP, for example.

The following chapter will conclude the work in this thesis and will collate suggestions for further work which have arisen throughout this study.

10. Conclusions and Suggestions for Further Work

Turbo-Discharging is a novel concept which makes use of IC engine exhaust gas energy. The work from the turbine is transferred back to the engine crankshaft by depressurising the exhaust gas and hence the engine pumping work during the exhaust stroke is reduced. The exhaust system depressurisation also allows for a number of key secondary benefits that can be more significant than the pumping work benefits alone. These benefits combine to offer significant improvements in engine fuel economy and performance.

The research presented in this thesis has used thermodynamic modelling, one-dimensional gas dynamics modelling and experimental investigation to quantify the benefits of using Turbo-Discharging on an automotive naturally aspirated four cylinder four-stroke spark ignition gasoline engine and has identified the mechanisms through which these benefits are realised.

This chapter summarises the major conclusions from this work. It also identifies future opportunities and suggests areas for further investigation of Turbo-Discharging.

10.1 Conclusions

The major conclusions from the research that has been undertaken are as follows:

1. A Turbo-Discharging system has been applied to an engine for the first time and has identified that benefits in engine pumping mean effective pressure (PMEP) and brake specific fuel consumption (bsfc) through reducing the exhaust system pressure are achievable.
2. Thermodynamic and one dimensional modelling and experimentation have shown that depressurising the exhaust system during the exhaust stroke, whilst the piston is moving, allows a reduction in gas exchange pumping work to help improve the evacuation of burned gases from the cylinder, or if sufficiently depressurised it allows for a positive work extraction from the gas exchange part of the cycle. For example, at 3000 rpm, 6 bar BMEP it has been shown it is possible to achieve no net pumping work with a Turbo-Discharged engine when the equivalent NA engine would have 200 mbar of PMEP.
3. The benefit of reduced cylinder residual gas fraction (RGF) was found to be significant. The increased expansion of exhaust gases into the depressurised exhaust results in a reduction in hot residual gas fraction of 1% at part load conditions. It was identified in the thermodynamic model and its benefit quantified through 1-D modelling and experimentation.
4. The arising cylinder depressurisation leads to increased acceleration of the gas through the intake valve, which then improves cylinder scavenging if there is an overlap between the exhaust and intake valve events. A reduction in RGF of 0.7% can be observed for an exhaust pressure of 0.8 bar at 2000 rpm, peak load, corresponding to a potential increase in BMEP of 3.7%.
5. A modelling investigation has shown that Turbo-Discharging offers advantages in both maximum achievable engine load and fuel efficiency at wide-open throttle (WOT), increasing the achievable load by up to 12% compared to the equivalent NA engine operating under the same boundary conditions.
6. Turbo-Discharging efficacy, defined as the power or capacity of the Turbo-Discharging system to depressurise the exhaust system, is useful to compare the effectiveness of the system between different conditions. This is applicable to any naturally aspirated internal combustion engine fitted with a Turbo-Discharging system, and will allow for

the performance of Turbo-Discharging systems to be quantified. It has been shown that the validated Turbo-Discharging model can achieve efficacies of up to 60% at part load conditions of less than 4 bar brake mean effective pressure (BMEP) but is limited to less than 20% efficacy under full load conditions.

7. Valve event timing has been identified as a significant factor affecting the primary benefit of Turbo-Discharging. The importance of optimising the high pressure valve opening to balance in-cylinder expansion work with exhaust gas energy content has been identified. For example, at full engine load and 4000 rpm, a reduction in PMEP of 24% was achieved by varying the high pressure valve opening by 20° crank angle, corresponding to a 1.1% improvement in bsfc.
8. Exhaust and intake valve overlap is particularly influential in the level of depressurisation achievable. For optimal exhaust system depressurisation, it is important to minimise valve overlap, however, charge motion and scavenging may benefit from valve overlap. It may be possible with adjustable cam timing and valve event duration systems to optimise for part load conditions, and then extend the valve event to allow valve overlap for more optimum high load conditions.
9. It is important to optimise Turbo-Discharging turbomachine sizing for PMEP. Turbomachine sizes that generate the greatest depressurisation may do so at the expense of engine fuel efficiency due to its influence on reducing expansion of the gas in-cylinder whilst the piston is still travelling to BDC.
10. Exhaust system depressurisation has been investigated on an experimental rig and a resulting benefit in knock margin has been identified. A reduction in RGF of 1.5-2% allows for up to a 2 Nm benefit with no ignition timing advance, and up to 5 Nm with advanced ignition timing.

10.2 Further Work

This work has for the first time successfully investigated Turbo-Discharging on an internal combustion engine. A number of suggestions for further work have been made throughout this thesis, which are summarised as follows.

1. The most significant aspect which has not been discussed in this work is the interaction between Turbo-Discharging and turbocharging systems. It is important to identify whether Turbo-Discharging can offer significant benefits on a turbocharged engine, or if it adversely impacts turbocharger and engine system performance. This is crucial due to the increasing popularity of turbocharged engines, not just in passenger cars but across all internal combustion engines.
2. Turbo-Discharging should be considered for types of engine other than NA gasoline engines. It has been suggested that benefits will be most significant on throttled gasoline engines; however, there may be circumstances where smaller benefits in fuel efficiency are worth the added complexity of the Turbo-Discharging system. As such, future studies should consider compression ignition applications, including stationary power and other large engines.
3. When calibrating valve flow coefficients for the NA and Turbo-Discharged engine models it was identified that common methods of measuring valve flow coefficients do not take into account the proximity of the piston and the impact of this on the flow through the valve. As a consequence most valve flow coefficients are modified to match a measured pressure drop. Measuring valve flow coefficients at a range of valve lifts and piston positions would mean these values could be input directly into the 1-D model to include these physical effects.
4. Low mass flows through the Turbo-Discharging turbine at low engine speeds and loads results in low turbomachine shaft powers compared to turbocharging systems. This means the turbine and compressor operate for longer periods in parts of the steady state performance maps which are commonly unmapped. The 1-D modelling software extrapolates the measured data into these regions which may result in inaccuracies. Measuring these parts of the maps would allow for greater confidence in the predicted performance.
5. This work has considered steady state performance of a Turbo-Discharging system. Transient performance is of equal importance in passenger car applications, and hence

should be the subject of further work. The transient effects of Turbo-Discharging on a turbocharger system should also be investigated.

6. When discussing the secondary benefits of Turbo-Discharging, experimental work was undertaken on the engine to identify the effect of depressurisation on knock margin. The result of this work was promising; however, it was not possible to translate this into a calibrated 1-D knock model. Further work should therefore be conducted on the effect of depressurisation on knock margin across the engine speed and load range.
7. A potential performance benefit of Turbo-Discharging was identified where it may be possible to use the depressurisation to generate a ram or supercharging effect through drawing fresh charge through the cylinder. This was not investigated due to the use of a port fuel injected engine and the consequential reduction in fuel efficiency. The use of a direct injection fuel system would allow this to be investigated.

References

ACEA (2010), European Automobile Manufacturers' Association, http://www.acea.be/ accessed 28-03-2010.

Alamgir , M. & Sastry , A.M. (2008), Efficient Batteries for Transportation Applications, *2008 Convergence Transportation Electronics Association and SAE International, SAE Technical Paper 2008-21-0017.*

Attard, W., Watson, H.C. & Konidaris, S. (2007), Highly Turbocharging a Flow Restricted Two Cylinder Small Engine – Turbocharger Development, *SAE Technical Paper 2007-01-1562.*

Baines, N.C. (2005), Fundamentals of Turbocharging, *First edition, Concepts NREC, White River Junction, Vermont.*

Berkheimer, J., Tang, J., Boyce, B. & Aswani, D. (2014), Electric Grid Integration Costs for Plug-In Electric Vehicles, *SAE Int. J. Alt. Power. edn, SAE Technical Paper 2014-01-0344.*

Blair, G.P., Drouin, F. M. M. (1996), Relationship Between Discharge Coefficients and Accuracy of Engine Simulation, *SAE International 962527.*

Boyle, G., Everett, B. & Ramage, J. (2003), Energy Systems and Sustainability, *First edn, Oxford University Press, Oxford.*

Brooker , A., Thornton , M. & Rugh , J. (2010), Technology Improvement Pathways to Cost-effective Vehicle Electrification, *SAE Technical Paper 2010-01-0824.*

Buchmann, I. (2001), Batteries in a Portable World, *Second edn, Cadex Electronics Inc., Canada.*

Cambustion (2014), Fast CO and CO2 Analyser for Engine Exhaust, http://www.cambustion.com/products/ndir500 accessed 26-01-2014.

Carberry , B., Grasi , G., Guerin , S., Jayat , F. & Konieczny , R. (2005), Pre-Turbocharger Catalyst - Fast Catalyst Light-Off Evaluation, *SAE Technical Paper 2005-01-2142.*

Conklin, J.C. & Szybist, J.P. (2010), A Highly Efficient Six-stroke Internal Combustion Engine Cycle with Water Injection for In-Cylinder Exhaust Heat Recovery, *Energy, 35, no. 4, pp. 1658-1664.*

de Almeida, A.T., Ferreira, F.J.T.E. & Fong, J.A.C. (2011), Standards for Efficiency of Electric Motors, *Industry Applications Magazine, IEEE, 17, no. 1, pp. 12-19.*

Ekenberg, M. (2002), Method For Controlling The Charging Pressure At A Turbocharged Combustion Engine, And A Corresponding Combustion Engine, Patent 6883319, US.

Elmqvist-Möller, C., Johansson, P., Grandin, B. & Lindström, F. (2005), Divided Exhaust Period – A Gas Exchange System for Turbocharged SI Engines, *SAE Technical Paper 2005-01-1150*.

Fiat Powertrain Technologies S.p.A (2009), MultiAir - The Ultimate Air Management Strategy, www.fptmultiair.com accessed 25-03-2010.

Fink, D.A., Cumpsty, N.A. & Greitzer, E.M. (1992), Surge dynamics in a free-spool centrifugal compressor system, *Journal of Turbomachinery, 114, no. 2, pp. 321-332.*

Garrett, T.K., Steeds, W. & Newton, N. (2001), The Motor Vehicle, *Elsevier Butterworth-Heinemann.*

Greitzer, E.M. (1976), Surge And Rotating Stall In Axial Flow Compressors - 2. Experimental Results And Comparison With Theory, *Journal of Engineering for Power, Transactions ASME, 98 Ser A, no. 2, pp. 199-217.*

Han , D., Han , S., Han , B. & Kim , W. (2007), Development of 2.0L Turbocharged DISI Engine for Downsizing Application, *SAE Technical Paper 2007-01-0259.*

Heywood, J.B. (1988), Internal Combustion Engine Fundamentals, *McGraw-Hill.*

Honeywell International Inc (2010), Garrett by Honeywell http://www.turbobygarrett.com/ accessed 28-03-2010.

Hussain, Q.E., Brigham, D.R. & Maranville, C.W. (2009), Thermoelectric Exhaust Heat Recovery for Hybrid Vehicles, *SAE Technical Paper 2009-01-1327.*

Ibrahim, E.A., Szybist, J.P. & Parks, J.E. (2010), Enhancement of automotive exhaust heat recovery by thermoelectric devices, *Proceedings of the Institution of Mechanical Engineers, Part D: Journal of Automobile Engineering, 224, no. 8, pp. 1097-1111.*

Ikezoe , M., Hirata , N., AMEMIYA, , Chika, Miyamoto , T., Watanabe , Y., Hirai , T. & Sasaki , T. (2012), Development of High Capacity Lithium- Ion Battery for NISSAN LEAF, *SAE Technical Paper 2012-01-0664.*

Konieczny , R., Müller , W., Cherington , B., Presti , M., Jayat , F., Davies , M.J. & Murphy , P.R. (2008), Pre-Turbocharger-Catalyst - Catalytic Performances on an Euro V Type Diesel Engine and Robust Design Development, *SAE Technical Paper 2008-01-0768.*

Lei, V.M., Nejedly, M., Houst, V. & Kares, V. (2012), Dual Boost Compressor Development, 10th International Conference on Turbochargers and Turbocharging, *Institution of Mechanical Engineers, London, pp. 345.*

Lüddecke, B., Filsinger, D. & Ehrhard, J. (2012), On Mixed Flow Turbines for Automotive Turbocharger Applications, *International Journal of Rotating Turbomachinery, pp 14.*

Lumsden , G., OudeNijeweme , D., Fraser , N. & Blaxill , H. (2009), Development of a Turbocharged Direct Injection Downsizing Demonstrator Engine, *SAE Technical Paper 2009-01-1503.*

Luttermann, C., Schünemann, E. & Klauer, N. (2006), Enhanced VALVETRONIC Technology for Meeting SULEV Emission Requirements, *SAE Technical Paper 2006-01-0849.*

Martins , J., Goncalves , L.M., Antunes , J. & Brito , F.P. (2011), Thermoelectric Exhaust Energy Recovery with Temperature Control through Heat Pipes, *SAE Technical Paper 2011-01-0315.*

Martyr, A.J. & Plint, M.A. (2007), Engine Testing Theory and Practice, *Third edition, Elsevier, UK.*

Miller , J., Auer , J. & Maher , B. (2007), Ultracapacitors - The Boost for Hybrid Vehicles, *SAE Technical Paper 2007-01-3468.*

Mori , M., Yamagami , T., Oda , N., Hattori , M., Sorazawa , M. & Haraguchi , T. (2009), Current Possibilities of Thermoelectric Technology Relative to Fuel Economy, *SAE Technical Paper 2009-01-0170.*

National Motor Museum Trust Limited (2010), http://www.nationalmotormuseum.org.uk/?location_id=335&item=52&offset=0 accessed 08-03-2010.

Oxford English Dictionary (2013) - *"compound, v.", "efficacy, n."*.

Payri , F., Serrano , J.R., Piqueras , P. & GarcÃa-Afonso , O. (2011), Performance Analysis of a Turbocharged Heavy Duty Diesel Engine with a Pre-turbo Diesel Particulate Filter Configuration, *SAE Technical Paper 2011-37-0004.*

Ricardo plc (2009), Ricardo WAVE, *8.2nd edition, UK.*

Ringler, J., Seifert, M., Guyotot, V. & Hübner, W. (2009), Rankine Cycle for Waste Heat Recovery of IC Engines, *SAE Technical Paper 2009-01-0174.*

Roth , D.B., Keller , P. & Sisson , J. (2010), Valve-Event Modulated Boost System, *SAE Technical Paper 2010-01-1222.*

Ryder, O. & Sharp, N. (2010), The Impact Of Future Engine And Vehicle Drivetrains On Turbocharging System Architecture, *9th International Conference on Turbochargers and Turbocharging, Institution of Mechanical Engineers, London, pp. 1*.

Sergaki, E.S. (2012), Electric Motor Efficiency Optimization As Applied To Electric Vehicles, *Power Electronics, Electrical Drives, Automation and Motion (SPEEDAM), 2012 International Symposium on, pp. 369.*

Shahed, S.M. & Bauer, K.H. (2009), Parametric Studies of the Impact of Turbocharging on Gasoline Engine Downsizing, *SAE Technical Paper 2009-01-1472.*

Simon, C., Lang, K., Feigl, P. & Bock, E. (2010), Turbocharger seal for zero oil consumption and minimised blow-by, *MTZ worldwide, 71, no. 4, pp. 36-41.*

SMMT (2010), http://www.smmt.co.uk/home.cfm accessed 28-03-2010.

Societe Rateau (1924), Improvements in or relating to Internal Combustion Engines, Patent GB 179926, France.

Stone, R. (1985), Introduction to internal combustion engines, *Macmillan.*

Tavčar, G., Bizjan, F. & Katrašnik, T. (2011), Methods For Improving Transient Response Of Diesel Engines & Influences Of Different Electrically Assisted Turbocharging Topologies, *Proceedings of the Institution of Mechanical Engineers, Part D: Journal of Automobile Engineering, 225, no. 9, pp. 1167-1185.*

Taylor , J., Fraser , N., Dingelstadt , R. & Hoffmann , H. (2011), Benefits of Late Inlet Valve Timing Strategies Afforded Through the Use of Intake Cam In Cam Applied to a Gasoline Turbocharged Downsized Engine, *SAE Technical Paper 2011-01-0360.*

Teng, H., Regner, G. & Cowland, C. (2007), Waste Heat Recovery of Heavy-Duty Diesel Engines by Organic Rankine Cycle Part I: Hybrid Energy System of Diesel and Rankine Engines, *SAE Technical Paper 2007-01-0537.*

Tennant , D. W. H. & Walsham , B.E. (1989), The Turbocompound Diesel Engine, *SAE Technical Paper 890647.*

Turner, J.W.G., Blake, D., Moore, J., Burke, P., Pearson, R.J., Patel, R., Blundell, D., Chandrashekar, R., Matteucci, L., Barker, P. & Card, C. (2010), The Lotus Range Extender Engine, *SAE Technical Paper 2010-01-2208*.

Turner, J.W.G., Marshall, D., Patel, R., Popplewell, A., Richardson, S., Barker, L., Martin, J., Lewis, A.J.G., Akehurst, S. & Brace, C.J. (2014), The Application of the SuperGen Electromechanical Centrifugal Supercharger to the Ultraboost Extreme Downsizing Engine, *Aachen Colloquium, Aachen Colloquium, Aachen.*

Turner, J.W.G., Pearson, R.J. & Kenchington, S.A. (2005), Concepts for improved fuel economy from gasoline engines, *International Journal of Engine Research, 6, no. 2, pp. 137-157.*

Uehara , T., Takahashi , Y., Oki , R., Hirasawa , T., Kamijyo , Y., Ando , I., Teraya , R. & Nakamura , M. (2012), Development of the New THS-II Powertrain for Compact Vehicles, *SAE Technical Paper 2012-01-1017.*

VanDyne, E. (2011), Superturbocharger For Engine Downsizing, *Engine Downsizing, Institution of Mechanical Engineers, London.*

Wang Zhong & Yuan Yin-nan (2008), The design of the 42V power system in turbocharged diesel enginr, *Vehicle Power and Propulsion Conference, 2008. VPPC '08. IEEE, pp. 1.*

Weerasinghe, W.M.S.R., Stobart, R.K. & Hounsham, S.M. (2010), Thermal Efficiency Improvement In High Output Diesel Engines A Comparison Of A Rankine Cycle With Turbo-Compounding, *Applied Thermal Engineering, 30, no. 14–15, pp. 2253-2256.*

Westin, F., Grandin, B. & Ångström, H.E. (2000), The Influence of Residual Gases on Knock in Turbocharged SI-Engines, *SAE Technical Paper 2000-01-2840.*

Williams, A.M. (2011), Internal combustion engine exhaust arrangement with reduced pumping losses, Patent GB2457326, F02B35/02, UK.

Woschni, G. (1967), A universally applicable equation for the instantaneous heat transfer coefficient in the internal combustion engine, *SAE Technical Paper 670931.*

Zhuge , W., Huang , L., Wei , W., Zhang , Y. & He , Y. (2011), Optimization of an Electric Turbo Compounding System for Gasoline Engine Exhaust Energy Recovery, *SAE Technical Paper 2011-01-0377.*